Moisture transport and shape stability of wood exposed to humidity variations a numerical study

Reijnen, S.

Award date:
2012

MOISTURE TRANSPORT AND SHAPE STABILITY OF WOOD EXPOSED TO HUMIDITY VARIATIONS

- A numerical study

Diploma thesis by

STIJN REIJNEN

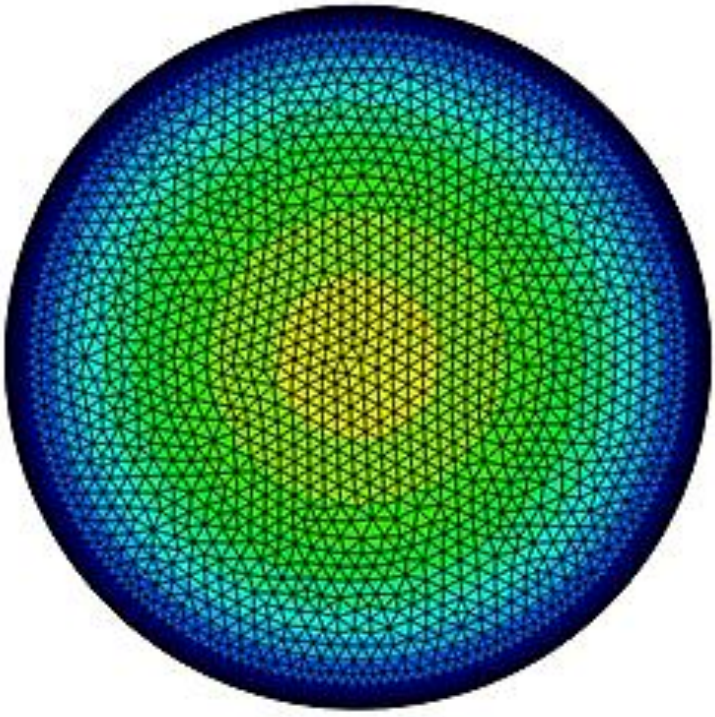

TU/e Technische Universiteit Eindhoven University of Technology

Department of Structural Design

The Faculty of the Built Environment

Technische Universiteit
Eindhoven
University of Technology

MOISTURE TRANSPORT AND SHAPE STABILITY OF WOOD EXPOSED TO HUMIDITY VARIATIONS- A numerical study

Diploma thesis by

STIJN REIJNEN

Version: 1e
31-08-2012

Version 2nd:
18-10-2012

Version 3th:
12-11-2012

Supervisors:

Prof. Dr. ir. André Jorissen, Structural Design, TU/ Eindhoven
Dr. ir. Henk Schellen, Building Physics, TU/ Eindhoven
Prof. Dr. ir. Akke Suiker, Structural Design, TU/ Eindhoven
Dr. Roger Groves, Aerospace Engineering, TU/ Delft
Dr. Bart Ankersmit, ICN, Amsterdam

Abstract

Due to its hygroscopic behaviour, wood is sensitive to variations in humidity. As a consequence of changing environmental conditions and the hygro-expansional behaviour of wood it tends to deform. When these deformations exceed the elastic limit, it could lead to permanent deformations. Often a substantial part of a museum's collection is painted on wood, so called panel paintings. Nowadays, methods of conservation are mainly based upon practical experience which resulted in strict condition requirements. More knowledge about the behaviour of these panel paintings as a result of changing environmental conditions could lead to a more permanent solution and a reduction in costs.

Without numerical simulation it would be impossible to predict the deformation due to the complex behaviour of wood, when exposed to humidity variations. This master's dissertation examines the possibility of ABAQUS CAE standard to model moisture movement and shape stability.

Several finite element models were created and exposed to a step change of 70% to 30% relative humidity (RH). This report is composed in a constructive order. Part 1: commencing with the introduction of the theoretical background. Part 2: The possibility to perform a mass diffusion analysis within a multi-physical environment using the toolbox for a heat transfer. To verify the accuracy of this procedure, a numerical model has been developed, based on research done by Jakiela, Bratasz and Kozlowski, 2008 [37]. Similar to Jakiela, Bratasz and Kozlowski, a lime wood cylindrical model has been developed and exposed to a sudden change of 70% to 30% relative humidity. Corresponding results were obtained with respect to moisture transport and stress field development. The calculated results are extensively discussed and some critical annotations are made.

Panel paintings are made from sawn wood. To smoothen the surface, several layers of gesso (mixture of hide glue, gypsum or sometimes ground chalk and water) and ossein (lime made from bones) were applied, after considerable sanding the panel surface becomes perfectly smooth. Shape stability of sawn wood depends strongly on the initial orientation within the stem. In the last chapter of this master's dissertation, the shape stability of sawn wood is examined. Structural orientations such as the conical angle, growth ring and spiral grain as well as mechanical properties such as the modulus of elasticity, modulus of shear and hygroexpansional coefficients play a significant role in shape stability. Three numerical models were developed to investigate the influence of these structural components and mechanical properties on shape stability. The results demonstrated how twist, crook, cup and bow deformation depend on these parameters. It is concluded that the influence of these parameters not only depends on the quantity of the parameter, but also on the capability of the wood board to adapt this material parameter.

Finally, the influence of a gesso layer on the shape stability is examined. Changing diffusivity, elasticity and thickness seems to affect the shape stability enormously. As a result of the interaction of these parameters, the behaviour of the wood board is different from the board without a gesso layer. Depending on the diffusivity of the gesso layer, it can lead to strong short time behaviour.

Keywords: panel painting, finite element method, moisture transport, strain development, shape stability, heat transfer, mass diffusion, driving potential, shrinking, swelling, ABAQUS

Acknowledgements

This diploma thesis was written during the summer of 2012 at the Division of Structural Design and Construction Technology at the Technical University of Eindhoven, The Netherlands.

Firstly, I want to thank my supervisors Prof. André Jorissen, Dr. Henk Schellen and Prof. Akke Suiker for their expert guidance, support and most importantly, allowing me to explore an unknown, new and interesting field of research. I wish to thank my supervisors Dr. Roger Groves from the Delft University of Technology for his time and helping me in the early stage with technical information and Dr. Bart Ankersmit from the ICN for his interest and providing the project with test material.

A special thanks to the "Sheriff of Melbourne" Loy Kop, for all the time he spent reviewing the thesis English.

Nijmegen, 27 August 2012

Stijn Reijnen

Samenvatting

Als gevolg van hygroscopiciteit is hout gevoelig voor wisselingen in de relatieve luchtvochtigheid. Ten gevolge van wisselende omgevingscondities en de hygroexpansie van hout kan vervorming optreden. Wanneer deze vervormingen de elasticiteitsgrens voorbij streven, zal permanente vervorming het gevolg zijn.

Veelal is een aanzienlijk deel van de collectie van een museum op hout geschilderd, een zogenaamd paneelschilderij. De huidige conservering methoden zijn veelal gebaseerd op jaren van praktische ervaring dit heeft geresulteerd in strenge eisen aan de directe omgeving waarin het paneel zich bevindt. Meer wetenschap betreffende het gedrag van hout als gevolg van wisselende klimatologische omstandigheden kunnen aanleiding geven tot een betere en meer permanente oplossing. Zonder het gebruik van numerieke simulaties is het onmogelijk betrouwbare voorspellingen te doen met betrekking tot vervorming als gevolg van het complexe gedrag van hout wanneer het reageert op vochtveranderingen. Dit afstudeerwerk onderzoekt de mogelijkheid om met ABAQUS CAE vochttransport door hout te simuleren en de vormstabiliteit te onderzoeken, zonder gebruik te maken van subroutines.

Verschillende eindige elementenmodellen zijn ontwikkeld waarmee de reactie op een verandering van 70% naar 30% relatieve luchtvochtigheid (RH) is berekend. Dit afstudeerwerk is opbouwend chronologisch samengesteld. Deel 1: Theoretische achtergrond. Deel 2: wordt ingegaan op de mogelijkheid om vochttransport en vorm stabiliteit te simuleren met behulp van een warmte transportanalyse in plaats van een massa-diffusieanalyse in een multi-fysische omgeving. Ter verificatie van de correctheid van deze aanpak is een numeriek model ontwikkeld gebaseerd op eerder onderzoek van Jakiela, Bratasz en Kozlowski, 2008 [37]. Een eindig elementenmodel in de vorm van een cilinder van lindenhout is blootgesteld aan een verandering van 70% naar 30% relatieve luchtvochtigheid. De verkregen resultaten blijken in overeenstemming te zijn met het werk van Jakiela, Bratasz en Kozlowski, 2008 [37].

Beschilderde panelen zijn vaak gemaakt van planken. Om het oppervlak glad te krijgen worden verschillende lagen gesso en beenderlijm aangebracht, die na gestaag schuren perfect glad dient te worden. De vormstabiliteit van planken is sterk afhankelijk van de plaats welk het in de stam heeft gehad. De laatste hoofdstukken van dit afstudeerwerk hebben betrekking op vormstabiliteit. Het blijkt dat de constructieve opbouw zoals de conische vorm, jaarring oriëntatie en vezel oriëntatie maar ook mechanische eigenschappen zoals de elasticiteitmodulus, schuifmodulus en hygroexpansie coëfficiënten hier een belangrijke rol in spelen. Drie numerieke modellen zijn er ontwikkeld om deze constructieve en mechanische eigenschappen te onderzoeken met betrekking tot vormstabiliteit. Uit de resultaten wordt verklaard hoe twist-, krom-, cup- en buigvervorming wordt aangedreven. Er wordt geconcludeerd dat niet alleen de grootte van de parameter maar ook de mogelijkheid tot ontwikkeling van deze parameter, welk afhankelijk is van de initiale oriëntatie in de stam, een belangrijke rol speelt.

De invloed van een gessolaag met betrekking tot vormstabiliteit is onderzocht. Veranderingen in de diffusiecoëfficiënt, elasticiteit en dikte van de laag blijken grote gevolgen te hebben voor de vormstabiliteit. Als gevolg van een gessolaag ontstaat er in sommige gevallen zelf een geheel nieuw type vervorming die zonder gesso nooit zou optreden. Het aanbrengen van een gessolaag blijkt ook invloed te hebben op de initiële ontwikkeling van twist-, krom-, cup- en buigvervorming.

Quantities and symbols

AH	=	Absolute Humidity $[kg/m^3]$
RH	=	Relative Humidity [%]
SH	=	Specific Humidity $[kg/m^3]$
SG	=	Specific Gravity [-]
MC	=	Moisture Content [%]

A	=	Area $[m^2]$
a	=	Thermal diffusivity $[m^2 \cdot s^{-1}]$
c_p	=	Specific heat capacity $[J \cdot kg^{-1}K^{-1}]$
D	=	Diffusion coefficient $[m^2 \cdot s^{-1}]$
D_C	=	Moisture concentration diffusion coefficient $[m^2 \cdot s^{-1}]$
D_u	=	Moisture content diffusion coefficient $[kg \cdot m^{-1} \cdot s^{-1}]$
D_P	=	Water vapour pressure diffusion coefficient $[kg \cdot m^{-1} \cdot s^{-1} \cdot Pa^{-1}]$
D_w, D_V	=	Water vapour content diffusion coefficient $[m^2 \cdot s^{-1}]$
E_x, E_y	=	Elastic modulus $[N \cdot m^{-2}]$
e_w	=	Actual vapour pressure $[Pa]$
e_w^*	=	Equilibrium vapour pressure $[Pa]$
ε_u	=	moisture induced strain $[-]$
G	=	Shear modulus $[N \cdot m^{-2}]$
g	=	Moisture flux at surface $[kg \cdot m^{-2}s^{-1}]$
h	=	Heat transfer coefficient $[W \cdot m^{-2}K^{-1}]$
J	=	Diffusion flux $[mol \cdot m^{-2}s^{-1}]$
k	=	Conductivity of the material $[W \cdot m^{-1}K^{-1}]$
M_w	=	Absolute quantity of water $[kg]$
m_i	=	Mass concentration $[kg]$
m_v	=	Mass of water vapour $[kg]$
$m_{dry-air}$	=	Mass of dry air $[kg]$
m_o	=	Mass of water in the wood sample $[kg]$
m_0	=	Mass of the oven dry wood $[kg]$
P_w	=	Vapour pressure $[Pa]$
P_{ws}	=	Equilibrium vapour pressure $[Pa]$
q	=	Density of heat flow rate $[W \cdot m^{-2}]$
R_g	=	Swollen volume density $[kg \cdot m^{-3}]$
S	=	Surface area (of material volume) $[m^2]$
S	=	Solubility $[ppm]$
s	=	Solubility [-]

T_0	=	Initial temperature $[K]$
T_s	=	Sink temperature $[K]$
T, θ	=	Temperature $[K]$
t	=	Time $[s]$
$\dot{U}$	=	Material time rate of internal energy $[J \cdot s^{-1}]$
u	=	Moisture content [%]
u_f	=	Moisture content at fibre saturation point [%]
V	=	Volume $[m^3]$
V_{air}	=	Absolute volume $[m^3]$
V_0	=	Oven dry volume $[m^3]$
W_0	=	Oven dry mass $[kg]$
W_m	=	Mass of the wet wood $[kg]$
w	=	Water vapour content $[kg \cdot m^{-3}]$
x	=	Position $[m]$
α	=	Matrix of the hygroexpansional coefficients (swelling) [-]
α_v	=	Volumetric swelling [%]
α_t	=	Tangential swelling coefficient [-]
α_l	=	longitudinal swelling coefficient [-]
α_r	=	Radial swelling coefficient [-]
β	=	Moisture transfer coefficient $[kg \cdot m^{-2} s^{-1}]$
β_t	=	Tangential volumetric shrinkage [-]
β_r	=	Radial volumetric shrinkage [-]
β_v	=	Volumetric shrinkage [-]
β_l	=	longitudinal volumetric shrinkage [-]
γ	=	Shear modulus $[N \cdot m^{-2}]$
∇T	=	Temperature gradient $[K \cdot m^{-1}]$
Δu	=	Change of moisture content [%]
ε	=	Strain [-]
κ_s	=	Soret factor [-]
λ	=	Thermal conductivity (k) $[W \cdot m^{-1} K^{-1}]$
ν	=	Poissons ratio [-]
ρ	=	Density $[kg \cdot m^{-3}]$
ρ	=	density of the material $[kg \cdot m^{-3}]$
ρ_0	=	Density $[kg \cdot m^3]$
σ	=	Stress $[Pa]$
ϕ	=	Concentration $[mol \cdot m^{-3}]$

Definitions:

ABAQUS:	Finite Element Software.
Absolute Humidity (AH):	Absolute humidity represents the total mass of water in a certain volume of air and water vapour.
Absorption:	Refers to absorbing one volume of mass into another volume of mass.
Adsorption:	Refers to the action of a substance in attracting and holding other mass volumes on its surface.
Angiosperms:	Type of tree (deciduous).
Bark:	The bark is responsible for protection against fungi, insects or other threats, located around the tree.
Bound water:	Bound water is the water that is in the cell wall and chemically bounded.
Bow deformation:	Bending of sawn wood perpendicular to the width of sawn wood.
Cambium:	The cambium is responsible for radial growth.
Cartesian coordinate system:	Coordinate system with X, Y and Z directions perpendicular to eachother.
Chemical potential:	Chemical potentials can be defined as 'factors' potentially driving the diffusive process (driving potentials).
COMSOL:	Finite Element Software.
Conduction:	Energy transfer by free electrons or vibrations of molecules within a solid.
Convection:	Energy transfer by bulk motion of matter.
Crook deformation:	Bending of sawn wood in the lateral direction.
Cup deformation:	Bending of sawn wood perpendicular to the length direction of sawn wood.
Cylindrical coordinate system (CCS):	Coordinate system with radial (R), tangential (T) and longitudinal (L) directions.

Diffusion:	The random movement of particles due to kinetic energy from an area where they are highly concentrated to an area where they are less concentrated. The rate of their motion is a function of temperature, viscosity and mass of the particles.
Driving potentials:	Driving potentials can be defined as 'factors' potentially driving the diffusive process (chemical potentials).
Earlywood:	Wood grown in spring time.
Equilibrium Moisture Content (EMC):	If the surrounding moisture content is kept constant, dry wood will keep on absorbing water until it is in equilibrium with its surrounding; this is called the Equilibrium Moisture Content.
Evaporation:	Molecules near the surface of a liquid which have enough kinetic energy (by heating) to escape.
Fibre Saturation Point (FSP):	The point where all the free water in the cavities has evaporated during desorption is called the Fibre Saturation Point (FSP).
Free water:	Water that fills the wood cavities.
Gesso:	Mixture of hide glue, gypsum or sometimes ground chalk and water.
Growth rings:	Annual rings of a tree.
Gymnosperms:	Type of tree (coniferous).
Heartwood:	Depending on the wood species, after 20 or 30 years, a tree begins the inward conversion of sapwood into heartwood.
Hygro-expansion:	Volumetric shrinkage/swelling.
Hygroscopicity:	Wood is able to absorb and desorb water in the cell wall with respect to the moisture content of the surrounding atmosphere, this is called hygroscopic behaviour.
Latewood:	Wood grown in the autumn/summer.
Moisture Content (MC):	Ratio between the mass of water in the wood sample and the mass of the oven dry wood.
Ossein:	Lime made from bones.
Pigment Volume Concentration (PVC):	The ratio of inert materials within gesso.
Pith:	Centre of the tree.

Radiation:	Energy transfer by (electromagnetic) -radiation generated by the thermal motion of charged particles in matter.
Relative Density (RD):	Relative dry wood density is a very important indicator, it is related to strength, surface hardness, shrinking and swelling. Wood with higher relative density generally shrinks and swells more than wood with a lower relative density.
Relative Humidity (RH):	Relative Humidity (RH) describes the quantity of water vapour in a mixture of air and water vapour.
Sapwood:	The sapwood is responsible for vertical, upwards saps transport.
Specific Gravity (SG):	Ratio between the density of a substance and the density of a standard (mostly water).
Specific Humidity (SH):	Specific humidity is the ratio between the mass of water vapour in a certain mass of dry air.
Tracheids:	In softwood tracheids are responsible for the vertical sap transport.
Twist deformation:	Twisting of sawn wood around the lengthwise direction.
Wood Density (WD):	Ratio between the oven dry weight and the current volume.

Contents

Part 2: Numerical

0 Introduction

Preservation of worldwide cultural heritage is very important. Different materials demand different conservation methodologies. Often a feeling, founded on years of experience, takes an important role in making the decision which method of conservation is to be applied. History teaches that this approach does not (always) deliver the desired results. Despite the invaluable experience of this empirical approach, it is not (always) sufficient. Thorough knowledge of the more or less changing environmental factors, mainly characterized by temperature, humidity and light, where the "art" is located, the resulting internal stresses and deformations in the wooden panel, as well as the response of the paint layers, could lead to a more permanent solution. This master's dissertation focusses on the crossroad between Science and Art.

A panel painting is a painting that is painted on wood. Not many people are aware that famous paintings, painted by great masters, are painted on wood. The Mona Lisa by Leonardo da Vinci is an example. The Mona Lisa is painted on a wooden panel made from poplar and is almost 500 years old. Wood, and the better known canvas, varies widely in material properties. In order not to expose the artefacts to big changes in temperature and relative humidity, museums, annually invest much money in the climatic control of the spaces where art is exhibited and stored.

Strict requirements, completely based on empirical evidence, should protect the art against degradation. Besides the cultural responsibility, there is also a financial stimulation to review the current way of thinking and to try to provide a scientific basis. Wood is sensitive to fluctuations in relative humidity. Absorption from and desorption of moisture to the immediate environment is unfortunately not without conflict. Absorption and desorption of moisture give rise to swelling and shrinking. The mechanical properties depend strongly upon their orientation. This directional dependency can lead to unwanted shape deformation and strain development. Deformations exceeding the elastic range can lead to permanent deformation.

This master's dissertation examines the possibility of ABAQUS CAE to model moisture transport and shape stability. Commencing with the very basics of the structure of hardwood, softwood, shrinking, swelling, stress, strain, creep and creep recovery. Subsequently a detailed discussion about creating a constitutive model will be presented. Finally, several numerical models are used to examine the effect of changing environmental conditions on moisture transport, structural parameters, changing mechanical parameters and the effect of a gesso layer on shape stability.

0.1 Problem statement

The conservation of panel paintings by museums is mainly based upon practical experience. In an attempt to protect our cultural heritage against degradation, museums apply strict condition requirements, 55% (±5.0%) relative humidity. Besides the cultural responsibility, there is also a financial stimulation to review the current way of thinking and to try to provide a scientific basis. More knowledge about the behaviour of these panel paintings as a result of changing environmental conditions could lead to a more permanent solution. Due to the complex behaviour of wood when exposed to humidity variations, it is almost impossible to predict the deformation without the use of numerical simulations. For this reason more knowledge about numerically modelling of wood is needed.

0.2 Objective

The objective of this research can be divided into four sub-objectives:

1) To examine the possibility of ABAQUS CAE standard to model moisture movement and shape stability.
2) To examine the influence of changing environmental conditions on shape stability.
3) To investigate the influence of changing material parameters on shape stability.
4) To investigate the influence of a coating layer and changing coating parameters on shape stability.

0.3 Research question

In order to meet the research objectives as mentioned in 0.2, the following research questions have to be answered:

1) Is it possible to perform a mass diffusion analysis within a multi-physical environment using the toolbox for a heat transfer analysis with ABAQUS CAE standard?
2) Is it possible to model the structural orientation such as the conical angle, growth ring and spiral grain and how do these structural parameters influence the shape stability of sawn wood?
3) What is the influence of changing mechanical parameters such as the modulus of elasticity, modulus of shear and hygro-expansional coefficients on shape stability of sawn wood ?
4) What is the influence of a gesso layer on the shape stability of sawn wood?

Part 1: Theory

1 Structure of hardwood and softwood

1.1 Introduction

Wood is a heterogeneous, hygroscopic, cellular and anisotropic material. It is a non-uniform material in composition. It has the ability to attract and hold water molecules from the surrounding environment. It is built from cells like all other living organisms and the material properties are directionally dependent.

Trees may be divided into two categories: angiosperms (hardwood/deciduous) and gymnosperms (softwood/coniferous). A more common division is to distinguish between deciduous and coniferous trees. The name deciduous means in Latin 'to fall' which means that these trees loses their leaves. Common species are oak and poplar. Coniferous trees does not lose their leaves or needles. Common species are spruces and pines.

1.2 Wood structure

The physical properties are highly dependent on the structure. Wood is an organic material, predominantly made of cellulose fibres and lignin. The cross section of a tree is divided in the pith, sapwood, heartwood, cambium and bark, see figure 1.1.

Pith: the pith is the centre of the tree. **Sapwood**: the sapwood is responsible for vertical, upwards saps transport (outer part) and sapwood is lighter of colour (in most cases) than heartwood. **Heartwood**: general speaking, after 20 or 30 years, a tree begins the inward conversion of sapwood into heartwood. Because the heartwood is naturally preserved with organic substances, all functions cease. The only functionality for heartwood is the provision of strength and stability of the tree. **Cambium**: the cambium is responsible for radial growth. In the cambium layer cells are split and sent inwards to form new sapwood and outwards to form bark. **Bark**: the bark is responsible for protection against fungi, insects or other threats. Vertical downwards sap transport transmits through the inner bark.

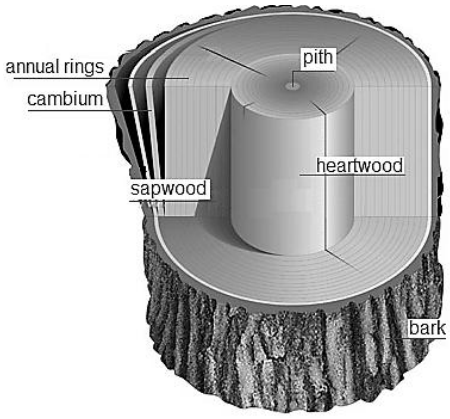

Figure 1.1: Structure of wood (www.visual.merriam-webster.com)

1.3 Structure of hardwood

Hardwood is from an anatomical point of view more complex than softwood. Hardwood is built up from more different cell types like fibres (figure 1.2: F), tracheids (responsible for the vertical sap transport) and parenchyma (storage tissue), are all built with different cell types. There is also more variation in arrangement of these cells. Hardwood uses vessels for vertical sap transport. When the cross section is observed, the ends of these vessels look like pores (figure 1.2: P). Big cells form vessels and small cells forms fibres. Vessels are a long series of longitudinal short cells. These vessels are responsible for vertical sap transport. The fibres look like tracheids, but they are definitely not the same. Fibres are much smaller in diameter and shorter in length. Tracheids are specific for softwood. Fibres are responsible for supporting tissue, see Martenson 1992 [1] and Madison 1980 [10].

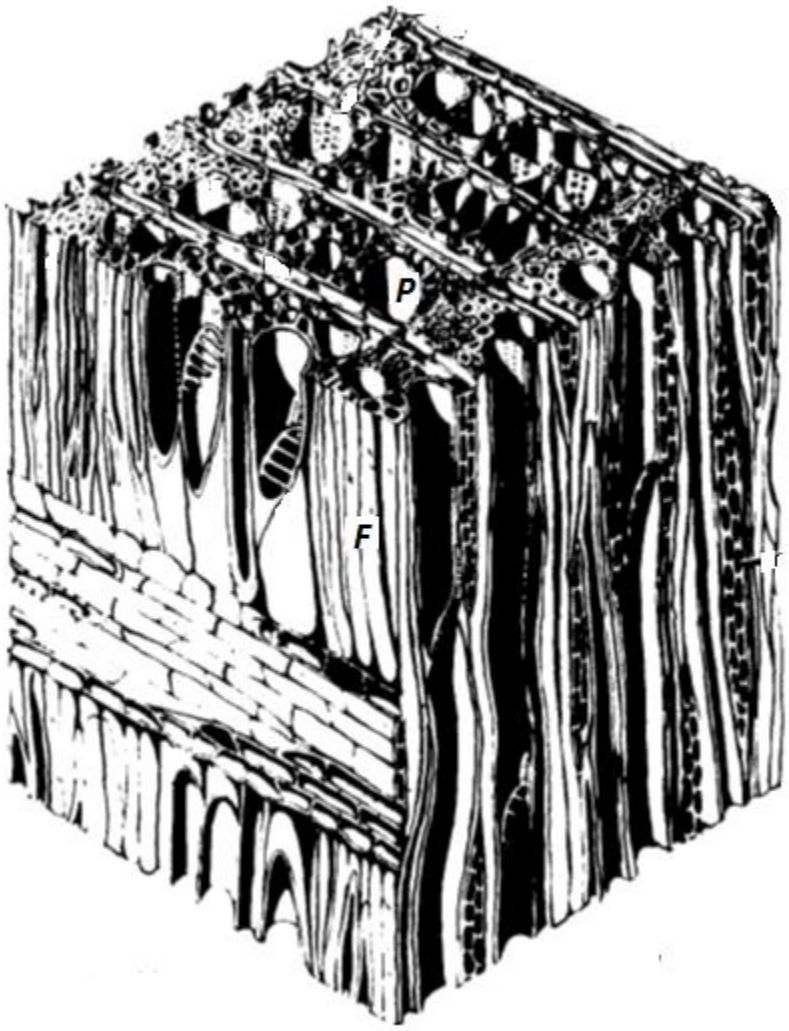

Figure 1.2: Structure of hardwood, yellow poplar (U.S. Department of Agriculture Forest Service)

1.4 Structure of softwood

In softwood tracheids are responsible for the vertical sap transport (figure 1.3: T). Tracheids can be seen as fibres and vessel in one. They are responsible for sap transport and support. About 90-95% cell wall structure is built from tracheids. The rays (figure 1.3: R) in softwood are also smaller than those of hardwood. The rays are made from parenchymal cells. Radial parenchymal cells are distinguished from vertical parenchymal cells. Some softwood trees also have resin ducts (figure 1.3: RD) which transport resin in vertical direction. Within figure 1.3 sapwood and heartwood are distinguished with respect to the pith, cambium and the bark. Commonly, the heartwood is dark collard and the sapwood brighter. This is not consistent for all species. The heartwood is defined as the part of the tree where there are no living cells.

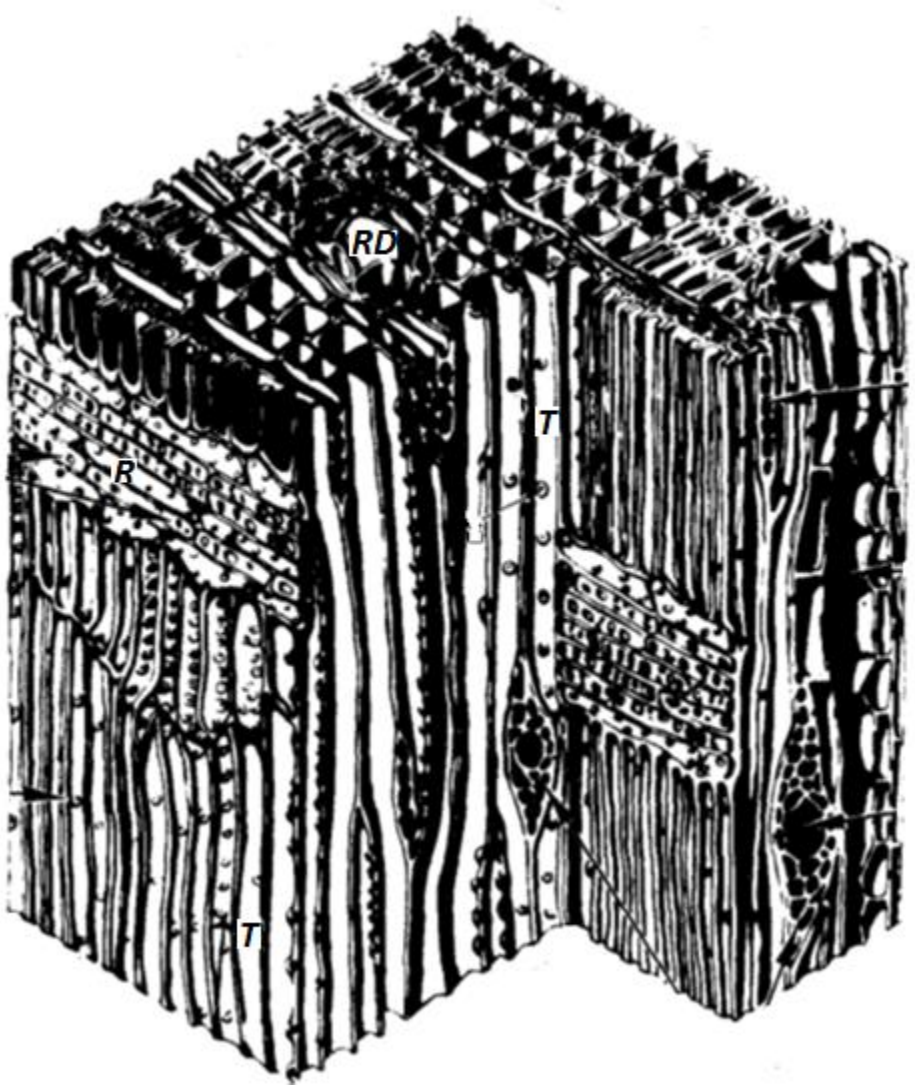

Figure 1.3: Structure of softwood (U.S. Department of Agriculture Forest Service).

1.5 Wood cells

Softwood is composed of two cell types: tracheids (90-95%) and ray cells (5-10%). Tracheids are relatively long (2-4 mm) and have an average width of 0.02-0.04 mm. The ray cells are 0.1-0.16 mm long and 0.002-0.050 mm width. It is known that hardwoods have vessels for conducting sap. Hardwoods contain several different cell types, each with different functions, such as supporting tissue (libriform fibres), conducting tissue (vessel elements) and storage tissue (parenchyma cells). Figure1.4 is a simplification and mainly applies to the tracheid (softwood). Rays do have the same main structure. The difference can be found in the orientation of the micro fibrils in the secondary wall, whilst the thickness of the individual layers within the cell wall varies, see Madison 1980 [10] and Martenson 1992 [1].

Wood cells are part of a bigger matrix of cells. Wood cells are divided in three different cell walls of which the secondary wall is divided into three layers, see figure 1.4.

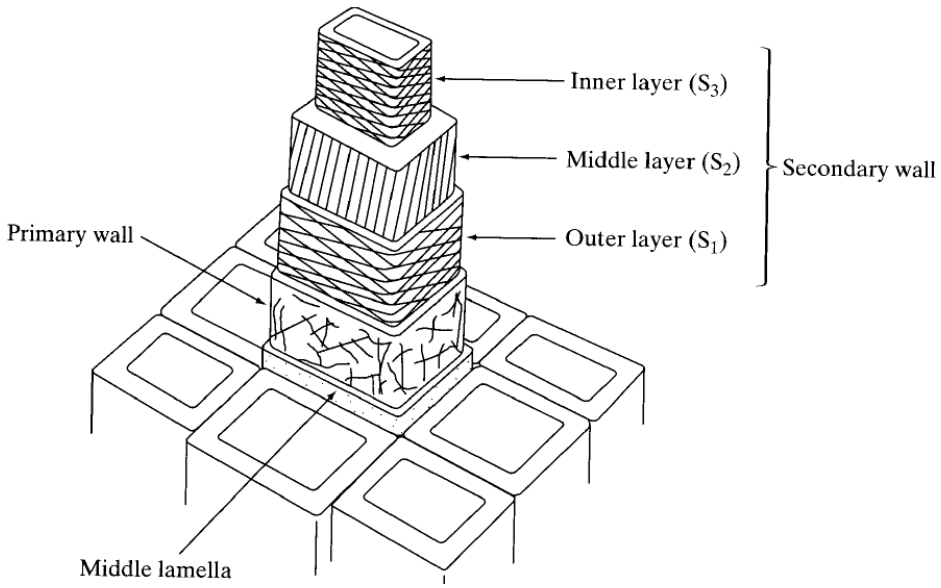

Figure 1.4: Cell wall structure (www.classes.mst.edu)

2 Shrinking and swelling of wood

2.1 Introduction

Furniture, old wooden instruments and panel paintings, require great care to keep them in a good condition. If good care is not taken cracks develop which is unwanted, see figure 2.1. Wood is sensitive to changes in moisture content, caused by climate changes. Wood drying out shrinks this reducing the dimensions of the sample. In contrast, wet wood swells, increasing the dimensions. Because of differences in moisture adsorption over the wood dimensions, a difference in deformation occurs, which may lead to cracks. To overcome the effect of shrinking and swelling, varnishes are used, but mostly this only slows down the process.

Humidity is a term for the quantity of water vapour in the air. There is an important relation between the moisture content in the air and the heat of the air. Warm air can hold more moisture than cold air. When the temperature of air increases, its capacity to hold moisture increases. A change in temperature correlates to a change in relative humidity, although the moisture content remains unchanged.

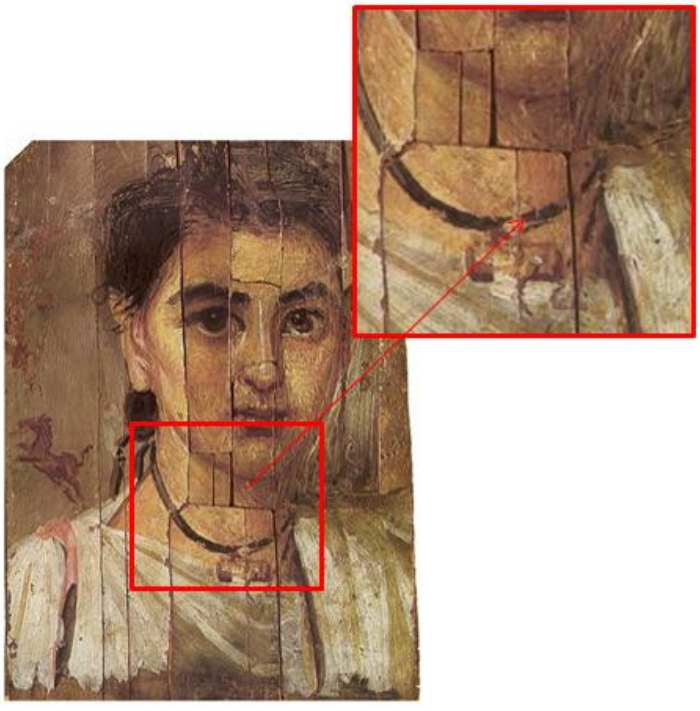

Figure 2.1: The boy from Fayum panel painting, the inset shows local cracking in the painting (Wikipedia).

2.2 Humidity

Humidity is a term for the amount of water vapour (moisture) in the air. The humidity can be expressed in three different ways: absolute humidity, relative humidity and specific humidity.

Absolute Humidity (AH):
Absolute humidity represents the total mass of water in a certain volume of air and water vapour.

$$AH = \frac{m_w}{V_{tot}} \qquad (2.1)$$

AH = Absolute Humidity $[kg/m^3]$
m_w = Total mass of water $[kg]$
V_{tot} = Total volume $[m^3]$

Relative Humidity (RH):
Relative Humidity describes the quantity of water vapour in a mixture of air and water vapour. The partial pressure of water vapour in the mixture of air and water is given in percentages of saturated vapour pressure under these conditions. When temperature increases, this leads to a change in relative humidity. When the temperature decreases, the relative humidity remains unchanged and some water vapour will change into water, this is called condensation.

$$RH = \frac{e_w}{e_w^*} 100\% \qquad (2.2)$$

RH = Relative Humidity [%]
e_w = Actual vapour pressure $[Pa]$
e_w^* = Saturation vapour pressure $[Pa]$

Specific Humidity (SH):
Specific humidity is the ratio between the mass of water vapour in a certain mass of dry air.

$$SH = \frac{m_v}{m_{dry-air}} \qquad (2.3)$$

SH = Specific Humidity $[-]$
m_v = Mass of water vapour $[kg]$
$m_{dry-air}$ = Mass of dry air $[kg]$

2.3 Specific Gravity and relative wood density

Specific gravity, wood density and relative density are very important indicators for wood.

Specific gravity is a dimensionless quantity; it is the ratio between the density of a substance and the density of a standard (mostly water):

$$SG = \frac{\rho_{object}}{\rho_{ref\,(water)}} \qquad (2.4)$$

SG = Specific gravity [-]
ρ_{object} = Density of substance $[kg/m^3]$
$\rho_{ref\,(water)}$ = Density of water $[kg/m^3]$

This differs from the more used relative wood density, the ratio between the oven dry weight and the current volume, equation (2.5).

$$\rho_0 = \frac{W_0}{V_0} \qquad (2.5)$$

ρ_0 = Relative dry wood density $[kg/m^3]$
W_0 = Oven dry mass $[kg]$
V_0 = Oven dry volume $[m^3]$

Relative dry wood density is a very important indicator (2.5). It is related to strength, surface hardness, shrinking and swelling. Wood with higher relative density generally shrinks and swells more than wood with a lower relative density. This is contrary to the thought that higher relative density means that hardwood is a strong wood and therefore more susceptible to shrinking and swelling than softwood, which is not true. The terms hardwood and softwood can be misleading when referring to literal hardness and softness. The classification hardwood and softwood is a classification based on the anatomical structure and not on the mechanical properties.

2.4 Moisture Content

The reason why wood reacts on water is because of its hygroscopic behaviour, see figure 2.2. Hygroscopic means that it is able to attract and hold water molecules from the surrounding air. If the surrounding moisture content is kept constant, dry wood will keep on absorbing water until it is in equilibrium with its surrounding. Without variation between inward or outward diffusion of vapour equilibrium is reached. This is called the Equilibrium Moisture Content (EMC).

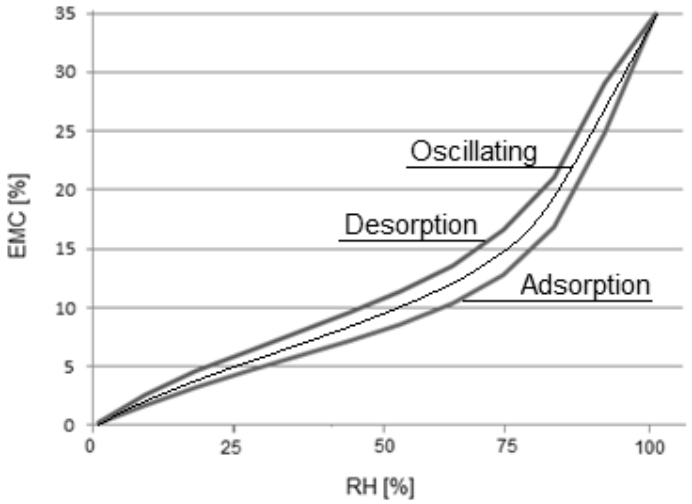

Figure 2.2: Relation between EMC and RH at a temperature of 21°C for white spruce.

The moisture content of wood is expressed according to:

$$u = \frac{m_w}{m_0} 100 \qquad (2.6)$$

u = Moisture content [%]
m_w = Mass of water in the wood sample $[kg]$
m_0 = Mass of the oven dry wood $[kg]$

The ratio between the adsorption equilibrium moisture content and desorption equilibrium moisture content of wood, is approximately constant, and has a value of about 0.85 (Friedrich, Kollmann, Côté, Kuenzi and Stamm, 1986 [19]). Figure 2.2 presents the relation between equilibrium moisture content and relative humidity when adsorption and desorption takes place. When the direction of sorption is not known, an oscillating curve between the adsorption and desorption curve maybe used, see figure 2.2. Additionally, the fact that the equilibrium moisture content varies considerably between species and even between heart and sapwood from the same species the oscillating curve can be a good approximation.

This oscillating approximation can be calculated as follows:

$$MC = \frac{1800}{W}\left[\frac{KRH}{1-KRH} + \frac{K_1 KRH + 2K_1 K_2 K^2 RH^2}{1 + K_1 KRH + K_1 K_2 K^2 RH^2}\right] \qquad (2.7)$$

W = $345 + 1.29T + 0.0135T^2$

K = $0.805 + 0.000736T - 0.00000273T^2$

K_1 = $6.27 - 0.00938T - 0.000303T^2$

K_2 = $1.19 - 0.0407T - 0.000293T^2$

T = temperature [°C]

Wood holds water in two different ways; water can be bound in the cell wall or be free. Bound water is the water that is in the cell wall and chemically bound, see figure 2.3.

Free water is water that fills the wood cavities. As wood dries, firstly the free water in the cavities evaporates. Evaporation of the free water has no effect on strength or dimension of the wood. If the drying continues, the bound water will be released from the cell wall, which leads to the deformation of the cell wall and eventually to the deformation of the wood.

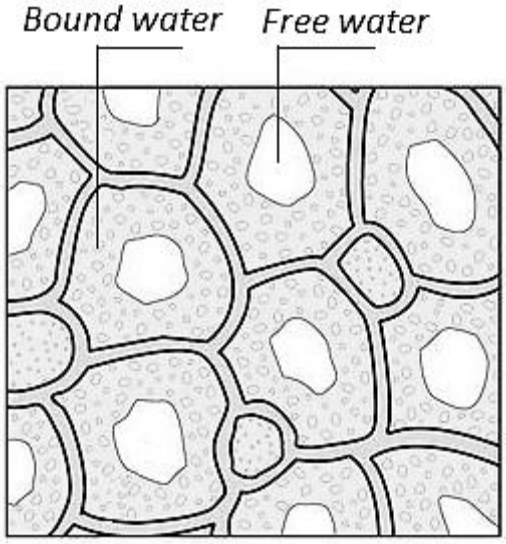

Figure 2.3: Bound and free water (www.workshopcompanion.com).

For low density wood species, generally, at the 27-30% moisture content and above, there is free water present in the cavities. The point where all the free water in the cavities has evaporated during desorption is called the Fibre Saturation Point; generally this is not an exact point but a range.

The moisture content below the fibre saturation point is a function of both the relative humidity and the temperature of the surrounding air, see Friedrich, Kollmann, Côté, Kuenzi and Stamm 1986 [19], Bratasz, Koslowski, Kozlowska and Rachwal 2006 [17] and Astrup, Hansen, Hoffmeyer and Damkilde [15].

2.5 Hygroscopicity

Wood is a hygroscopic material; *perhaps it is more descriptive that the cell walls of wood are hygroscopic*. Wood is able to absorb and desorb bound water in the cell wall with respect to the moisture content of the surrounding atmosphere. Figure 2.2 represents this hysteretic effect for white spruce. The figure represents the relation between the environmental relative humidity and the moisture equilibrium content of wood at T = 21 °C. For clarity, equilibrium moisture content means that there is equilibrium between the air moisture content and the bound moisture in the wood. This definition of equilibrium moisture content explains why the range of equilibrium moisture content increases from 0% until 31 – 35% as this is the generally Fibre Saturation Point of wood (white spruce FSP ~ 30%, mahogany FSP ~ 22-24%, beech or birch FSP ~ 32-34%).

2.6 Hygro-expansion

The volumetric shrinkage depends linearly upon the moisture content; see equations (2.8) and (2.9). Figure 2.4 shows the relation between volumetric shrinkage and the moisture content. The higher the density of the wood specimen, the larger is its volumetric shrinkage or swelling.

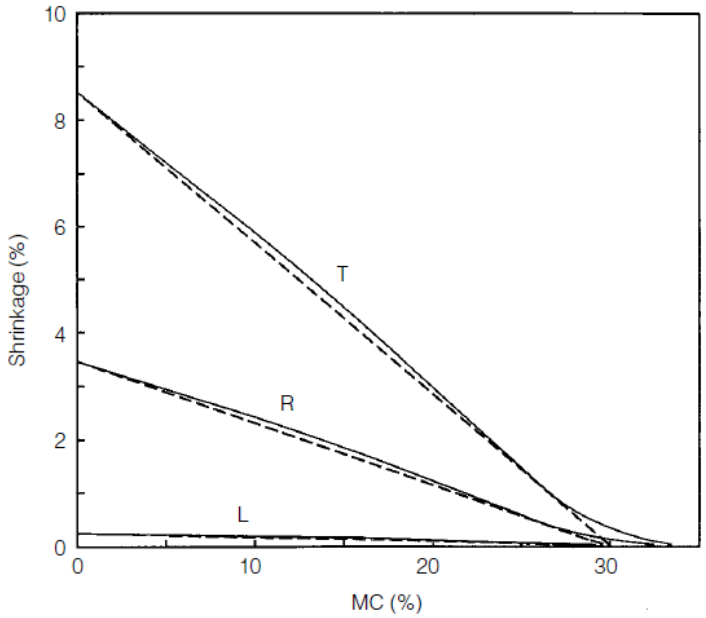

Figure 2.4: Relation between moisture content (MC) and volumetric shrinkage in the longitudinal (L), radial (R) and tangential (T) direction (solid line) and the linearized relation (dotted line) (C. Eckelman).

$$\alpha_v = u_f \rho_0 \qquad (2.8)$$

$$\beta_v = u_f R_g \qquad (2.9)$$

α_v = Volumetric swelling [%]
β_v = Volumetric shrinkage [%]
u_f = Moisture content at FSP [%]
ρ_0 = Oven dry density [kg/m^3]
R_g = Swollen volume density [kg/m^3]

Referring to figure 2.4, this linearity can be extrapolated towards the horizontal axis, at which the moisture content becomes 28 for white spruce, which is close to the average fibre saturation point. The volumetric coefficients of shrinkage and swelling can be computed from the tangential, radial and longitudinal components as the following equations show:

$$\beta_v = 1-(1-\beta_t)(1-\beta_r)(1-\beta_L) \qquad (2.10)$$

$$\alpha_v = (1+\alpha_t)(1+\alpha_r)(1+\alpha_L)-1 \qquad (2.11)$$

β_t, α_t = Tangential volumetric shrinkage/swelling coefficient [-]
β_r, α_r = Radial volumetric shrinkage/swelling coefficient [-]
β_L, α_L = Longitudinal volumetric shrinkage/swelling coefficient [-]

Neglecting the longitudinal effect, the small products of shrinkage and swelling coefficients, equation (2.10) and (2.11) can be simplified into:

$$\beta_v \approx \beta_t + \beta_r \qquad (2.12)$$

$$\alpha_v \approx \alpha_t + \alpha_r \qquad (2.13)$$

Unequal distributed change of moisture content induces strain in the wood, which can be referred to as moisture induced strain. This strain can be computed as:

$$\vec{\varepsilon}_u = \vec{\alpha}\,\Delta u \qquad (2.14)$$

ε_u = Moisture induced strain $[-]$
α = Hygro-expansional coefficients (swelling)[-]
Δu = Change of moisture content below the fibre saturation point $[\%]$

$$\alpha = \begin{bmatrix} \alpha_L \\ \alpha_T \\ \alpha_R \\ \gamma_0 \\ \gamma_0 \\ \gamma_0 \end{bmatrix} \qquad (2.15)$$

γ_0 = Shear strain of the hygro-expansion coefficient [-]

The vectors above refer to the longitudinal (L), tangential (T) and radial (R) directions of the wood cell structure, known as the principal directions.

The maximum hygro-expansion coefficients are calculated according to:

$$\alpha_{max} = \frac{a_{max} - a_{min}}{a_{min}} \cdot 100\% \qquad \text{Swelling} \qquad (2.16)$$

$$\beta_{max} = \frac{\beta_{max} - \beta_{min}}{\beta_{max}} \cdot 100\% \qquad \text{Shrinkage} \qquad (2.17)$$

a_{max} = Dimension of specimen at or above fibre saturation point [mm]
a_{min} = Dimension of specimen at the oven dry condition [mm]
β_{max} = Dimension of specimen at or below fibre saturation point [mm]
β_{min} = Dimension of specimen at the oven dry condition [mm]

The vector of the hygro-expansional coefficients contains the longitudinal, radial and tangential coefficients. The longitudinal direction will be ignored. The ratio between the tangential and the radial directions is approximately two.

In general the hygro-expansion coefficients can be measured in Cartesian directions (X,Y) with hygro-expansion coefficients (α_X, α_Y) other than the principal axes (R,T) with hygro-expansion coefficients (α_R, α_T), see figure 2.5. The hygro-expansion coefficients must be transformed with the help of Mohr's circle, see figure 2.6.

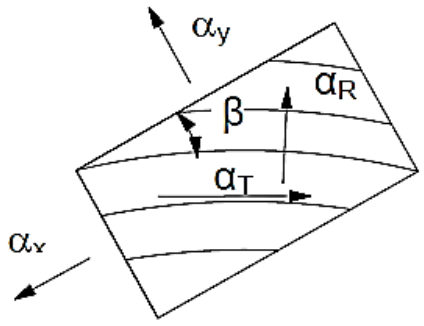

Figure 2.5: Cutting plane and principal directions.

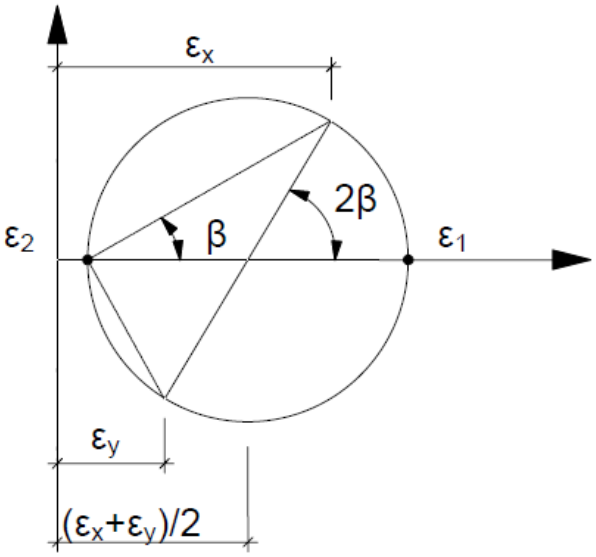

Figure 2.6: Mohr's circle for strain transformation (shrinkage).

Figure 2.6 illustrates how to compute to principal strains using Mohr's circle. Accordingly equation (2.18) represents the radius (R) of the circle and equations (2.19) reflect the principal strains, ε_1 and ε_2.

$$R = \frac{\varepsilon_x - \varepsilon_y}{2\cos(2\beta)} \tag{2.18}$$

$$\varepsilon_1, \varepsilon_2 = \frac{\varepsilon_x + \varepsilon_y}{2} + \frac{\varepsilon_x - \varepsilon_y}{2\cos(2\beta)} \tag{2.19}$$

Substitution of the strains by the hygro-expansion coefficients results in:

$$\alpha_R = \frac{\alpha_x + \alpha_y}{2} - \frac{\alpha_x - \alpha_y}{2\cos(2\beta)} \tag{2.20}$$

$$\alpha_T = \frac{\alpha_x + \alpha_y}{2} + \frac{\alpha_x - \alpha_y}{2\cos(2\beta)} \tag{2.21}$$

α_x, α_y = Hygro-expansion coefficients in x- and y- direction [-]

α_R, α_T = Hygro-expansion coefficients in the R- and T- direction of the wood cell structure [-]

2.7 Shrinking and swelling in different directions

Water is found bound and free in wood. Shrinking of wood happens when the free water has already been evaporated and the chemically bound water in the cell wall reduces (below fibre saturation point). Evaporation of the chemically bound water in the cell wall causes the lignin-hemicellulose matrix to shrink and the micro fibrils to become packed more closely. Because the outer part dries quicker than the inner part, a difference in shrinkage, resulting in tension perpendicular to the grain between the outer and inner parts occurs which causes cracking, see figure 2.7. The quantity of shrinking is proportional to the loss of moisture below the saturation point. If 1 % moisture below the fibre saturation point is lost, the wood shrinks one-thirtieth of the total possible shrinkage, see Eckelman 2000 [14], Friedrich, Kollmann, Cote, Kuenzi and Stamm 1986 [19], as indicated by figure 2.4.

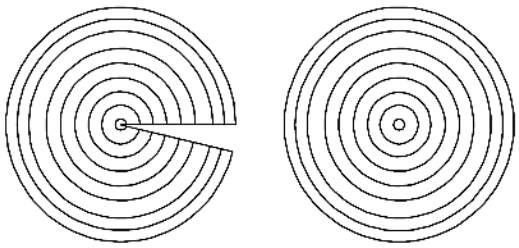

Figure 2.7: Cracking parallel to the grain (C. Eckelman [14]).

2.8 Shrinking and swelling in relation to the grain direction

It is known that there is a difference between tangential and radial shrinkage, see figure 2.4, and that cracks can develop when wood dries, see figure 2.7. There is more than one reason for this behaviour. The most important reasons and influence factors can be explained as follows: Different wood species have different properties, and show different shrinking and swelling behaviour. One thing is always the same for all species: wood shrinks the most in the tangential direction, about two times more than in the radial direction, see figure 2.4. Swelling in the longitudinal direction is small and is usually ignored (general 0.1%-0.2%).

The difference between shrinkage in the tangential en radial directions causes characteristic splitting of the log section as shown in figure 2.7. The split which is the result of these differences in shrinking occurs usually along a ray. Rays are supposed to have a constraining effect in the radial direction. Because of the structure of wood, rays differ between wood species. Consequentially the influence of the rays differs among wood species.

Figure 2.8 [14] shows the effect on shrinking for different grain oriented wood pieces, according to Bratasz,Koslowski, Kozlowska and Rachwal 2000 [17].

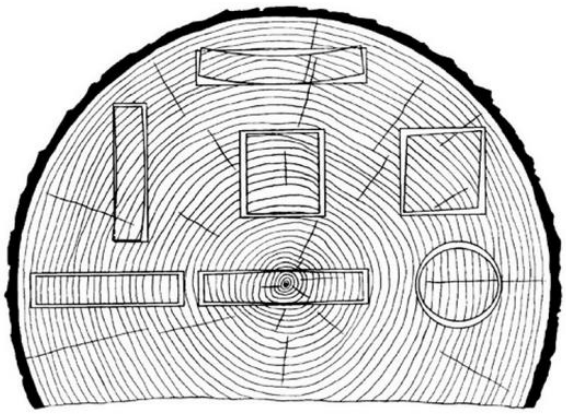

Figure 2.8: The effect on shrinking and swelling
Depending on the grain orientation (C. Eckelman [14]).

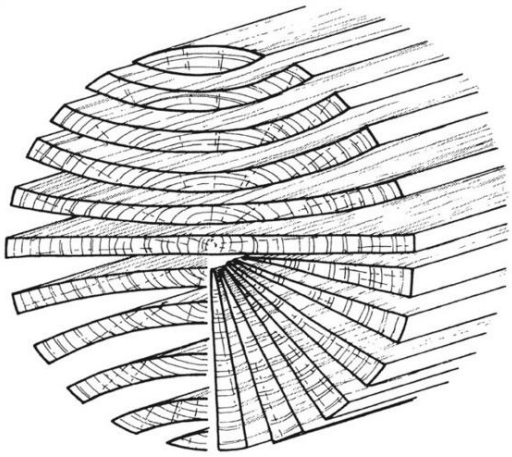

Figure 2.9: Flat sawn planks and radial sawn planks (C. Eckelman [14]).

The mechanical constraint caused by a frame around a panel painting can induce stresses in the panel with all possible consequences. Generally, wood can sustain 0.5% to 1.0% deformation in the elastic region. Values above this limit induce plastic deformation. When a panel deforms because of changing moisture content due to environmental fluctuations, these stresses can cause cupping of the planks in the panel, or warping (cupping) of the whole panel, including the frame. Another cause for cupping can be non-uniform moisture diffusion due to applied coatings. The last important source for cupping of panel paintings is the direction of the grain or growth-ring. Quarter sawn planks (this is radially sawn) stay flat when the moisture content changes, see figure 2.9. Flat sawn planks will cup with a changing moisture content.

More information about warping, cupping, crook, bow and twist deformation, see chapter 10.

3 Stress-strain, creep and creep recovery behaviour

3.1 Elasticity

Elasticity is the property of a material to recover its initial state after removing the load. All materials have a certain limit of stress for which lower stresses belong to elastic behaviour and above this limit to plastic behaviour. Plasticity is the property of a material that does not recover its initial state after unloading. When a material is loaded above this plastic limit, no more stress can be taken by the material. Rather different than steel, the elastic limit of wood is an arbitrary concept. When small elastic deformations are imposed for a period of time, the elastic deformations can turn into plastic deformations. When the moisture content (MC) in the wood is higher than the fibre saturation point (FSP), the moisture content is assumed to have no influence on the moduli of elasticity, shear moduli and Poisson's ratio. If the moisture content is under the fibre saturation point it is assumed that the moduli of elasticity, shear and Poisson's ratio are effected by the moisture, as well by temperature. Furthermore, the moduli of elasticity, shear and Poisson's ratio differ between different species of wood; see Kollmann and Cote [2].

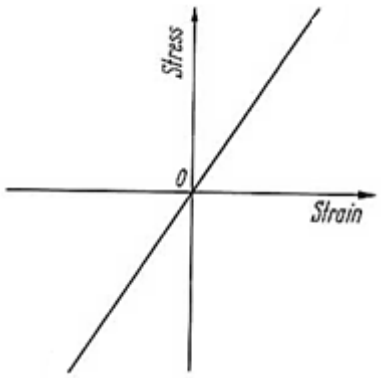

Figure 3.1: Ideal linear elastic behaviour (Kollmann F., Cote W 1968).

3.2 Stress-strain behaviour

For such a complicated material as wood, one should not expect ideal elastic behaviour, as described by Hooke's law, see figure 3.1. The stress-strain diagram is therefore not the same as for an ideal elastic body. Ideally behaving materials seem hard to be found in nature, but a material like rubber approaches this behaviour quite well. It is important to note that the stress-strain curve for an ideal elastic body does not need to be straight line, but the strain must be completely reversible. For example; vulcanized Hevea rubber is stretched at 20°C to a 700% elongation, the stress-strain curve will look like figure 3.2. When volcanic Hevea rubber is stretched within the elastic region and subjected to a cycle of loading and unloading, this can be carried out without energy loss due to the fact that the permanent deformation is ignorable. At any stage of deformation within the elastic region, after unloading the deformation will revert back to the initial state, see Kollmann and Cote [2].

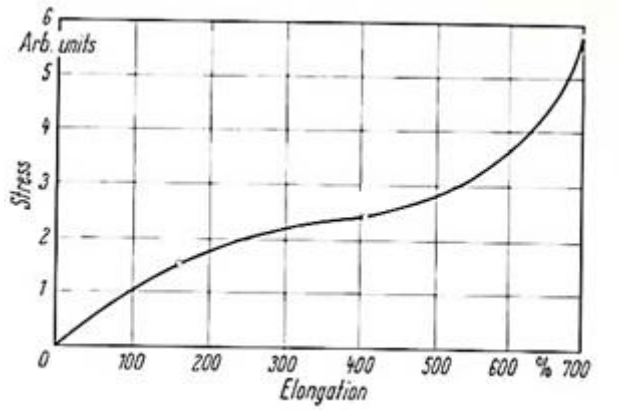

Figure 3.2: Stress-strain curve of vulcanized Hevea rubber (Kollmann F., Cote W 1968).

If the same strain cycle is applied to an elastic-plastic material like wood, the outcome will not be ideal as with volcanic Hevea rubber, see figure 3.3. Loading wood from O – A' followed by unloading will lead to permanent deformation of O – B'. In order to recover this permanent deformation a stress of O – C' in the compression direction must be applied. Compression with a magnitude of O – C' will lead to the stress-strain curve B' – C'. Compression to the absolute maximum will lead to a stress-strain curve C' – D' and removal of the compressive load will lead to curve D' – E' , resulting in the negative permanent deformation E' – O. By increasing the load stress-strain curve E' – F' will occur, making the loop compleet, see Kollmann and Cote [2].

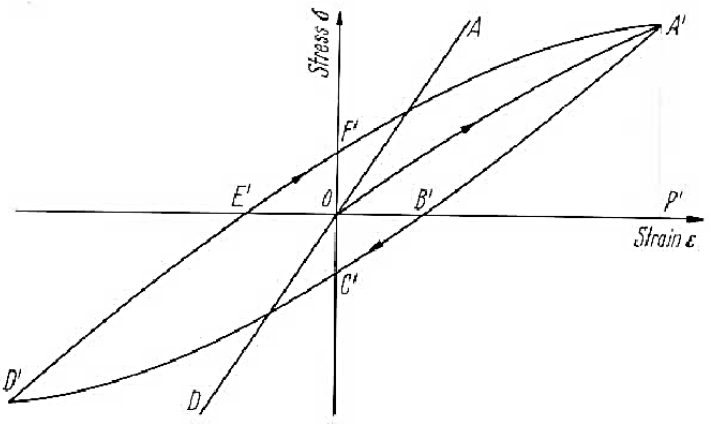

Figure 3.3: Stress-strain curve for wood (Kollmann F., Cote W 1968).

Applying cyclical stress only in one direction, depending on the stress level, the permanent deformation will be increased with each cycle, see figure 3.4. Alternatively, the stress strain-curves can approach an ideal elastic behaviour with increasing load cycles, see figure 3.5.

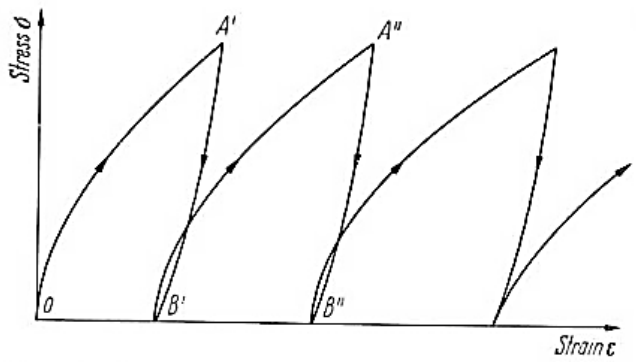

Figure 3.4: Stress-strain cycles for repeated loading and unloading with increasing plasticity (Kollmann F., Cote W 1968).

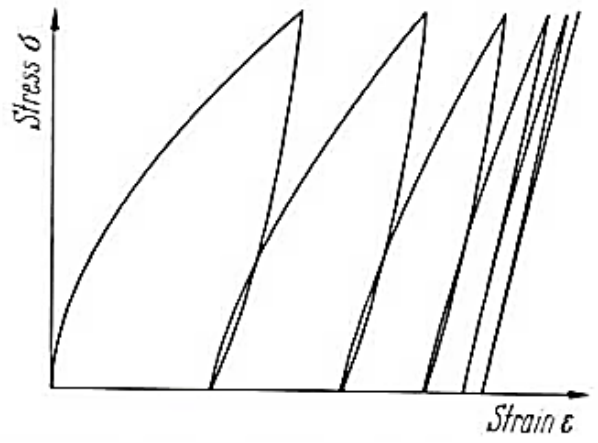

Figure 3.5: Stress-strain cycles for repeated loading and unloading with increasing approach to the ideal elastic behaviour (Kollmann F., Cote W 1968).

3.3 Creep and creep recovery

Increasing deformation when stressed at an equal level is called creep. It occurs as a result of long term exposure to stresses that are below the yield strength of the material.

If a stress is applied at t = 0 there is an instantaneous elastic deformation O – A, see figure 3.6. This instantaneous deformation is followed by a retarded deformation called creep A – B. Along the curve A – B the stress is held at a constant level. When at $t = t_1$ the initial stress is removed, an instantaneous elastic recovery appears, B – C1. This instantaneous elastic recovery is followed by creep recovery, C1 – C2. The recovery after D is very small and can be neglected so the permanent deformation is D – E.

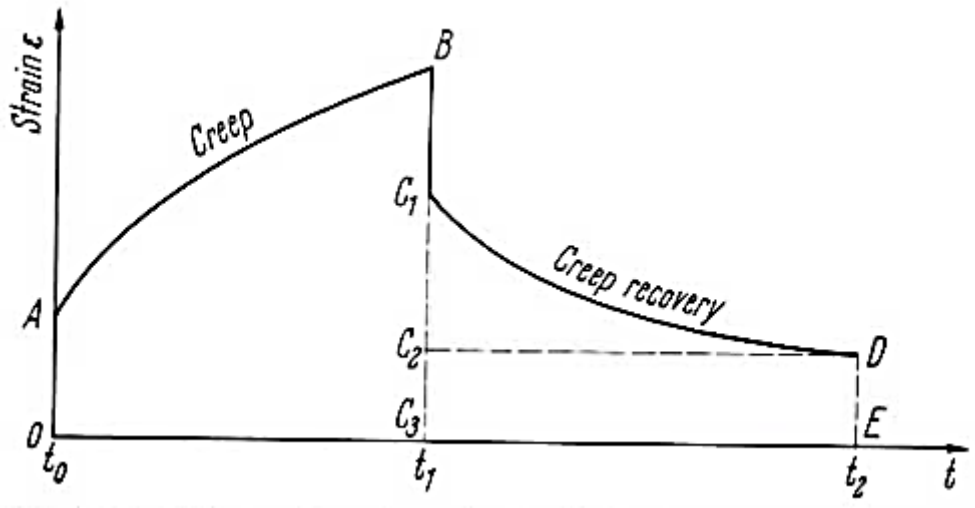

Figure 3.6: Creep and creep recovery (Kollmann F., Cote W 1968).

The creep A – B consists of two components. The first one is an elastic creep C1 – C2. This is the primary creep. The non-recoverable component C2 – C3 is called the secondary creep which is permanent deformation, see Kollmann and Cote, (1968) [2].

4 Local coordinate system

4.1 Wood structure

The macrostructure of wood is formed by concentric annual rings, called growth rings, see figure 1.1. Beside the growth ring orientation also the conical shape of the tree and the spiral grain orientation play an important role. A good constitutive model contains all these components.

4.2 Cylindrical coordinate system

Local coordinate systems are often aligned with the material axes in a structure. Because of the concentric growth a cylindrical coordinate system is generally used to model wood, see figure 4.1. The pattern used in the sawmilling process determines the position of the pith. The mechanical response of sawn timber depends on the position of the pith (material central axis). During the drying process of sawn timber, the orientation of the pith influences the deformation, see chapter 9. When modelling the drying process of wood, these material orientations and the position of the pith have to be considered in the model.

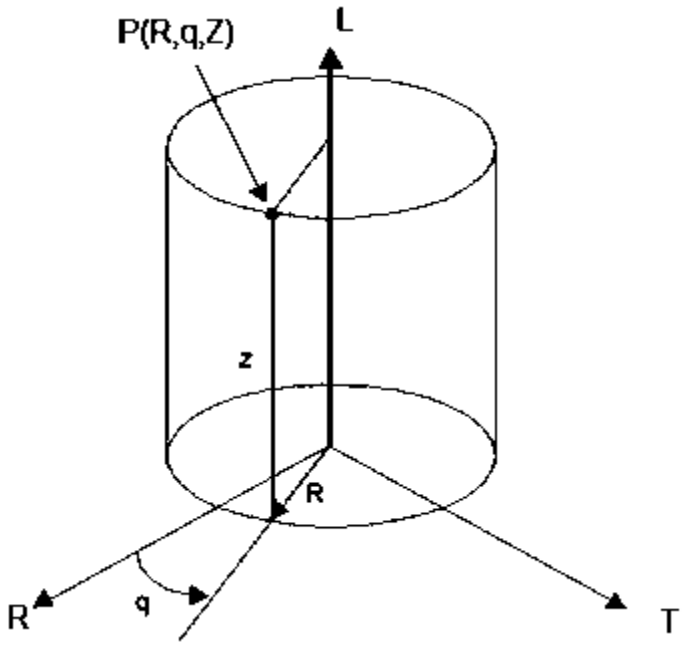

Figure 4.1: Cylindrical coordinate system, radial (R), tangential (T) and longitudinal (L) (manual Solid Work).

When a user defines a local coordinate system in ABAQUS, the axes are indicated by X, Y, Z (standard rectangular Cartesian coordinate system), X', Y', Z' (transformed rectangular Cartesian coordinate system) and R, T, Z (cylindrical coordinate system).

Generally a local cylindrical coordinate system is assumed to be capable of simulating the orthotropic behaviour due to the growth ring orientation. This is doubtful because of the following reasons. By inserting a coordinate system by default, being Cartesian or cylindrical, it is always assumed that the directional properties are perpendicular to each other. Because of the spiral grain orientation, this would be impossible with respect to the radial and tangential direction. By applying a default coordinate system it is assumed that the mechanical behaviour in each direction can be regarded to be independent of the distance from the pith or the longitudinal direction. It has been experientially observed that the longitudinal moduli of elasticity, the longitudinal moisture expansion coefficient and elastic strain parameter vary from pith to bark.

4.3 Defining a cylindrical coordinate system in ABAQUS

Within ABAQUS CAE, the global coordinate system is the default material coordinate system. The user can choose between several local systems. The coordinate system can be rectangular, cylindrical or spherical.

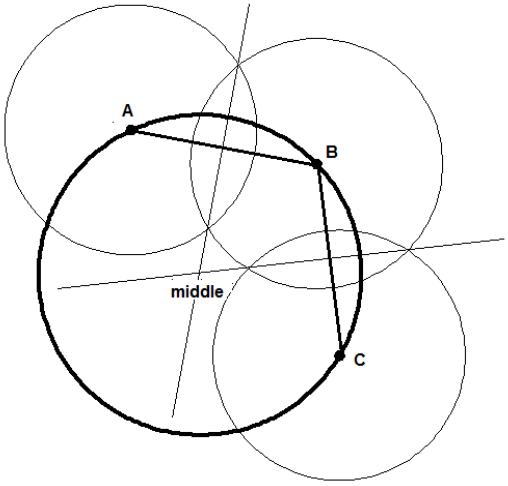

Figure 4.2: Graphical determination of pith.

In case of modelling sawn timber, it is possible to assign the origin of the local coordinate system in a logical fashion; this origin is called the pith, see figure 4.2. For example, in case of a plank coming from a panel painting, see figure 4.3-A, first the pith needs to be identified with the help of a plane geometry, see figure 4.2 and 4.3-B. When the pith of the tree has been identified, choose a reference point P(x,y) on the growth ring to calculate the angle (φ) between the pith and the reference point, see figure 4.3-B. Transpose (φ) to the plank edge, see figure 4.3-C. Now the origin of the local coordinate system from the plank is known o(x,y), see figure 4.3-D.

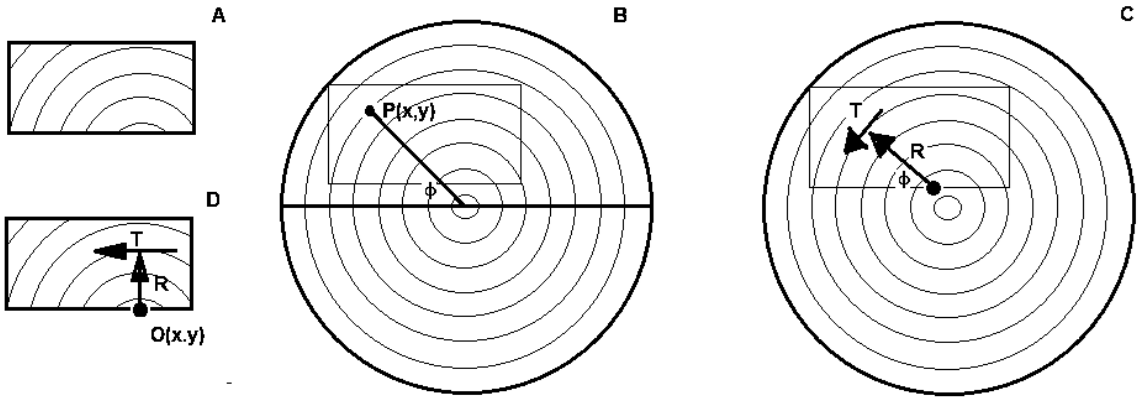

Figure 4.3: Graphical determination of coordinate system origin.

Figure 4.5 and figure 4.6 are examples of cylindrical coordinate systems used for the material orientation in a wood system and a plank system.

This spiral orientation is related to the entire system and not to individual axes. The ease to model a spiral grain orientation depends strongly upon the dimensional properties of the model (wood board). Applying a spiral grain orientation to a three-dimensional wooden cylinder taken from the heart is much more complicated than modelling sawn timber. Because within sawn timber the spiral grain orientation is cut through, it is no real spiral anymore and easy to model, see figure 4.4.

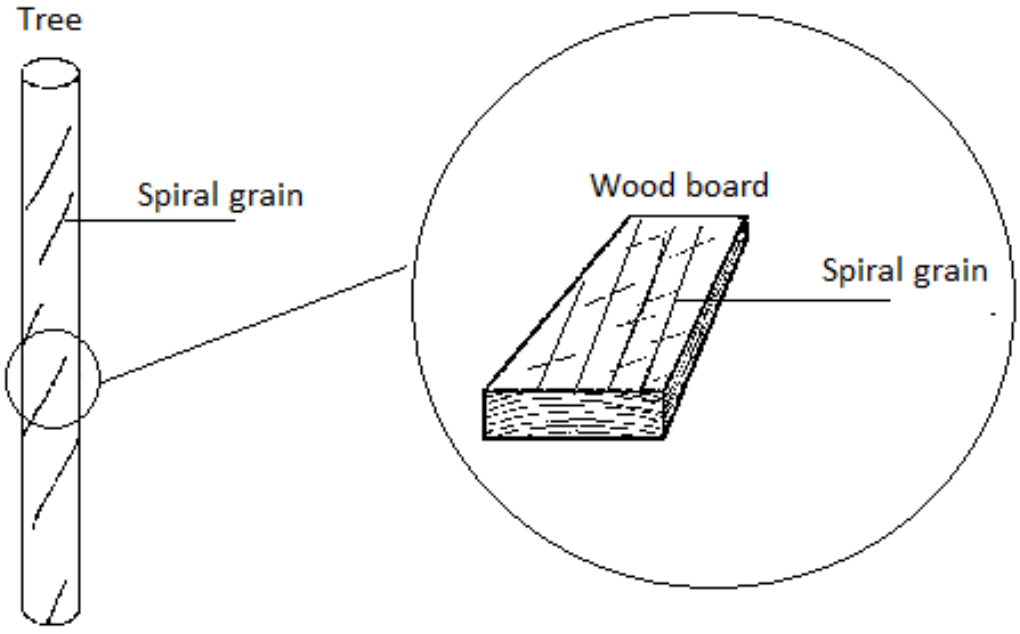

Figure 4.4: Spiral grain from tree to wood board

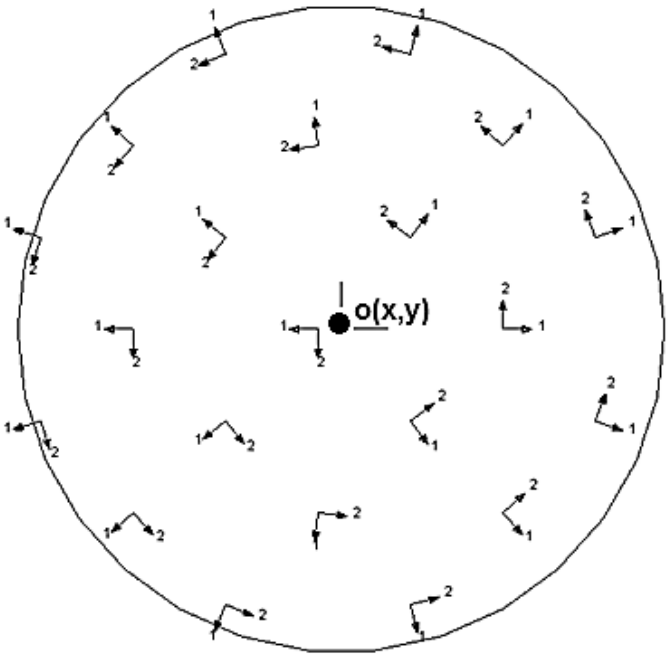

Figure 4.6: ABAQUS cylindrical coordinate system, wood model.

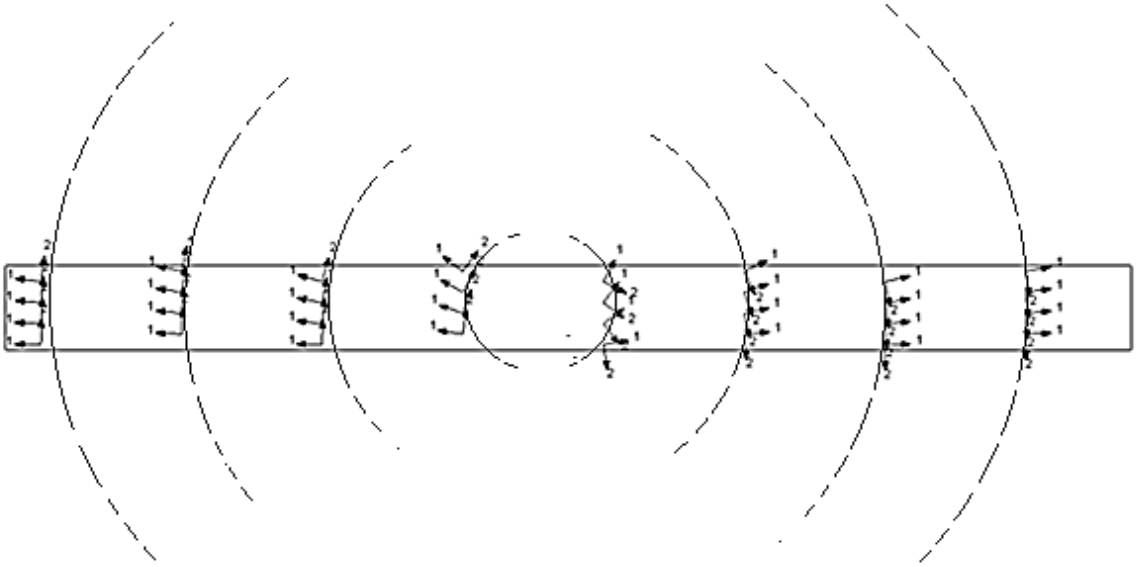

Figure 4.6: ABAQUS cylindrical coordinate system, plank model.

5 Energy and mass transport

5.1 Introduction

From a physical viewpoint, there are several transport phenomena that occur in nature, namely conduction, convection, radiation and diffusion. These transport phenomena concern the exchange of mass (water molecules), energy (heat) and momentum (force) within systems. These transport quantities vary greatly.

Heat transfer and mass transfer are, from an engineering viewpoint, among the most common transport phenomena. Heat transfer concerns conversion and exchange of thermal energy and heat between physical systems. Thermal energy can be defined as part of the total internal energy within a thermodynamic system that results in the system temperature. Heat can be defined as the energy transferred from one thermodynamic system to another by interaction. Heat transfer can be divided into various mechanisms such as conduction, convection and radiation [20] [24], see the list of definitions.

Mass transfer can be defined as the net movement of mass from one location to another. Mass transfer can be divided into various mechanisms such as absorption, adsorption and evaporation (drying). Absorption and adsorption are different phenomena, but both involve transfer of mass.

From an engineering viewpoint, the physical process of mass transfer is known as convective transport. Diffusion is energy transport without bulk motion and differs from convection, which uses bulk motion to move particles from one place to another. Diffusion is the tendency of particles to spread out due to kinetic energy and distribute evenly throughout a volume [21] [22].

The energy transport phenomenon is grounded in two primary concepts: conservation laws and constitutive equations. Conservation laws are formulated as continuity equations, describing the transport of a conserved quantity, such as mass, energy and momentum. Constitutive equations describe the response of that material to external influences. These external influences can be forces or field variables. A good example is Fourier's law of heat conduction, describing the response of heat flux to the temperature gradient:

$$\vec{q} = -k\vec{\nabla}T \qquad (5.1)$$

$\vec{q}$ = Heat flux $[W \cdot m^{-1}]$

k = Conductivity of the material $[W \cdot m^{-1}K^{-1}]$

$\vec{\nabla}T$ = Temperature gradient $[K]$

Almost all physical transport phenomena involve a system which seeks for the lowest energy state (the principle of minimum potential energy). These systems always seek a true thermodynamic equilibrium. When thermal equilibrium has been reached and there is no gradient, the transport stops and has reached equilibrium. All transport systems seek their own equilibrium. A heat transfer system seeks thermal equilibrium.

Two transport phenomena will be discussed: heat conduction (energy transfer) and molecular diffusion (mass transfer). There is a strong similarity between these two transport phenomena. Both transport phenomena are driven by diffusion. In case of heat conduction this is called heat diffusion and in case of mass transfer this is called mass diffusion. This similarity becomes clear when one compares Fourier's law of heat conduction (5.2) and Fick's law of molecular diffusion (5.3) [21] [22], which in a one-dimensional form read:

$$q_x = -k\frac{dT}{dx} \qquad \textit{Fourier's law of heat conduction} \qquad (5.2)$$

$$J_x = -D\frac{\partial \phi}{\partial x} \qquad \textit{Fick's law of molecular diffusion} \qquad (5.3)$$

q_x = Heat flux $[W \cdot m^{-1}]$
k = Thermal conductivity $[W \cdot m^{-1}K^{-1}]$
T = Temperature $[K]$

J_x = Diffusion flux $[mol \cdot m^{-1}s^{-1}]$
D = Diffusion coefficient $[m \cdot s^{-1}]$
ϕ = Concentration $[mol \cdot m^{-3}]$

5.2 Mass transfer

Between two systems, whose concentration differ, there is a natural tendency for mass transfer. Due to mass transfer, both systems seek equilibrium, minimizing the difference in concentration. A method for modelling mass transfer is given by Fick's law, equation 5.3.

Adolf Fick (1829 – 1901) was a German Physicist and physiologist. He introduced his law of diffusion in 1855. Fick's first law of diffusion (5.3) relates the diffusive flux to the concentration in steady state conditions. Systems in steady state conditions contain properties that are not time dependent. For any property P, the partial derivative with respect to time equals zero, equation (5.4) [21] [22].

$$\frac{dP}{dt} = 0 \qquad \textit{Steady state} \qquad (5.4)$$

Fick's first law (5.3) describes the flow or flux from regions of high concentration to regions of low concentration. The magnitude of this flux is proportional to the spatial gradient of the concentration.

$$\frac{\partial \phi}{\partial x} \quad = \text{Driving force behind the process}$$

Equation (5.3) describes molecular diffusion in one dimension. In two or more dimensions, Fick's first law of diffusion can be written with help of a gradient operator ∇ :

$$\vec{J} = -D\vec{\nabla}\phi \qquad (5.5)$$

$$\vec{\nabla}\phi = \left(\frac{\partial \phi}{\partial x}, \frac{\partial \phi}{\partial y}, \frac{\partial \phi}{\partial z}\right) \quad \textit{Three dimensional gradient operator} \qquad (5.6)$$

Fick's first Law of diffusion is only valid when no change in diffusion concentration takes place. Because the diffusion concentration commonly changes over time, physical properties change over time. For this reason, a "non-steady-state" or "transient" diffusion law is needed. This law is provided by Fick's second Law (5.7), see appendix A: Derivation of Fick's second law.

$$\frac{\partial \phi}{\partial t} = D\left(\frac{\partial^2 \phi}{\partial x^2}\right) \qquad (5.7)$$

In the case of two or more dimensions:

$$\frac{\partial \phi}{\partial t} = D\vec{\nabla}^2 \phi \qquad (5.8)$$

$$\vec{\nabla}^2 = \left(\frac{\partial^2 \phi}{\partial x^2} + \frac{\partial^2 \phi}{\partial y^2} + \frac{\partial^2 \phi}{\partial z^2}\right) \qquad \textit{Laplace operator}$$

5.3 Heat conduction

The concept of heat transfer starts with the famous English scientist Sir Isaac Newton (1643 - 1723). Isaac Newton wrote in his 1701 paper entitled "Scala Graduum Caloris" his specific ideas about heat convection and presented what is nowadays known as Newton's law of cooling: equation (5.9). In his paper, Newton uses the "caloric" theory, developed by the French chemist Antoine Lavoisier (1743 – 1794) to explain the transfer of heat. Lavoisier proposed that caloric was a tasteless, odourless, massless, and colourless substance which flows from one body into another and the loss of caloric substance would equal the increased or lost temperature. This is the reason why Newton's law of cooling uses bulk motion to calculate loss and increasing temperature. It seems logical that the caloric theory was never fully accepted and later proven to be wrong, because the theory essentially states that heat could not be created or destroyed. If one rubs his hands together it becomes clear to him this is not the case and heat can be generated. Benjamin Thompson (1753 – 1814) developed the idea that heat was generated by friction which is a form of motion. Benjamin Thompson's ideas were not immediately accepted but did help to establish the law of conservation of energy in the 19th century. The English physicist, James P. Joule (1818 – 1889), demonstrated with his experiments the relationship between mechanical work and the nature of heat and this led to the development of the first law of thermodynamics (conservation of energy). In the 19th century, the development of the kinetic theory stated that heat or energy is generated by the random motion of atoms and molecules. This kinetic theory helped to develop the concept of conduction of heat [25].

The French mathematician and physicist, Joseph Fourier (1768 – 1830), used Newton's law of cooling to develop his law of heat convection. Newton's law of cooling suggested a relationship between the temperature difference and the amount of heat transferred. Fourier took Newton's equations and rewrote it as a convection equation. Fourier also developed the concept of heat flux and temperature gradient. Fourier used the same process to develop his law of heat conduction (5.12), also known as Fourier's law [25].

$$\frac{dQ}{dt} = \alpha A\left(T - T_A\right) \qquad \textit{Newton's law of cooling} \qquad (5.9)$$

Q = Thermal energy $[J]$

A = Surface area of body $[m^2]$

T = Temperature of object body $[K]$

T_A = Surrounding temperature $[K]$

α = Heat transfer coefficient $[W/m^2K]$

Since $Q = c_p T$, where c_p is the heat capacity, equation (5.9) becomes:

$$\frac{dT}{dt} = \frac{\alpha A}{c_p}\left(T - T_A\right) = k\left(T - T_A\right) \qquad (5.10)$$

The solution to this differential equation is:

$$T = T_A + \left(T_0 - T_A\right)\exp\left(-\alpha t\right) \qquad (5.11)$$

See appendix B: Solution to Newton's cooling equation.

Newton's law of cooling is a solution to the differential equation given by Fourier's law.

$$q_x = -k\frac{dT}{dx} \qquad \textit{Fourier's law} \qquad (5.12) = (5.1)$$

Note the similarity between Fick's law of molecular diffusion and Fourier's law of heat conduction. In case of non-steady state heat conduction, Fourier's equation becomes equation (5.13), similar to equation (5.7).

$$\frac{dT}{dt} = a\frac{\partial^2 T}{\partial x^2} \qquad (5.13)$$

With;

$$a = \frac{\lambda}{\rho c_p} \qquad (5.14)$$

a = Thermal diffusivity $[m^2 \cdot s^{-1}]$

λ = Thermal conductivity (k) $[W \cdot m^{-1}K^{-1}]$

ρ = Density $[kg \cdot m^3]$

c_p = Specific heat capacity $[J \cdot kg^{-1}K^{-1}]$

Example 1: Transient one dimensional heat conduction (appendix C)

Example 2: A temperature step at the surface of a semi-infinite thick slab (appendix D)

6 Diffusion coefficients and driving potentials

6.1 Driving potentials

Driving potentials can be defined as 'factors' potentially driving the diffusive process. Temperature, moisture content and pressure are examples of driving potentials. Because these potentials act as a driving force behind the process, they take an important place within equations describing the diffusion process. Fick's law and Fourier's law are examples of equations using driving potentials. The potentials appear in these equations as gradients. So, the gradient of the driving potential is eventually responsible for the diffusive flux. The gradient (grad.) defines the steepness of the slope of the variation of any quantity in space. From a mathematical viewpoint, the gradient can be defined as the rate of increase of a scalar field, which is a vector field.

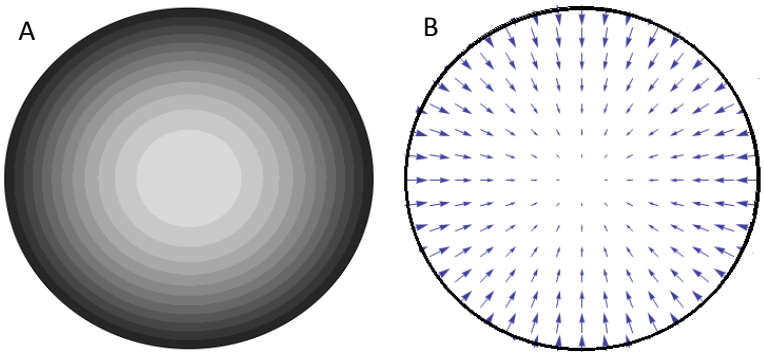

Figure 6.1: Scalar and vector field.

The gradient of f is written as: $grad\ f = \vec{\nabla} f$ $\vec{\nabla}$ = *gradient operator*

Figure 6.1-A represents a scalar field and figure 6.1-B the two dimensional vector field of this scalar field and the size of the gradient is expressed by the size of the arrows.

Formally, the gradient can be defined as the multi-dimensional derivative of f .

For example: if $f : R^3 \to R$ $\quad gradf = \vec{\nabla} f = \left(\frac{\partial f}{\partial x}, \frac{\partial f}{\partial y}, \frac{\partial f}{\partial z} \right)$

Look at Fourier's equation (6.1), and see the driving potential *T*:

$$q_x = -k\frac{\partial T}{\partial x} \qquad (6.1) = (5.2)$$

Within wood science, moisture concentration (ϕ), moisture content (u), water vapour pressure (P) and water vapour content (w) are often used as driving potential.

Table 6.1: Driving potentials and diffusion coefficients

Driving Potential	Diffusion Coefficient
Moisture concentration (C) $\phi = \frac{m_{wheight-moisture-volume}}{V_{volume}}$ $[kgm^{-3}]$	$D_\phi[m^2 s^{-1}]$
Moisture content (u) $u = \frac{m_w}{m_0}100$ [%]	$D_u[kgm^{-1}s^{-1}]$
Water vapour pressure (P) $P_w = \frac{RHP_{ws}}{100\%}$ [Pa]	$D_P[kgm^{-1}s^{-1}Pa^{-1}]$
Water vapour content (w) $w = \frac{\rho_{mass-vapour}}{\rho_{dry-air}}$ $m_{dry-air} = 1.2[kg/m^3]$ [-]	$D_w[m^2 s^{-1}]$

B. Time [27] concludes that that the chemical potential is the essential driving force for moisture transport through wood. Time states that the chemical potential results from the gradient of water vapour pressure. In other words, the chemical potential is a pushing force or driving force behind moisture transport, based upon vapour pressure gradient.

The term chemical potential seems to come from plant physiology as well as water activity and osmotic pressure. From plant physiology, the chemical potential of water can be defined as the free energy per mole of water [28]. In other words, chemical potential is the potential of a substance to do work or move something. Because work is the movement of an object due to an applied force, chemical potential is the ability to move, or diffuse a solute through a solvent. Chemical potential in the case of water is also called water potential (in plant physiology, water potential and chemical potentials are not the same). Defining the chemical potential as the ability to do work is consistent with the definition from ABAQUS.

6.2 The cup method

Different methods exist to examine and evaluate the diffusion coefficient (D) of wood. The most frequently used method is the so called "Cup method". With this method, a wood specimen is fastened on top of a cup serving as a lid, see figure 6.2. Due to the difference in relative humidity between the cup and the surrounding environment, a water vapour flow through the wooden specimen occurs. By weighing the cup at regular intervals and plotting this as a function of time, the diffusion coefficient can be found by calculating the slope of the sorption curve. If the moisture process is behaving according to Fick's law, the diffusion coefficient can be calculated from the slope of the curve.

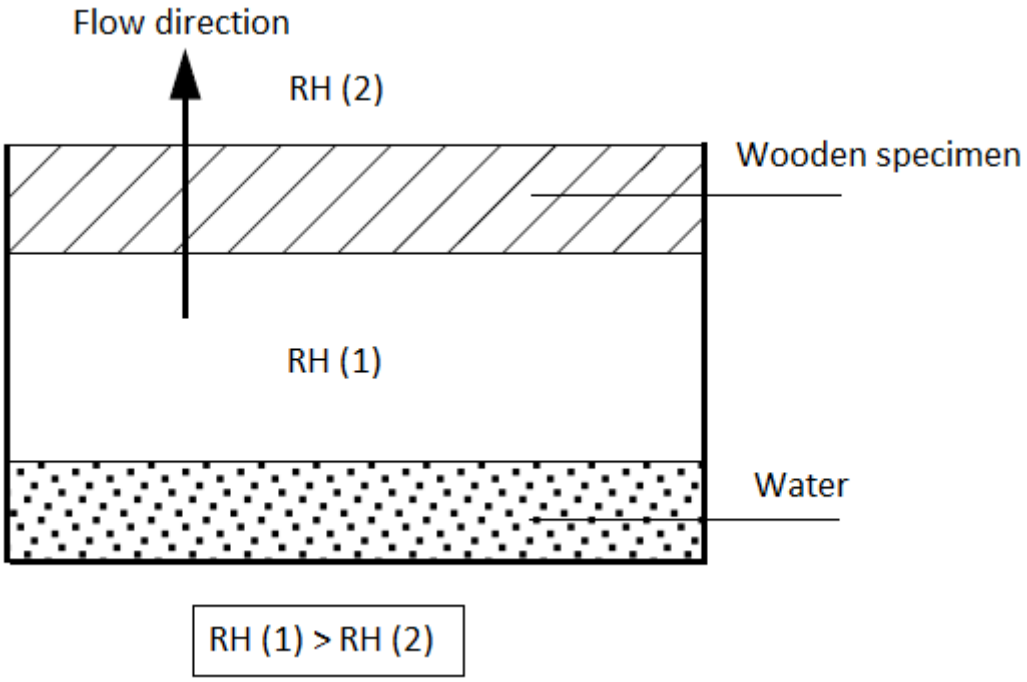

Figure 6.2: The cup method

6.3 Driving potentials and their diffusion coefficients

To calculate moisture diffusion in wood commonly, moisture concentration (ϕ) or moisture content (u) are used as driving potentials. Moisture concentration can be calculated as follows:

$$\phi = \frac{m_w}{V} \qquad (6.2)$$

ϕ = Moisture concentration $[kg \cdot m^{-3}]$
m_w = Mass $[kg]$
V = Volume $[m^3]$

Moisture content can be calculated as follows:

$$u = \frac{m_w}{m_0} 100\% \qquad (6.3) = (2.7)$$

u = Moisture content [%]
m_w = Mass of the water in the wood sample $[kg]$
m_0 = Mass of the oven dry wood $[kg]$

Moisture concentration and moisture content are essentially the same. The relation between moisture content and moisture concentration can be shown as follows:

$$m_w = \frac{um_0}{100} \qquad (6.4)$$

$$m_w = \phi V \qquad (6.5)$$

$$\frac{um_0}{100} = \phi V \qquad (6.6)$$

$$\phi = \frac{um_0}{100 \cdot V} \qquad (6.7)$$

$$\phi = u\frac{m_0}{V} \qquad (6.8)$$

$$\frac{m_0}{V} = \rho_0 \qquad (6.9)$$

ρ_0 = Wood dry density $[kg \cdot m^{-3}]$

The relation between the moisture concentration by volume and the moisture content by weight of wood:

$$\phi = u\rho_0 \qquad (6.10)$$

Wood is most often only a part of a bigger structure, consisting of many other layers and different materials as in panel paintings, see figure 6.3. Different materials show different material properties. Because of this different behaviour, it is wise to use a driving potential which is consistent for different materials. Water vapour pressure [*P*] and water vapour content [*w*] are such driving potentials.

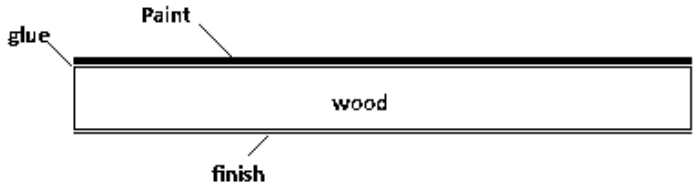

Figure 6.3: Different layers of panel painting.

The diffusion coefficient with water vapour pressure (D_P) can easily be transferred into a diffusion coefficient with water vapour content (D_V) as shown by Time [27]:

$$D_V = 461.4TD_P \qquad (6.11)$$

T = temperature in [K]

Because water vapour content (*w*) and moisture concentration (ϕ) share the same diffusion coefficient in units, see table 6.1, the above transformation can also be used to transform the pressure potential diffusion coefficient into the moisture concentration diffusion coefficient. Note that moisture concentration content [*w*] is essentially the same as equilibrium moisture content.

Table 6.2: Fick's first and second law with different diffusion coefficients.

Diffusion coefficient	First law	Second law
Diffusion coefficient with water vapour pressure	$q_X = -D_p \frac{\partial P}{\partial x}$	$\frac{\partial C}{\partial t} = D_P \cdot \frac{\partial^2 P}{\partial x^2}$
Diffusion coefficient with moisture concentration	$q_X = -D_\phi \frac{\partial \phi}{\partial x}$	$\frac{\partial \phi}{\partial t} = D_\phi \cdot \frac{\partial^2 \phi}{\partial x^2}$
Diffusion coefficient with moisture content	$q_X = -D_u \frac{\partial u}{\partial x}$	$\frac{\partial C}{\partial t} = D_u \cdot \frac{\partial^2 u}{\partial x^2}$

7 Procedures to model moisture movement using ABAQUS

ABAQUS uses Fourier's law of heat conduction to calculate heat transfer within a heat transfer analysis. ABAQUS uses an extension of Fick's law to perform a mass diffusion analysis. Due to the analogy between Fourier's equation and Fick's equation one can model mass diffusion using a heat transfer analysis and vice versa.

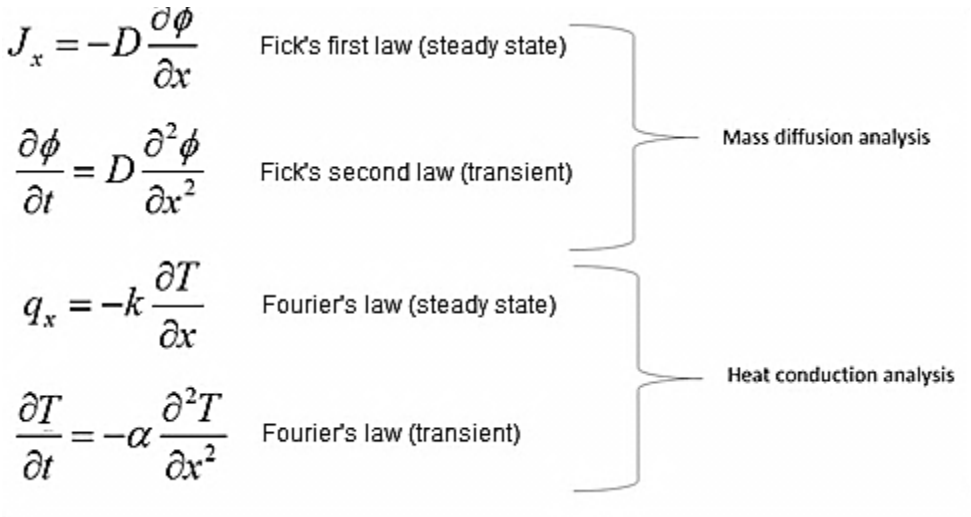

Although one can calculate mass diffusion using a transient heat transfer analysis, heat transfer analysis and mass diffusion analysis are not the same. For example, heat transfer analysis based on Fourier's law can only use a temperature gradient as the driving force behind the diffusive process. Within mass diffusion analysis other driving forces (ABAQUS calls this a chemical potentials) can control the diffusive process. Pressure, temperature and concentration are examples of field variables which can be used as driving potential.

ABAQUS has developed a strong capability over a long time to solve multi-physics problems. The advantage of ABAQUS multi-physics is the ease with which multi-physics problems can be solved. It has the ability to utilise the same model, element library, material data and load history. A single-physic analysis can easily be extended to a multi-physics analysis, without the need for additional tools, interfaces or simulation methodology.

For the specific case of modelling moisture movement through wood, the multi-physical thermal – mechanical coupling is of importance. By coupling the thermal field variables from a heat conduction analysis as a predefined field to a static stress analysis, one can easily calculate thermal expansion and thermal stress field [26].

7.1 ABAQUS uncoupled heat transfer analysis

The uncoupled heat transfer analysis is capable to model solid body heat conduction with temperature-dependent conductivity, internal energy, general convection and radiation boundary conditions. The focus of this paragraph will be heat transfer in materials due to convection/diffusion.

The basic energy balance used by ABAQUS:

"Energy balance (conservation of energy) states that the change in internal energy of a closed system is equal to the amount of heat supplied to the system, minus the quantity of work performed by the system on its surroundings, equation (7.1)".

$$\int_V \dot{U} dV = \int_S q dS + \int_V r dV \qquad (7.1)$$

V = Volume of a solid material $[m^3]$

S = Surface area of material volume $[m^2]$

$\dot{U}$ = Material time rate of internal energy (the change of internal energy in time) $[J \cdot s^{-1}]$

q = Heat flux per unit area of the material body, flowing into the body $[W \cdot m^{-2}]$

r = Heat supplied into/out of the body per unit volume; this is the work performed by the system on the surroundings $[W \cdot m^{-3}]$

The basic energy balance states that the change of internal heat energy equals the heat flux per unit area flowing into the body and the heat per unit volume flowing into the body. The heat flux per unit area flowing into the body is governed by Fourier's law of thermal conduction

The boundary conditions:

T = $T(x,t)$, prescribed temperature $[K]$

q = $q(x,t)$, prescribed surface heat flux per area $[W \cdot m^{-2}]$

r = $r(x,t)$, prescribed volumetric heat flux per volume $[W \cdot m^{-3}]$

q = $h \cdot (T - T_0)$, surface convection $[W \cdot m^{-2}]$

h = $h(x,t)$, the film coefficient $[W \cdot m^{-2} K^{-1}]$

$(T - T_0)$ = difference between inside and outside temperature (sink temperature) $[K]$

ABAQUS can solve the following types of heat transfer problems:

Uncoupled heat transfer analysis:

These are heat transfer problems involving conduction, forced convection, and boundary radiation. Uncoupled heat transfer analysis calculates the temperature field, without knowledge of stress/deformation state. This procedure solves pure heat transfer problems. These heat transfer problems can be steady state (time excluded/transient), unsteady state (time included) and linear or non-linear.

Sequentially coupled thermal-stress analysis:

When stress/displacement is dependent of a temperature field, but there is no inverse dependency, it is called a sequentially coupled thermal-stress analysis. A sequentially coupled thermal-stress analysis first solves the pure heat transfer problem, and then reads the temperature solution into a stress analysis as a predefined field. In the stress analysis, the temperature can vary with time and position, but is not changed by the stress analysis solution.

Two analyses have to be done. First a heat transfer analysis and, secondly, a thermal- stress analysis. ABAQUS allows the use of different meshes between these two models.

Fully coupled thermal-stress analysis:

A fully coupled thermal-stress analysis is used when thermal, electrical and mechanical solutions effect each other strongly. For example, spot welding is such process where thermal, electrical and mechanical solutions are strongly dependent on each other. These problems can be steady state (time excluded/transient), unsteady state (time included) and linear or nonlinear.

Adiabatic analysis:

Is used in cases where mechanical deformation causes heating, but the event is so rapid that this heat has no time to diffuse through the material an adiabatic analysis can be performed.

Coupled thermal-electrical analysis:

Is used in cases where heat is generated due to the flow of electrical current through a conductor.

Cavity radiation:

In an uncoupled heat transfer, cavity radiation can be included.

7.2 ABAQUS mass diffusion analysis

An ABAQUS mass diffusion analysis can model the transient and steady-state diffusion of one material through another. For example: hydrogen through metal. It requires the use of mass diffusion elements such as DC2D3 or DC3D4, depending on the model. ABAQUS mass diffusion analysis can be used to model temperature and pressure driven mass diffusion.

The basic solution variable is the "normalized concentration (ϕ)"also called the activity of the diffusing material. Firstly, some fundamental definitions will be explained.

Solubility:

Is the ability of a liquid (called the solute) to dissolve into a solid (called the solvent) to become a homogenous unit of solute and solvent. The solubility depends on the solute, solvent, temperature and pressure. The degree of solubility can be measured as the degree of saturation of a solvent, however the addition of more water than the solubility (or degree of saturation) will not make any difference.

In ABAQUS, the solubility of a material can be specified in the *solubility edit material dialog box*. Solubility (s) is used to define the "normalized concentration (ϕ)" of the diffused material in the diffusing phase in a mass diffusion process. Taking the solubility equal to 1, the concentration equals the normalized concentration, see equation 7.3.

Diffusivity:

In heat transfer analysis, the diffusivity of heat is called thermal diffusivity.

$$a = \frac{k}{\rho \cdot c_p} \qquad (7.2)$$

a = Thermal diffusivity $[m^2 \cdot s^{-1}]$

k = Thermal conductivity (λ) $[W \cdot m^{-1}K^{-1}]$

ρ = Density $[kg \cdot m^{-3}]$

c_p = Specific heat capacity $[J \cdot kg^{-1}K^{-1}]$

In mass transfer analysis this is called the diffusivity of mass.

Normalized concentration:

The normalized concentration of a solute diffusing with a solvent can be calculated as follows:

$$\phi = \frac{c}{s} \qquad (7.3)$$

c = Mass concentration $[kg \cdot m^{-3}]$

S = Solubility $[ppm]$

The governing equation that ABAQUS uses to calculate the diffusive flux is an extension of Fick's law of diffusion, see equation 5.3. The difference can be found in the fact that the equations used by ABAQUS allow for a non-uniform solubility of the solute (the diffusing substance) through the solvent (the base material) and for mass diffusion driven by gradients of temperature and pressure.

$$J = -sD \cdot \left[\frac{\partial \phi}{\partial x} + \kappa_s \frac{\partial}{\partial x} (\ln(T - T^Z)) + \kappa_P \frac{\partial p}{\partial x} \right] \qquad (7.4)$$

$D(c,T,f)$ = Diffusivity $[m^2 \cdot s^{-1}]$
$s(T,f)$ = Solubility $[ppm]$
$\kappa_s(C,T,f)$ = Soret factor, providing diffusion because of a temperature gradient $[-]$
T = Temperature $[K]$
T^Z = Value of the absolute zero on the temperature scale used $[-]$
$\kappa_p(C,T,f)$ = Pressure stress factor, providing diffusion, driven by the gradient of the pressure stress $[-]$
C = Concentration of the diffusing material $[kg \cdot m^{-3}]$
f = Other predefined field variables (potential) $[-]$

Fick's law of mass diffusion is a linear equation. The extended law used by ABAQUS becomes non-linear since $D(c,\theta,f), \kappa_s(c,\theta,f)$ and $\kappa_p(c,\theta,f)$ depend on the concentration.

Diffusion is assumed to be driven by the gradient of a general chemical potential. The relation between Fick's law and the general chemical potential can be found in appendix E.

To define diffusivity in ABAQUS, a law option must be selected to specify how you want to define diffusivity behaviour. The user can choose between two options:

- Select the "general law" when you want to use the general chemical potential mass diffusion:

$$J = -sD \cdot \left[\frac{\partial \phi}{\partial x} + \kappa_s \frac{\partial}{\partial x} (\ln(T - T^Z)) + \kappa_P \frac{\partial p}{\partial x} \right] \qquad (7.5)$$

- Select "Fick's law" when you want to use Fick's diffusion law:

$$J = -D \cdot \left(\frac{\partial \phi}{\partial x} + s\kappa_p \frac{\partial p}{\partial x} \right) \qquad (7.6)$$

  Note that equation (7.6) can be driven by the gradient of concentration and by the gradient of pressure.

This extended form of Fick's equation can be used as an alternative to the driving potential. The difference between the extended form of Fick's law and the driving potential equation can be found in the fact that the extended form of Fick's law automatically converts $\kappa_s(c, \theta, f)$ because $s = s(\theta)$. Thus, diffusivity is the relation between the concentration flux (J) of the diffusing material and the gradient of the chemical potential. The driving potential is that part of the diffusion equation which is responsible to drive the mass diffusion process. In other words, in case of temperature driven mass diffusion it does not really matter which procedure you choose.

Part 2: Numerical

8 Modelling isothermal moisture movement in wood, using ABAQUS transient heat conduction

8.1 Introduction

When a wooden cylinder is exposed to varying environmental conditions, especially fluctuations in the relative humidity, due to the hygroscopic behaviour of wood, moisture will transfer through the wooden cylinder. Fluctuations in these surrounding conditions, especially fluctuations in relative humidity below the fibre saturation point, result in deformation in the form of shrinking or swelling. If these deformations do not exceed the elastic range, theoretically there is no problem. Beyond this elastic range, the so called plastic range, the wooden cylinder no longer returns into the initial state after removing of the load. This is called plastic deformation. Jakiela, Bratasz and Kozlowski [37] developed a numerical model describing moisture movement due to changing environmental conditions to calculate the related stress field. This model has been applied to lime wood cylinders. Schellen and Schijndel [36] verified the work done by Jakiela, Bratasz and Kozlowski with help of a numerical COMSOL (multiphysics engineering simulation software) model.

Chapter 8 discusses the validation of the research done by Jakiela at al [37] and Schellen et al [36]. The outcome of these researches will be validated by an ABAQUS finite element model. To validate the outcome by Jakiela and Schellen, an ABAQUS transient heat conduction analysis is performed. By using a transient heat conduction analysis procedure instead of mass diffusion analysis, the possibility to apply a transient analysis procedure to model moisture transport will be examined. One of the possible great advantages of using ABAQUS CAE (Complete ABAQUS Environment) is the ease of modelling. Within the CAE, it is possible to perform a heat conduction analysis and apply the outcome as a predefined field to a static stress / strain analysis. This is a so called sequentially coupled thermal-stress analysis. A sequentially coupled thermal strain analysis can be used when stress/displacement is dependent on a temperature field but there is no inverse dependency.

The aim of chapter 8 is to model the moisture movement in a wooden cylinder in response to a step change of 70 % – 30% relative humidity, which corresponds to an equilibrium moisture change (in time) of 14 % - 6 %. These results will be used to calculate the internal stress field and evaluate the risk of damage.

Most of the material parameters are directly copied from the work done by Jakiela and Schellen et al. Missing values are taken from Time [27], de Wit [20] and [38].

* *More information about developing a constitutive model, see chapter 4.*

* *More information about analysis procedures, see chapter 7.*

8.2 Sequentially coupled multi-physics analysis

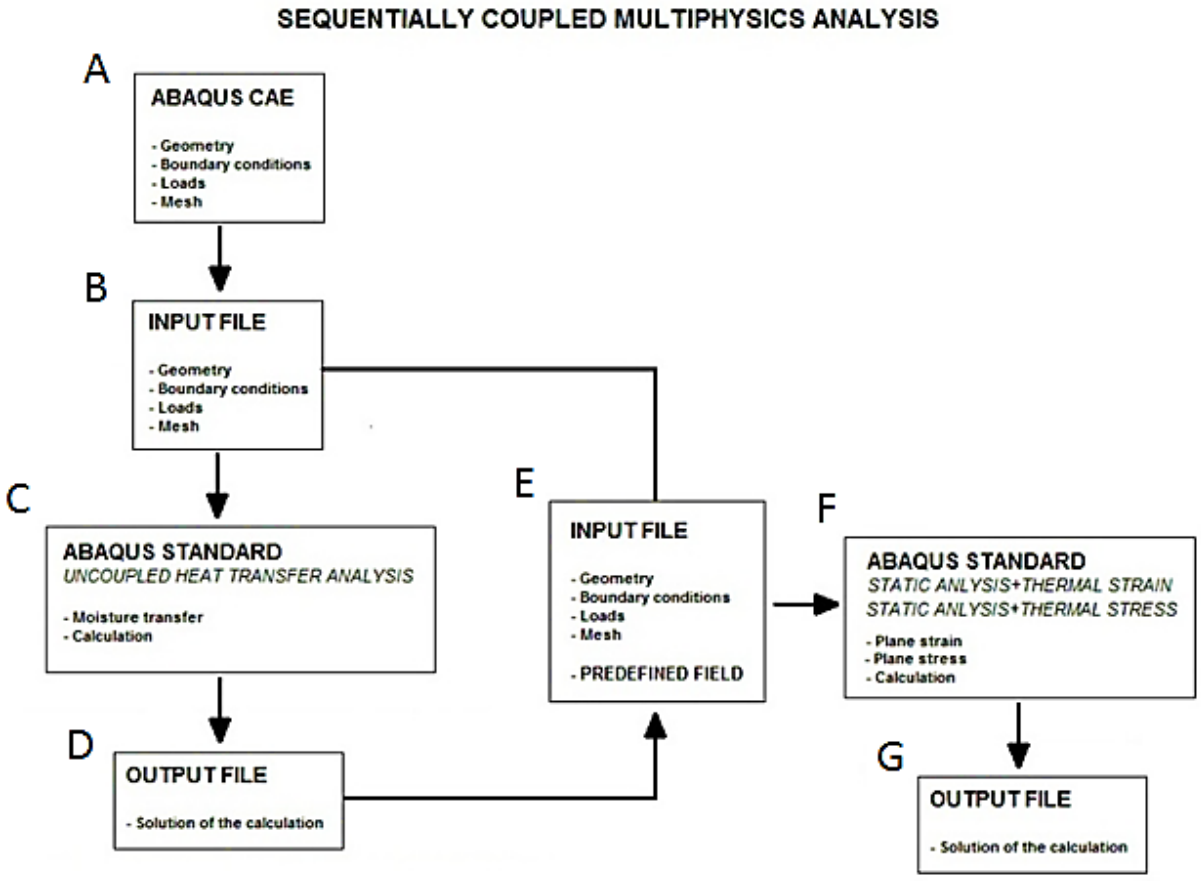

Figure 8.1: Sequentially coupled multi-physics analysis ABAQUS.

Figure 8.1 represents a stepwise scheme of the multi-physics environment.

A: In this step, the geometry of the structure will be developed, the boundary conditions will be applied, the loads will be applied and the model will be properly meshed.
B: The model from step (A) will form an input file containing all the properties as discussed in (A).
C: The input file from step (B) will be exposed to an uncoupled heat transfer analysis to determine the heat field.
D: This is the solution from step (C). This will be used as an input file for the next analysis.
E: The temperature field from the previous analysis will serve as a predefined field to calculate the corresponding strain field within a static analysis.
F: The input files from (B) and (E) will be used to perform a static analysis with thermal strain calculation.
G: The outcome from step (F), thermal stress and strain field.

8.3 ABAQUS model

Geometry:

Ø = 0.13 m lime wood, see figure 8.2.

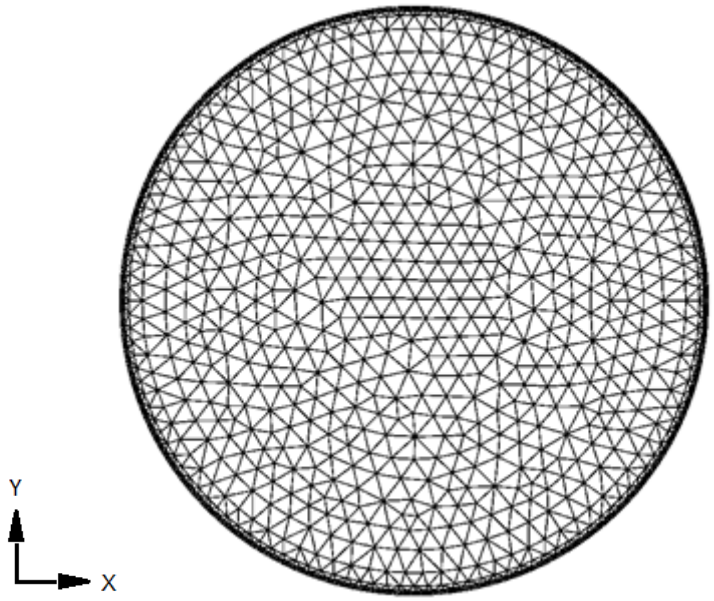

Figure 8.2: Lime wood ABAQUS model.

Hygro thermal equation:

Thermal transport within the ABAQUS model is based upon equation:

$$\rho c_p \frac{\partial T}{\partial t} = \frac{\partial}{\partial x}\left(\lambda \frac{\partial T}{\partial x}\right) \qquad (8.1)$$

Water vapour transport by diffusion is based upon equation:

$$\frac{\partial u}{\partial t} = \frac{\partial}{\partial x}\left(D_u \frac{\partial u}{\partial x}\right) \qquad (8.2)$$

Boundary conditions:

Thermal:

$$q = h \cdot (T_0 - T_S) \qquad (8.3)$$

q = heat flux at surface $[W \cdot m^2]$

h = heat transfer coefficient (7.7, based on M. de Wit) $[W \cdot m^{-2} K^{-1}]$

$$h = \frac{Q}{A \cdot \Delta T} \qquad Q \text{ = heat flow } [W]$$

T_0 = 20 °C

T_S = Surface temperature [°C]

T_∞ = 20 °C

Hygric:

$$g = \beta \cdot (u_0 - u_S) \qquad (8.4)$$

g = moisture flux at surface $[kg \cdot m^{-2} s^{-1}]$

β = moisture transfer coefficient (0.003, based on M. de Wit) [20] $[kg \cdot m^{-2} s^{-1}]$

u_0 = 14 [%]

u_S = 6[%]

t = 0 [s]

t_∞ = ∞

RH_0 = 70 [%]

RH_∞ = 30 [%]

The model surface is constraint (type: coupling) to a reference point in space. The constraint degree of freedom is UR3 (vertical movement). By coupling the surface to a reference point in space, rigid body rotation cannot take place and the model is free to move horizontal in UR1 and UR2 direction.

Material properties:

Mean dry density = 530 $[kg \cdot m^{-3}]$

Modulus of elasticity:

Table 8.1: Modulus of elasticity of lime wood (S. Jakiela [37])

RH [%]	Tangential direction [MPa]	Radial direction [MPa]
20	600	1120
35	490	900
50	450	820
65	420	770

Mechanical stress and strain:

$$\begin{pmatrix} \varepsilon_x \\ \varepsilon_y \\ \gamma_{xy} \end{pmatrix} = \begin{pmatrix} \frac{1}{E_x} & -\frac{\nu_{xy}}{E_y} & 0 \\ -\frac{\nu_{yx}}{E_x} & \frac{1}{E_y} & 0 \\ 0 & 0 & \frac{1}{G_{xy}} \end{pmatrix} \begin{pmatrix} \sigma_x \\ \sigma_y \\ \tau_{xy} \end{pmatrix} + \begin{pmatrix} \alpha_x \\ \alpha_y \\ 0 \end{pmatrix} \Delta\theta + \begin{pmatrix} \kappa_x \\ \kappa_y \\ 0 \end{pmatrix} \Delta w \qquad (8.5)$$

ε_x, ε_y = Normal strain components $[-]$

γ_{xy} = Shear strain components $[-]$

E_x, E_y = Moduli of elasticity $[N \cdot m^{-2}]$

ν_{xy}, ν_{yx} = Poisson's ratio $[-]$

G_{xy} = Shear modulus $[N \cdot m^{-2}]$

σ_x, σ_y = Normal stress components $[N \cdot m^{-2}]$

α_x, α_y = Linear thermal expansion coefficient $[m \cdot m^{-1} \cdot K^{-1}]$

$\Delta\theta$ = Temperature increment $[K]$

Δw = Moisture content increment $\left[kg \cdot m^{-3}\right]$

κ_x, κ_y = Linear relative deformation due to changing moisture content $[m \cdot m^{-1} \cdot (kg \cdot m^3)^{-1}]$

Equation (8.5) describes the stress and strain relation by means of the generalized Hooke's law for an anisotropic material. Concerning a wooden cylinder within isothermal conditions, there will be no contributions due to thermal expansion. As a result of this condition, the strain calculated depends on the moduli of elasticity (E_x E_y), the normal stress components and the hygro-expansional coefficients (κ_x κ_y).

Dimensional change coefficient:

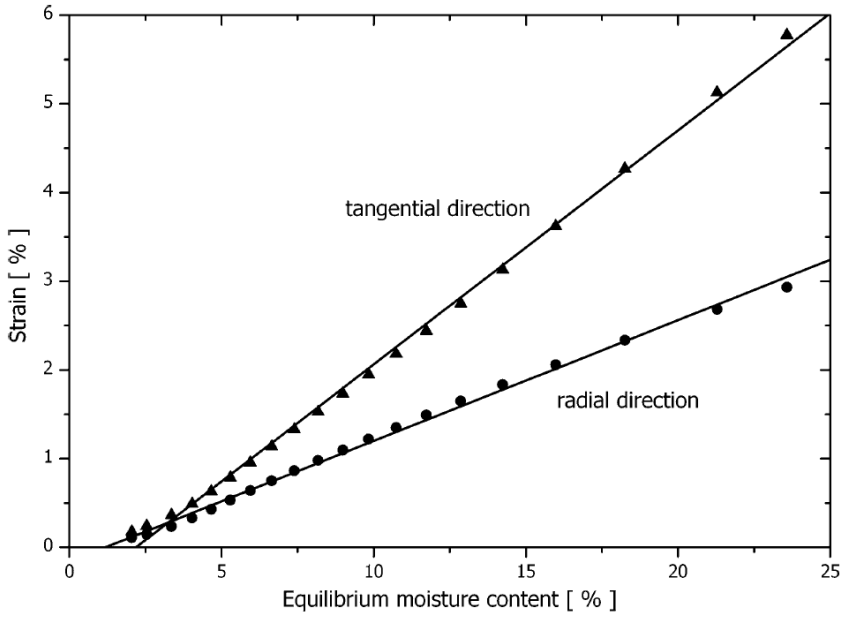

Figure 8.3: Dimensional change of lime wood in the radial and tangential direction plotted as a function of equilibrium moisture content (EMC) (S. Jakiela).

The dimensional change (swelling) coefficient (α_R, α_T) can be determined from the slope of figure 8.3. Figure 8.3 shows the tangential and radial strain as a function of the equilibrium moisture content. The expansion coefficients (α_R, α_T) can be determined by calculating the slope of the graph.

α_R = 0.13
α_T = 0.28

Moisture diffusion coefficient:

Table 8.2: Moisture diffusion coefficient as a function of equilibrium moisture content (EMC) (S. Jakiela).

Equilibrium moisture content [%]	Radial diffusion coefficient [m^2/h]	Tangential diffusion coefficient [m^2/h]	Longitudinal diffusion coefficient [m^2/h]
0	0.0003888	0.0003888	0.0009
0.05	0.0004751	0.0004751	0.00504
0.055	0.0004841	0.0004841	0.00535
0.07	0.0005137	0.0005137	0.00567
0.085	0.0005461	0.0005461	0.00585
0.09	0.0005572	0.0005572	0.00567
0.135	0.0006690	0.0006690	0.00454
0.18	0.0008026	0.0008026	0.00307
0.23	0.0009690	0.0009690	0.00210
0.28	0.0012029	0.0012029	0.00135

Equilibrium moisture content (EMC) as a function of Relative humidity (RH) at 20° C:

$$EMC = \frac{1800}{W}\left[\frac{K(RH)}{1-K(RH)} + \frac{K_1K(RH) + 2K_1K_2K^2(RH)^2}{1+K_1K(RH)+K_1K_2K^2(RH)^2}\right] \qquad (8.6) = (2.8)$$

$$K = 0.805 + 0.000736T - 0.00000273T^2 \qquad (8.7)$$

$$K_1 = 6.27 - 0.00938 \cdot T - 0.000303 \cdot T^2 \qquad (8.8)$$

$$K_2 = 1.19 + 0.0407 \cdot T - 0.000293 \cdot T^2 \qquad (8.9)$$

RH = Relative humidity [%]
T = Temperature $[^{\circ}C]$

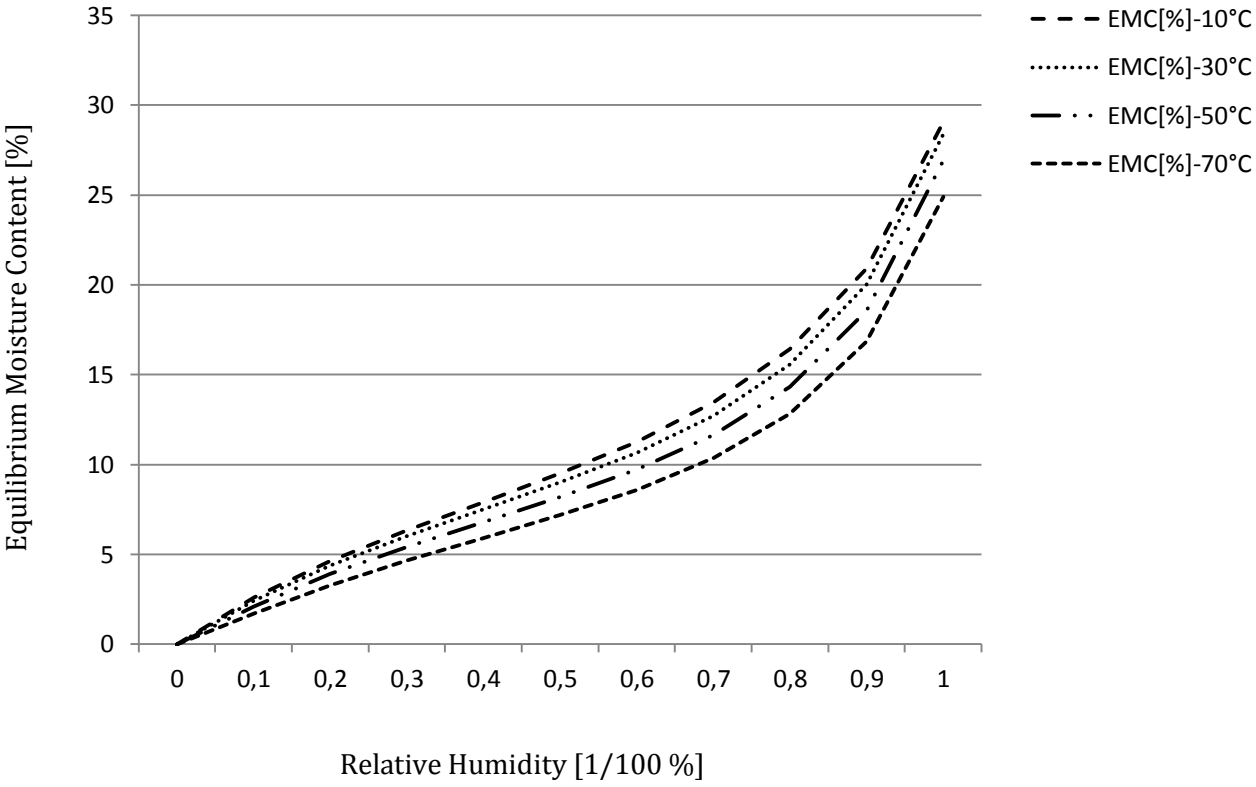

Figure 8.4: Equilibrium moisture content (EMC) as a function of relative humidity (RH) at 10 °C, 20 °C, 30 °C and 40 °C.

8.4 Results

The wooden cylinder is in equilibrium with its surrounding at t = 0. The relative humidity at $t = 0$ equals 70% which corresponds to 14% of equilibrium moisture content, see figure 8.4. At $t = 1$ the surrounding conditions suddenly change. The relative humidity at $t = 1$ drops from 70% to 30%, this corresponds to 6% equilibrium moisture content. The environment is kept constant at RH_1 = 30% after that. From $t = 1$ the wooden cylinder is slowly drying as it releases moisture. From $t = 1$ the wooden cylinder seeks for a new equilibrium with its surrounding condition. With help of ABAQUS finite element model the time to reach complete equilibrium was calculated at ~ 40 days, see appendix F. The process to this new equilibrium will be discussed now.

8.4.1 Distribution of moisture content after 24 hours and 10 days

Figure 8.5 represents the scalar field of the changing moisture content of the wooden cylinder after 24 hours. Figure 8.5 shows that after 24 hours the inner core is still at the initial 14% moisture content. The surface of the wooden cylinder shows a fast transition in moisture content.

Moisture concentration after 24h:

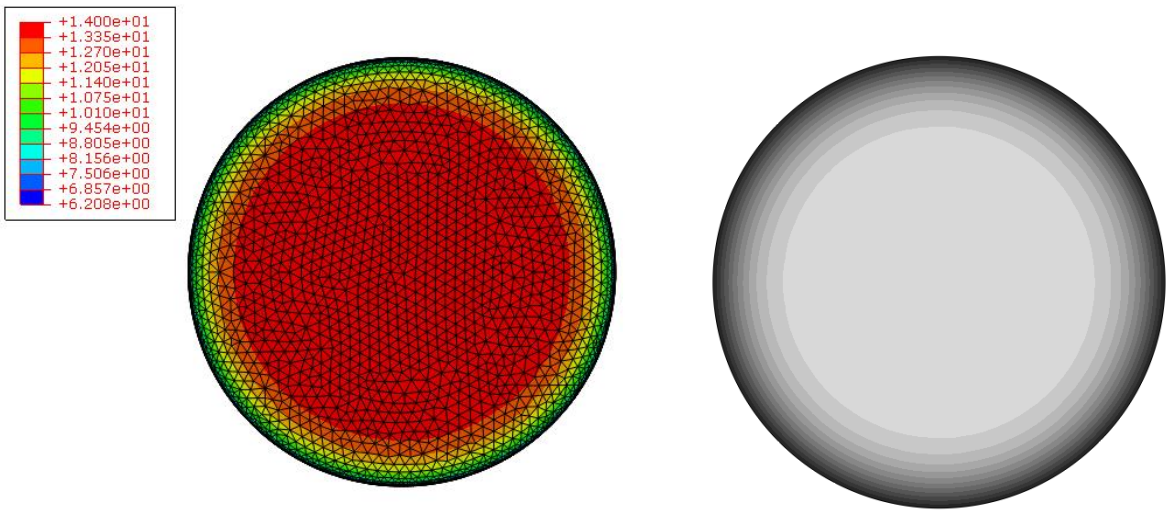

Figure 8.5: Moisture content (MC) scalar field of wooden cylinder exposed to a change in relative humidity (RH) from 70% down to 30% after 24 h.

Figure 8.6 shows the changing moisture content of different depths from the surface as a function of time. The selected distances from surface up to 10 mm inside the wooden cylinder, illustrate a non-linear diffusion process. Figure 8.6 shows that the change in moisture content is maximal at the surface. The first 1 mm to 5 mm from the surface level instantaneously changes its moisture content. The core of the cylinder lying deeper than 1 centimetre does not experience any change in the moisture content before 3 hours. After 24 hours, at 1 centimetre from the surface, the moisture content reduces from 14% to 11% moisture content. After 24 hours, at 0.5 mm from the surface, the moisture content drops from 14% down to 9%. Figure 8.6 shows that although the response may not be quick, the cylinder seeks for new equilibrium; see figure 8.9 and appendix F.

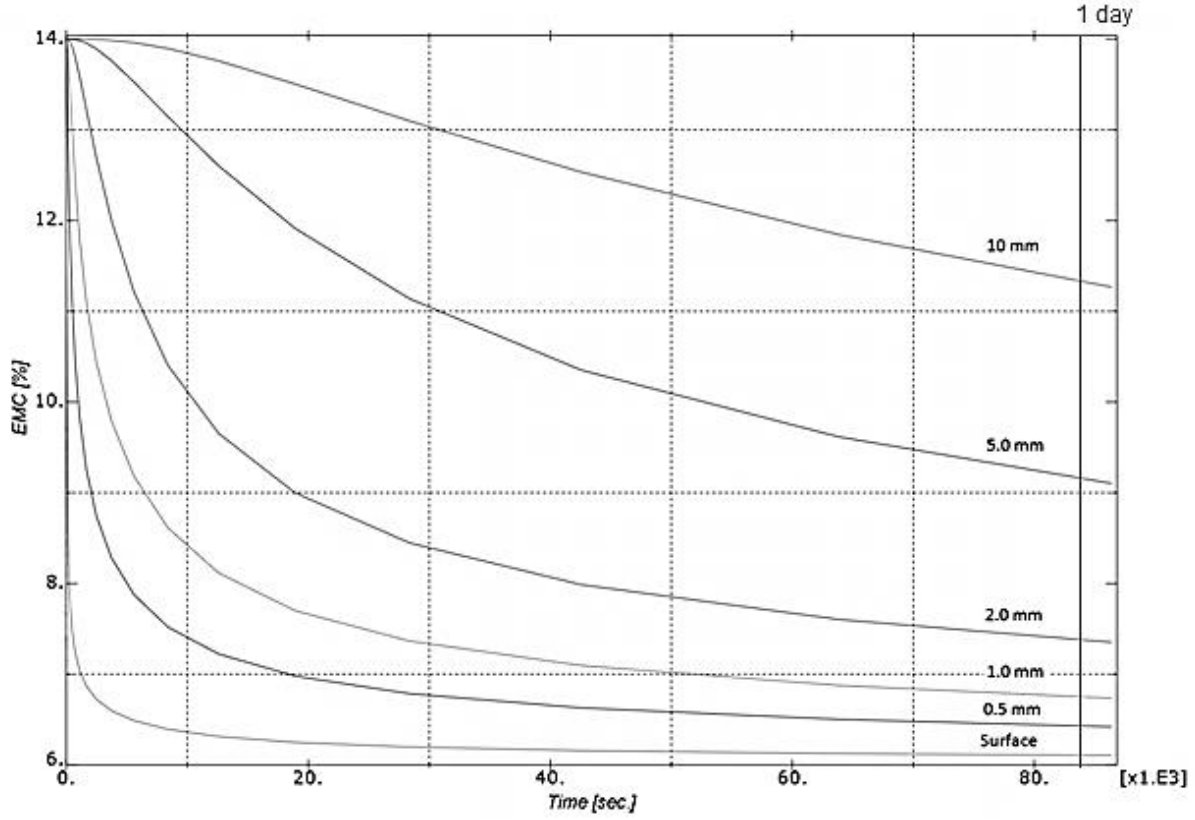

Figure 8.6: Distribution of moisture content at selected distances from the surface up to 10 mm into a wooden cylinder with a step change of 14% MC to 6% MC which is equal to 70% RH to 30% RH after 24 h.

Figure 8.7 shows the moisture distribution in the wooden cylinder after a drying period of 10 days. The inner core of the cylinder reduces from 14% moisture content to 11% moisture content.

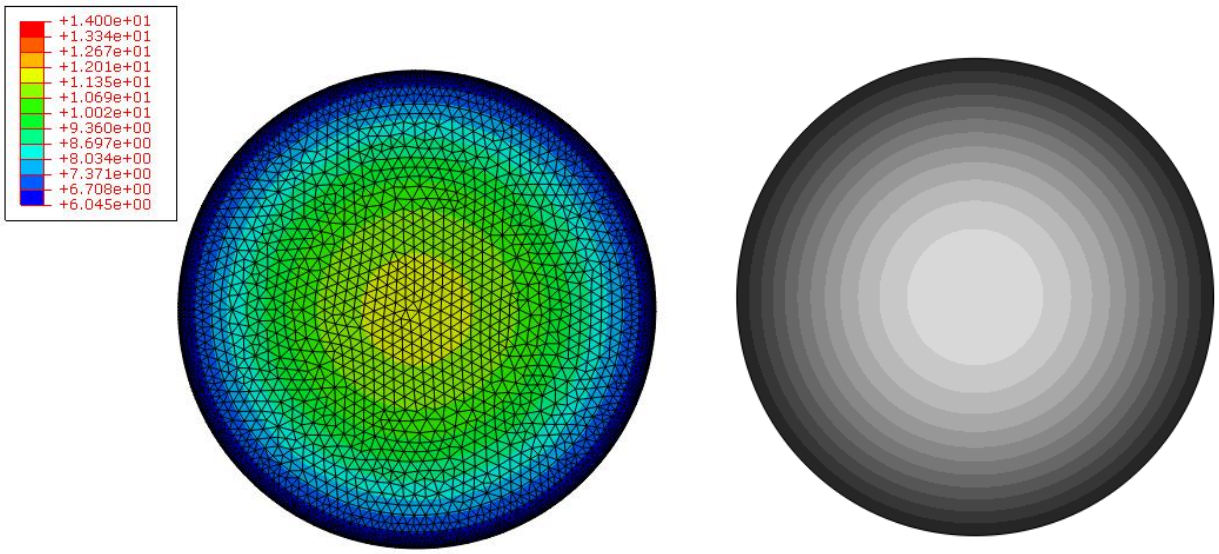

Figure 8.7: Moisture content (MC) scalar field of wooden cylinder exposed to a change in relative humidity (RH) from 70% down to 30% after 10.

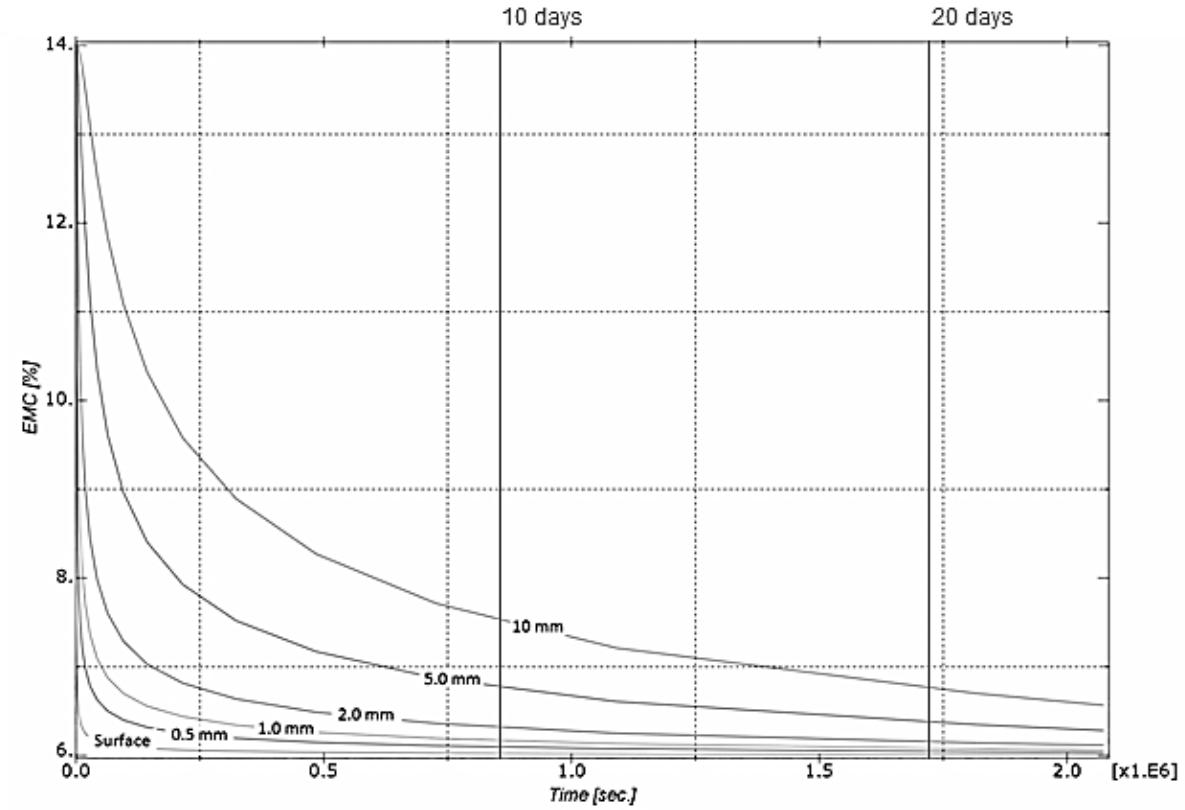

Figure 8.8: Distribution of moisture content (MC) at selected distances from the surface up to 10 mm into a wooden cylinder with a step change of 14% to 6% equal to 70% to 30% relative humidity (RH) after 10 and 20 days.

8.4.2 Stress development in radial and tangential direction

Figure 8.9 shows the calculated radial stress at different depths from the surface as a function of time. Because the wooden cylinder is releasing moisture, the cylinder slowly shrinks into the direction of the centre. The radial stress due to shrinkage increases in the direction towards the cylinder centre.

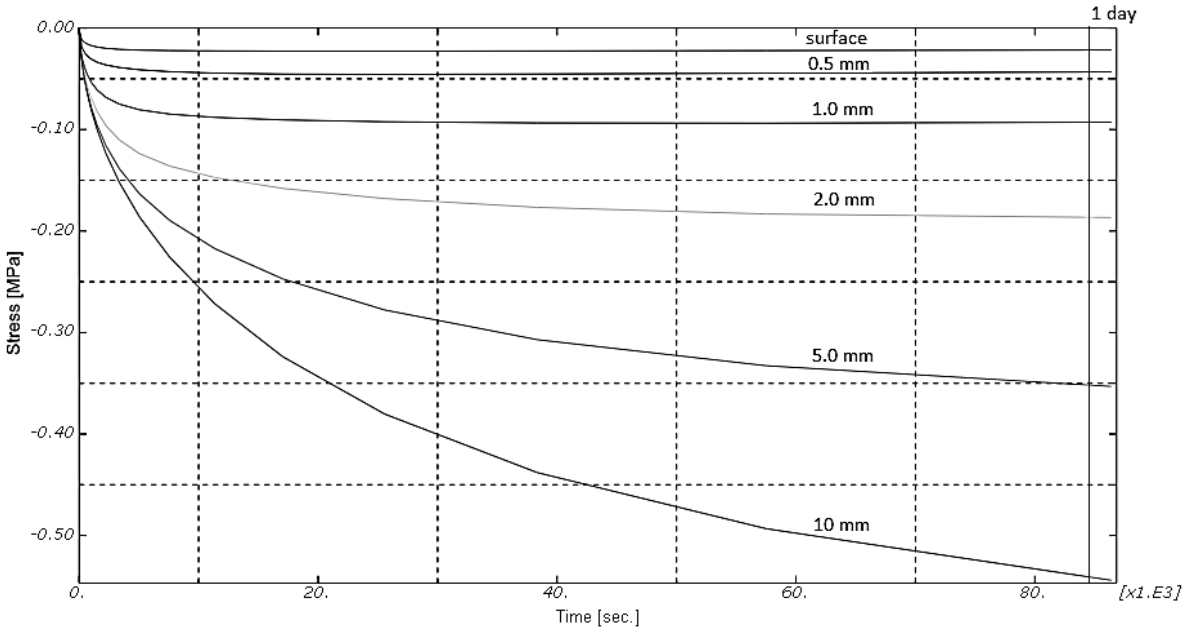

Figure 8.9: Radial stress at selected distances from the surface up to 10 mm into a wooden cylinder with a step change of 14% to 6% moisture content (MC) equal to 70% to 30% relative humidity (RH) after 24 h.

Figure 8.10 shows the development of tangential stress at different depths from the surface as a function of time. The maximum tangential strength of ~ 5.5 MPa (S. Jakiela [37]) has been exceeded. The elastic range of ~ 2.5 MPa (S. Jakiela [37]) has been exceeded more than 2 times. With continues drying of the interior layers, the stress slowly decreases. This slow decrease is the result of the slow vanishing of the moisture gradient as the interior layers dry.

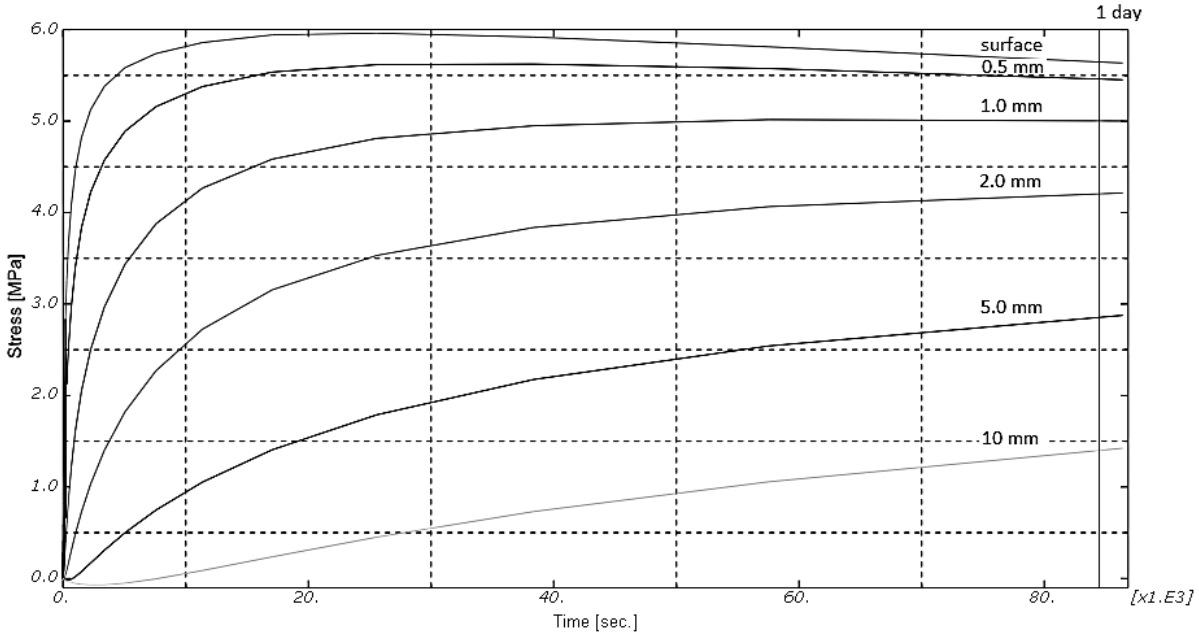

Figure 8.10: Tangential stress at selected distances from the surface up to 10 mm into a wooden cylinder with a step change of 14% to 6% moisture content (MC) equal to 70% to 30% relative humidity (RH) after 24 h.

8.4.3 Strain development in radial and tangential direction

Figure 8.11 shows the development of radial strain in compression perpendicular to the grain at different depths from the surface as a function of time. Generally, the maximum elastic strain at which wood begins to plastically deform lies around the 0.004. As one can see, this critical value is rapidly exceeded. Equivalent to the tangential stress development, the radial strain shows a steep slope at the surface, which gradually decreases when going deeper into the material.

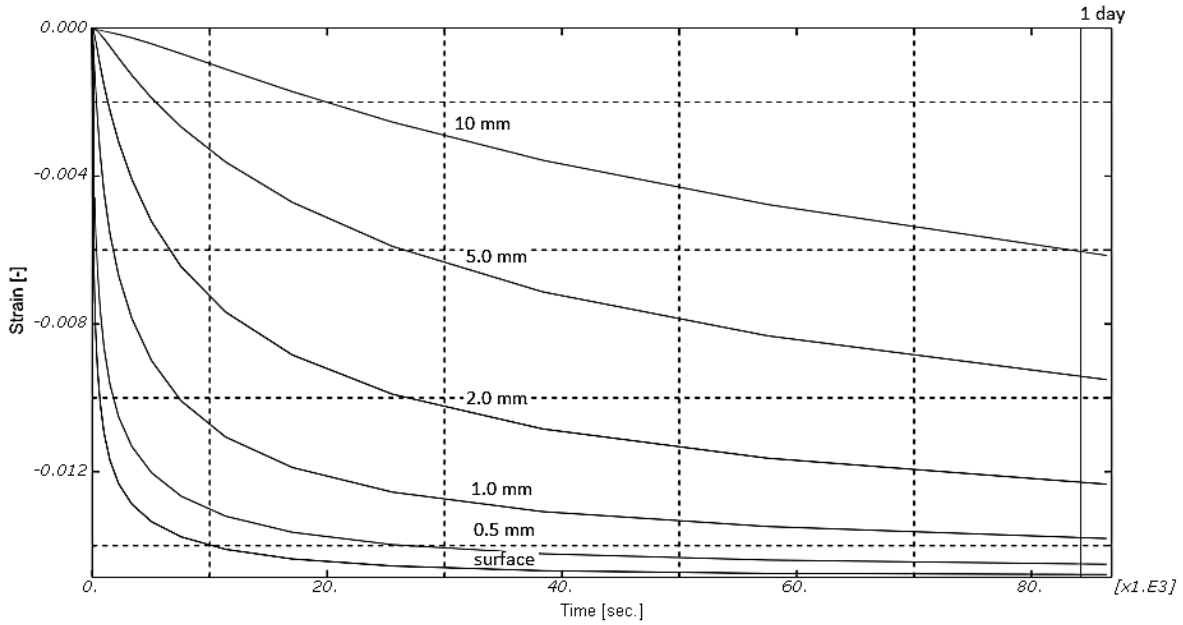

Figure 8.11: Radial strain at selected distances from the surface up to 10 mm into a wooden cylinder with a step change of 14% to 6% moisture content (MC) equal to 70% to 30% relative humidity (RH) after 24 h.

Figure 8.12 shows the development of tangential strain in compression perpendicular to the grain at different depths from the surface as a function of time.

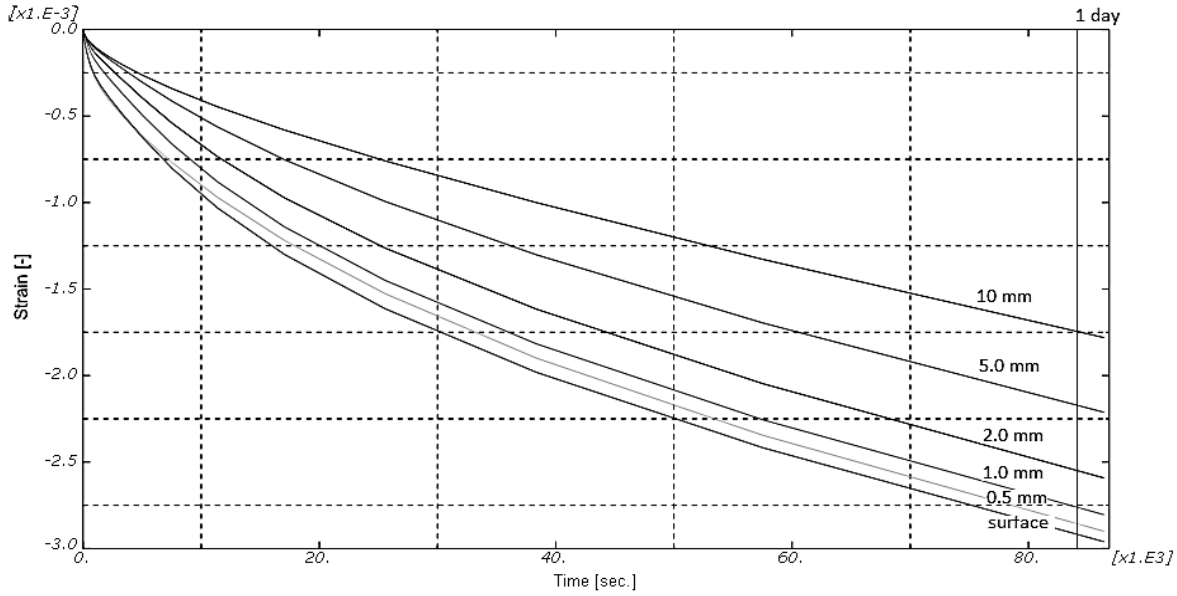

Figure 8.12: Tangential strain at selected distances from the surface up to 10 mm into a wooden cylinder with a step change of 14% to 6% moisture content (MC) equal to 70% to 30% relative humidity (RH) after 24 h.

8.5 Verification

The results of the ABAQUS model are compared to the results from Jakiela et al [37] and Schellen and Schijndel [36]. The results found by Schellen and Schijndel were computed with help of a numerical model within COMSOL as a comparative benchmark of the research done by Jakiela et al. The material properties which were implemented into the ABAQUS finite element model were taken from Jakiela et al [37], which are given in figure 8.13 and 8.15.

Comparing the moisture distribution computed with help of ABAQUS after 24 hours (figure 8.6) and the results found by Jakiela et al [36] (figure8.13), it can be concluded that these results are very much the same.

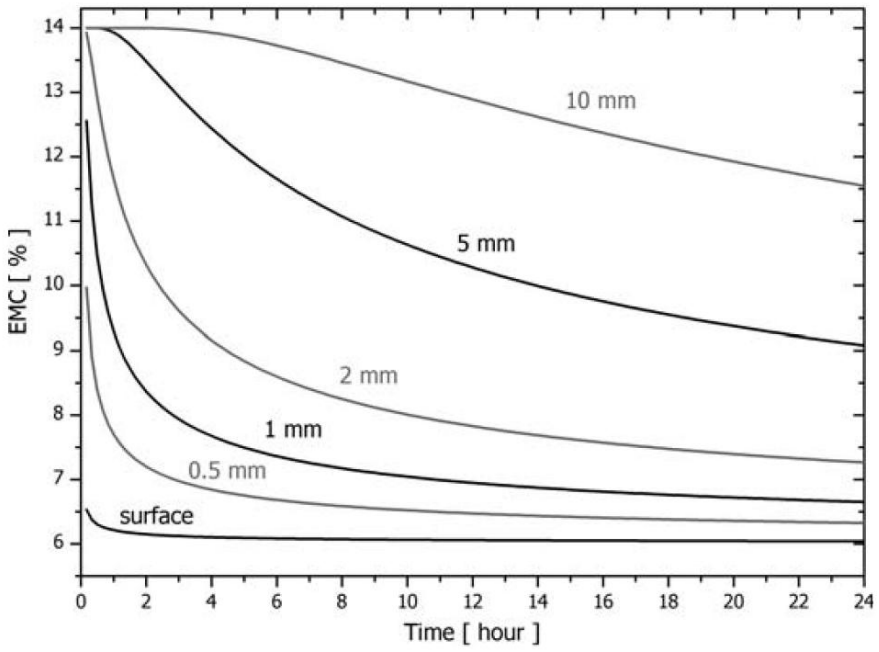

Figure 8.13: Calculation of change in distribution of moisture content (MC) at selected distances from the external surface of a wooden cylinder for a step change of 70 % - 30 % relative humidity after 24 h. (RH) (S. Jakiela)

A slight difference can be found in the slope of the surface line in the very beginning of the process. This difference has been calculated to be smaller than 5%. The slope of the line representing the moisture distribution at surface level found by Schellen, Schijndel and Bratasz et al seems to be slightly steeper. This difference is probably a result of a small difference in the vapour transfer coefficient. This difference in vapour transfer coefficient (β) is the result of different hygric boundary conditions. Within the ABAQUS model, the moisture content was prescribed at the boundary and within the COMSOL model, the vapour pressure was prescribed at the boundary, see equations (8.10) and (8.11).

ABAQUS:

$$g = \beta(u_0 - u_S) \qquad (8.10)$$

β = 0.003, based on M. de Wit [20]

COMSOL:

$$g = \beta(p_0 - p_S) \qquad (8.11)$$

β = 1.5E-6, based on Schellen [36]

Figure 8.14 shows the results of a small change in the vapour transfer coefficient on the slope of the curve. As the vapour transfer coefficient reduces, the slope of the moisture distribution at the surface seems to decrease.

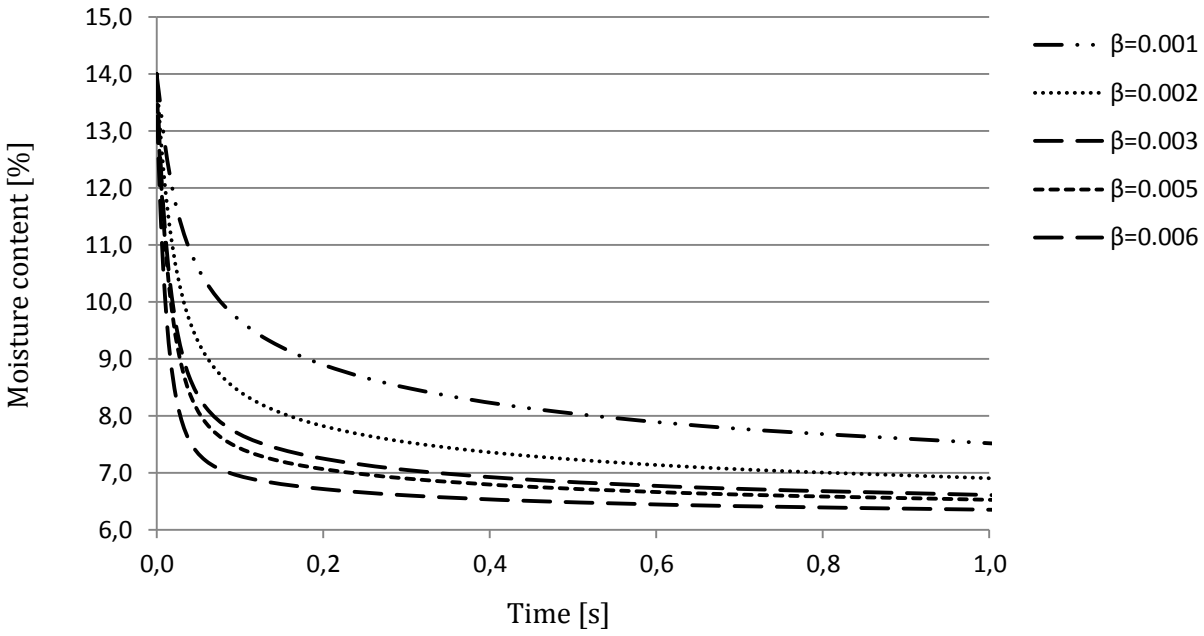

Figure 8.14: Dependency of the surface moisture content distribution upon the vapour transfer coefficient (β).

Comparing the tangential stresses computed with help of ABAQUS after 24 hours (figure 8.10) and the results found by Jakiela et al [37], see figure8.15. There seems to be almost difference in the maximum tangential stress.

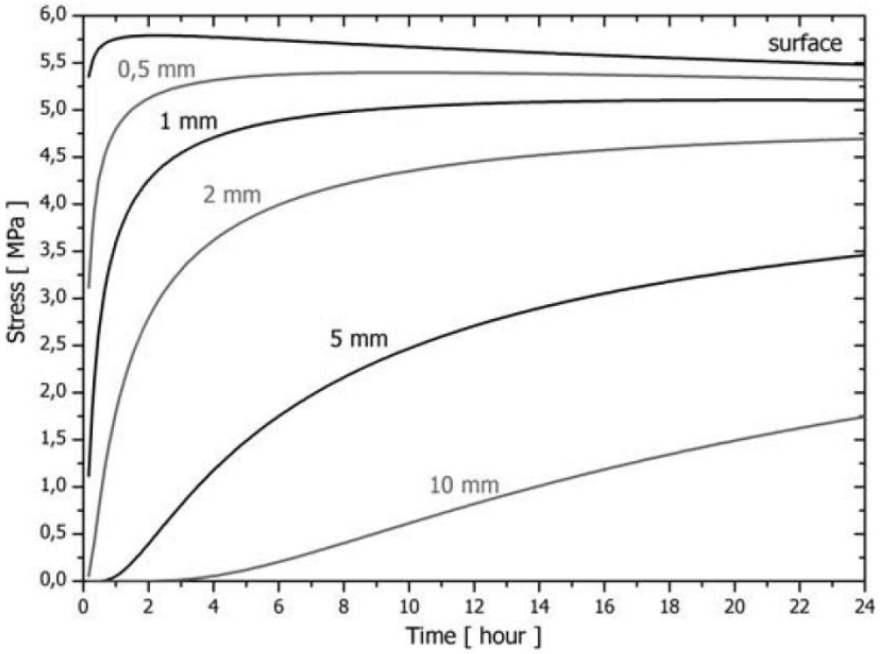

Figure 8.15: Tangential stress developing in wood as a result of the gradient of moisture content after 24 h. (S. Jakiela)

8.6 Conclusion

Modelling moisture distribution, using the transient heat conduction analysis procedure from ABAQUS was successful. Also the coupling of the heat conduction analysis with the static analysis has been successful.

It is shown that moisture distribution is strongly non-linear. The first few millimetres from surface level responds very quickly to a changing relative humidity. The corresponding stress development in tangential direction (6.0 MPa) exceeds the maximum stress (5.5 MPa) and elastic limit (2.5 MPa) as defined by Jakiela [37]. Previous research has proven that the diffusion of moisture through wood is not pure Fickian, as calculated by ABAQUS. Suppose that the moisture distribution through wood obeys Fick's law of mass diffusion, this would always lead to very high stress development at surface level as shown by ABAQUS. As a result, cracking of the surface level would be almost instantaneous. Practical research and experience has proven that this is not the case. As a result, a non-Fickian or multi-Fickian model has been developed by others, describing the process of moisture distribution through wood more realistically. This non-Fickian or multi-Fickian model predicts a much less steep gradient at the surface in correspondence with practical observations, see figure 8.16.

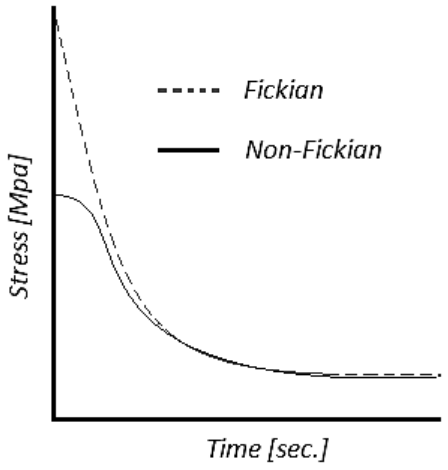

Figure 8.16: Fickian and Non-Fickian stress development in wood due to changing moisture content.

Although in practice the stress development at the surface level does not obey a pure Fickian process, still a strong gradient in moisture content gives rise to considerable drying stresses also due to the differential shrinkage being restrained.

The analysis performed with ABAQUS showed that the core of the lime wood cylinder lying deeper than 1 cm does not experience any change in moisture content for 3 hours. Stress decreases slowly as the moisture gradient gradually vanishes on a progressive drying occurs of the interior layers. Comparing the moisture distribution and stress field calculations by ABAQUS shows to be in good agreement with the result from Jakiela et al [37] , Schellen and Schijndel [36].

9 Shape stability of sawn timber

9.1 Introduction

Sawn timber, when exposed to changing environmental conditions shrinks or swells. The deformation of sawn timber exposed to changing environmental conditions can be a serious problem. For example, museums are forced to use expensive climate conditioning installations to condition their wooden collections, such as panel paintings and antique wooden furniture. These climate conditioning installations are responsible for keeping the relative humidity at around 55%. This strict requirement, mainly based on many years of practical experience, comes with great costs to the museums. But, not only museums are affected by this problem, all industry producing wooden products for construction or interior decoration must take account of this hygroscopic behaviour of wood. For both museums and industry, it is important to investigate how the material properties, the internal structure and changing environmental conditions influence the shape deformation. More knowledge could lead to monetary savings and stable wooden products.

Without numerical simulation, it is almost impossible to predict the deformation resulting from changing environmental conditions. A proper constitutive model that takes into account the directional dependency of the material, wood properties and the orientation of the fibres (spiral grain orientation) is necessary to accurately predict the deformation.

Chapter 9 discusses the finite element simulations in relation to the stability of sawn timber exposed to changing environmental conditions. Four types of deformation will be discussed: cup, twist, crook and bow, as well as the influence of the conical angle and spiral grain on shape stability.

The finite element simulations performed in this chapter are all done with ABAQUS finite element software, using a sequentially coupled Temperature-Displacement analysis and multi-physic heat transfer - static stress/strain analysis. The material properties are taken from Kollmann [2] for pine; missing values are taken from Blumer [18] and Ormarsson [6].

It has been experientially observed that the longitudinal moduli of elasticity and the longitudinal moisture expansion coefficient vary from pith to bark. This behaviour will be neglected and the moduli of elasticity and expansion coefficient will be regarded as being constant. Also, the elastic strain parameters will be assumed to be independent of the distance from the pith and regarded as being constant. More information about varying material properties in longitudinal direction and from pith to bark can be found in Ormarsson et al [6].

9.2 Types of deformation

Sawn timber exposed to changing environmental conditions could cup, twist, crook or bow. These types of deformations can occur individually or combined, see figure 9.1. The stability of sawn timber strongly depends upon the orientation of the fibres and the growth ring. It is essential to have detailed information about the original position of the sawn timber within the tree stem and the orientation of the fibres.

The conical angle (angle between pith and fibre direction) of a tree can be regarded as being constant from the bottom to the top of the tree. Because the diameter decreases from the bottom to the top of the tree, the conical angle sine is negative. The conical angle is generally regarded as being constant -0.5°.

In this report, cup, twist, crook and bow deformation will always be determined as shown by figure 9.1, using displacement δ (cup, crook and bow) and the angle ϕ (twist).

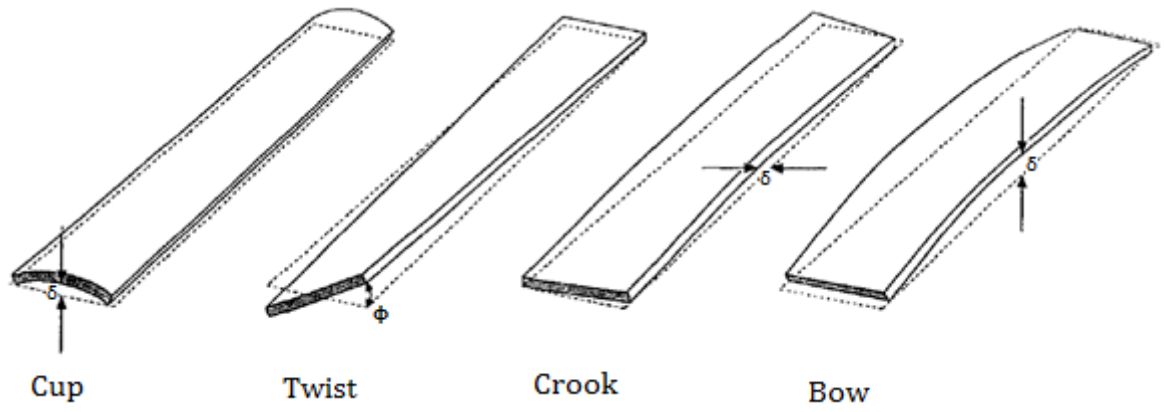

Figure 9.1: Different deformation types (Ormarsson, 1999 [6]).

9.3 Numerical setup

9.3.1 Models

Three numerical models where developed, all with different pith orientation. The first model is called Wood Board -1 (WB-1), second model is called Wood Board -2 (WB-2) and the third model is called Wood Board -3 (WB-3), see figure 9.2.

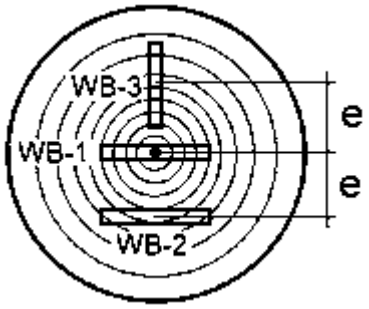

Figure 9.2: WB-1, WB-2 and WB-3 stem orientation.

Table 9.1: Dimension of wood beards.

	Spiral grain [degrees]	Conical angle [degrees]	Pith distance from centre [mm]	Thickness of wood board [mm]	Length of wood board [mm]	Width of wood board [mm]
WB-1	-4,0°	-0,5°	0	15	1000	200
WB-2	-0.0°	0°	-107.5	15	1000	200
WB-3	-0.0°	0°	107.5	15	1000	200

The pith of WB -1 is in its centre. WB -1 has a conical angle of -0.5°, a spiral grain of -4.0° and growth ring orientation as denoted by figure 9.2. The pith of WB -2 is located at e = 107.5 mm from the middle of the wood board. WB -2 has no conical angle, no spiral grain orientation and a growth rings orientation, as denoted by figure 9.2. The pith of WB -3 is located at e = 107.5 mm from the middle of the wood board. WB -3 has no conical angle, no spiral grain orientation and a growth ring orientation as denoted by figure 9.2.

Table 9.2: Wood boards loaded by a quick change of environmental condition.

Time [s]	Relative Humidity [%]	WB -1	WB -2	WB -3
t_0	RH_0	70 %	70 %	70 %
t_1	RH_∞	30 %	30 %	30 %

At $t = 0$ WB-1, WB-2 and WB-3 are in equilibrium with its direct environment of 70% relative humidity, corresponding to 14% moisture content. At $t = 1$, WB-1, WB-2 and WB-3 where exposed to a step change of 70% relative humidity to 30% relative humidity, corresponding to a decrease in moisture content from 14% to 6%.

It should be noted that the deformations displayed in this chapter are at a high scale factor. The deformations represented by figures are oversized representations of real world deformation.

9.3.2 Material data

Table 9.3: Coefficients of hygro-expansion (Kolmann [2]).

Unities	Coefficients of hygro expansion
$\alpha_L[m/m\%]$	3.0e-05
$\alpha_T[m/m\%]$	3.6e-03
$\alpha_R[m/m\%]$	1.9e-03

Table 9.4: Moduli of elasticity (Kolmann [2]).

Unities	Modulus of elasticity
$E_L[MPa]$	13553
$E_T[MPa]$	616
$E_R[MPa]$	1232

Table 9.5: Shear moduli (Kolmann [2]).

Unities	Shear modulus
$G_{LT}[MPa]$	836
$G_{LR}[MPa]$	788
$G_{TR}[MPa]$	79

Table 9.6: Poisson's ratio (Kolmann [2]).

Unities	Poison's ratio
$\nu_{LT}[-]$	0.4
$\nu_{LR}[-]$	0.4
$\nu_{TR}[-]$	0.4

Table 9.7: Diffusion coefficients (Jakiela).

Radial diffusion [m^2/h]	Tangential diffusion [m^2/h]	Longitudinal diffusion [m^2/h]	Moisture content [%] wood
0.0003888	0.0003888	0.0009	0
0.0004751	0.0004751	0.00504	5
0.0004841	0.0004841	0.00535	5.5
0.0005137	0.0005137	0.00567	7
0.0005461	0.0005461	0.00585	8.5
0.0005572	0.0005572	0.00567	9
0.0006690	0.0006690	0.00454	13.5
0.0008026	0.0008026	0.00307	18
0.0009690	0.0009690	0.00210	23
0.0012029	0.0012029	0.00135	28

Table 9. 8: Density and specific heat capacity (Jakiela).

Unities	
$\rho[kg/m^3]$	530
$C_P[J/kgK]$	0.0015

9.3.3 Boundary conditions

Thermal:

$$q = h(T_0 - T_S) \qquad (9.1)$$

q = Heat flux at surface $[W \cdot m^{-2}]$

h = Heat transfer coefficient (7.7) $[W \cdot m^{-2}K^{-1}]$

T_0 = 20 °C

T_∞ = 20 °C

Hygric:

$$g = \beta(u_0 - u_S) \qquad (9.2)$$

g = Moisture flux at surface $[W \cdot m^{-2}]$

β = Moisture transfer co-efficient (0.003, by de Witt [20]) $[W \cdot m^{-2}K^{-1}]$

u_0 = 14 [%]

u_S = 6[%]

t = 0 [s]

t_∞ = ∞

RH_0 = 70 [%]

RH_∞ = 30 [%]

The four center nodes in the middle of the wood board have the following displacement boundary conditions: node 1 (U1, U2, U3), node 2(U3), node 3(U1, U3) and node 4 (U3).

9.4 Results

As a consequence of the changing moisture content from 14% to 6%, shape deformation occurs. This shape deformation is numerically calculated and will serve as a reference value in the upcoming chapters.

Figures 9.3 to 9.9 illustrate the shape deformation of WB -1, WB -2 and WB -3 due to this changing moisture content. Table 9.9 shows the deformation quantities schematized in figure 9.1.

Table 9.9: Deformation due to changing moisture content, 14% - 6% after 10 days.

Deformation	Twist [degrees]	Bow [mm]	Cup [mm]	Crook [mm]
WB-1	2,00	0,00	0,00	0,00
WB-2	0,00	4,61	0,46	0,00
WB-3	0,00	0,00	0,00	-2,27

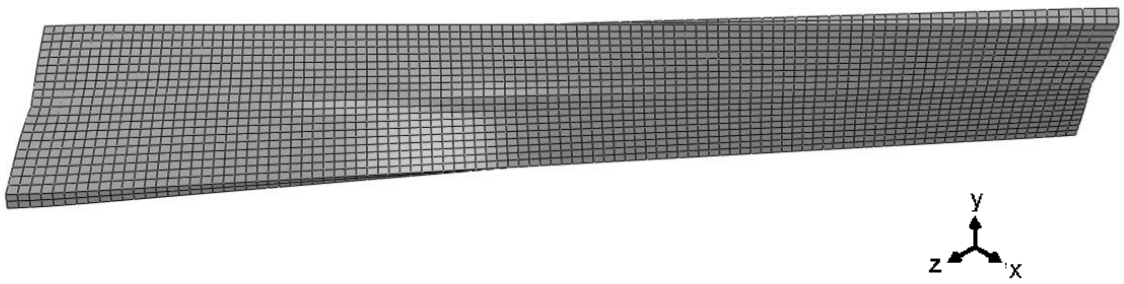

Figure 9.3: Twist deformation WB-1.

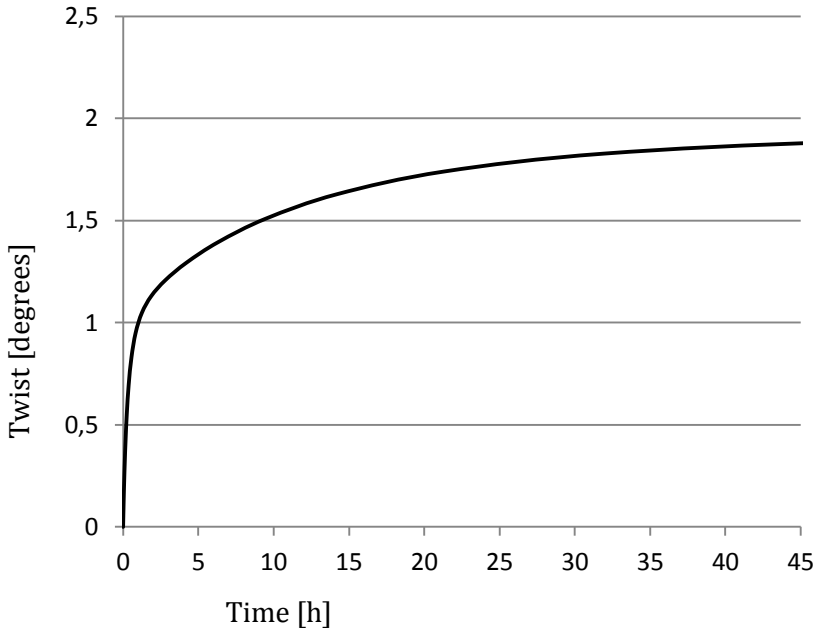

Figure 9.4: Twist [degrees] as a function of time [h], WB -1.

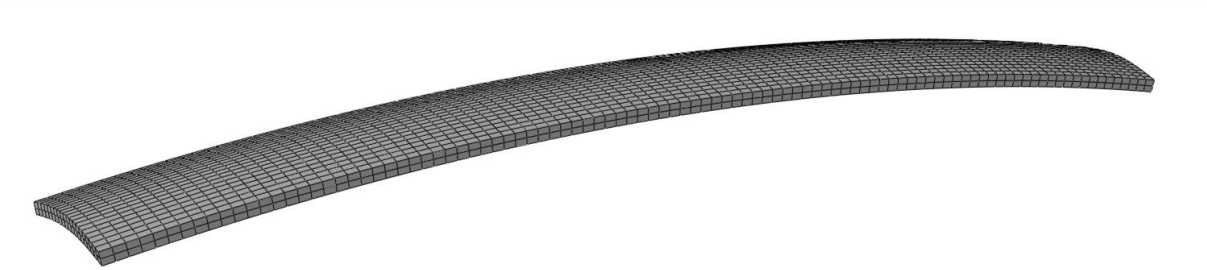

Figure 9.5: Cup and bow deformation WB-2.

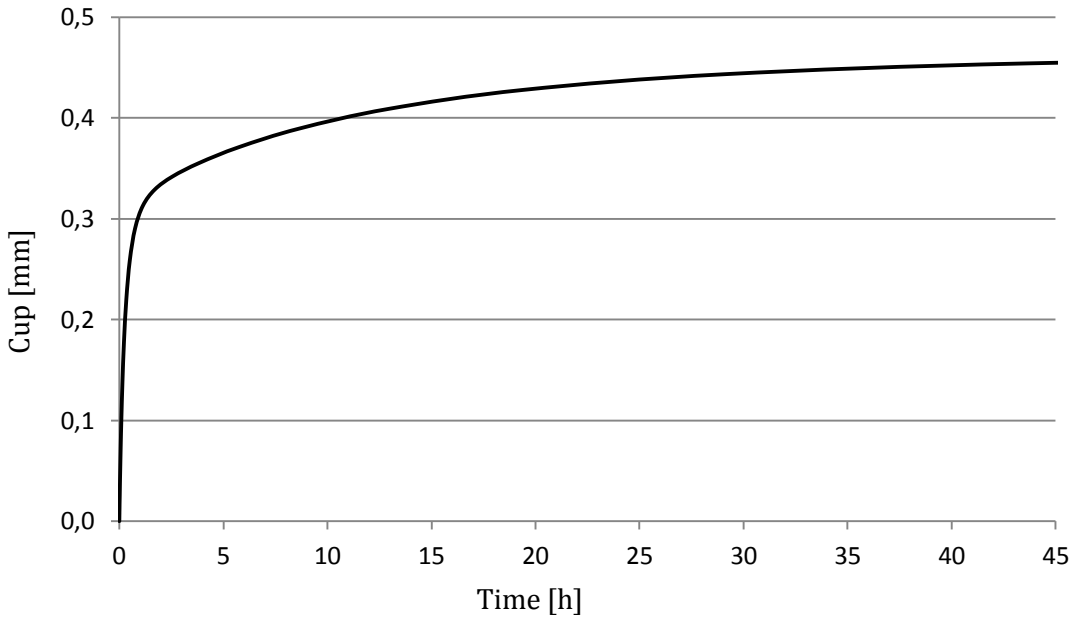

Figure 9.6: Cup [mm] as a function of time [h], WB -2.

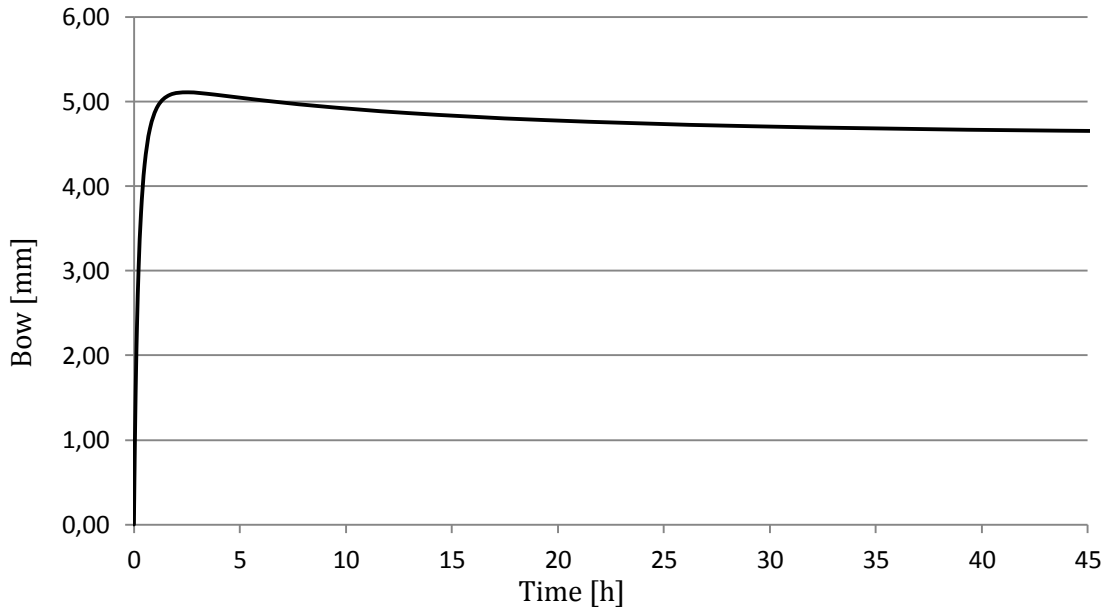

Figure 9.7: Bow [mm] as a function of time [h], WB -2.

Figure 9.8: Crook deformation WB-3.

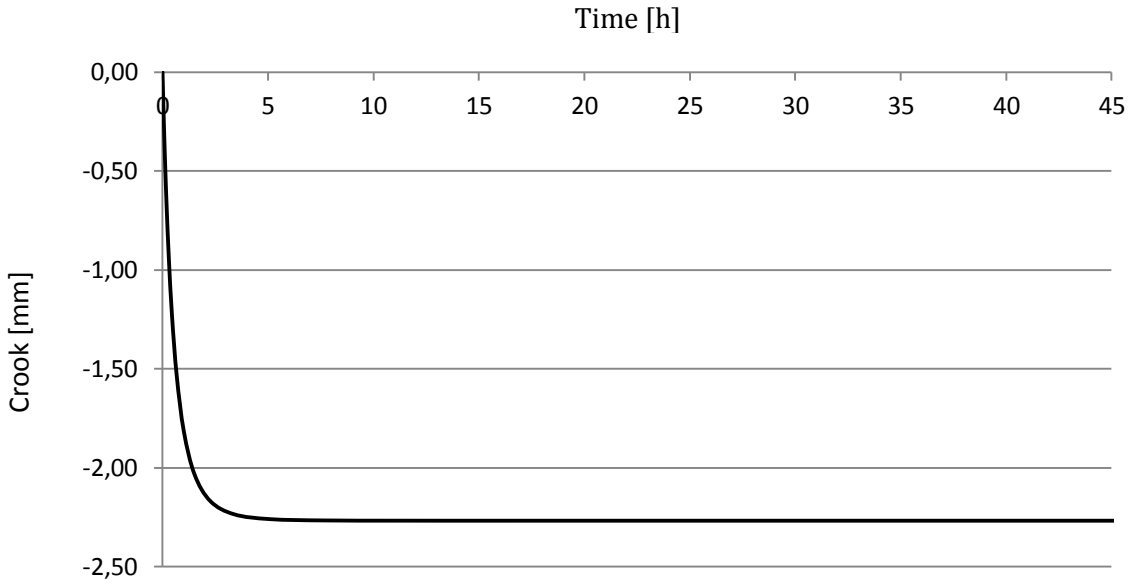

Figure 9.9: Crook [mm] as a function of time [h], WB -3.

9.5 Conclusion

Twist deformation under drying conditions is mainly the result of the spiral grain orientation. Without a spiral grain orientation, WB -1 would be stable and twist deformation would not occur. The strong relation between twist deformation and spiral grain orientation is a consequence of the wood board being much stiffer in the longitudinal direction, compared to the radial and tangential direction. Because the spiral grain equals the direction of the longitudinal material properties, placing the spiral grain under an angle of -4.0° results in a relatively great diagonal stiffness and, as a consequence, under drying conditions twist deformation of the wood board will occur. Although the model used by Ormarsson is dimensionally quite different, the result shown in figure 10.4 is in agreement with the result found by Ormarsson [6]. The wooden boards studied by Ormarsson were 3.0 m long, 100 x 10 mm in cross section and exposed to a change in moisture content from 27 % to 10.75 %. After 1 day of drying, Ormarsson calculated a twist deformation of 2.5 degrees. Figure 10.4 shows a strong twist gradient in the early stage of the drying process, as a consequence of progressive drying, this twist rate slowly decreases until equilibrium is reached. This strong twist rate in the early stage is a consequence of the average moisture content decreasing very quickly in the first few hours, see figure 9.10. This strong twist rate in the early stage of the drying process was also found by Ormarsson [6].

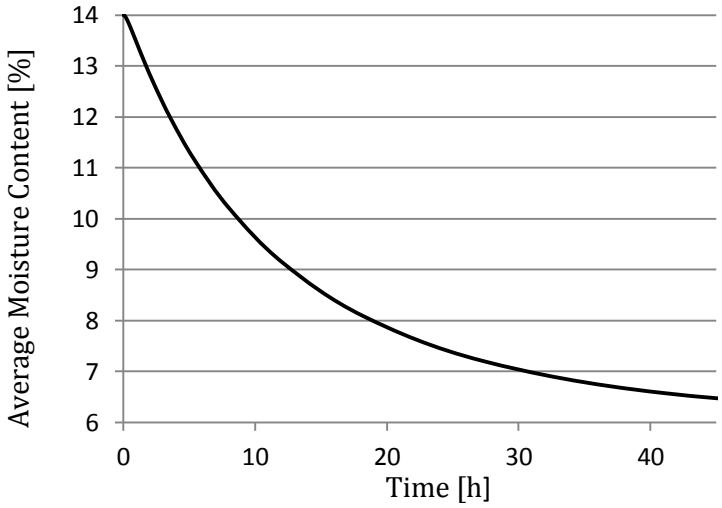

Figure 9.10: The average moisture content decreases very quickly in the first few hours.

Cup deformation is caused by the difference between radial and tangential shrinkage. Since shrinkage is greater in the tangential than in the radial direction, cup deformation develops. Also in the case of cup development, the rate of increase is the greatest in the early stage of the drying process. Crook deformation depends strongly on the distance between the pith and the centre of the wood board in case of WB -3, see figure 9.2. A wood board, originally taken close to the pith, will show a stronger crook deformation than one taken further away from the pith because further away from the pith the growth rings become relative straight, which make the wood board more stable, see figure 9.11. Ormarsson did not investigate crook deformation.

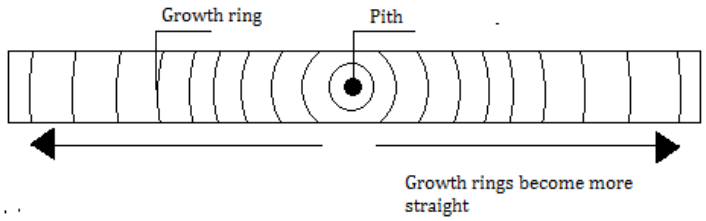

Figure 9.11: Further away from the pith the growth rings become relative straight.

Wood board -1 does not show bow deformation because it is stable due to its growth ring orientation, see figure 9.2. This is opposite to wood board -2 which shows significant bow deformation, see figure 9.7. The difference between wood board -1 and wood board -2 is clearly the orientation of the growth ring.

It is known that the direction of cupping depends upon the orientation of the growth rings. If the growth rings point upwards, the cupping direction will be downwards. In case of bow deformation, this is the opposite. The position of the pith, which is the centre of the growth rings, determines the direction of bowing. If the pith is located above the board, the bowing direction will be the same.

The reason for bowing cannot be the difference between radial and tangential shrinkage. The wood boards are exposed to equal drying condition at each surface, so unequal drying of the top and bottom surfaces can not also be the reason for this behaviour. It becomes doubtful whether bowing is the result of material properties or a consequence of the local cylindrical coordinate system. In the latter case it is doubtful if this bow effect would take place in a real world situation.

One possible explanation could be that bow deformation is the result of unequal material property distribution over the cross section as a consequence of the modelled local cylindrical coordinate system assuming to represent the growth ring orientation. Comparing the distribution of the local coordinate systems of wood board -1 and wood board -2, wood board -1 shows equal distribution of the local coordinate systems but wood board -2 does not show this equal distribution, see figure 9.12 and 9.13.

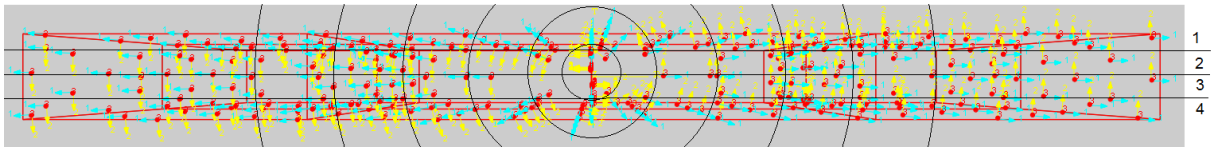

Figure 9.12: WB-1 Local coordinate system, longitudinal stiffness distribution.

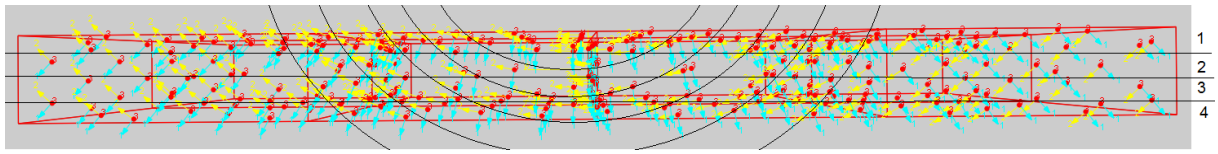

Figure 9.13: WB-1 Local coordinate system, longitudinal stiffness distribution.

Figure 9.12 shows an equal distribution of coordinate systems across intersection layers 1, 2, 3 and 4. Figure 9.13 does not show an equal distribution of coordinate systems across intersection layers 1, 2, 3 and 4 due to the horizontal cut off of the growth rings. This could explain bow deformation but does not have to be the real world situation. Ormarsson [6] also calculates bow deformation, but did not explain the effect. Figure 9.14 shows that increasing the distance between the pith and the wood board results in a decreasing bow deformation. It is the same reason why the crook deformation decreases when increasing the distance between the pith and the wood board centre, see figure 9.14.

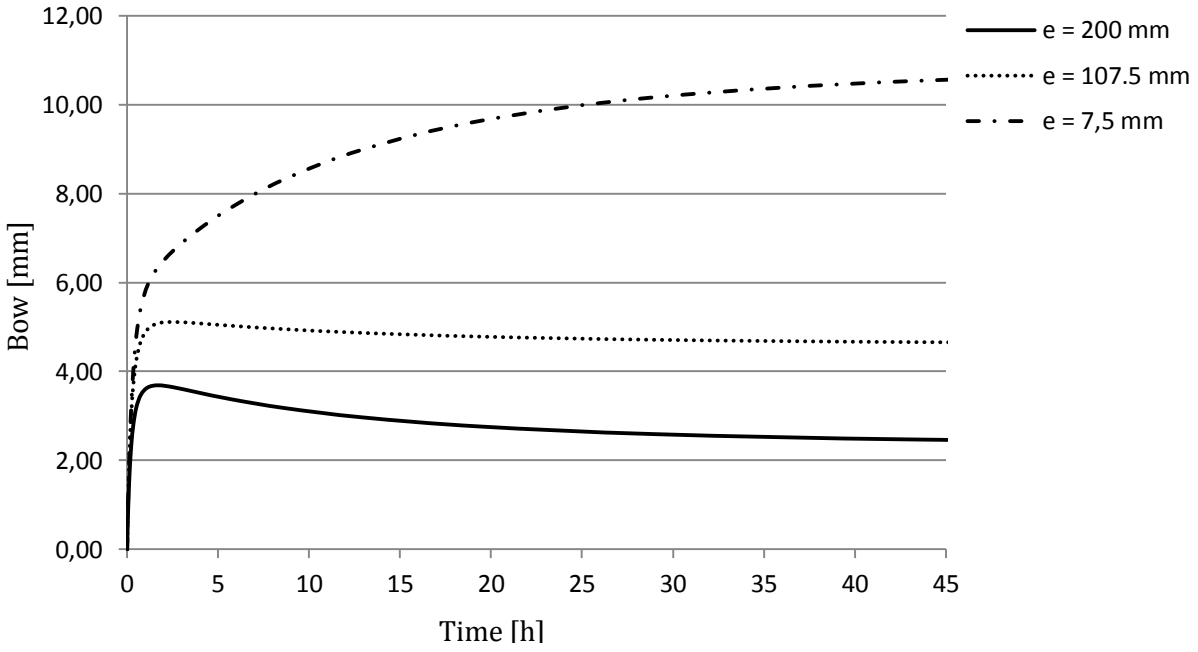

Figure 9.14: Influence of the distance between pith and wood board centre on bow deformation.

10 Influence of material parameters on shape stability

10.1 Introduction

This chapter discusses the influence of changing mechanical properties in regard to shape stability, for which each mechanical property was reduced by 50% and compared to a reference value.

$$
\begin{aligned}
E_L^{red} &= \frac{E_L^{ref}}{2} & G_L^{red} &= \frac{G_L^{ref}}{2} & \alpha_L^{red} &= \frac{\alpha_L^{ref}}{2} \\
E_T^{red} &= \frac{E_T^{ref}}{2} & G_T^{red} &= \frac{G_T^{ref}}{2} & \alpha_T^{red} &= \frac{\alpha_T^{ref}}{2} \\
E_R^{red} &= \frac{E_R^{ref}}{2} & G_R^{red} &= \frac{G_R^{ref}}{2} & \alpha_R^{red} &= \frac{\alpha_R^{ref}}{2}
\end{aligned}
\qquad (10.1)
$$

In line with chapter 9, the same numerical models are used to investigate the influence of changing mechanical properties. Wood board -1 is used to investigate the influence of these changing mechanical properties on twist deformation. Wood board -2 is used to investigate the influence of these changing mechanical properties on bow and cup deformation and wood board -3 is used to investigate the influence of these changing mechanical properties on crook deformation.

10.2 Wood board -1: Influence of changing E, G, α on twist deformation

10.2.1 Reduced elastic moduli

Figure 10.1 shows the result of reducing the elastic moduli (E) with 50 % of its reference value on twist deformation after a drying period of 45 hours. Reducing the elastic moduli (E) resulted in an overall increase of twist deformation. Calculations showed that the tangential elastic modulus has the smallest influence on twist deformation, +5.0% after a drying period of 45 hours. Reducing the longitudinal and radial elastic moduli increases twist deformation by +10 % after a drying period of 45 hours.

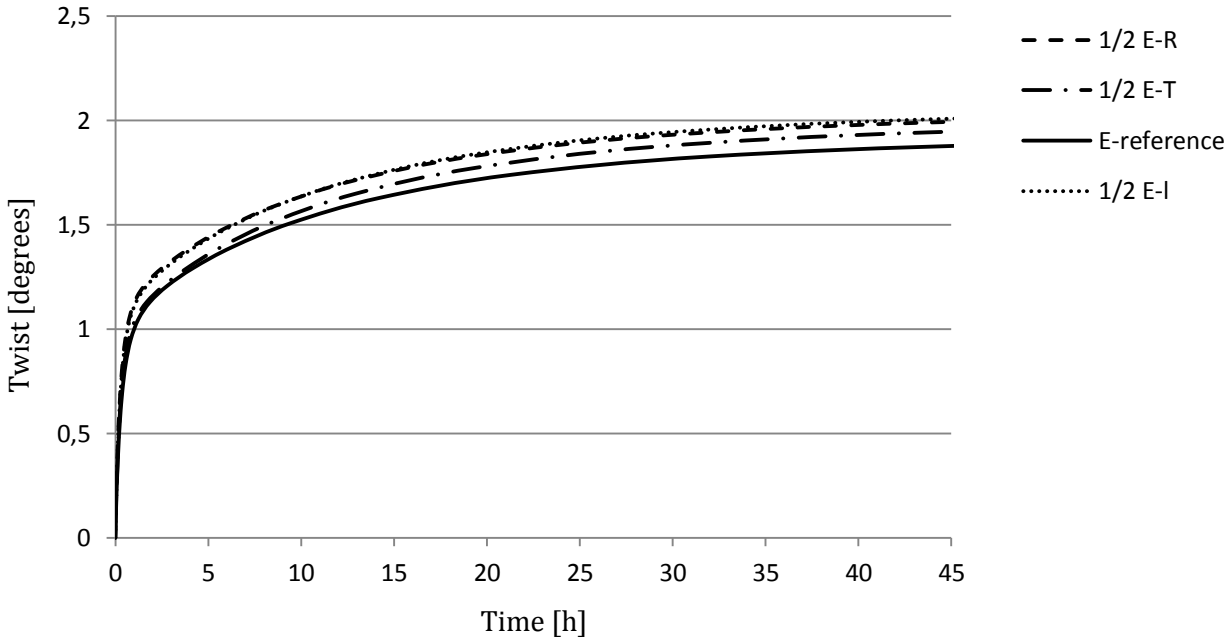

Figure 10.1: WB-1, influence of changing elastic moduli on twist deformation, step change of 70% - 30% RH after 45 h.

10.2.2 Reduced shear moduli

Figure 10.2 shows the results of reducing the shear moduli (G) with 50% of its reference value on twist deformation after a drying period of 45 hour. Equal to the reduction of the elastic moduli, reducing the shear moduli resulted in an overall increase of twist deformation. Calculations showed that reducing G-LT, influences the twist deformation the least, compared to the other shear moduli, namely +10.0% after a drying period of 45 hours. Reduction of G-LR and G-TR, have the largest influence, namely +20% after a drying period of 45 hours.

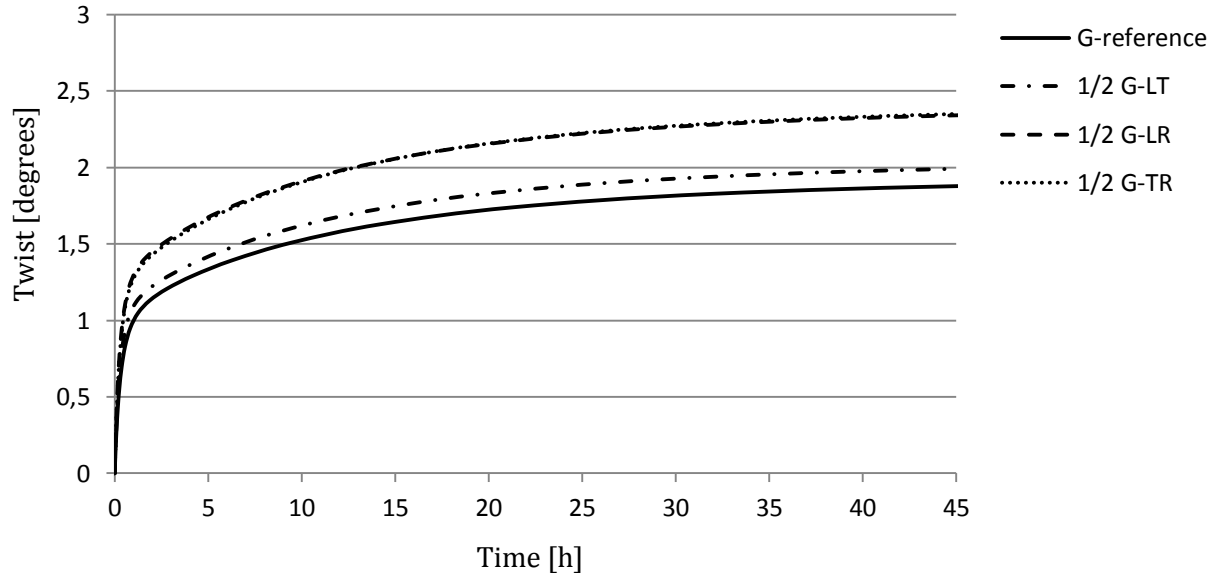

Figure 10.2: WB-1, influence of changing shear moduli on twist deformation, step change of 70% - 30% RH after 45 h.

10.2.3 Reduced hygro-expansion

Figure 10.3 shows the results of reducing the hygro-expansion coefficient (α) with 50% of its reference value on twist deformation after a drying period of 45 hours. Figure 11.3 shows a relatively strong influence of the hygro-expansion coefficient with respect to twist deformation. Reducing the tangential hygro-expansion coefficient resulted in a significant twist reduction compared to the radial and longitudinal hygro-expansion coefficients. Reduction of the tangential hygro-expansion coefficient results in -100 % decrease of twist deformation after a drying period of 45 hours. Reducing the radial and longitudinal hygro-expansion coefficient respectively results in an increase of +28.0% and +17.0% of twist deformation after a drying period of 45 hours.

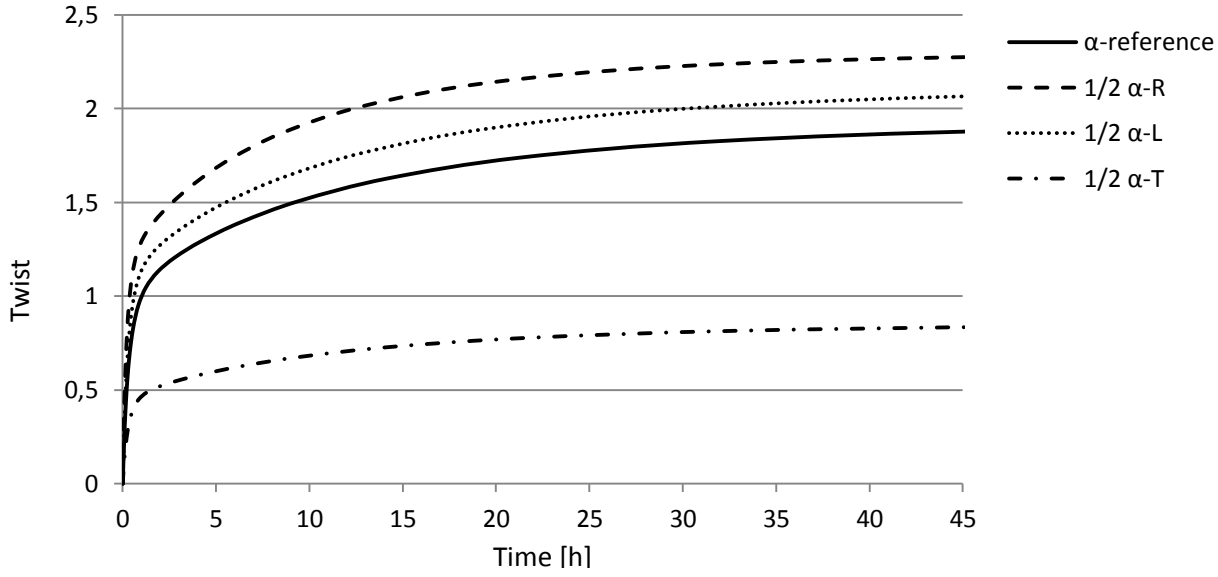

Figure 10.3: WB-1, influence of changing coefficient of hygro-expansion on twist deformation, step change of 70% - 30% RH after 45 h.

10.2.4 Conclusion

Reducing the tangential, longitudinal and radial elastic moduli (E), increases twist deformation. The tangential elastic modulus has the least influence on twist deformation, +5.0% after a drying period of 45 hours. Reducing the longitudinal and radial elastic moduli results in increasing twist deformation of +10% after a drying period of 45 hours. After a drying period of 6 days, these increments have slightly reduced. After a drying period of 6 days, reduction of the tangential elastic modulus resulted in +4.0% twist increment. Reduction of the longitudinal and radial elastic moduli resulted in +8.0% twist increment after a drying period of 6 days.

The wooden boards studied by Ormarsson [6] are 3.0 m long, 100 x 10 mm in cross section and exposed to a change in moisture content (MC) from 27 % to 10.75 %. Ormarsson [6] calculated an increment of +10% twist deformation when reducing the tangential elastic modulus. This seems to be in line with the calculated +8.0 %. Ormarsson concludes that reducing the longitudinal elastic modulus does not affect the twist deformation and reducing the radial elastic modulus decreases twist deformation. This is in contradiction with the current results. This contradiction can be the result of different dimensional properties, different environmental conditions, differences in the constitutive model and differences in the strain model (Ormarsson for example included a mechano-sorptive strain parameter).

Calculations showed that reducing G-LT, influences the twist deformation the least, compared to the other shear moduli, namely +10.0% after a drying period of 45 hours. Reduction of G-LR and G-TR, have the largest influence, namely +20% after a drying period of 45 hours. After a drying period of 6 days reducing G-LT results in +7.0% more twist deformation, reducing G-LR and G-TR resulted in + 25% more twist deformation. These values differ from the results calculated by Ormarsson, see [6].

Reducing the tangential hygro-expansional coefficient shows the most significant influence on the twist development. Reducing the tangential hygro-expansional coefficient with 50% of its reference value resulted in -125% twist deformation after a drying period of 45 hours and -55% after a drying period of 6 days. Ormarsson [6] concluded that reducing the tangential hygro-expansional coefficient shows the most significant influence on twist deformation. This is in agreement with the current results. Ormarsson calculated a decrease of – 40 % after a drying period of 6 days; this is also in line with current results.

10.3 Wood board -2: Influence of changing E, G, α on cup deformation

10.3.1 Reduced elastic moduli

Figure 10.4 shows the results of reducing the elastic moduli (E) with 50% of its reference value on cup deformation after a drying period of 45 hours. Figure 10.4 shows that reducing the tangential elastic modulus result in -18% decrease of cup deformation after a drying period of 45 hours. Reduction of the radial elastic modulus does not influence the cup deformation. Reducing the longitudinal elastic modulus resulted in a +6.0% increase of cup deformation after a drying period of 45 hours.

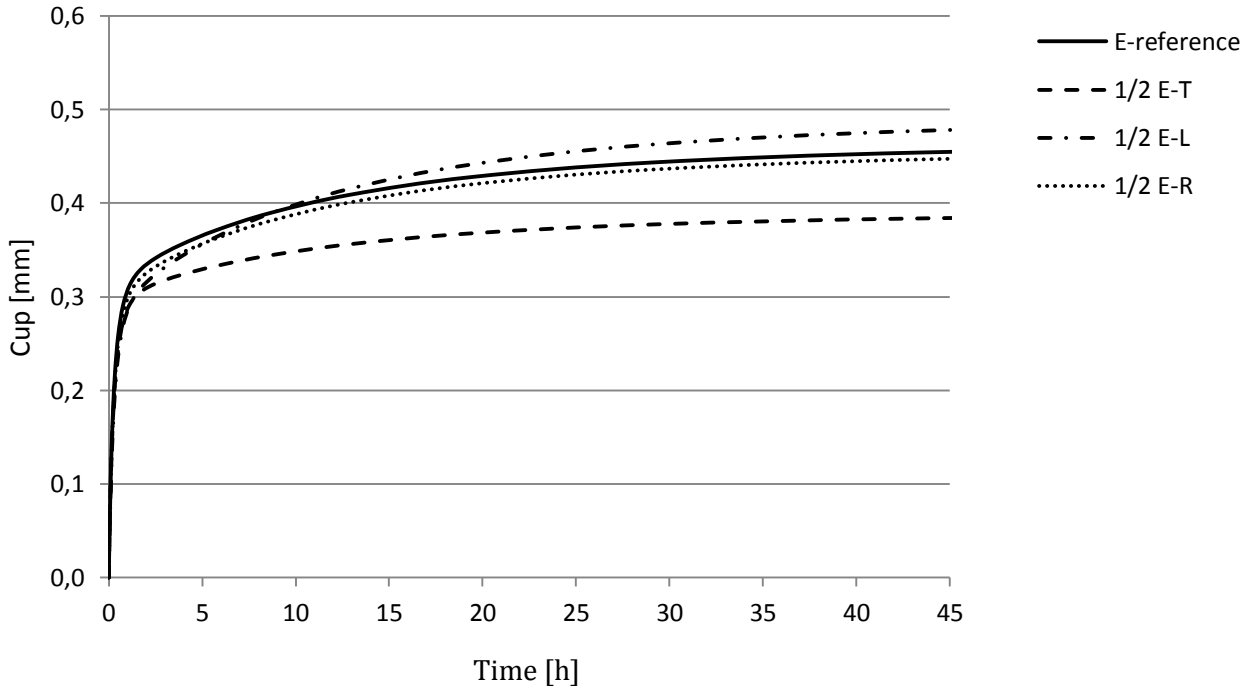

Figure 10.4: WB-2, influence of changing elastic moduli on cup deformation, step change of 70% - 30% RH after 45 h.

10.3.2 Reduced shear moduli

Figure 10.5 shows the results of reducing the shear moduli (G) with 50% of its reference value on cup deformation after a drying period of 45 hour. The influence of G-LR and G-TR compared to the reference value can be neglected. The influence of G-LT is significant larger, +15% after a drying period of 45 hours.

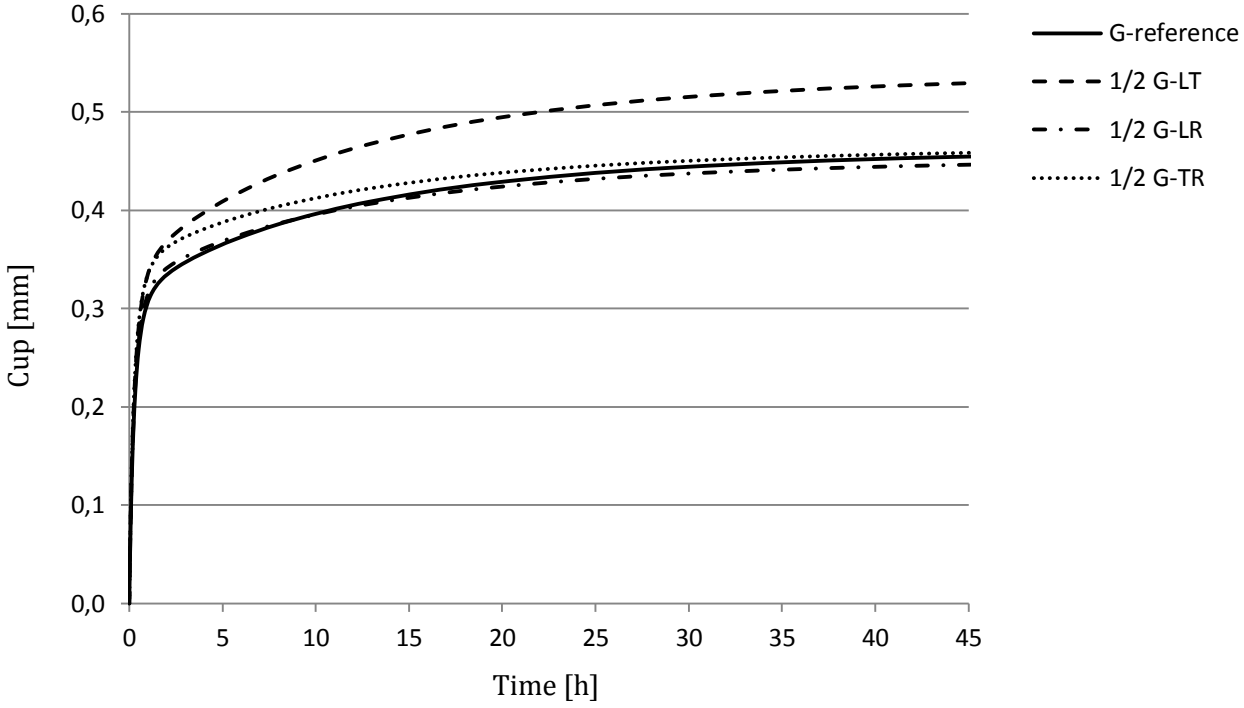

Figure 10.5: WB-2, influence of changing shear moduli on cup deformation, step change of 70% - 30% RH after 45 h.

10.3.3 Reduced hygro-expansion

Figure 10.6 shows the results of reducing the hygro-expansion coefficient (α) with 50% of its reference value on cup deformation after a drying period of 45 hours. The influence of the longitudinal hygro-expansion coefficient can be neglected. Reducing the radial hygro-expansion coefficient with 50% of its reference value resulted in +85.0% increase of cup deformation after a drying period of 45 hours. Reducing the tangential hygro-expansion coefficient with 50% of its reference value, results in -130% decreasing cup deformation after a drying period of 45 hours.

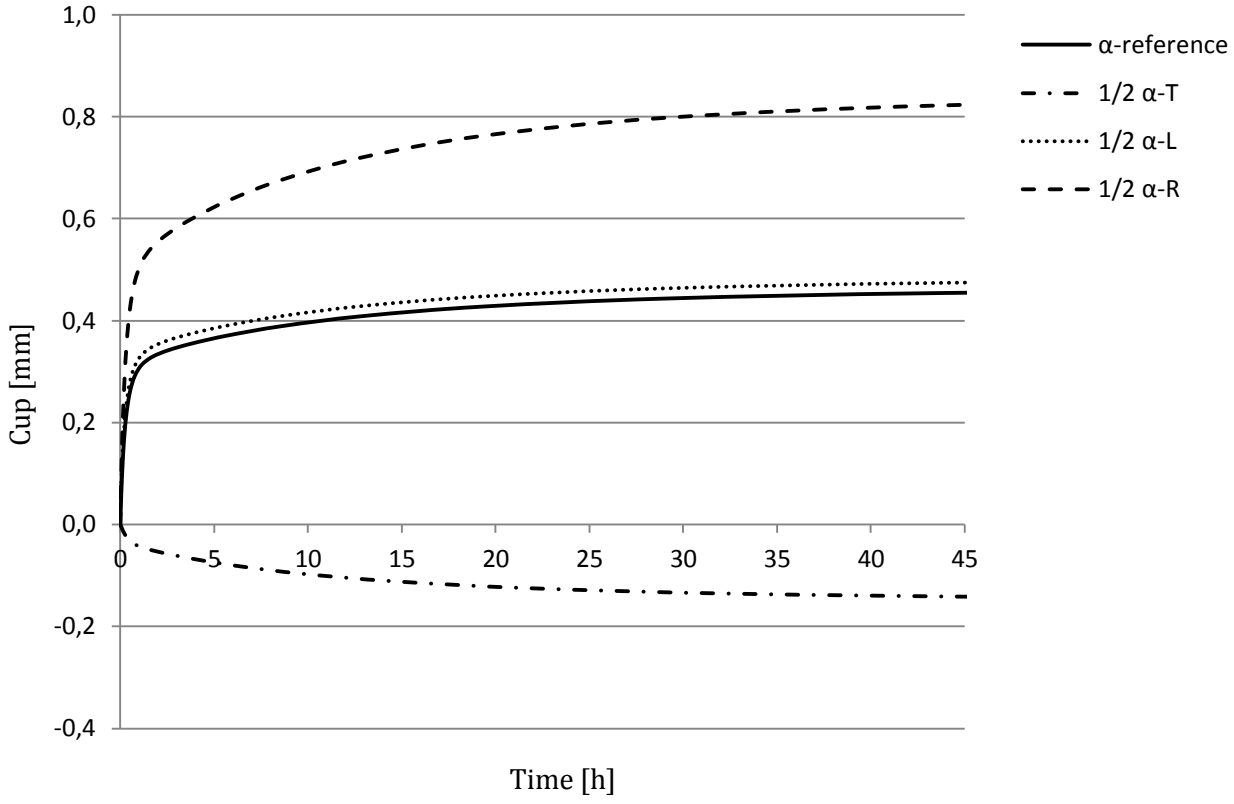

Figure 10.6: WB-2, influence of changing coefficient of hygro-expansion on cup deformation, step change of 70% - 30% RH after 45 h.

10.3.4 Conclusion

Reduction of the radial elastic modulus does not influence the cup deformation. Reducing the longitudinal elastic modulus resulted in +6.0% increase of cup deformation after a drying period of 45 hours. Reduction of the tangential elastic modulus resulted in -18% decrease of cup deformation after a drying period of 45 hours. No significant difference can be found after a drying period of 6 days which means that after 45 hours equilibrium has been reached.

Because cup deformation is mainly the result of a difference in tangential and radial mechanical properties, one would expect significant influence of these mechanical properties on cup deformation. In case of the tangential elastic moduli, this seems to correspond with our expectation (+18%). But reduction of the radial elastic modulus does not seem to have influence on this deformation. The reason for this behaviour can be found in the difference between radial and tangential elastic moduli for pine wood. By reducing the radial elastic modulus (1232 MPa) by 50%, this value (616 MPa) equals the tangential modulus which is 616 MPa. Consequentially, there is no longer any difference between radial and tangential stiffness. But, reduction of the tangential elastic modulus (616 MPa) by 50% results in a four times stiffer radial mechanical behaviour. This effect seems to be represented by figure 10.4. These calculated results differ from the results calculated by Ormarsson [6].

The influence of reducing G-LR and G-TR compared to the reference value can be neglected. The influence of G-LT is significant larger, +15% after a drying period of 45 hours. No significant difference has been found after a drying period of 6 days which means that after 45 hours equilibrium has been reached. These calculated results are in agreement with the results calculated by Ormarsson [6].

The influence of reducing the longitudinal hygro-expansion coefficient can be neglected compared to its reference value. Reducing the radial hygro-expansion coefficient with 50% of its reference value, results in +85.0% increase of cup deformation after a drying period of 45 hours. Reducing the tangential hygro-expansion coefficient with 50% of its reference value, resulted in -130% decreasing cup deformations. The tangential coefficient of hygro-expansion is mainly responsible for cup deformation. Reducing this value with 50% results in a significant decrease of cup deformations seems to be logical. Note that reducing the tangential hygro-expansion coefficient with 50% of its reference value resulted in cup deformation in opposite direction, see figure 10.6. This effect was also found by Ormarsson. The calculated results are in quantitative agreement with the results calculated by Ormarsson [6].

10.4 Wood board -2: Influence of changing E, G, α on bow deformation

10.4.1 Reduced elastic moduli

Figure 10.7 shows the results of reducing the elastic modulus (E) with 50% of its reference value on bow deformation after a drying period of 45 hours. Reduction of the longitudinal elastic modulus with 50% of its reference value results in -35% decrease of bow deformation after a drying period of 45 hours. Reduction of the tangential and radial elastic modulus with 50% of its reference value respectively results in +5% and +10% increase of bow deformation after a drying period of 45 hours.

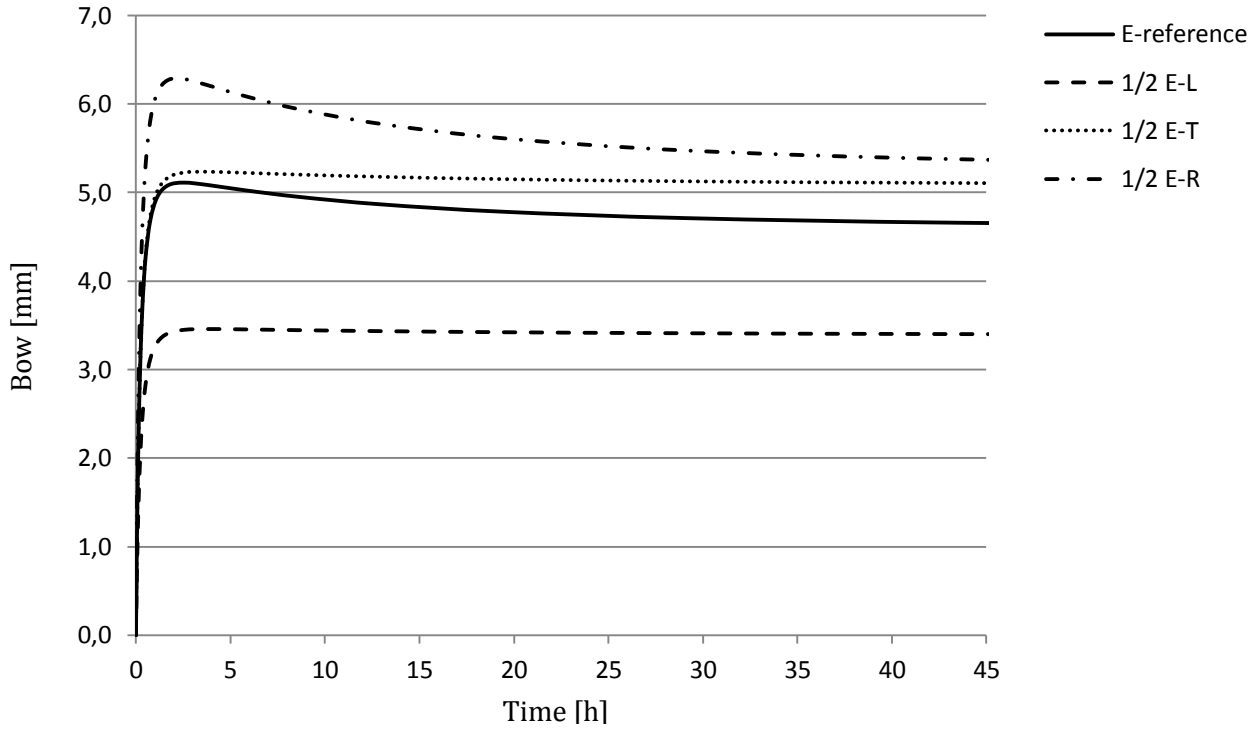

Figure 10.7: WB-2, influence of changing elastic moduli on bow deformation, step change of 70% - 30% RH after 45 h.

10.4.2 Reduced shear moduli

Figure 10.8 shows the results of reducing the shear modulus (G) with 50% of its reference value on bow deformation after 45 hours. Figure 10.8 shows that reducing the G-TR with 50% of its reference value does not influence bow deformation. Reducing the G-LT with 50% of its reference value results in -17% bow deformation and reducing the G-TR with 50% of its reference value results in +6% bow deformation after a drying period of 45 hours.

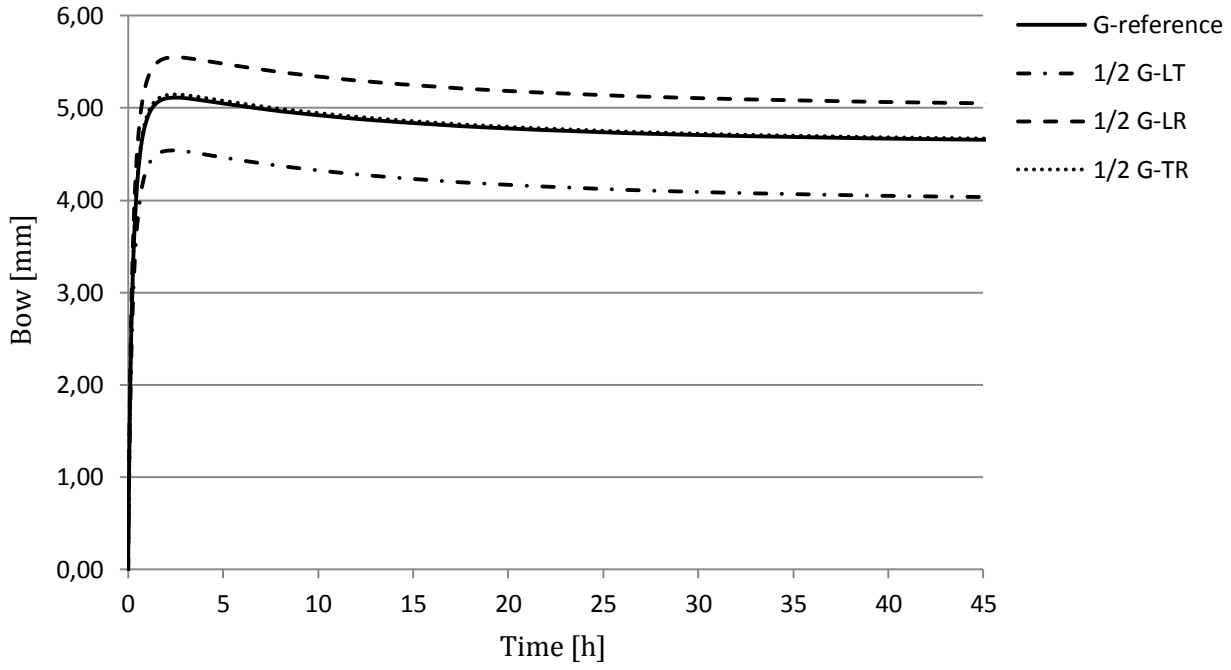

Figure 10.8: WB-2, Influence of changing shear moduli on bow deformation, step change of 70% - 30% RH after 45 h.

10.4.3 Reduced hygro-expansion

Figure 10.9 shows the results of reducing the hygro-expansion coefficient (α) with 50% of its reference value on bow deformation after a drying period of 45 hours. The longitudinal hygro-expansion coefficient does not influence bow deformation. Reduction of the radial coefficient of hygro-expansion with 50% of its reference value results in +45% bow deformation after a drying period of 45 hours. Reduction of the tangential coefficient of hygro-expansion seems to influence bow deformation quite significantly, -95.0% after a drying period of 45 hours.

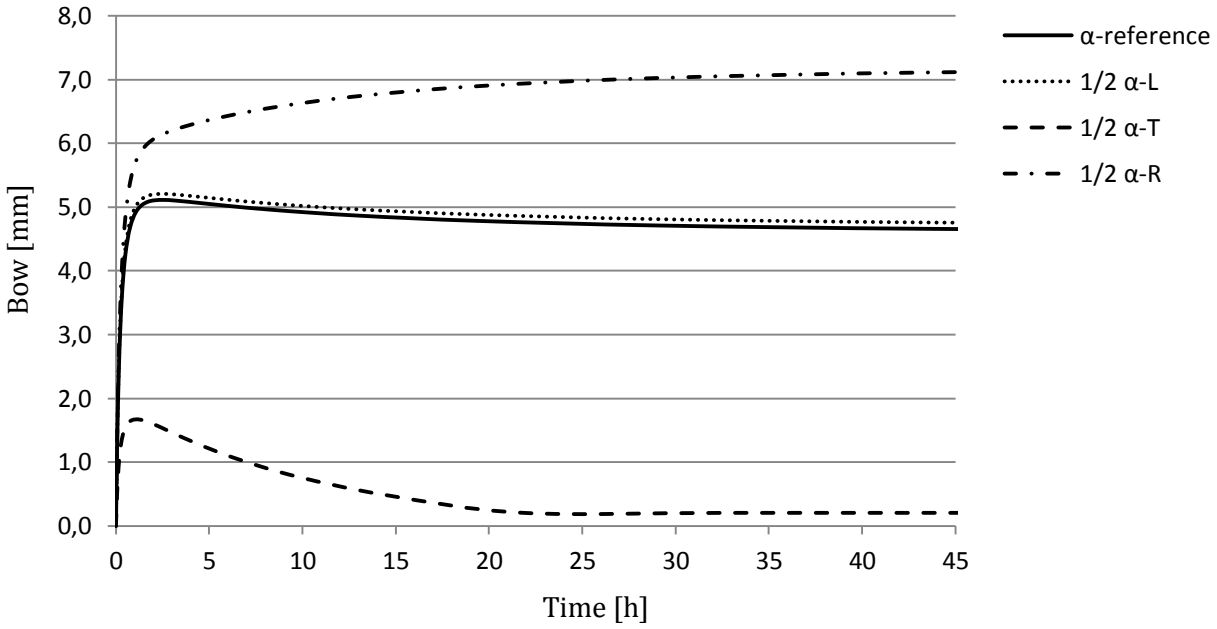

Figure 10.9: WB-2, influence of changing coefficient of hygro-expansion on bow deformation, step change of 70% - 30% RH after 45 h.

10.4.4 Conclusion WB-2, bow deformation:

Reducing the longitudinal elastic modulus with 50% of its reference value, results in a significant decrease of bow deformation of -35% after a drying period of 45 hours and -26% after a drying period of 6 days. Reduction of the radial elastic modulus with 50% of its reference value resulted in +10% increase of bow deformation and +15% after a drying period of 6 days. Reduction of the tangential modulus of elasticity with 50% of its reference value resulted in a relative small increase of +5% bow deformation and +10% bow deformation after a drying period of 6 days. Reducing the radial elastic modulus influences the short time behaviour. Reducing the radial elastic modulus gives rise to a steep rate of bow deformation in the first 2.5 hours. These results seem to differ with the result calculated by Ormarsson [6]. Ormarsson calculated the greatest influence by reducing the radial elastic modulus instead of the longitudinal elastic modulus. Although these results seem to be in contrast with the results calculated by Ormarsson, the longitudinal elastic modulus having most influence on bow deformation confirms the theory that bow deformation is the result of unequal local coordinate distribution over the cross section, resulting in unequal longitudinal stiffness distribution over the cross section, see chapter 9.

Reducing the G-TR with 50% of its reference value does not influence bow deformation. Reducing the G-LT with 50% of its reference value resulted in -17% bow deformation and after a drying period of 6 days this becomes -27% bow deformation. Reducing the G-TR with 50% of its reference value resulted in +6% bow deformation after a drying period of 45 hours and after a drying period of 6 days this becomes +9%. These results are in agreement with the calculations made by Ormarsson [6].

The longitudinal hygro-expansion coefficient does not influence bow deformation. Reduction of the radial hygro-expansion coefficient with 50% of its reference value results in +45% bow deformation after a drying period of 45 hours and +56% after a drying period of 6 days. Reduction of the tangential coefficient of hygro-expansion significantly influences bow deformation, -95.0% after a drying period of 45 hours and -90% after a drying period of 6 days. These results differ from the results calculated by Ormarsson [6]. Ormarsson concludes that reducing the longitudinal hygro-expansion coefficient leads to a significant reduction of bow deformation (-100%). Although these results seem to be in contrast with the results calculated by Ormarsson, the longitudinal hygro-expansion coefficient having most influence on bow deformation confirms the theory that bow deformation is the result of unequal local coordinate distribution over the cross section resulting in unequal longitudinal hygro-expansion over the cross section, see chapter 10.

10.5 Wood board -3: Influence of changing E, G, α on crook deformation

Reducing the longitudinal, tangential and radial elastic moduli seems to have no effect, compared to the reference value. Also, reduction of the shear moduli does not seem to affect the crook deformation. Figure 10.10 show that only a reduction of the radial hygro-expansion coefficient significantly influences crook deformation, -61% after a drying period of 45 hours.

10.5.1 Conclusion

Reduction of the elastic moduli and shear moduli seems to have no effect on the crook deformation. The only mechanical property influencing this crook behaviour seems to be the radial coefficient of hygro-expansion. The radial coefficient of hygro-expansion shows a significant reduction of crook deformation, -61% after a drying period of 45 hours. This reduction of -61% is reached in the first 5 hours and will remain unchanged for the rest of the drying period. Because the direction of deformation equals the radial direction, one would expect that reducing the radial stiffness would increase the crook deformation in this direction, but the very opposite seems to occur. Ormarsson [6] did not perform any calculations on the influence of reduced material properties with respect to crook deformation.

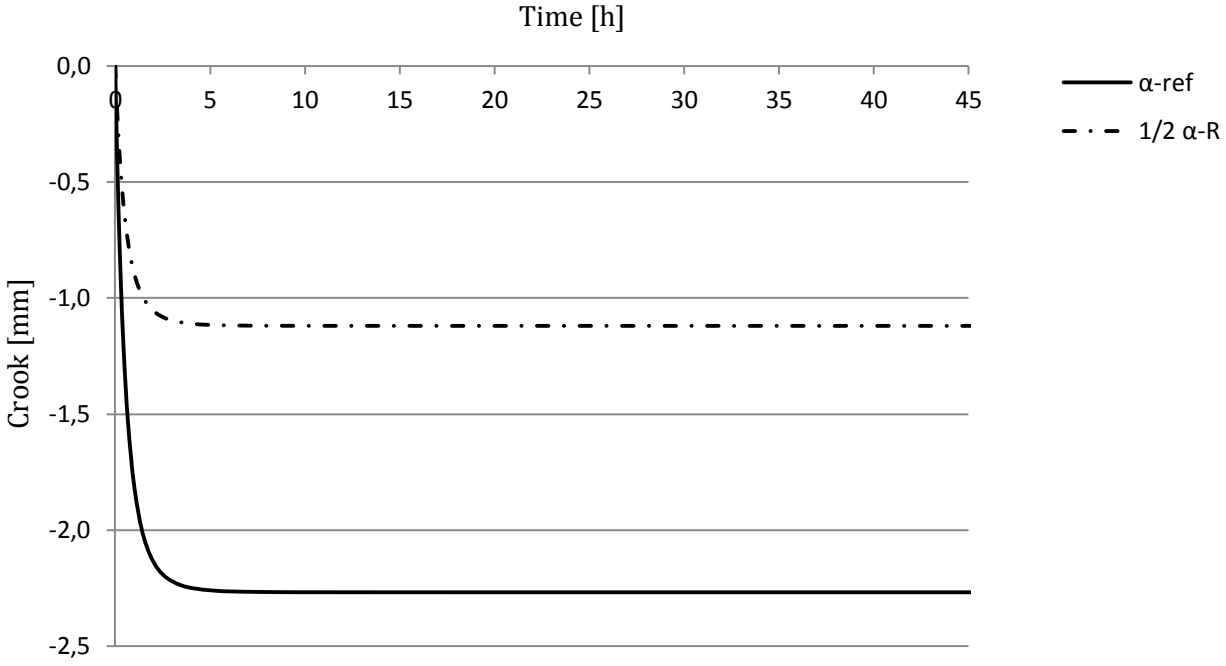

Figure 10.10: WB-3, influence of changing co-efficient of hygro-expansion on crook deformation, step change of 70% - 30% RH after 45 h.

11 Influence of gesso layer on shape stability

11.1 Introduction

A panel painting is a painting made on a wooden panel. It is not well known, but a lot of famous paintings are actually panel paintings, such as The Mona Lisa by Leonardo Da Vinci, Assunta by Titian, Primavera by Botticelli and Samson and Delilah by Rubens. Artists had clear reasons to choose wood instead of canvas, see paragraph 11.2: *short history of panel paintings.* One of the main reasons was availability and stability. Before an artist could start his painting he had to prepare the panel with several layers of gesso (mixture of hide glue, gypsum or sometimes ground chalk and water) ossein (lime made from bones) or other materials. After several layers and considerable sanding, the panel surface became perfectly smooth if properly done.

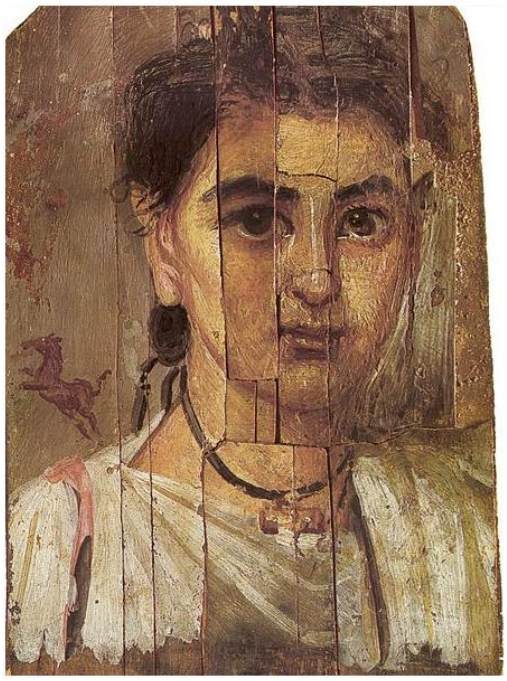

Figure 11.1: *Portrait of a boy from Fayum, National Museum of Warsaw, second half of 2nd century, painter is unknown.*

The Portrait of a boy from Fayum was found in an Egyptian tomb, at the oasis of Al-Fayyu, see figure 11.1. It is part of a series of tablet paintings, which were made during a period from 1st to the 4th century. The tablets show the head and shoulders of the dead person. The tablets where placed on the coffins of wealthy persons, see [39].

This chapter discusses the influence of a gesso layer on the shape stability of wood boards. The numerical models of wood board -1 and wood board -2 from the previous chapter are expanded with a gesso layer. The influence of this gesso layer on shape stability will be discussed for the same drying conditions as previous in chapter 9 and 10 (70% RH to 30% RH).

11.2 Short history of panel paintings [39]

In ancient Greece and Rome, wood was used as a support for encaustic paintings. Encaustic paintings are paintings made with colours that are dissolved in molten wax. Also, the first Byzantine icons, made in the 6th century, were painted on wood with the same encaustic technique. Orthodox churches, in the late 20th century, were still using the same technique to make their icons. Icons are religious pictures, mostly painted on wood, inextricably bound with the church. Until the Gothic period, painting on wood was not common in western and northern Europe. However, altar pieces made in this period where painted on wood. Painting on wood during the 13th and 14th centuries has proven to be practical. Most of the paintings from this period and the 15th century that have survived are panel paintings. They are less vulnerable to damage than canvas paintings. From the 15th century onwards, canvas became more popular as a supporting material for paint. During the 16th century altar pieces had less gilding (gold), so it was not necessary to use a solid wooden and perfectly flat panel any longer. Canvas is also relatively cheap, light and portable. These factors made canvas more popular. In the 16th century, in Venice Italy, big wall paintings where almost always painted on canvas. The small paintings where still made on wood support. Painters from Flanders and the Netherlands kept using the wooden panels for their landscapes and portraits. With the increase in international trade, new wood species came to Europe, (mahogany etc.) which encouraged the continued use of wood. In the 19th century, some artists, such as William Blake (1757-1827) and Samuel Palmer (1805-1881), revived the medieval and early Renaissance techniques of wood painting. This technique of painting did not suit other artists such as Impressionists and Post-Impressionists. 20th century artists were, due to industrialisation, able to use manufactured wood panels, such as block board, plywood and hardboard. When it comes to conservation, or stabilisation of panel paintings, it was opined that: as a treatment, it is better to do nothing (quote from Greenwich, England conference on Comparative Lining Techniques), the first conference discussing the treatment of panel paintings. The reasons for an artist to paint on wood are tempered by cost, practicality and availability. It is unknown why some famous painters switched from one medium to another , such as Titian's Assunta (panel) and Titian's Pesaro Altar pieces (canvas), Botticelli's Primavera (panel) and Botticelli's Birth of Venus (canvas) as well as Ruben's Samson and Delilah (panel) and Ruben's Garden of love (canvas). Why these painters used both in the same period will probably never be known. In the history of panel painting conservation, events occurred that are still not understood to this day. For example, hundreds of Renaissance panel paintings were sent to St. Petersburg, Russia and transferred to canvas. Every century and every decade ignites further thought. Compare the book written by Rembrandt titled: "Inleyding tot de Hooge Schoole der Schilderkunst", (An introduction to the higher school of painting), compared to the invention and use of X-ray scanning, optical laser technology and dendrochronology science, during the 20th and 21st centuries, a lot of changes have occurred. However, conservators and scientists are still not able to answer important questions. Questions such as: what happens to a panel painting, if it has been preserved for years in a constant condition and then exposed to slow or even rapid cycles of change in relative humidity? What happens if a panel painting is moved from a dry climate, where it has been for years, then suddenly moved to a climate controlled museum? Even the writers of the document from the Getty Institutions are unable to answer these questions, because no one has ever investigated this topic in a scientific way, see [39].

11.3 Mechanical behaviour of gesso

Gesso is a mixture of hide glue, gypsum or sometimes ground chalk and water. Different artist have different recipes for making gesso. Sometimes inert materials as zinc and clay are incorporated. The ratio of inert materials to hide glue has a great influence on the mechanical behaviour of gesso. This ratio of inert materials is called the PVC ratio (Pigment Volume Concentration). The higher the pigment volume ratio, the weaker, stiffer and less hygro-expansionally responsive the gesso becomes. Consequentially, more hide glue means stronger, more elastic and more hygro-expansional responsive the gesso becomes, see figure 11.2 [39].

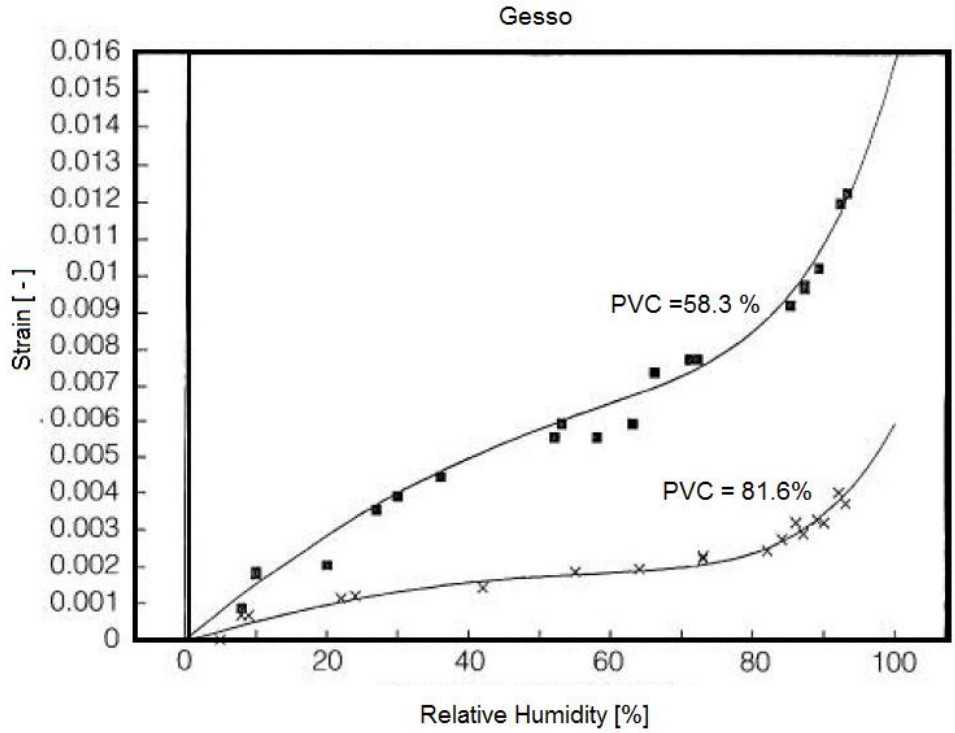

Figure 11.2: Influence of pigment volume ratio on strain (Getty Institute).

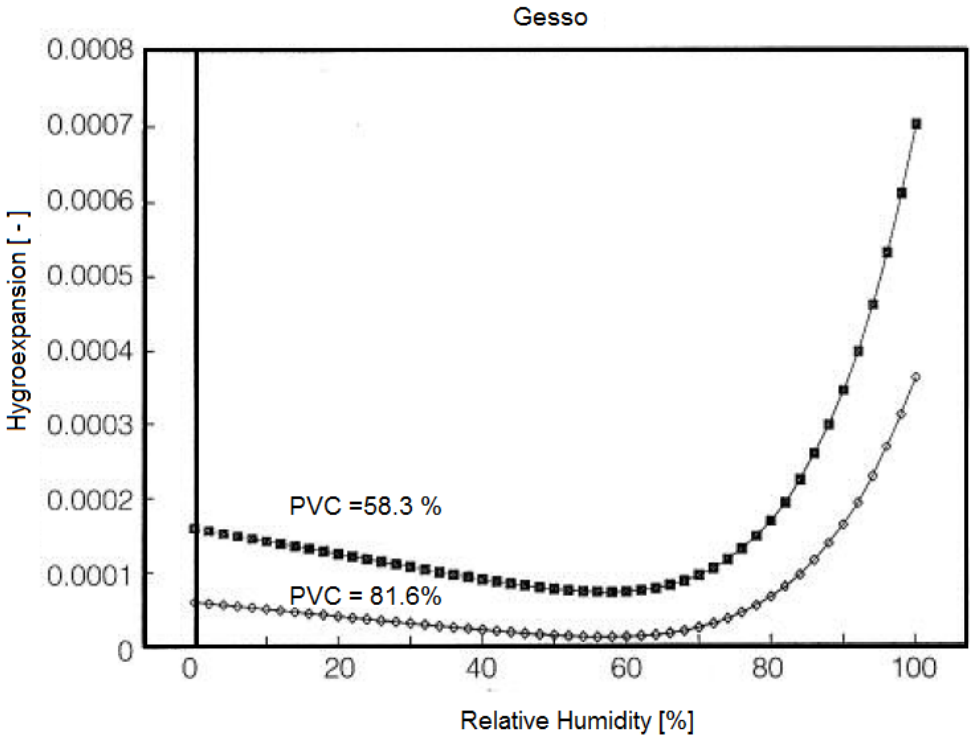

Figure 11.3: Influence of PVC on hygro-expansion (Getty Institute).

Figures 11.2 and 11.3, respectively, represent the behaviour of two different pigment volume ratio values on strain and hygro-expansional behaviour of gesso. Figure 11.2 shows that a pigment volume ratio of 58.3% has a maximum change of 1.5% over the entire relative humidity range. The higher pigment volume ratio mixture (81.3%) has a maximum change of 0.6% over the entire relative humidity range.

Overall, it can be concluded that the pigment volume ratio affects the mechanical behaviour of gesso quite significantly. The mechanical behaviour of gesso is also affected by other aspects, such as light and ageing. This is outside the scope of this master thesis. More information can be found in: Structural Conservation of Panel Paintings [39].

This chapter discusses the influence of the elastic modulus (E) and diffusivity of gesso (D) on shape stability of wood board -1 and wood board -2, see figure 11.4.

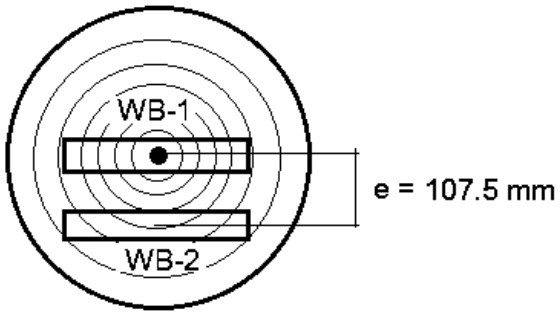

Figure 11.4: Wood board stem orientation.

11.4 Dimensional and mechanical properties

Figure 11.5 and table 11.1 respectively represent the dimension of the wood boards and the structural parameters. The type of wood used is pine. Material data of pine is directly adopted from chapter 10.

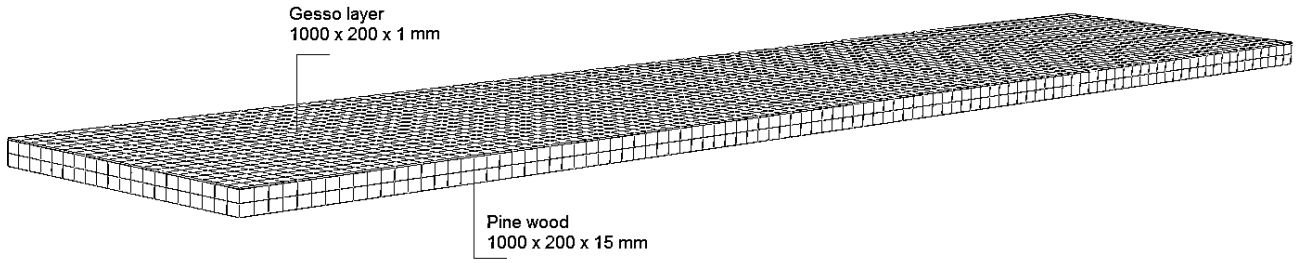

Figure 11.5: Dimensions WB-1 and WB-2.

Table 11.1: Dimensions WB-1, WB-2 and gesso layer.

	Spiral grain [degrees]	Conical angle [degrees]	Pith distance from centre [mm]	Dimensions wood board [mm]	Dimensions gesso layer [mm]
WB-1	-4,0°	-0,5°	0	1000 x 200 x 15	1000 x 200 x 1
WB-2	-0.0°	0°	-107.5	1000 x 200 x 15	1000 x 200 x 1

Mechanical properties of Gesso:

Density (ρ) = 1300 $[kg \cdot m^{-3}]$
Elasticity (E) = 760 $[MPa]$ based on 58.3% PVC
Poisson's ratio (ν) = 0.481
Diffusivity (D) = 104e-6 $[m^2 \cdot h^{-1}]$
Yield strain (ε_y) = 0.0025 [%]

Table 11.2: Hygro-expansion of gesso.

Relative Humidity [%]	Hygro expansion
0	6.0e-05
10	5.0e-05
20	4.1e-05
30	3.1e-05
40	2.0e-05
50	1.0e-05
60	1.1e-05
70	3.2e-05
80	7.1e-05
90	1.6e-04
100	3.5e-0.4

The material properties of gesso are adopted from: The Getty institute and the Getty Museum, Structural Conservation of Panel Paintings "Proceeding of a symposium at the J.Paul Getty Museum" April 1995, Part 6: History and Conservation, Scientific Research see [39].

11.5 Influence of thickness gesso layer on moisture transport

Figure 11.6 shows the effect of a changing gesso layer thickness on moisture transport through the wood board. Figure 11.6 represents the moisture content in the centre of the wood board. Figure 9.41 clearly shows that a thicker gesso layer slows down the process of moisture release. This is not surprising, because a thicker layer gives rise to a longer distance for the moisture to travel before reaching the surface.

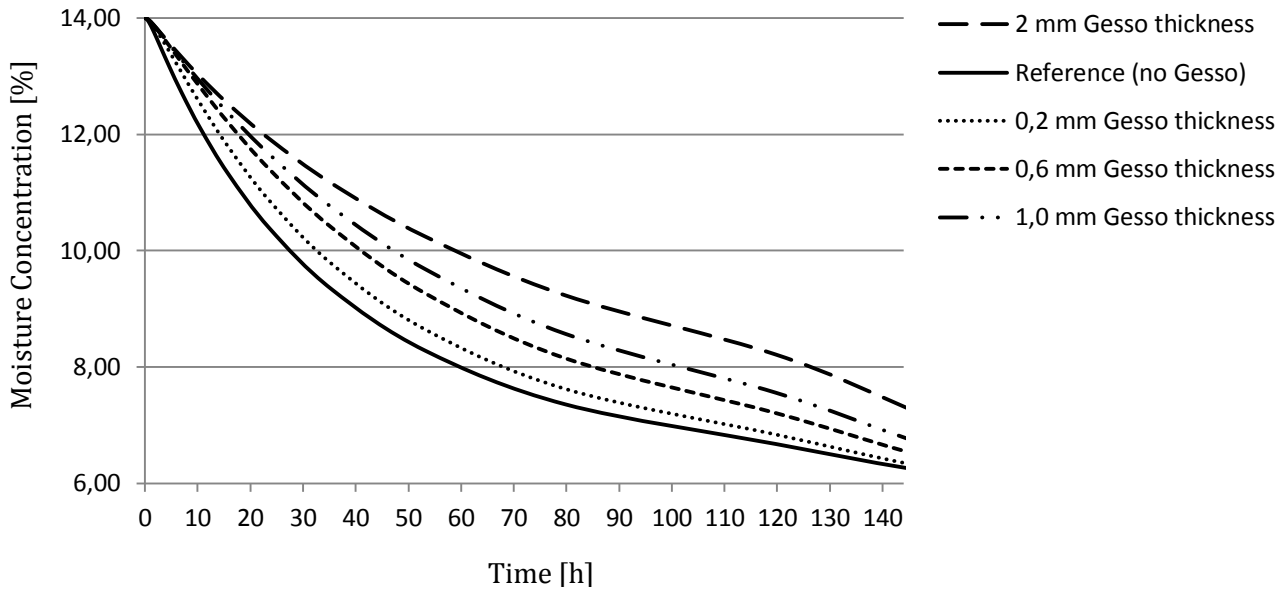

Figure 11.6: Influence of thickness of gesso layer on moisture transport.

11.6 Influence of changing elastic modulus of gesso on shape stability

11.6.1 Wood board -1: Twist deformation

Figure 11.8 shows the influence of changing elastic moduli on twist deformation of a 1.0 mm thick gesso layer after a drying period of 24 hours. It looks like figure 11.8 shows first negative twisting (clockwise) and after 4 hours of drying positive twisting (counter clockwise), see figure 11.7. This changing of twist direction is most unusual. Consequentially figure 11.8 showing pure twist deformation, is most unlikely. Note that the lines of figure 11.8 only represent the angular rotation between the pith and the wood board edge as shown by figure 11.7. This means that negative rotation (clockwise) does not necessarily mean twist deformation; it could also represent cup deformation. Proceeding research has shown that this is indeed the case, see figure 11.8.

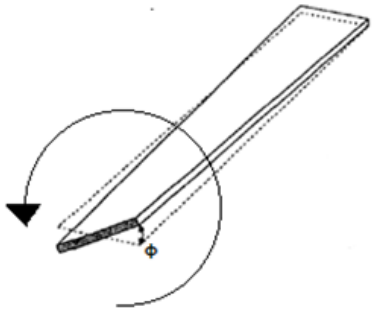

Figure 11.7: Counter clockwise twist

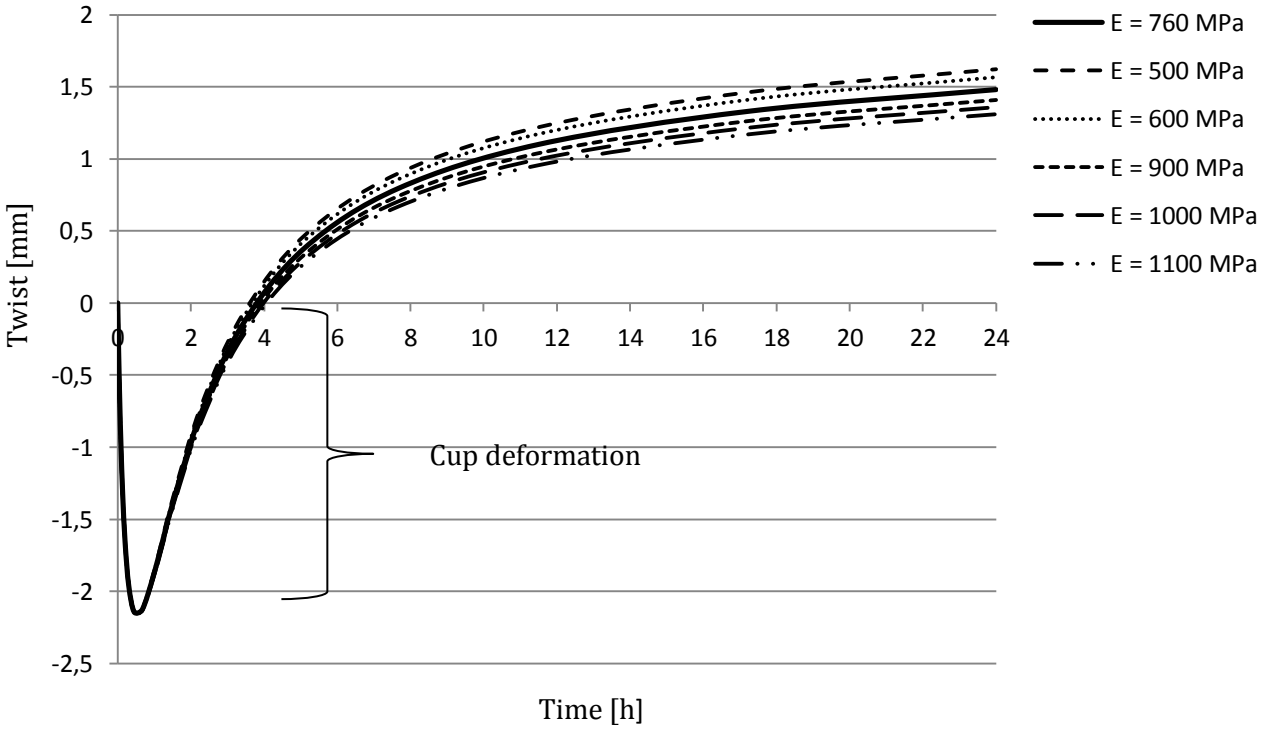

Figure 11.8: WB-1, influence of elasticity gesso on twist deformation.

Figure 11.8 shows between 0 and 2 hours increasing “cup” deformation because, the gesso layers slow down the outflow of moisture. Between 2 and 4 hours, this cupping effect decreases and after 4 hours ”twist” deformation begins to develop.

Figure 11.8 clearly shows that an increasing stiffness of the gesso layer results in a decrease of twist deformation. The solid line represents the reference elastic moduli of the gesso layer, which is 760 MPa. The reference layer shows a twist deformation of 2.6° after a drying period of 6 days. The same wood board, without the gesso layer, shows a twist deformation of 3.4° after a drying period of 6 days. This means 30% constraint of twist deformation due to 1.0 mm gesso layer after a drying period of 6 days.

11.6.2 Wood board -1: Bow deformation

Figure 11.9 shows the development of bow deformation. Notice that wood board -1 did not show bow deformation without the gesso layer, see chapter 9. Figure 11.9 shows strong, short time behaviour. The first 2 hours it shows a maximum bow deformation of 35 mm. After these first 2 hours it slowly reaches its equilibrium state which is much smaller, between 18 mm and 10 mm of bow deformation.

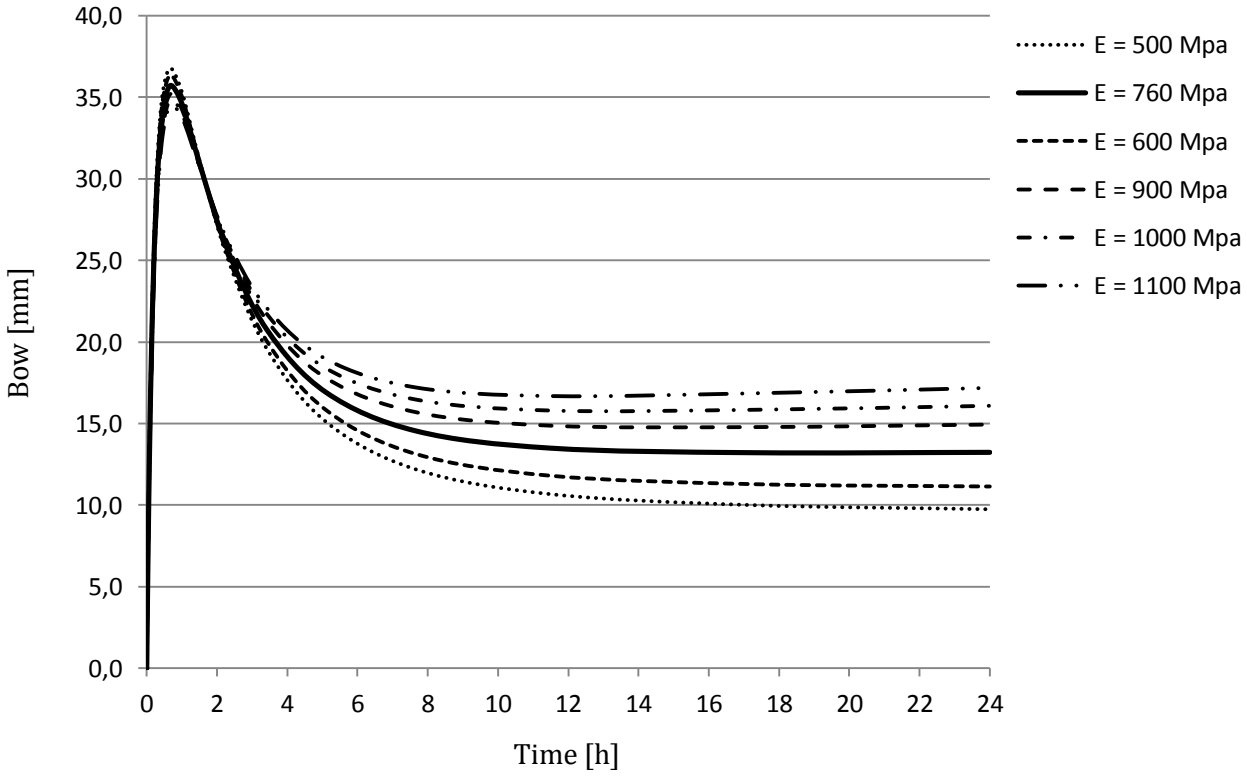

Figure 11.9: WB-2, influence of elasticity gesso on bow deformation.

11.6.3 Wood board -2: Cup deformation

Figure 11.10 represents the influence of the elastic moduli of gesso on cup deformation. The reference cup deformation is represented by the 760 MPa solid line, which shows a final cup deformation of 2.9 mm after a drying period of 1 day and 0.9 mm after a drying period of 6 days. Without a gesso layer, the same wood board shows an average cup deformation of 0.5 mm after a drying period of 6 days. Figure 1.10 shows a short time maximum cup deformation of approximately 3.5 mm and progressive recovery until equilibrium has been reached. Figure 11.10 show that a stiffer gesso layer results in a greater cup deformation

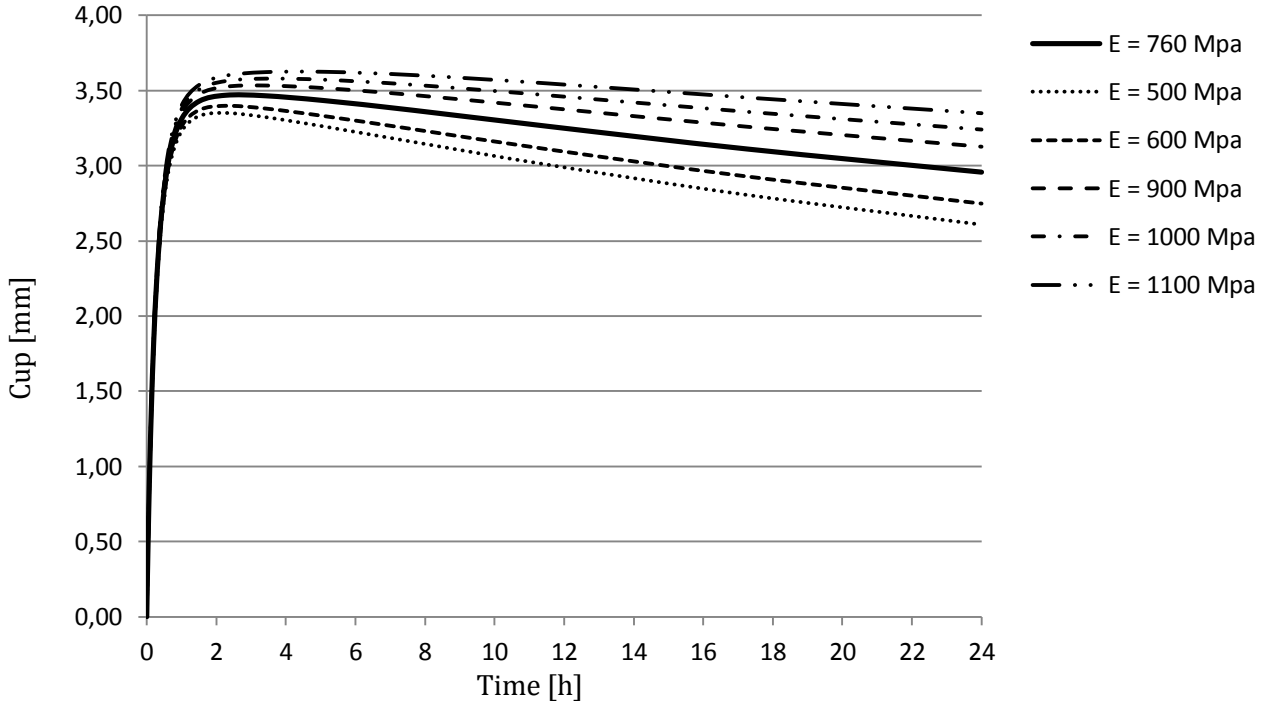

Figure 11.10: WB-2, influence of elasticity gesso on cup deformation.

11.6.4 Wood board -2: Bow deformation

Figure 11.11 shows the effect of changing the elastic modulus of the gesso layer on bow deformation of WB-2. Figure 11.11 clearly shows that changing the elastic modulus of the gesso layer does not influence the short time maximum behaviour and final equilibrium behaviour very much. The maximum short time bow deformation lies around the 34 mm and the final equilibrium bow deformation lies around the 25 mm after a drying period of 24 hours.

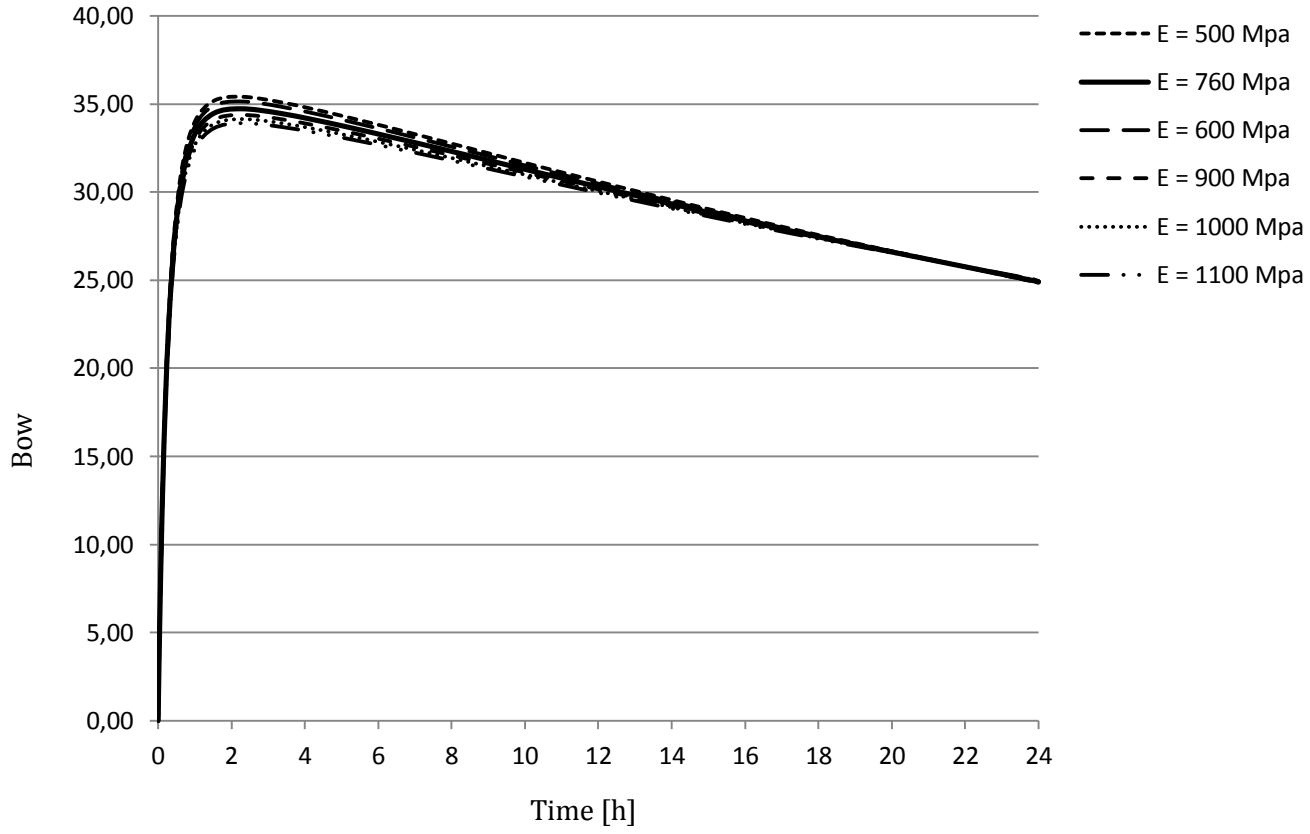

Figure 11.11: WB-2, influence of elasticity gesso on bow deformation.

11.6.5 Conclusion

Applying a 1.0 mm thick gesso layer on a sawn wood board seems to have a great influence on the shape stability. As a consequence of a gesso layer, unequal moisture transfer between the top and bottom surface develops.

In case of wood board -1, a stiffer gesso layer seems to reduce the twist. Applying a gesso layer on wood board -1 results in cup and twist deformation. Because the gesso layer slows down the moisture transport in one direction under rapid drying conditions, the wood board develops a tendency to cup. After 2 hours and continuing drying, this short time cup behaviour slowly disappears and after 4 hours wood board -1 slowly starts to develop twist deformation. Without a gesso layer wood board -1 would not show any cup deformation at all, only twist deformation. The reference layer shows a twist deformation of 2.6° after a drying period of 6 days. The same wood board, without the gesso layer, shows a twist deformation of 3.4° after a drying period of 6 days. This means 30% constraint of twist deformation due to 1.0 mm gesso layer after a drying period of 6 days.

Increasing the elastic moduli resulted in a greater bow deformation in case of wood board -1. Figure 11.9 shows strong, short time behaviour. In the first 2 hours it shows a maximum bow deformation of 35 mm. After these first 2 hours it slowly reaches its equilibrium state, which is much smaller, between 18 mm and 10 mm of bow deformation.

The reason for this strong short time bow deformation (between t = 0 and t = 2 h.) of figure 11.9 can be found in the diffusion properties of pine wood. Because of the longitudinal direction of the cellular structure, the diffusivity in this direction, compared to the radial and tangential direction, is approximately 10 times stronger. If one takes a good look at figure 9.3, one will notice that the pith is slightly drawn inside due to this relatively strong longitudinal diffusivity. In the case of figures 9.3 there is no gesso layer applied, consequentially the pith's location is in the centre of the wood board. In case of figure 11.9, due to the gesso layer, the pith is located slightly out of centre. Because the wood board is exposed to a strong drying situation from 70% to 30% relative humidity and because of the relatively strong longitudinal diffusivity, a bending moment develops. This explains the strong, short time bow deformation. With progressive drying of the wood board, this deformation slowly recovers until it reaches its final equilibrium state.

Figure 11.10 show that a stiffer gesso layer results in a greater cup deformation. Because of the unequal moisture transfer between top and bottom as a result of the gesso, a relatively strong short time-cup deformation develops of ~ 3.5 mm after a drying period of 2 hours. After 2 hours, with continuous drying, this strong cup effect decreases to 2.9 mm after 24 hours and 0.9 mm after 6 days of drying. Without a gesso layer, the same wood board shows an average cup deformation of 0.5 mm after a drying period of 6 days. These two values clearly approach each other.

Figure 11.11 shows that changing the elastic modulus of the gesso layer does not influence the short time maximum behaviour and final equilibrium behaviour very much. The maximum short time bow deformation lies around 34 mm and the final equilibrium bow deformation lies around 25 mm. Note that the maximum bow deformation of wood board -1 and wood board -2 are the same (35 mm), regardless of the fact that both wood boards have completely different growth

ring orientations. It seems that the growth ring orientation has no effect on the short time bow deformation. This difference in growth ring orientation between wood board -1 and wood board -2 becomes clear when looking at the recovery phase. Wood board -1 without a gesso layer does not bow at all shows a strong ability to recover, see figure 11.9. Wood board -2 which does show bow deformation without a gesso layer shows significant less recovery. This effect is in agreement with the expectations.

11.7 Influence of changing the diffusivity of gesso on shape stability

11.7.1 Wood board -1: Twist deformation

Figure 11.12 shows the effect of a changing diffusivity of the gesso layer on twist deformation of wood board -1. Figure 11.12 shows that a high diffusivity results in a faster twist development and that a lower diffusivity results in a slower twist development, all with respect to a drying period of 24 hours.

Note that the lines of figure 11.12 only represent the angular rotation between pith and wood board edge as shown by figure 11.7. This means that negative rotation does not necessarily mean twist deformation; it could also represent cup deformation. Further research has shown that this is indeed the case; see also paragraph 11.6.1, figure 11.8 and figure 11.12 for more information. Because the gesso layer slows down the moisture transport in one direction under rapid drying conditions, the wood board develops a tendency to cup. Depending on the diffusion coefficient, between the 30 min. and 2 hours as a result of continuing drying this short time cup behaviour slowly disappears and twist deformation starts to develop.

It has been calculated that the average twist deformation after 6 days is at approximately2.5°. This is in agreement with the result as presented in paragraph 11.6.1 which calculated a twist deformation of 2.6°.

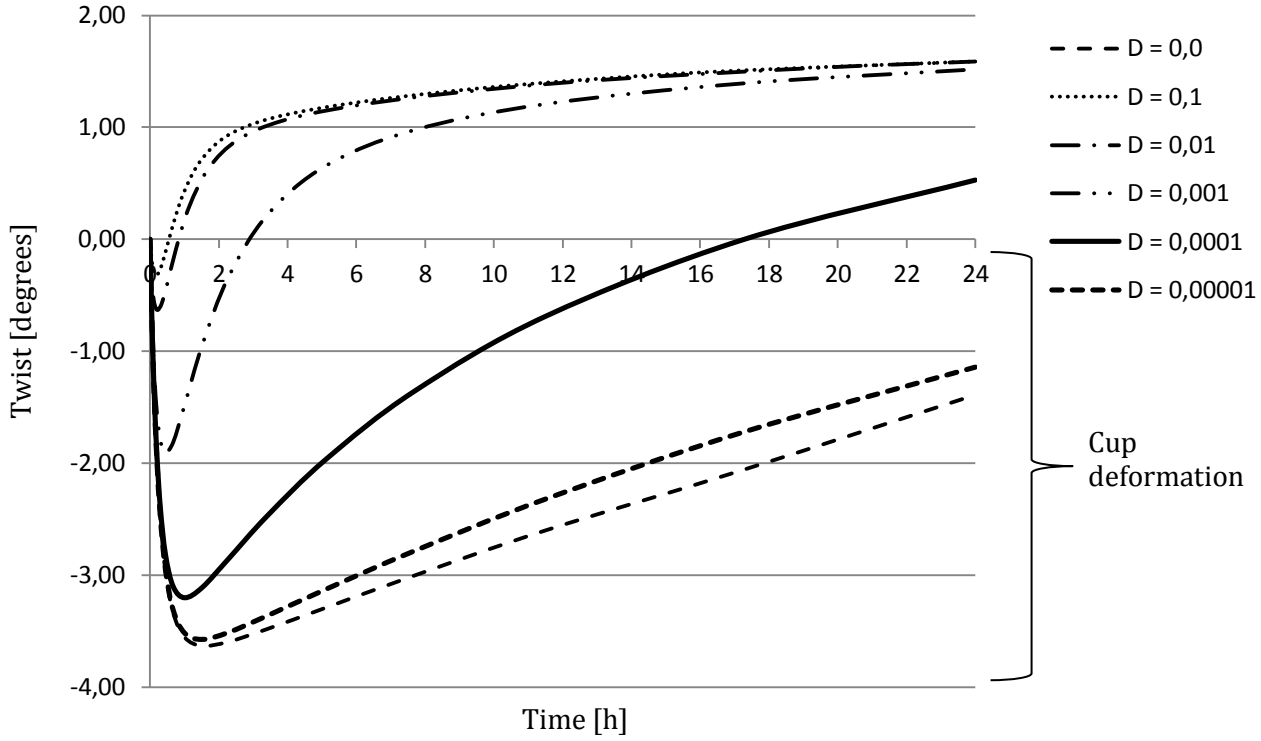

Figure 11.12: WB-1, influence of diffusivity gesso on twist deformation.

11.7.2 Wood board -2: Cup deformation

Figure 11.13 shows the influence of changing diffusivity of gesso on cup deformation. Figure 11.13 shows that increasing the diffusivity results in smaller maximum short time behaviour and decreasing the diffusivity results in increasing the maximum short time behaviour. Comparing the cup behaviour of wood board -2 with and without a gesso layer (see 10.3.2), applying a gesso layer results in a significant greater final cup deformation. Figure 11.13 shows that decreasing the diffusivity results in slow recovery of this short time behaviour. Increasing the diffusion coefficient consequentially holds faster moisture transport through the gesso layer, resulting in smaller cup deformation. Comparing these results with the reference board from paragraph 10.3, it can be concluded that applying a gesso layer significantly influences the final cup deformation.

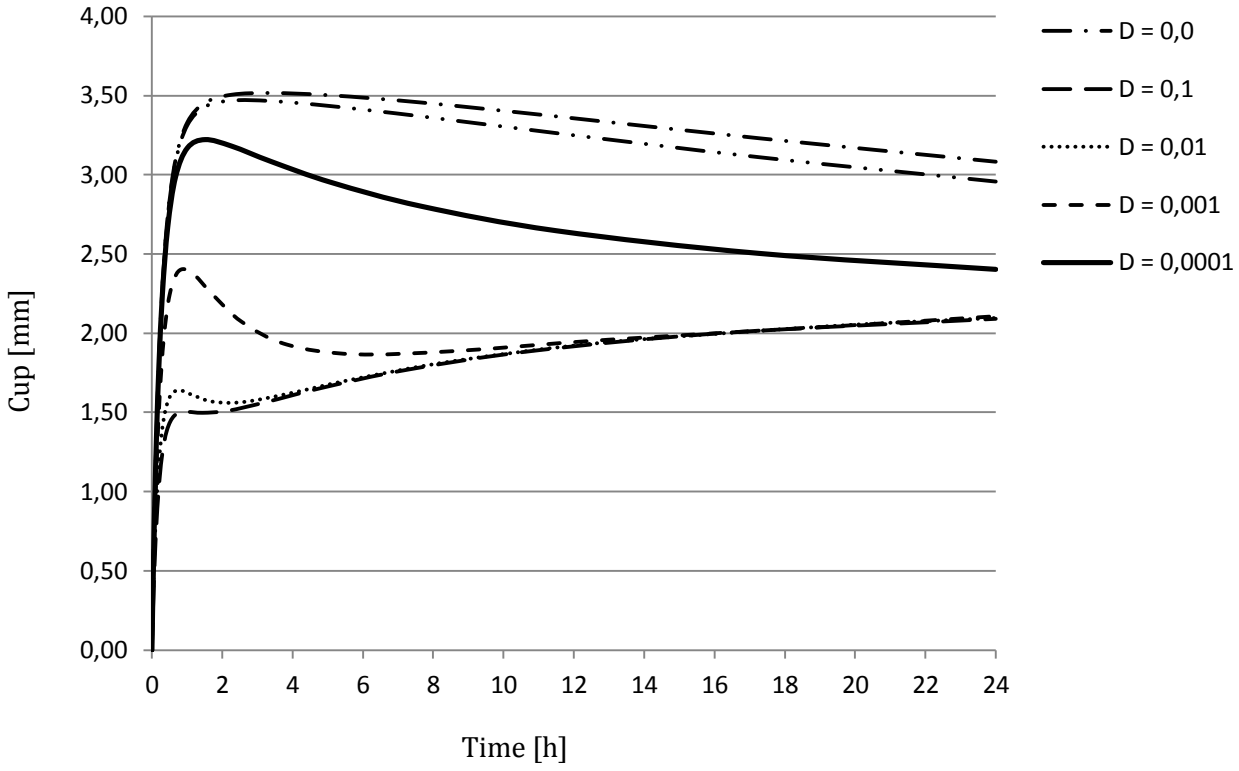

Figure 11.13: WB-2, influence of diffusivity gesso on cup deformation.

11.7.3 Wood board -2: Bow deformation

Figure 11.14 shows the results of changing diffusivity on bow deformation. Figure 11.14 shows that decreasing the diffusion coefficient results in an increment of short time maximum bow deformation. Figure 11.14 also shows that a decrement of diffusivity results in a slower recovery of this short time deformation. Comparing these results with the reference board from paragraph 10.4, both calculations show a final bow deformation of ~ 5.0 mm after a drying period of 6 days.

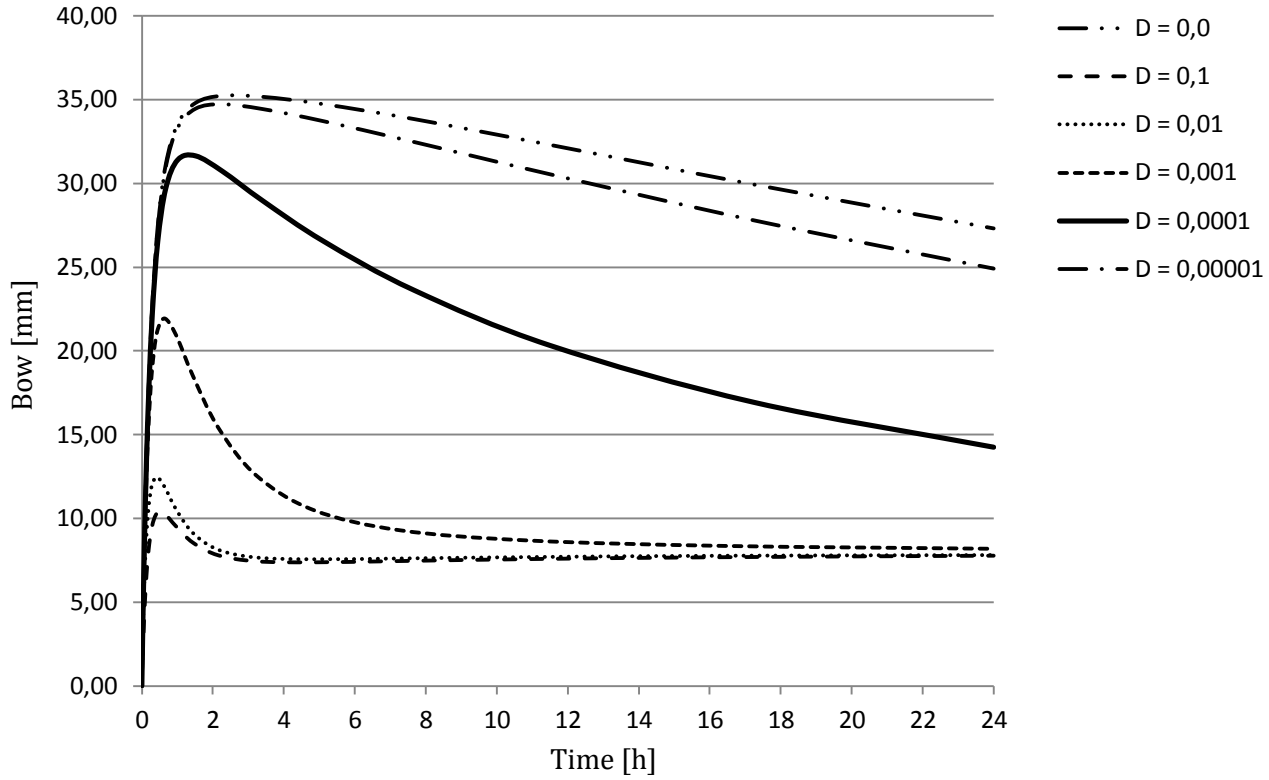

Figure 11.14: WB-2, influence of diffusivity gesso on bow deformation.

11.7.4 Conclusion

Changing the diffusivity of the gesso layer of wood board -1 shows that a high diffusivity results in a faster twist development and that a lower diffusivity results in a slower twist development. Because the gesso layer slows down the moisture transport in one direction under rapid drying conditions, the wood board develops a tendency to cup. Depending on the diffusion coefficient, this is between 30 min. and 2 hours. As a result of continuing drying this short time cup behaviour slowly disappears and twist deformation starts to develop, for more information see paragraph 11.6.1, figure 11.8 and figure 11.12. It has been calculated that the average twist deformation after 6 days is approximately 2.5°. This is in agreement with paragraph 11.6.1 which calculated a twist deformation of 2.6°.

Comparing the cup behaviour of wood board -2 with and without a gesso layer (see 10.3.2), applying a gesso layer results in a significantly greater final cup deformation compared to the reference wood board from paragraph 10.3.

Decreasing the diffusion coefficient results in an increment of short time maximum bow deformation and in a slower recovery of this short time deformation. Comparing these results with the reference board from paragraph 10.4, both calculations show a final bow deformation of ~ 5.0 mm after a drying period of 6 days.

The effect of changing the diffusion coefficient shows a significantly greater effect than changing the elastic moduli of the gesso layer on the shape stability. A relatively small diffusivity of the gesso layer always resulted in stronger short time behaviour and relatively slow recovery of this process. Although changing the diffusion coefficient does affect the shape stability more than changing the elastic moduli, it does not affect the long-time behaviour as much as changing the elastic modulus does. Applying a gesso layer and changing the diffusivity did not influence the final twist and bow deformation (for t_∞) when compared to the outcome of the wood boards without a gesso layer. In case of cup deformation this is different; applying a gesso layer had a great influence on the final cup deformation (for t_∞) when compared to the outcome of the wood board without a gesso layer.

12 Concluding remarks

12.1 General

Compared to other structural materials, wood is quite complex. This complex behaviour is the result of wood being a heterogeneous, hygroscopic, cellular and anisotropic material. Without numerical simulation, it is almost impossible to predict the deformation, due to the complex behaviour of wood exposed to moisture. A proper constitutive model, takes account of the directional dependency of the material, the behaviour being strongly influenced by changing moisture content, wood properties, orientation of the fibres (spiral grain orientation) and all non-linear / non-Fickian processes necessary to predict the behaviour.

For accurate time dependent predictions, such a numerical model should include a proper total strain model, taking account for the moisture content, time and temperature. This constitutive model should also take account of the structural orientation of wood such as growth ring orientation, spiral grain direction and conical angle.

It is assumed that a local cylindrical coordinate system is capable to simulate the orthotropic behaviour as a result of the growth ring orientation. This seems to be doubtful because of the following reasons: By default, inserting a coordinate system (Cartesian or cylindrical) assumes that the directional properties are perpendicular to each other. Considering the spiral orientation of the fibres, representing the longitudinal direction, this would be impossible with respect to the radial and tangential direction. It also has been experientially observed that the longitudinal moduli of elasticity, the longitudinal moisture expansion coefficient and elastic strain parameter vary from pith to bark.

Within ABAQUS finite element software, it is shown that due to the analogy between Fourier's law of heat conduction and Fick's law of mass diffusion, it is possible to solve a moisture movement problem with a heat transfer analysis. Careful implementation, proper material data and using an appropriate driving potential deserves full attention. Wood is most often only part of a bigger construction, consisting of many other layers and different materials as in panel paintings. Different materials come with different material properties. Because of this different behaviour, it is wise to use a driving potential, which is consistent for different materials. Water vapour pressure [P] and water vapour content [w] are such driving potentials. Unfortunately, moisture transport below fibre saturation point cannot be regarded as being a pure Fickian process. In case of short time moisture movement simulations, one should use a non-Fickian or multi-Fickian model.

A wooden cylinder exposed to a change in relative humidity from 70% to 30%, shows that moisture distribution is strongly non-linear. The first few millimetres from surface level respond very quickly to changing relative humidity. As a result, cracking of the surface level would be almost instantaneous. Practical research and experience has proven that this is not the case.

As a result, a non-Fickian or multi-Fickian model has been developed (described in literature but not implemented, this is outside the scope of this master thesis), describing the process of moisture distribution through wood more realistically. This non-Fickian or multi-Fickian model predicts a much less steeper gradient at surface level, corresponding to practical experience.

When sawn timber is exposed to moisture variation it can cup, twist, crook or bow. The stability of sawn timber depends upon the original orientation within the stem. It is essential to have detailed information about the position of the sawn timber within the tree stem and the orientation of the fibres. It has been proven that cupping is the result of different radial and tangential properties. Twisting is mainly the result of the spiral grain orientation. Crook and bow deformation are both the result of an equal distribution of longitudinal stiffness.

Some material parameters greatly influence the type of deformation. The influence of a parameter can differ strongly with respect to the same type of deformation, but between different structural orientations of wood boards. Changing the longitudinal elastic moduli, for instance, has respective other consequences for a wood board cut from the centre of a tree, compared to a wood board sawn quartered. It can be concluded that the influence of a material parameter does not only depend on the quantity, but also on the capability of the wood board to develop this material parameter.

Applying a 1.0 mm gesso layer significantly influences the shape stability. Moisture transport through a gesso layer depends upon the diffusivity and the thickness of the gesso layer. As a result of the thickness, diffusivity and elasticity of such a gesso layer, completely new combinations of deformations occur, compared to the same wood board without a gesso layer. Depending on the diffusivity of the gesso layer it can develop strong short time behaviour with maximum strain development. As a result of progressive drying, this short time behaviour generally disappears and the system reaches for its equilibrium state. Step changes of this scale, 70% to 30% relative humidity, always result in relatively large strain development exceeding the elastic strain of wood and gesso, sometimes multiple times.

12.2 Conclusions

1) *Is it possible to perform a mass diffusion analysis within a multi-physical environment using the toolbox for a heat transfer analysis with ABAQUS CAE standard?*

   Modelling moisture distribution, using the transient heat conduction analysis procedure from ABAQUS was successful. Also the coupling of the heat conduction analysis with the static analysis (multi-physical) has been successful. Comparing the calculated moisture distribution and stress field by ABAQUS and the result from Jakiela et al [37] and Schellen et al [36] are in agreement.

1) *Is it possible to model the structural orientation such as the conical angle, growth ring and spiral grain and how do these structural parameters influence the shape stability of sawn wood?*

   Modelling a conical angle has been successful. To model the concentric growth, generally a cylindrical coordinate system is assumed to be capable of simulating the orthotropic behaviour due to the growth ring orientation. This is concluded to be doubtful, see paragraph 4.2. The ease to model a spiral grain orientation depends strongly upon the dimensional properties of the model. Applying a spiral grain orientation to a three-

dimensional wooden cylinder taken from the heart is much more complicated than modelling sawn timber, see paragraph 4.3.

It has been numerically proven that: Twist deformation under drying conditions is mainly the result of the spiral grain angle which is the angle between the pith and the fibre direction. With increasing spiral grain angle, twist deformation increases. When the spiral grain angle is set to zero, no twist deformation will develop. Cup deformation is caused by the difference between radial and tangential shrinkage. Crook deformation depends strongly on the distance between the pith and the centre of the wood board. A wood board, originally taken close to the pith, will show a stronger crook deformation than one taken further away from the pith. It becomes doubtful whether bowing is the result of material properties or a consequence of the local cylindrical coordinate system. In the latter case it is doubtful if this bow effect would take place in a real world situation. See paragraph 9.5 for more detailed conclusions.

2) *What is the influence of changing mechanical parameters such as the modulus of elasticity, modulus of shear and hygro-expansional coefficients on shape stability of sawn wood?*

Twist: The most significant influence on the twist deformation is obtained for the longitudinal elastic modulus, radial elastic modulus and the tangential hygro-expansion (increase of twist deformation). The tangential elastic modulus and the G-LT shear modulus have the least influence on twist deformation. More detailed information about the influence of reducing material properties on twist deformation: see paragraph 10.2.4.

Cup: The most significant influence on the cup deformation is obtained for the radial hygro-expansion (increase of cup deformation) and the tangential hygro-expansion (decrease of cup deformation).Reduction of the radial elastic modulus does not influence the cup deformation. The influence of G-LR shear modulus, G-TR shear modulus and the longitudinal hygro-expansion coefficient can be neglected; the influence of G-LT is significantly larger compared to G-LR and G-TR. More detailed information about the influence of reducing material properties on cup deformation: see paragraph 10.3.4.

Bow: The most significant influence on the bow deformation is obtained for the longitudinal elastic modulus, tangential hygro-expansion (decrease of bow deformation) and the radial hygro-expansion coefficient (increase of bow deformation). Reducing the tangential and radial elastic modulus resulted in a relative small increase of bow deformation. Reducing the G-TR and the longitudinal hygro-expansion does not influence bow deformation and reducing G-LT has almost twice as much influence as reducing G-LR. More detailed information about the influence of reducing material properties on bow deformation: see paragraph 10.4.4.

Crook: The only mechanical property which significantly influences the crook deformation seems to be the radial coefficient of hygro-expansion. More detailed information about the influence of reducing material properties on crook deformation: see paragraph 10.5.1.

3) *What is the influence of a gesso layer on the shape stability of sawn wood?*

It has been concluded that a thicker gesso layer slows down the process of moisture release. This does not surprise, because a thicker layer equals a longer distance for the moisture to travel before reaching the surface.

As a consequence of a gesso layer, unequal moisture transfer between the top and bottom surface develops resulting in different short time (30 min up to 2 hours) behaviour when compared with the models without a gesso layer. Generally this short time behaviour contains a strong short time relatively strong deformation development. Applying a gesso layer does not influence the final deformation (for t_∞) when compared to the outcome of the wood boards without a gesso layer. Only in case of cup deformation this is different; applying a gesso layer had a great influence on the final cup deformation (for t_∞) when compared to the outcome of the wood board without a gesso layer.

In some cases, applying a gesso layer, can lead to the development of new types of deformation when compared with the reference model without a gesso layer. For example wood board -1 did not show cup deformation before applying the gesso layer, it only showed twist deformation.

The effect of changing the diffusion coefficient shows a significantly greater effect than changing the elastic moduli of the gesso layer on the shape stability. A relatively small diffusivity of the gesso layer always resulted in stronger short time behaviour and relatively slow recovery of this process.

12.3 Relevance

One of the possible great advantages of using ABAQUS CAE (Complete ABAQUS Environment) is the ease of modelling. Within the CAE, it is possible to perform a heat conduction analysis and apply the outcome as a predefined field to a static stress / strain analysis. This is a so called sequentially coupled thermal-stress analysis. The multi-physical environment of ABAQUS CAE makes it possible to perform complicated calculations combining mechanical, heat and moisture loads, modelling complicated structures like panel paintings.

These results provide more insight in the mechanical behaviour of sawn wood and can be used to develop a more permanent solution for the conservation problem. Detailed information about the influence of different structural orientations can lead to a more precise and direct method of solving the deformation problem for different types of deformation. These results can also contribute to the development of a constitutive model able to predict deformation due to changing environmental conditions more precisely.

Coating layers like gesso seems to have great influence on the deformation behaviour of sawn wood when exposed to changing environmental conditions. Coating layers like gesso can lead to unexpected types of deformation. This knowledge can be used to develop a more permanent solution of conservation for individual panel paintings with different coatings. Because of the impact of applied coatings on the deformation of sawn wood further research is desirable

BIBLIOGRAPHY

[1] Martenson A.: Mechanical behaviour of wood exposed to humidity variations. Lund Institute of Technology, department of structural engineering, Lund, Sweden (1992).

[2] Kollmann F., Cote W.: Principles of Wood science and Technology: 1 Solid Wood. Institute fur Holzforschung und Holztechnik , Munchen, Germany / College of Forestry, Syracuse, New York (1968).

[3] Toratti T.: Creep of timber beams in a variable environment. Helsinki University of Technology, Report 31 (1992).

[4] Svensson S.:. Internal Stress in Wood Caused by Climate Variations, Lund Institute of Technology (1997).

[5] Mirianon F. Fortino S. and Toratti T.: A method to model wood by using ABAQUS finite element software, VTT (2008).

[6] Ormarsson s. Dahlblom O. Petersson H.: A numerical study of the shape stability of sawn timber subjected to moisture variations, Lund Institute of Technology (1997).

[7] Blumer S.: Moisture Induced Stresses and Deformations in Parquet Floors - An experimental and Numerical Study, Lund University, Division of Structural mechanics (diploma thesis), Lund, Sweden (2006).

[8] Mackenzie-Helnwein P, Hanhijärvi A.: Computational analysis of quality reduction during drying of lumber due to irrecoverable deformation, Journal of Engineering Mechanics 1006 – 1016 (2003).

[9] Hofmeijer H.: Linear Finite Element Method (FEM),Technical University of Eindhoven, Department of Structural Design and Construction Technology (Lecture Notes), Eindhoven, Netherlands (2000).

[10] Madison S.: Structure of Wood, Wisconsin, United States Department of Agriculture Forest Service,USA (1980).

[11] Wiselius S.: Hout vademecum, 7e druk, Stichting Centrum Hout SCH, Almere,Netherlands (1994).

[12] Saupe S.: Plant physiology, College of St. Benedict / St. Jon's University;Biology Department, Minnesota, USA (2011).

[13] Madison S.: Shrinking and swelling of wood in use, United States Department of Agriculture Forest Service, Wisconsin, USA (1957).

[14] Eckelman C.:The shrinking and swelling of wood and its effect on furniture, University Cooperative Extension Service West Lafayette, West Lafayette,USA (2000).

[15] Astrup T, Hansen K, Hoffmeyer P and Damkilde L.: Moisture transport in wood – an experimental and numerical study. Department of civil engineering, Technical University of Denmark, Copenhagen, Denmark.

[16] Kozlowski R, Bratasz L, Lasyk L and Lukomski M.: Allowable microclimatic variations for painted wood: direct tracing of damage development, The research was supported by grant PL0086 from Iceland, Liechtenstein and Norway through the European Economy Area Financial Mechanism (2006).

[17] Bratasz L, Koslowski R, Kozlowska A and Rachwal B.: Sorption of moisture and dimensional change of wood species used in historic objects, Institute of Catalysis and Surface Chemistry, Polish Academy of Sciences, Krakow, Poland (2006).

[18] Blumer S.: Moisture Induced Stresses and Deformations in Parquet Floors- An experimental and Numerical Study, Lund University, Division of Structural mechanics (diploma thesis), Lund, Sweden (2006).

[19] Friedrich F, Kollmann P, Côté W, Kuenzi E and Stamm A.: Principles of Wood Science and Technology: Solid Wood Springer-Verlag, Berlin, Heidelberg, New York (1986).

[20] Wit, de M.: Heat air and Moisture in Building Envelopes, University of Technology Eindhoven, Eindhoven, Netherlands (2009).

[21] Wikipedia: http://en.wikipedia.org/wiki/Diffusion

[22] Wikipedia: http://en.wikipedia.org/wiki/Molecular_diffusion

[23] Kaseb S, El-Hariry G.: Basic of heat transfer: Course Part A: Introduction to Electronics Cooling, Mechanical Power Engineering Department, Faculty of Engineering Cairo University, Cairo, Egypt (2006).

[24] Jiji Latif M.: Heat Conduction, Third Edition, Department of Mechanical Engineering, City University of New York, New York, USA (2009).

[25] Theodore L.: Heat Transfer Applications for the Practicing Engineer, John Wiley & Sons, Hobooken, NU (2009).

[26] ABAQUS documentation: ABAQUS Analysis User's Manual and ABAQUS Theory Manual

[27] Time B.: Hygroscopic moisture transport in wood, A thesis presented for the degree of Dr.ir. Norwegian University of Science and Technology, Department of Building and Construction Engineering, Trondheim, Norway (1998).

[28] http://www.appstate.edu/~neufeldhs/pltphys/waterpotential.htm

[29] Frandsen H., Damkilde L., Svensson S.: A revised multi-Fickian moisture transport model to describe non-Fickian effects in wood, Aalborg University, Department of Civil Engineering, Aalborg, Denmark. Technical University of Denmark, Lyngby, Denmark (2007).

[30] Wadso L.: Describing non-Fickian water-vapour sorption in wood, Lund University,Department of Building Material, Lund, Sweden (1994).

[31] Krabbenhoft K., Damkilde L.: A model for non-Fickian moisture transfer in wood, Technical University of Denmark, Department of Civil Engineering, Lungby, Denmark. Aalborg University Esbjerg, Institute of Chemistry and applied Engineering Science, Esbjerg, Denmark (2004).

[32] Robert H.: XVIIIth Convention of the Julius-Hirschberg-Gesellschaft,Oktober 14th–16th 2004, Innsbruck, Germany.

[33] Cunningham M.: A model to explain anomalous moisture sorption in wood under step function driving forces, Wood and fibre science 27(3) (1996).

[34] Salin J.: Mass transfer from wooden surfaces and internal moisture non-equilibrium, Drying Technology 14(10) (1996).

[35] Absetz I., Koponen S.: Fundamental diffusion behaviour of wood, In Hoffmeyer P. (editor), International Conference on Wood Water Relations, Copenhagen, Denmark (1997).

[36] Schellen H., van Schijndel J.: Numerical modeling of moisture related mechanical stress in wooden cylindrical objects using COMSOL: a comparative benchmark, Eindhoven University of Technology, Department of Building and Architecture, Eindhoven, Netherlands (2011).

[37] Jakiela S., Bratasz L., Kozlowski R.: Numerical modeling of moisture movement and related stress field in lime wood subjected to changing climate conditions, Wood Science Technology (2008).

[38] Mirianon F., Fortino S and Toratti T.: A Method to model wood by using ABAQUS finite element software, part 1: Constitutive model and computational details, VTT publications 687, Finland (2008).

[39] The Structural Conservation of Panel Paintings, proceedings of a symposium at the J.Paul Getty Museum april 1995, The Getty Conservation Institute, Los Angeles, USA, 1998.

Appendix A: Derivation of Fick's second law

Fick's second law of diffusion describes how diffusive concentration changes in time to an unsteady state. Fick's second law can be derived from Fick's first law and law of mass conservation (law of mass conservation: the mass in an isolated system remains constant over time):

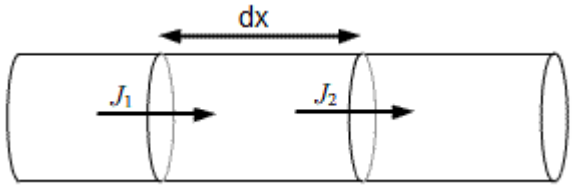

$$C = \frac{m}{V}$$
$$V = A \cdot dx \qquad \text{(A-1)}$$

C = Concentration
V = Volume
M = Mass
A = Area
dx= Distance

$$\frac{\partial c}{\partial t} = \textit{The changing concentration in time}$$

The changing concentration in time equals the difference between the incoming mass and the outflowing mass (law of mass conservation).

So,

$$\frac{\partial c}{\partial t} = \frac{\frac{m_{in}}{t} - \frac{m_{out}}{t}}{V} = \frac{\frac{\Delta m}{t}}{V} \qquad \text{(A-2)}$$

$$\frac{\partial c}{\partial t} = \frac{\frac{m_{in}}{t} - \frac{m_{out}}{t}}{A \cdot dx} = \frac{\frac{m_{in}}{tA} - \frac{m_{out}}{tA}}{dx} \qquad \text{(A-3)}$$

$$J = flux = \frac{m_{in}}{tA} \qquad \text{(A-4)}$$

$$\frac{\partial c}{\partial t} = \frac{J_{in} - J_{out}}{dx} = \frac{\partial (J)}{\partial x} \qquad \text{(A-5)}$$

From Fick's first law:

$$J = -D\frac{\partial C}{\partial x} \tag{A-6}$$

So,

$$\frac{\partial c}{\partial t} = \frac{\partial\left(-D\frac{\partial C}{\partial x}\right)}{\partial x} = \frac{\partial}{\partial x}\left(-D\frac{\partial C}{\partial x}\right) = D\frac{\partial^2 C}{\partial x^2} \tag{A-7}$$

This is Fick's second law:

$$\frac{\partial c}{\partial t} = D\frac{\partial^2 C}{\partial x^2} \tag{A-8}$$

Appendix B: Solution to Newton's cooling equation

$$\frac{dT}{dt} = -\alpha\left(T - T_A\right) \tag{B-1}$$

Change of variables: $y = T_S - T_A$

$$\frac{dy}{dt} = -\alpha y \quad \rightarrow \quad \frac{dy}{y} = -\alpha dt \tag{B-2}$$

$$\ln(y) = -\alpha t + C \tag{B-3}$$

$$y = \exp\left(-\alpha t + C\right) \quad \rightarrow \quad y = \exp\left(-\alpha t\right)\exp\left(C\right) \tag{B-4}$$

$\exp\left(C\right)$ is a constant

$$T - T_A = y_0 \exp\left(-\alpha \cdot t\right) \tag{B-5}$$

$$T = T_A + \left(T_0 - T_A\right)\exp\left(-\alpha t\right) \tag{B-6}$$

Appendix C: Example 1

Example 1: Transient one dimensional heat conduction

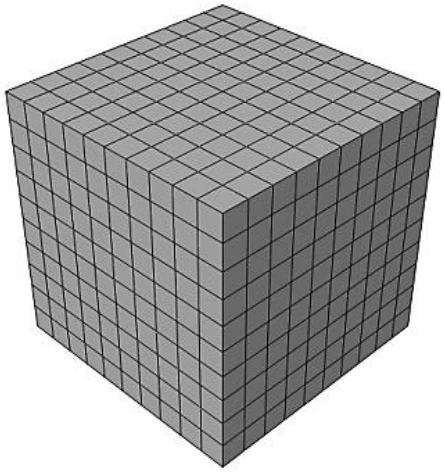

Input:

Initial temperature (T_0) = 50 °C
Final temperature (T) = 1 °C
Material density (ρ) = 997, 3 $[kg \cdot m^3]$
water)
Specific heat capacity (c_p) = 4.1813 $[J \cdot kg^{-1}K^{-1}]$
Thermal conductivity (k) = 0.6 $[W \cdot m^{-2}K^{-1}]$

A volume of water with an initial temperature of 50 °C cools down, conduction takes place along all six planes. Firstly, calculate the conduction process with help of Newton's law for cooling and compare the results with a finite element simulation with help of ABAQUS.

$$T = T_A + (T_0 - T_A)\exp(-\alpha \cdot t) \quad \textit{Newton's cooling law} \qquad \text{(C-1)}$$

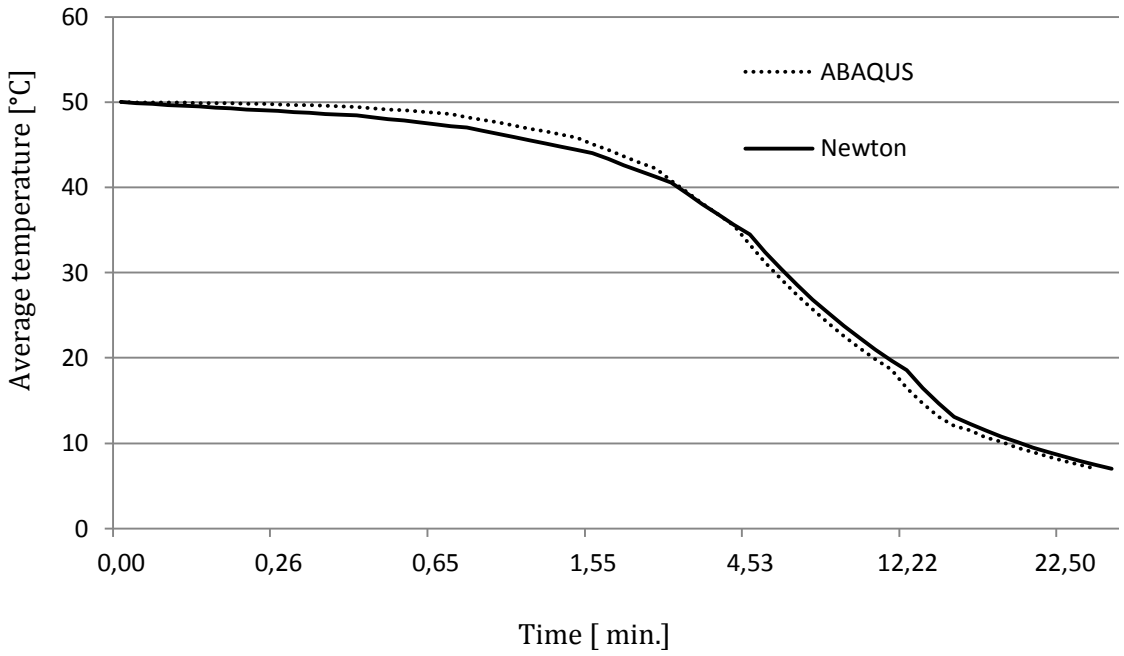

Appendix D: Example 2

Example 2: A temperature step at the surface of a semi-infinite thick slab

A semi-infinite thick slab is suddenly heated from T_0 up to Ts. The diffusive flux of heat can be calculated in time and in space for this specific one-dimensional case.

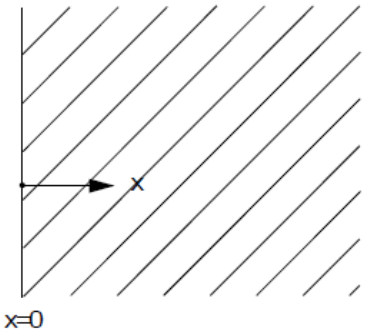

Figure 5.5: Semi-infinite thick slab (M. de Wit).

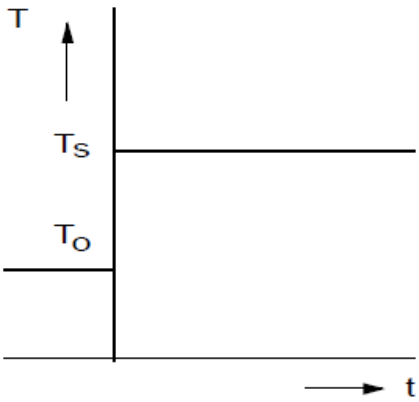

Figure 5.6: A temperature step at the surface of a semi-infinite thick slab as a function of time t (M. de Wit).

The initial boundary conditions are:

$$t < 0 \qquad T(x,t) = T_0$$

$$x = 0 \quad and \quad t \geq 0 \qquad T(0,t) = T_0 + \Delta T_s$$

$$x \to \infty \quad and \quad t \geq 0 \qquad T(\infty,t) = T_0$$

Input:

Initial temperature (T_0) = 10 °C
Final temperature (Ts) = 30 °C
Thermal diffusivity (α) = 1

$$T(x,t) = T_0 + \Delta T_s erfc\left(\frac{x}{2\sqrt{at}}\right)$$ (See M. de Wit [20] for more information) (D-1)

$T(x,t)$ = the temperature in x-direction
T_0 = the initial temperature
T_s = the increase or suddenly decrease in temperature
ΔT_s = T_s - T_0
x = the distance in x-direction into the slab
t = time
a = thermal diffusivity

Where erfc(Z) is the complementary error function (Gauss error integral):

$$erfc(Z) = \frac{2}{\sqrt{\pi}} \int_Z^{\infty} \exp(-\xi^2) d\xi$$ (D-2)

So erfc(0)=1 and erfc(∞)=0

Within Microsoft Excel and Mathemathica (software program), a complementary error function is standard implemented. If this would not be the case, a good approximation can be made with equation (5.26) and (5.27) (error smaller then 1%).

$$erfc(Z) = \frac{\sqrt{\pi}}{2Z + \sqrt{(\pi-2)^2 \cdot Z^2 + \pi}} \cdot \exp(-Z^2)$$ (D-3)

$$erfc\left(\frac{x}{2\sqrt{at}}\right) = \frac{\sqrt{\pi}}{2\left(\frac{x}{2\sqrt{at}}\right) + \sqrt{(\pi-2)^2 \cdot \left(\frac{x}{2\sqrt{at}}\right)^2 + \pi}} \cdot \exp\left(-\left(\frac{x}{2\sqrt{at}}\right)^2\right)$$ (D-4)

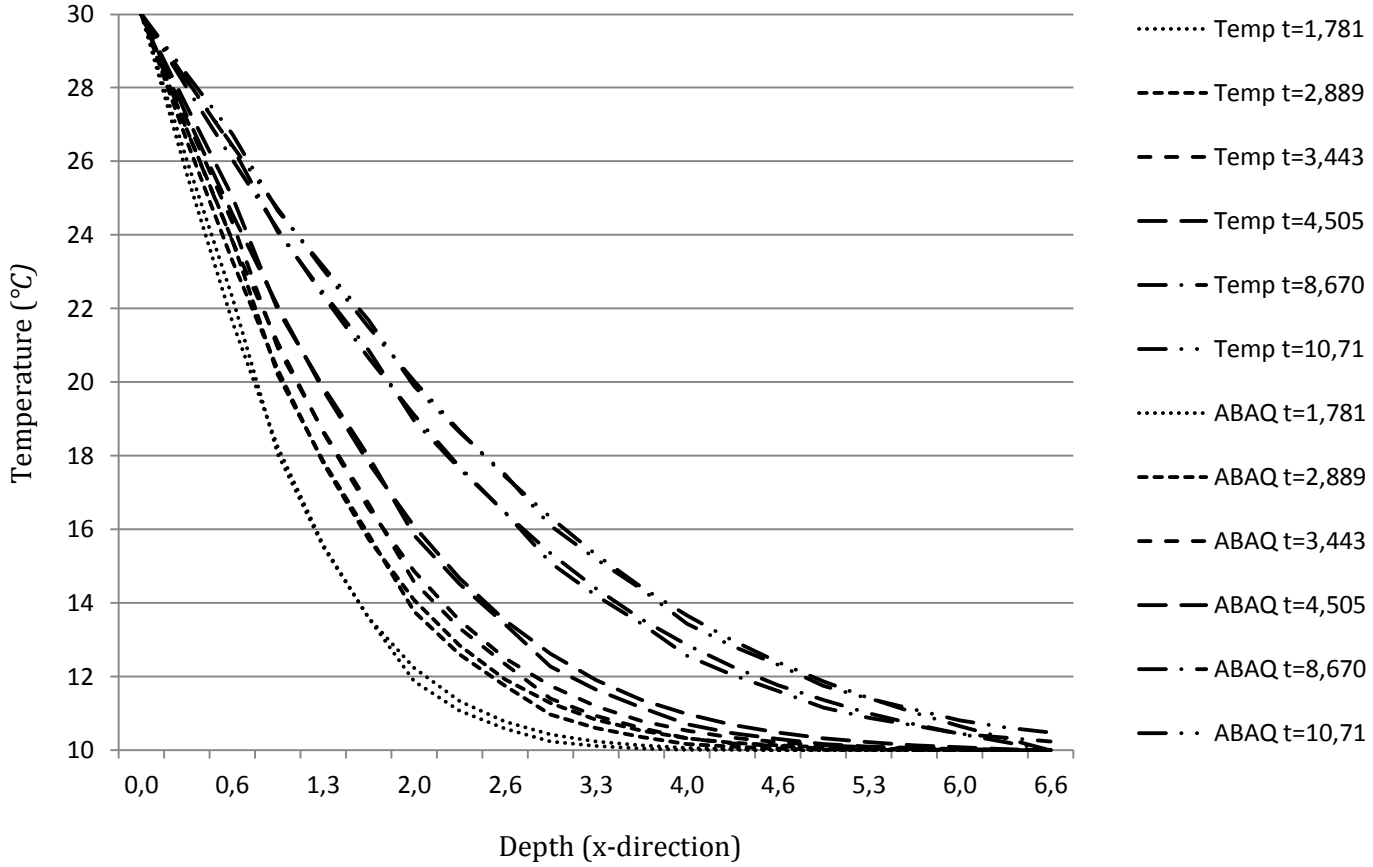

Temp = temperature of body calculated with approximation equation [°C]
ABAQ = temperature of body calculated by ABAQUS [°C]
t = time interval determined by ABAQUS [s]

Appendix E: Relation between Fick's law and the general chemical potential

Diffusion is assumed to be driven by the gradient of a general chemical potential. The relation between Fick's law and the general chemical potential can be established as follows:

$$J = -D \cdot \frac{\partial c}{\partial x} \tag{E-1}$$

The concentration of the diffusing material can be written as a function of the normalized concentration and the solubility, equation (F-2).

$$\phi = \frac{c}{s} \rightarrow c = s \cdot \phi \tag{E-2}$$

Takes the partial differential, using the product rule, resulting in equation (F-3).

$$\frac{\partial c}{\partial x} = \phi \frac{\partial s}{\partial x} + s \frac{\partial \phi}{\partial x} \tag{E-3}$$

Substitute equation (F-3) into equation (F-1).

$$J = -D \cdot \frac{\partial c}{\partial x} \rightarrow -D \cdot \left(s \frac{\partial \phi}{\partial x} + \phi \frac{\partial s}{\partial x} \right) \tag{E-4}$$

The solubility (s) is a function of the temperature (θ), $s = s(\theta)$.

$\phi \frac{\partial s}{\partial x}$ and can be written as follows, equation (F-5).

$$\phi \frac{\partial s(\theta)}{\partial x} = \frac{c}{s} \frac{\partial s}{\partial \theta} \frac{\partial \theta}{\partial x} \tag{E-5}$$

Substitution of equation (F-5) into equation (F-4):

$$J = -sD \cdot \frac{\partial \phi}{\partial x} - D \frac{c}{s} \frac{\partial s}{\partial \theta} \frac{\partial \theta}{\partial x} \tag{E-6}$$

The first term of this equation, $-sD \cdot \frac{\partial \phi}{\partial x}$, describes the normalized concentration and the second term, $-D \frac{c}{s} \frac{\partial s}{\partial \theta} \frac{\partial \theta}{\partial x}$, describes the temperature-driven diffusion, respectively. The first term (normalized concentration driven-diffusion term) is identical to that given in the general mass diffusion equation used by ABAQUS equation. The second term (temperature driven-diffusion term) is recovered in the general relation if:

$$\kappa_s = \frac{c \cdot (\theta - \theta^Z)}{s^2} \frac{\partial s}{\partial \theta} \tag{E-7}$$

Appendix F: Moisture movement

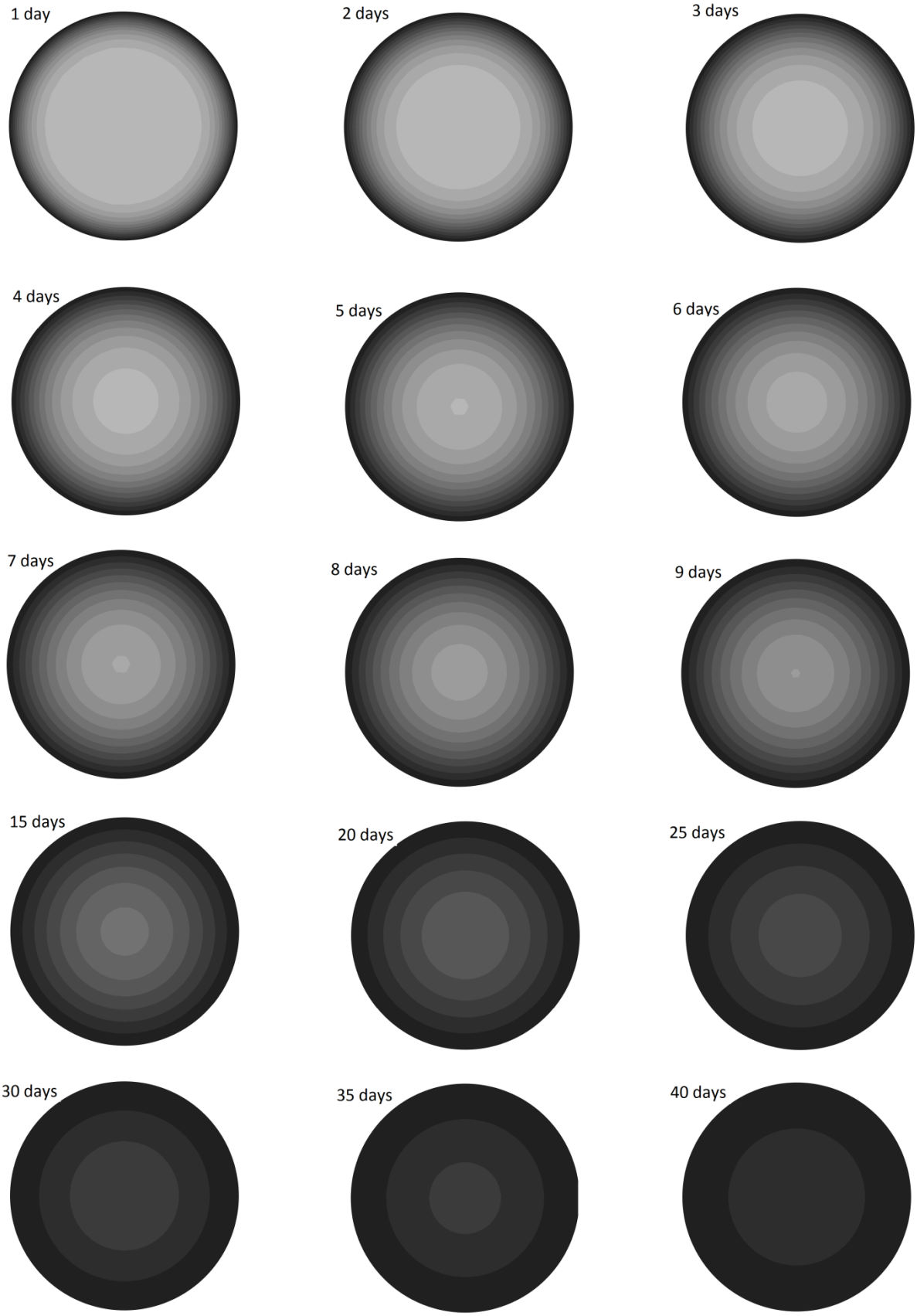

Appendix G: Data shape stability of sawn timber and the influence of gesso

WB-1-Twist

Displ [mm]	1/2 Width	Twist [degrees]	time [sec.]	time (h)	TWIST
0,0001	100	6,99931E-05	0	0	
0,0002	100	0,000138902	0	0	
0,0005	100	0,000276697	0	0	
0,0008	100	0,000483339	1	0	
0,0014	100	0,000793186	1	0	
0,0022	100	0,0012577	1	0	
0,0034	100	0,001953895	2	0	
0,0052	100	0,002996879	3	0	
0,0080	100	0,004558435	4	0	
0,0120	100	0,006894229	7	0	
0,0181	100	0,010383256	10	0	
0,0272	100	0,015584108	15	0	
0,0407	100	0,023312792	23	0	
0,0606	100	0,034745417	34	0	
0,0900	100	0,051543269	52	0	
0,1326	100	0,075981608	78	0	
0,1938	100	0,11103106	117	0	E-reference
0,2798	100	0,160285098	175	0	
0,3972	100	0,227561597	263	0	
0,5515	100	0,315962395	394	0	
0,7441	100	0,426307683	591	0	
0,9691	100	0,555246903	887	0	
1,2114	100	0,694041395	1330	0	
1,4482	100	0,829688022	1995	1	
1,6574	100	0,949556223	2993	1	
1,8293	100	1,04801199	4489	1	
1,9724	100	1,129961166	6734	2	
2,1080	100	1,207610452	10100	3	
2,2576	100	1,293301282	15151	4	
2,4333	100	1,393891686	22726	6	
2,6334	100	1,508478423	34089	9	
2,8428	100	1,628337234	51134	14	
3,0367	100	1,739343516	76700	21	
3,1902	100	1,827253141	115051	32	
3,2903	100	1,884528887	172576	48	
3,3418	100	1,914009524	258864	72	
3,3620	100	1,92554739	388296	108	
3,3675	100	1,928695095	518400	144	

Displ [mm]	1/2 Width	ist [degre	time [sec.]	time (h)	TWIST
0,0001	100	6,75E-05	0	0	
0,0002	100	0,00011	0	0	
0,0003	100	0,000174	0	0	
0,0005	100	0,00027	0	0	
0,0007	100	0,000414	0	0	
0,0011	100	0,00063	1	0	
0,0017	100	0,000953	1	0	
0,0025	100	0,001438	1	0	
0,0038	100	0,002165	2	0	
0,0057	100	0,003254	3	0	
0,0085	100	0,004886	4	0	
0,0128	100	0,007328	6	0	
0,0192	100	0,010978	9	0	
0,0287	100	0,016425	14	0	
0,0428	100	0,024533	21	0	
0,0638	100	0,036557	32	0	
0,0947	100	0,054287	47	0	1/2 E-I
0,1400	100	0,080212	71	0	
0,2053	100	0,117652	106	0	
0,2980	100	0,17075	160	0	
0,4260	100	0,244094	239	0	
0,5963	100	0,341663	359	0	
0,8112	100	0,464796	539	0	
1,0637	100	0,609438	808	0	
1,3338	100	0,764166	1212	0	
1,5915	100	0,911762	1818	1	
1,8089	100	1,036287	2727	1	
1,9767	100	1,132395	4091	1	
2,1102	100	1,208853	6136	2	
2,2383	100	1,282232	9204	3	
2,3863	100	1,36699	13806	4	
2,5662	100	1,470025	20709	6	
2,7757	100	1,589974	31064	9	
2,9993	100	1,71794	46596	13	
3,2114	100	1,839353	69893	19	
3,3843	100	1,938304	104840	29	
3,5009	100	2,005043	157260	44	
3,5633	100	2,040751	235890	66	
3,5887	100	2,055297	353835	98	
3,5962	100	2,059595	518400	144	

Displ [mm]	1/2 Width	ist [degre	time [sec.]	time (h)	TWIST
0,0001	100	6,94E-05	0	0	
0,0002	100	0,000113	0	0	
0,0003	100	0,000179	0	0	
0,0005	100	0,000278	0	0	
0,0007	100	0,000425	0	0	
0,0011	100	0,000647	1	0	
0,0017	100	0,00098	1	0	
0,0026	100	0,001478	1	0	
0,0039	100	0,002226	2	0	
0,0058	100	0,003346	3	0	
0,0088	100	0,005023	4	0	
0,0131	100	0,007533	6	0	
0,0197	100	0,011286	9	0	
0,0295	100	0,016885	14	0	
0,0440	100	0,025218	21	0	
0,0656	100	0,037572	32	0	
0,0974	100	0,055781	47	0	1/2 E-R
0,1438	100	0,082394	71	0	
0,2108	100	0,120799	106	0	
0,3058	100	0,175205	160	0	
0,4368	100	0,250246	239	0	
0,6107	100	0,349874	359	0	
0,8296	100	0,475287	539	0	
1,0859	100	0,622168	808	0	
1,3593	100	0,778762	1212	0	
1,6192	100	0,927624	1818	1	
1,8375	100	1,052697	2727	1	
2,0049	100	1,148575	4091	1	
2,1365	100	1,223932	6136	2	
2,2610	100	1,295237	9204	3	
2,4037	100	1,376936	13806	4	
2,5767	100	1,476002	20709	6	
2,7780	100	1,591256	31064	9	
2,9927	100	1,714191	46596	13	
3,1964	100	1,830802	69893	19	
3,3625	100	1,925816	104840	29	
3,4744	100	1,98989	157260	44	
3,5343	100	2,024156	235890	66	
3,5587	100	2,038113	353835	98	
3,5659	100	2,042228	518400	144	

Displ [mm]	1/2 Width	ist [degre	time [sec.]	time (h)	TWIST
0,0001	100	6,13E-05	0	0	
0,0002	100	0,0001	0	0	
0,0003	100	0,000158	0	0	
0,0004	100	0,000245	0	0	
0,0007	100	0,000376	0	0	
0,0010	100	0,000572	1	0	
0,0015	100	0,000865	1	0	
0,0023	100	0,001306	1	0	
0,0034	100	0,001966	2	0	
0,0052	100	0,002955	3	0	
0,0077	100	0,004437	4	0	
0,0116	100	0,006655	6	0	
0,0174	100	0,009971	9	0	
0,0260	100	0,01492	14	0	
0,0389	100	0,02229	21	0	
0,0580	100	0,033225	32	0	
0,0861	100	0,049359	47	0	1/2 E-T
0,1274	100	0,072974	71	0	
0,1870	100	0,107129	106	0	
0,2717	100	0,155669	160	0	
0,3891	100	0,222911	239	0	
0,5458	100	0,312706	359	0	
0,7445	100	0,426579	539	0	
0,9794	100	0,56112	808	0	
1,2322	100	0,705957	1212	0	
1,4750	100	0,845046	1818	1	
1,6814	100	0,963298	2727	1	
1,8427	100	1,055658	4091	1	
1,9736	100	1,130666	6136	2	
2,1023	100	1,204335	9204	3	
2,2528	100	1,29053	13806	4	
2,4365	100	1,395736	20709	6	
2,6506	100	1,518309	31064	9	
2,8790	100	1,649101	46596	13	
3,0958	100	1,773202	69893	19	
3,2725	100	1,874347	104840	29	
3,3918	100	1,942591	157260	44	
3,4556	100	1,979108	235890	66	
3,4816	100	1,993982	353835	98	
3,4892	100	1,998377	518400	144	

Displ [mm]	1/2 Width	Twist [degrees]	time [sec.]	time (h)	TWIST
0,0001	100	6,99931E-05	0	0	
0,0002	100	0,000138902	0	0	
0,0005	100	0,000276697	0	0	
0,0008	100	0,000483339	1	0	
0,0014	100	0,000793186	1	0	
0,0022	100	0,0012577	1	0	
0,0034	100	0,001953895	2	0	
0,0052	100	0,002996879	3	0	
0,0080	100	0,004558435	4	0	
0,0120	100	0,006894229	7	0	
0,0181	100	0,010383256	10	0	
0,0272	100	0,015584108	15	0	
0,0407	100	0,023312792	23	0	
0,0606	100	0,034745417	34	0	
0,0900	100	0,051543269	52	0	
0,1326	100	0,075981608	78	0	
0,1938	100	0,11103106	117	0	G-reference
0,2798	100	0,160285098	175	0	
0,3972	100	0,227561597	263	0	
0,5515	100	0,315962395	394	0	
0,7441	100	0,426307683	591	0	
0,9691	100	0,555246903	887	0	
1,2114	100	0,694041395	1330	0	
1,4482	100	0,829688022	1995	1	
1,6574	100	0,949556223	2993	1	
1,8293	100	1,04801199	4489	1	
1,9724	100	1,129961166	6734	2	
2,1080	100	1,207610452	10100	3	
2,2576	100	1,293301282	15151	4	
2,4333	100	1,393891686	22726	6	
2,6334	100	1,508478423	34089	9	
2,8428	100	1,628337234	51134	14	
3,0367	100	1,739343516	76700	21	
3,1902	100	1,827253141	115051	32	
3,2903	100	1,884528887	172576	48	
3,3418	100	1,914009524	258864	72	
3,3620	100	1,92554739	388296	108	
3,3675	100	1,928695095	518400	144	

Displ [mm]	1/2 Width	ist [degre	time [sec.]	time (h)	TWIST
0,0001	100	0,0001	0	0	
0,0002	100	0,0001	0	0	
0,0003	100	0,0002	0	0	
0,0005	100	0,0003	0	0	
0,0007	100	0,0004	0	0	
0,0011	100	0,0006	1	0	
0,0016	100	0,0009	1	0	
0,0025	100	0,0014	1	0	
0,0037	100	0,0021	2	0	
0,0056	100	0,0032	3	0	
0,0084	100	0,0048	4	0	
0,0126	100	0,0072	6	0	
0,0189	100	0,0108	9	0	
0,0282	100	0,0162	14	0	
0,0422	100	0,0242	21	0	
0,0628	100	0,0360	32	0	
0,0933	100	0,0535	47	0	1/2 G-LT
0,1379	100	0,0790	71	0	
0,2022	100	0,1159	106	0	
0,2936	100	0,1682	160	0	
0,4197	100	0,2405	239	0	
0,5877	100	0,3367	359	0	
0,7997	100	0,4582	539	0	
1,0490	100	0,6010	808	0	
1,3158	100	0,7539	1212	0	
1,5706	100	0,8998	1818	1	
1,7858	100	1,0231	2727	1	
1,9521	100	1,1183	4091	1	
2,0846	100	1,1942	6136	2	
2,2120	100	1,2672	9204	3	
2,3594	100	1,3516	13806	4	
2,5387	100	1,4542	20709	6	
2,7474	100	1,5737	31064	9	
2,9701	100	1,7012	46596	13	
3,1814	100	1,8222	69893	19	
3,3537	100	1,9208	104840	29	
3,4700	100	1,9873	157260	44	
3,5322	100	2,0229	235890	66	
3,5575	100	2,0375	353835	98	
3,5650	100	2,0417	518400	144	

Displ [mm]	1/2 Width	ist [degre	time [sec.]	time (h)	TWIST
0,0001	100	7,93E-05	0	0	
0,0002	100	0,000129	0	0	
0,0004	100	0,000204	0	0	
0,0006	100	0,000317	0	0	
0,0008	100	0,000486	0	0	
0,0013	100	0,00074	1	0	
0,0020	100	0,00112	1	0	
0,0029	100	0,001689	1	0	
0,0044	100	0,002543	2	0	
0,0067	100	0,003823	3	0	
0,0100	100	0,00574	4	0	
0,0150	100	0,008608	6	0	
0,0225	100	0,012896	9	0	
0,0337	100	0,019294	14	0	
0,0503	100	0,028819	21	0	
0,0749	100	0,042942	32	0	
0,1113	100	0,063765	47	0	1/2 G-LR
0,1644	100	0,094209	71	0	
0,2412	100	0,13817	106	0	
0,3499	100	0,200499	160	0	
0,5002	100	0,286568	239	0	
0,6999	100	0,401015	359	0	
0,9519	100	0,545368	539	0	
1,2477	100	0,714825	808	0	
1,5639	100	0,89597	1212	0	
1,8653	100	1,068626	1818	1	
2,1194	100	1,214156	2727	1	
2,3152	100	1,326281	4091	1	
2,4705	100	1,415216	6136	2	
2,6191	100	1,500274	9204	3	
2,7904	100	1,598349	13806	4	
2,9985	100	1,717517	20709	6	
3,2409	100	1,856243	31064	9	
3,4995	100	2,004265	46596	13	
3,7450	100	2,144736	69893	19	
3,9452	100	2,259273	104840	29	
4,0803	100	2,336566	157260	44	
4,1527	100	2,377944	235890	66	
4,1822	100	2,394817	353835	98	
4,1909	100	2,399805	518400	144	

Displ [mm]	1/2 Width	ist [degre	time [sec.]	time (h)	TWIST
0,0001	100	7,7E-05	0	0	
0,0002	100	0,000126	0	0	
0,0003	100	0,000199	0	0	
0,0005	100	0,000308	0	0	
0,0008	100	0,000472	0	0	
0,0013	100	0,000718	1	0	
0,0019	100	0,001087	1	0	
0,0029	100	0,00164	1	0	
0,0043	100	0,002469	2	0	
0,0065	100	0,003712	3	0	
0,0097	100	0,005573	4	0	
0,0146	100	0,008358	6	0	
0,0219	100	0,012521	9	0	
0,0327	100	0,018736	14	0	
0,0488	100	0,027987	21	0	
0,0728	100	0,041708	32	0	
0,1081	100	0,061945	47	0	1/2 G-TR
0,1598	100	0,091548	71	0	
0,2344	100	0,134325	106	0	
0,3404	100	0,195038	160	0	
0,4869	100	0,278994	239	0	
0,6822	100	0,390842	359	0	
0,9290	100	0,532256	539	0	
1,2196	100	0,698739	808	0	
1,5312	100	0,87725	1212	0	
1,8293	100	1,047966	1818	1	
2,0815	100	1,192417	2727	1	
2,2770	100	1,304405	4091	1	
2,4339	100	1,394224	6136	2	
2,5858	100	1,481236	9204	3	
2,7623	100	1,582285	13806	4	
2,9773	100	1,705346	20709	6	
3,2277	100	1,848694	31064	9	
3,4950	100	2,001678	46596	13	
3,7488	100	2,146893	69893	19	
3,9558	100	2,265325	104840	29	
4,0956	100	2,345284	157260	44	
4,1704	100	2,388102	235890	66	
4,2010	100	2,405575	353835	98	
4,2100	100	2,410734	518400	144	

Displ [mm]	1/2 Width	Twist [degrees]	time [sec.]	time (h)	TWIST
0,0001	100	6,99931E-05	0	0	
0,0002	100	0,000138902	0	0	
0,0005	100	0,000276697	0	0	
0,0008	100	0,000483339	1	0	
0,0014	100	0,000793186	1	0	
0,0022	100	0,0012577	1	0	
0,0034	100	0,001953895	2	0	
0,0052	100	0,002996879	3	0	
0,0080	100	0,004558435	4	0	
0,0120	100	0,006894229	7	0	
0,0181	100	0,010383256	10	0	
0,0272	100	0,015584108	15	0	
0,0407	100	0,023312792	23	0	
0,0606	100	0,034745417	34	0	
0,0900	100	0,051543269	52	0	
0,1326	100	0,075981608	78	0	
0,1938	100	0,11103106	117	0	α-reference
0,2798	100	0,160285098	175	0	
0,3972	100	0,227561597	263	0	
0,5515	100	0,315962395	394	0	
0,7441	100	0,426307683	591	0	
0,9691	100	0,555246903	887	0	
1,2114	100	0,694041395	1330	0	
1,4482	100	0,829688022	1995	1	
1,6574	100	0,949556223	2993	1	
1,8293	100	1,04801199	4489	1	
1,9724	100	1,129961166	6734	2	
2,1080	100	1,207610452	10100	3	
2,2576	100	1,293301282	15151	4	
2,4333	100	1,393891686	22726	6	
2,6334	100	1,508478423	34089	9	
2,8428	100	1,628337234	51134	14	
3,0367	100	1,739343516	76700	21	
3,1902	100	1,827253141	115051	32	
3,2903	100	1,884528887	172576	48	
3,3418	100	1,914009524	258864	72	
3,3620	100	1,92554739	388296	108	
3,3675	100	1,928695095	518400	144	

Displ [mm]	1/2 Width	ist [degre	time [sec.]	time (h)	TWIST
0,0001	100	0,0001	0	0	
0,0002	100	0,0001	0	0	
0,0003	100	0,0002	0	0	
0,0005	100	0,0003	0	0	
0,0007	100	0,0004	0	0	
0,0011	100	0,0006	1	0	
0,0017	100	0,0010	1	0	
0,0026	100	0,0015	1	0	
0,0039	100	0,0022	2	0	
0,0058	100	0,0033	3	0	
0,0088	100	0,0050	4	0	
0,0132	100	0,0075	6	0	
0,0197	100	0,0113	9	0	
0,0295	100	0,0169	14	0	
0,0441	100	0,0252	21	0	
0,0656	100	0,0376	32	0	
0,0975	100	0,0559	47	0	1/2 α-L
0,1440	100	0,0825	71	0	
0,2113	100	0,1211	105	0	
0,3066	100	0,1757	160	0	
0,4383	100	0,2511	239	0	
0,6135	100	0,3515	359	0	
0,8347	100	0,4782	539	0	
1,0944	100	0,6270	808	0	
1,3723	100	0,7862	1212	0	
1,6374	100	0,9381	1818	1	
1,8611	100	1,0662	2727	1	
2,0337	100	1,1651	4091	1	
2,1710	100	1,2437	6136	2	
2,3027	100	1,3191	9204	3	
2,4548	100	1,4062	13806	4	
2,6398	100	1,5121	20709	6	
2,8551	100	1,6354	31064	9	
3,0848	100	1,7669	46596	13	
3,3029	100	1,8917	69893	19	
3,4806	100	1,9934	104840	29	
3,6005	100	2,0620	157260	44	
3,6646	100	2,0987	235890	66	
3,6908	100	2,1137	353835	98	
3,6985	100	2,1181	518400	144	

Displ [mm]	1/2 Width	ist [degre	time [sec.]	time (h)	TWIST
0,0001	100	5,74E-05	0	0	
0,0002	100	8,79E-05	0	0	
0,0002	100	0,000134	0	0	
0,0004	100	0,000202	0	0	
0,0005	100	0,000305	1	0	
0,0008	100	0,000459	1	0	
0,0012	100	0,00069	1	0	
0,0018	100	0,001036	2	0	
0,0027	100	0,001555	3	0	
0,0041	100	0,002332	5	0	
0,0061	100	0,003494	7	0	
0,0091	100	0,00523	11	0	
0,0136	100	0,00782	16	0	
0,0204	100	0,01167	24	0	
0,0303	100	0,017371	35	0	
0,0450	100	0,025758	53	0	
0,0663	100	0,037979	80	0	1/2 α-T
0,0969	100	0,05554	120	0	
0,1401	100	0,080264	180	0	
0,1991	100	0,11406	269	0	
0,2764	100	0,158362	404	0	
0,3720	100	0,213162	606	0	
0,4815	100	0,275862	909	0	
0,5948	100	0,340764	1364	0	
0,6988	100	0,400398	2045	1	
0,7837	100	0,449004	3068	1	
0,8484	100	0,486065	4602	1	
0,9016	100	0,516571	6903	2	
0,9557	100	0,547544	10355	3	
1,0197	100	0,584225	15532	4	
1,0970	100	0,628492	23298	6	
1,1849	100	0,678866	34947	10	
1,2758	100	0,73094	52420	15	
1,3585	100	0,77831	78630	22	
1,4224	100	0,814937	117945	33	
1,4629	100	0,838092	176917	49	
1,4829	100	0,849548	265376	74	
1,4903	100	0,853822	398064	111	
1,4921	100	0,854858	518400	144	

Displ [mm]	1/2 Width	ist [degre	time [sec.]	time (h)	TWIST
0,0001	100	8,51E-05	0	0	
0,0003	100	0,000148	0	0	
0,0004	100	0,000242	0	0	
0,0007	100	0,000384	0	0	
0,0010	100	0,000595	0	0	
0,0016	100	0,000913	1	0	
0,0024	100	0,00139	1	0	
0,0037	100	0,002105	1	0	
0,0055	100	0,003175	2	0	
0,0083	100	0,00478	3	0	
0,0125	100	0,007181	4	0	
0,0188	100	0,010772	6	0	
0,0282	100	0,016134	9	0	
0,0421	100	0,024124	14	0	
0,0628	100	0,035987	21	0	
0,0934	100	0,053515	32	0	
0,1383	100	0,079219	47	0	1/2 α-R
0,2033	100	0,116502	71	0	
0,2962	100	0,169711	105	0	
0,4257	100	0,24388	160	0	
0,6001	100	0,343827	239	0	
0,8242	100	0,47223	359	0	
1,0939	100	0,626711	539	0	
1,3913	100	0,797076	808	0	
1,6854	100	0,96556	1212	0	
1,9426	100	1,112911	1818	1	
2,1451	100	1,228886	2727	1	
2,3025	100	1,318997	4091	1	
2,4447	100	1,400414	6136	2	
2,6027	100	1,490901	9204	3	
2,7947	100	1,600828	13806	4	
3,0225	100	1,731255	20709	6	
3,2728	100	1,874479	31064	9	
3,5194	100	2,01563	46596	13	
3,7304	100	2,136377	69893	19	
3,8816	100	2,222856	104840	29	
3,9686	100	2,272625	157260	44	
4,0071	100	2,294689	235890	66	
4,0198	100	2,301948	353835	98	
4,0217	100	2,302995	518400	144	

WB-2-Cup

Displ [mm]	time [sec.]	time (h)	Cup
0,0001	0	0	
0,0002	1	0	
0,0003	1	0	
0,0004	1	0	
0,0007	2	0	
0,0010	3	0	
0,0015	4	0	
0,0023	6	0	
0,0034	9	0	
0,0051	14	0	
0,0076	21	0	
0,0113	32	0	
0,0167	47	0	
0,0246	71	0	
0,0360	106	0	
0,0520	160	0	
0,0738	239	0	E-reference
0,1024	359	0	
0,1377	539	0	
0,1781	808	0	
0,2201	1212	0	
0,2589	1818	1	
0,2904	2727	1	
0,3131	4091	1	
0,3290	6136	2	
0,3419	9204	3	
0,3553	13806	4	
0,3711	20709	6	
0,3894	31064	9	
0,4090	46596	13	
0,4278	69893	19	
0,4434	104840	29	
0,4541	157260	44	
0,4600	235890	66	
0,4624	353835	98	
0,4632	518400	144	

Displ [mm]	time [sec.]	time (h)	Cup
0,0001	0	0	
0,0002	1	0	
0,0003	1	0	
0,0004	1	0	
0,0006	2	0	
0,0009	3	0	
0,0013	4	0	
0,0020	6	0	
0,0030	9	0	
0,0044	14	0	
0,0066	21	0	
0,0099	32	0	
0,0146	47	0	
0,0216	71	0	
0,0317	106	0	
0,0458	160	0	
0,0653	239	0	1/2 E-L
0,0911	359	0	
0,1233	539	0	
0,1607	808	0	
0,2003	1212	0	
0,2375	1818	1	
0,2683	2727	1	
0,2915	4091	1	
0,3090	6136	2	
0,3248	9204	3	
0,3425	13806	4	
0,3638	20709	6	
0,3888	31064	9	
0,4155	46596	13	
0,4413	69893	19	
0,4625	104840	29	
0,4773	157260	44	
0,4854	235890	66	
0,4888	353835	98	
0,4898	518400	144	

Displ [mm]	time [sec.]	time (h)	Cup
0,0001	0	0	
0,0002	1	0	
0,0003	1	0	
0,0004	1	0	
0,0006	2	0	
0,0010	3	0	
0,0015	4	0	
0,0022	6	0	
0,0033	9	0	
0,0049	14	0	
0,0073	21	0	
0,0109	32	0	
0,0161	47	0	
0,0238	71	0	
0,0348	106	0	
0,0502	160	0	
0,0713	239	0	1/2 E-R
0,0990	359	0	
0,1332	539	0	
0,1724	808	0	
0,2133	1212	0	
0,2511	1818	1	
0,2818	2727	1	
0,3041	4091	1	
0,3199	6136	2	
0,3328	9204	3	
0,3463	13806	4	
0,3623	20709	6	
0,3809	31064	9	
0,4009	46596	13	
0,4200	69893	19	
0,4358	104840	29	
0,4467	157260	44	
0,4527	235890	66	
0,4552	353835	98	
0,4559	518400	144	

Displ [mm]	time [sec.]	time (h)	Cup
0,0001	0	0	
0,0002	1	0	
0,0003	1	0	
0,0004	1	0	
0,0007	2	0	
0,0010	3	0	
0,0015	4	0	
0,0023	6	0	
0,0034	9	0	
0,0051	14	0	
0,0076	21	0	
0,0113	32	0	
0,0167	47	0	
0,0246	71	0	
0,0360	106	0	
0,0520	160	0	
0,0738	239	0	G-reference
0,1024	359	0	
0,1377	539	0	
0,1781	808	0	
0,2201	1212	0	
0,2589	1818	1	
0,2904	2727	1	
0,3131	4091	1	
0,3290	6136	2	
0,3419	9204	3	
0,3553	13806	4	
0,3711	20709	6	
0,3894	31064	9	
0,4090	46596	13	
0,4278	69893	19	
0,4434	104840	29	
0,4541	157260	44	
0,4600	235890	66	
0,4624	353835	98	
0,4632	518400	144	

Displ [mm]	time [sec.]	time (h)	Cup
0,0001	0	0	
0,0002	1	0	
0,0003	1	0	
0,0005	1	0	
0,0007	2	0	
0,0011	3	0	
0,0016	4	0	
0,0024	6	0	
0,0036	9	0	
0,0054	14	0	
0,0080	21	0	
0,0120	32	0	
0,0177	47	0	
0,0262	71	0	
0,0383	106	0	
0,0554	160	0	
0,0788	239	0	1/2 G-LT
0,1095	359	0	
0,1478	539	0	
0,1919	808	0	
0,2381	1212	0	
0,2812	1818	1	
0,3165	2727	1	
0,3425	4091	1	
0,3615	6136	2	
0,3779	9204	3	
0,3955	13806	4	
0,4167	20709	6	
0,4413	31064	9	
0,4677	46596	13	
0,4931	69893	19	
0,5141	104840	29	
0,5286	157260	44	
0,5366	235890	66	
0,5399	353835	98	
0,5409	518400	144	

Displ [mm]	time [sec.]	time (h)	Cup
0,0001	0	0	
0,0002	1	0	
0,0003	1	0	
0,0004	1	0	
0,0006	2	0	
0,0010	3	0	
0,0015	4	0	
0,0022	6	0	
0,0033	9	0	
0,0049	14	0	
0,0073	21	0	
0,0109	32	0	
0,0161	47	0	
0,0238	71	0	
0,0348	106	0	
0,0502	160	0	
0,0768	239	0	1/2 G-LR
0,1063	359	0	
0,1427	539	0	
0,1842	808	0	
0,2271	1212	0	
0,2665	1818	1	
0,2982	2727	1	
0,3208	4091	1	
0,3361	6136	2	
0,3480	9204	3	
0,3599	13806	4	
0,3737	20709	6	
0,3896	31064	9	
0,4067	46596	13	
0,4231	69893	19	
0,4366	104840	29	
0,4459	157260	44	
0,4510	235890	66	
0,4531	353835	98	
0,4538	518400	144	

Displ [mm]	time [sec.]	time (h)	Cup
0,0001	0	0	
0,0002	1	0	
0,0003	1	0	
0,0005	1	0	
0,0008	2	0	
0,0011	3	0	
0,0017	4	0	
0,0026	6	0	
0,0038	9	0	
0,0057	14	0	
0,0085	21	0	
0,0127	32	0	
0,0189	47	0	
0,0278	71	0	
0,0405	106	0	
0,0585	160	0	
0,0828	239	0	1/2 G-TR
0,1146	359	0	
0,1535	539	0	
0,1978	808	0	
0,2433	1212	0	
0,2849	1818	1	
0,3182	2727	1	
0,3416	4091	1	
0,3572	6136	2	
0,3687	9204	3	
0,3797	13806	4	
0,3923	20709	6	
0,4069	31064	9	
0,4224	46596	13	
0,4373	69893	19	
0,4496	104840	29	
0,4581	157260	44	
0,4627	235890	66	
0,4646	353835	98	
0,4652	518400	144	

Displ [mm]	time [sec.]	time (h)	Cup	Displ [mm]	Displ+0,02	time [sec.]	time (h)	Cup	Displ [mm]	time [sec.]	time (h)	Cup	Displ [mm]	time [sec.]	time (h)	Cup
0,0001	0	0		0,0001	0,02	0	0		-0,0001	5	0		0,0002	0	0	
0,0002	1	0		0,0002	0,02	1	0		-0,0002	7	0		0,0003	1	0	
0,0003	1	0		0,0003	0,02	1	0		-0,0002	11	0		0,0005	1	0	
0,0004	1	0		0,0004	0,02	1	0		-0,0004	16	0		0,0007	1	0	
0,0007	2	0		0,0007	0,02	2	0		-0,0005	24	0		0,0010	2	0	
0,0010	3	0		0,0010	0,02	3	0		-0,0008	35	0		0,0016	3	0	
0,0015	4	0		0,0015	0,02	4	0		-0,0012	53	0		0,0024	4	0	
0,0023	6	0		0,0023	0,02	6	0		-0,0018	80	0		0,0035	6	0	
0,0034	9	0		0,0034	0,02	9	0		-0,0028	120	0		0,0053	9	0	
0,0051	14	0		0,0051	0,03	14	0		-0,0042	180	0		0,0079	14	0	
0,0076	21	0		0,0076	0,03	21	0		-0,0064	269	0		0,0118	21	0	
0,0113	32	0		0,0112	0,03	32	0		-0,0096	404	0		0,0176	32	0	
0,0167	47	0		0,0167	0,04	47	0		-0,0141	606	0		0,0262	47	0	
0,0246	71	0		0,0246	0,04	71	0		-0,0199	909	0		0,0386	71	0	
0,0360	106	0		0,0359	0,06	106	0		-0,0267	1364	0		0,0565	106	0	
0,0520	160	0		0,0519	0,07	160	0		-0,0338	2045	1		0,0818	160	0	
0,0738	239	0	α-reference	0,0737	0,09	239	0	1/2 α-L	-0,0402	3068	1	1/2 α-T	0,1165	239	0	1/2 α-R
0,1024	359	0		0,1022	0,12	359	0		-0,0462	4602	1		0,1623	359	0	
0,1377	539	0		0,1374	0,16	539	0		-0,0525	6903	2		0,2193	539	0	
0,1781	808	0		0,1778	0,20	808	0		-0,0602	10355	3		0,2855	808	0	
0,2201	1212	0		0,2198	0,24	1212	0		-0,0701	15532	4		0,3551	1212	0	
0,2589	1818	1		0,2585	0,28	1818	1		-0,0824	23298	6		0,4204	1818	1	
0,2904	2727	1		0,2900	0,31	2727	1		-0,0965	34947	10		0,4744	2727	1	
0,3131	4091	1		0,3127	0,33	4091	1		-0,1113	52420	15		0,5145	4091	1	
0,3290	6136	2		0,3287	0,35	6136	2		-0,1249	78630	22		0,5445	6136	2	
0,3419	9204	3		0,3416	0,36	9204	3		-0,1356	117945	33		0,5710	9204	3	
0,3553	13806	4		0,3550	0,38	13806	4		-0,1426	176917	49		0,6003	13806	4	
0,3711	20709	6		0,3708	0,39	20709	6		-0,1461	265376	74		0,6355	20709	6	
0,3894	31064	9		0,3892	0,41	31064	9		-0,1475	398054	111		0,6766	31064	9	
0,4090	46596	13		0,4088	0,43	46596	13		-0,1478	518400	144		0,7207	46596	13	
0,4278	69893	19		0,4277	0,45	69893	19						0,7630	69893	19	
0,4434	104840	29		0,4434	0,46	104840	29						0,7981	104840	29	
0,4541	157260	44		0,4541	0,47	157260	44						0,8222	157260	44	
0,4600	235890	66		0,4600	0,48	235890	66						0,8354	235890	66	
0,4624	353835	98		0,4624	0,48	353835	98						0,8409	353835	98	
0,4632	518400	144		0,4632	0,48	518400	144						0,8426	518400	144	

WB-2-Bow

Displ [mm]	time [sec.]	time (h)	Bow	Displ [mm]	time [sec.]	time (h)	Bow	Displ [mm]	time [sec.]	time (h)	Bow	Displ [mm]	time [sec.]	time (h)	Bow
0,0006	0	0		0,0004	0	0		0,0008	0	0		0,0006	0	0	
0,0010	0	0		0,0006	0	0		0,0012	0	0		0,0010	0	0	
0,0015	0	0		0,0010	0	0		0,0019	0	0		0,0015	0	0	
0,0024	0	0		0,0015	0	0		0,0030	0	0		0,0023	0	0	
0,0036	1	0		0,0023	1	0		0,0045	1	0		0,0036	1	0	
0,0054	1	0		0,0035	1	0		0,0068	1	0		0,0054	1	0	
0,0082	1	0		0,0053	1	0		0,0103	1	0		0,0081	1	0	
0,0123	2	0		0,0080	2	0		0,0155	2	0		0,0122	2	0	
0,0185	3	0		0,0121	3	0		0,0233	3	0		0,0184	3	0	
0,0278	4	0		0,0181	4	0		0,0350	4	0		0,0276	4	0	
0,0417	6	0		0,0272	6	0		0,0525	6	0		0,0413	6	0	
0,0624	9	0		0,0407	9	0		0,0786	9	0		0,0619	9	0	
0,0932	14	0		0,0608	14	0		0,1174	14	0		0,0925	14	0	
0,1390	21	0		0,0907	21	0		0,1750	21	0		0,1379	21	0	
0,2066	32	0		0,1349	32	0		0,2602	32	0		0,2050	32	0	
0,3057	47	0		0,1996	47	0		0,3848	47	0		0,3034	47	0	
0,4493	71	0	E-reference	0,2935	71	0	1/2 E-L	0,5654	71	0	1/2 E-R	0,4460	71	0	1/2 E-T
0,6539	106	0		0,4274	106	0		0,8224	106	0		0,6495	106	0	
0,9384	160	0		0,6140	160	0		1,1796	160	0		0,9330	160	0	
1,3210	239	0		0,8653	239	0		1,6588	239	0		1,3149	239	0	
1,8109	359	0		1,1884	359	0		2,2712	359	0		1,8055	359	0	
2,3991	539	0		1,5781	539	0		3,0039	539	0		2,3969	539	0	
3,0479	808	0		2,0106	808	0		3,8084	808	0		3,0529	808	0	
3,6922	1212	0		2,4433	1212	0		4,6027	1212	0		3,7089	1212	0	
4,2567	1818	1		2,8260	1818	1		5,2938	1818	1		4,2886	1818	1	
4,6838	2727	1		3,1193	2727	1		5,8115	2727	1		4,7324	2727	1	
4,9531	4091	1		3,3094	4091	1		6,1308	4091	1		5,0192	4091	1	
5,0822	6136	2		3,4095	6136	2		6,2715	6136	2		5,1689	6136	2	
5,1119	9204	3		3,4492	9204	3		6,2813	9204	3		5,2259	9204	3	
5,0840	13806	4		3,4578	13806	4		6,2097	13806	4		5,2345	13806	4	
5,0257	20709	6		3,4538	20709	6		6,0900	20709	6		5,2226	20709	6	
4,9505	31064	9		3,4451	31064	9		5,9405	31064	9		5,2023	31064	9	
4,8665	46596	13		3,4341	46596	13		5,7757	46596	13		5,1776	46596	13	
4,7830	69893	19		3,4219	69893	19		5,6134	69893	19		5,1513	69893	19	
4,7107	104840	29		3,4103	104840	29		5,4747	104840	29		5,1266	104840	29	
4,6582	157260	44		3,4009	157260	44		5,3756	157260	44		5,1072	157260	44	
4,6277	235890	66		3,3948	235890	66		5,3188	235890	66		5,0950	235890	66	
4,6141	353835	98		3,3918	353835	98		5,2939	353835	98		5,0891	353835	98	
4,6097	518400	144		3,3908	518400	144		5,2859	518400	144		5,0871	518400	144	

Displ [mm]	time [sec.]	time (h)	Bow	Displ [mm]		time [sec.]	time (h)	Bow	Displ [mm]	time [sec.]	time (h)	Bow	Displ [mm]	time [sec.]	time (h)	Bow
0,0006	0	0		0,0006		0	0		0,0007	0	0		0,0006	0	0	
0,0010	0	0		0,0009		0	0		0,0011	0	0		0,0010	0	0	
0,0015	0	0		0,0014		0	0		0,0017	0	0		0,0015	0	0	
0,0024	0	0		0,0021		0	0		0,0026	0	0		0,0024	0	0	
0,0036	1	0		0,0032		1	0		0,0039	1	0		0,0036	1	0	
0,0054	1	0		0,0049		1	0		0,0059	1	0		0,0055	1	0	
0,0082	1	0		0,0073		1	0		0,0089	1	0		0,0083	1	0	
0,0123	2	0		0,0110		2	0		0,0134	2	0		0,0124	2	0	
0,0185	3	0		0,0166		3	0		0,0201	3	0		0,0187	3	0	
0,0278	4	0		0,0249		4	0		0,0302	4	0		0,0280	4	0	
0,0417	6	0		0,0373		6	0		0,0452	6	0		0,0420	6	0	
0,0624	9	0		0,0559		9	0		0,0677	9	0		0,0629	9	0	
0,0932	14	0		0,0835		14	0		0,1012	14	0		0,0940	14	0	
0,1390	21	0		0,1245		21	0		0,1509	21	0		0,1401	21	0	
0,2066	32	0		0,1851		32	0		0,2243	32	0		0,2083	32	0	
0,3057	47	0		0,2738		47	0		0,3319	47	0		0,3082	47	0	
0,4493	71	0	G-reference	0,4024		71	0	1/2 G-LT	0,4878	71	0	1/2 G-LR	0,4529	71	0	1/2 G-TR
0,6539	106	0		0,5855		106	0		0,7099	106	0		0,6591	106	0	
0,9384	160	0		0,8401		160	0		1,0188	160	0		0,9460	160	0	
1,3210	239	0		1,1821		239	0		1,4341	239	0		1,3314	239	0	
1,8109	359	0		1,6199		359	0		1,9660	359	0		1,8252	359	0	
2,3991	539	0		2,1447		539	0		2,6046	539	0		2,4177	539	0	
3,0479	808	0		2,7226		808	0		3,3089	808	0		3,0712	808	0	
3,6922	1212	0		3,2953		1212	0		4,0082	1212	0		3,7198	1212	0	
4,2567	1818	1		3,7959		1818	1		4,6209	1818	1		4,2879	1818	1	
4,6838	2727	1		4,1733		2727	1		5,0845	2727	1		4,7175	2727	1	
4,9531	4091	1		4,4093		4091	1		5,3767	4091	1		4,9880	4091	1	
5,0822	6136	2		4,5192		6136	2		5,5166	6136	2		5,1170	6136	2	
5,1119	9204	3		4,5384		9204	3		5,5487	9204	3		5,1456	9204	3	
5,0840	13806	4		4,5034		13806	4		5,5181	13806	4		5,1157	13806	4	
5,0257	20709	6		4,4384		20709	6		5,4544	20709	6		5,0547	20709	6	
4,9505	31064	9		4,3558		31064	9		5,3723	31064	9		4,9762	31064	9	
4,8665	46596	13		4,2640		46596	13		5,2807	46596	13		4,8887	46596	13	
4,7830	69893	19		4,1730		69893	19		5,1896	69893	19		4,8017	69893	19	
4,7107	104840	29		4,0944		104840	29		5,1107	104840	29		4,7265	104840	29	
4,6582	157260	44		4,0377		157260	44		5,0535	157260	44		4,6720	157260	44	
4,6277	235890	66		4,0048		235890	66		5,0202	235890	66		4,6404	235890	66	
4,6141	353835	98		3,9902		353835	98		5,0054	353835	98		4,6263	353835	98	
4,6097	518400	144		3,9855		518400	144		5,0006	518400	144		4,6218	518400	144	

Displ [mm]	time [sec.]	time (h)	Bow	Displ [mm]	Displ+0,1	time [sec.]	time (h)	Bow	Displ [mm]	time [sec.]	time (h)	Bow	Displ [mm]	time [sec.]	time (h)	Bow
0,0006	0	0		0,0006	0,1006	0	0		0,0001	0	0		0,0007	0	0	
0,0010	0	0		0,0010	0,1010	0	0		0,0002	0	0		0,0011	0	0	
0,0015	0	0		0,0015	0,1015	0	0		0,0003	0	0		0,0016	0	0	
0,0024	0	0		0,0024	0,1024	0	0		0,0005	0	0		0,0025	0	0	
0,0036	1	0		0,0036	0,1036	1	0		0,0008	0	0		0,0038	1	0	
0,0054	1	0		0,0054	0,1054	1	0		0,0012	0	0		0,0058	1	0	
0,0082	1	0		0,0082	0,1082	1	0		0,0018	1	0		0,0087	1	0	
0,0123	2	0		0,0123	0,1123	2	0		0,0027	1	0		0,0132	2	0	
0,0185	3	0		0,0185	0,1185	3	0		0,0040	1	0		0,0198	3	0	
0,0278	4	0		0,0278	0,1278	4	0		0,0060	2	0		0,0297	4	0	
0,0417	6	0		0,0416	0,1416	6	0		0,0090	3	0		0,0445	6	0	
0,0624	9	0		0,0623	0,1623	9	0		0,0135	5	0		0,0667	9	0	
0,0932	14	0		0,0931	0,1931	14	0		0,0203	7	0		0,0997	14	0	
0,1390	21	0		0,1388	0,2388	21	0		0,0303	11	0		0,1488	21	0	
0,2066	32	0		0,2063	0,3063	32	0		0,0452	16	0		0,2213	32	0	
0,3057	47	0		0,3053	0,4053	47	0		0,0673	24	0		0,3278	47	0	
0,4493	71	0	α-reference	0,4487	0,5487	71	0	1/2 α-L	0,0996	35	0	1/2 α-T	0,4825	71	0	1/2 α-R
0,6539	106	0		0,6530	0,7530	106	0		0,1467	53	0		0,7039	106	0	
0,9384	160	0		0,9372	1,0372	160	0		0,2141	80	0		1,0136	160	0	
1,3210	239	0		1,3192	1,4192	239	0		0,3084	120	0		1,4335	239	0	
1,8109	359	0		1,8086	1,9086	359	0		0,4362	180	0		1,9779	359	0	
2,3991	539	0		2,3961	2,4961	539	0		0,6016	269	0		2,5422	539	0	
3,0479	808	0		3,0442	3,1442	808	0		0,8023	404	0		3,3908	808	0	
3,6922	1212	0		3,6877	3,7877	1212	0		1,0255	606	0		4,1540	1212	0	
4,2567	1818	1		4,2517	4,3517	1818	1		1,2476	909	0		4,8441	1818	1	
4,6838	2727	1		4,6785	4,7785	2727	1		1,4400	1364	0		5,3889	2727	1	
4,9531	4091	1		4,9477	5,0477	4091	1		1,5804	2045	1		5,7632	4091	1	
5,0822	6136	2		5,0768	5,1768	6136	2		1,6577	3068	1		5,9960	6136	2	
5,1119	9204	3		5,1069	5,2069	9204	3		1,6676	4602	1		6,1478	9204	3	
5,0840	13806	4		5,0794	5,1794	13806	4		1,6083	6903	2		6,2762	13806	4	
5,0257	20709	6		5,0218	5,1218	20709	6		1,4817	10355	3		6,4146	20709	6	
4,9505	31064	9		4,9473	5,0473	31064	9		1,2939	15532	4		6,5713	31064	9	
4,8665	46596	13		4,8642	4,9642	46596	13		1,0532	23298	6		6,7378	46596	13	
4,7830	69893	19		4,7815	4,8815	69893	19		0,7735	34947	10		6,8956	69893	19	
4,7107	104840	29		4,7098	4,8098	104840	29		0,4792	52420	15		7,0243	104840	29	
4,6582	157260	44		4,6578	4,7578	157260	44		0,2050	78630	22		7,1112	157260	44	
4,6277	235890	66		4,6276	4,7276	235890	66		0,2050	117945	33		7,1576	235890	66	
4,6141	353835	98		4,6141	4,7141	353835	98		0,2050	176917	49		7,1766	353835	98	
4,6097	518400	144		4,6097	4,7097	518400	144		0,2050	265376	74		7,1821	518400	144	
									0,2050	398064	111					
									0,2050	518400	144					

WB-3-Crook

Displ [mm]	time [sec.]	time (h)	Crook	Displ [mm]	time [sec.]	time (h)	Crook	Displ [mm]	time [sec.]	time (h)	Crook	Displ [mm]	time [sec.]	time (h)	Crook
-0,0001	0	0		-0,0002	0	0		-0,0001	0	0		-0,0002	0	0	
-0,0002	0	0		-0,0003	0	0		-0,0002	0	0		-0,0003	0	0	
-0,0004	0	0		-0,0004	0	0		-0,0004	0	0		-0,0004	0	0	
-0,0005	0	0		-0,0007	0	0		-0,0005	0	0		-0,0007	0	0	
-0,0008	1	0		-0,0011	1	0		-0,0008	1	0		-0,0011	1	0	
-0,0013	1	0		-0,0017	1	0		-0,0013	1	0		-0,0017	1	0	
-0,0019	2	0		-0,0025	2	0		-0,0019	2	0		-0,0025	2	0	
-0,0029	2	0		-0,0039	2	0		-0,0029	2	0		-0,0039	2	0	
-0,0044	4	0		-0,0059	4	0		-0,0044	4	0		-0,0058	4	0	
-0,0066	6	0		-0,0088	6	0		-0,0066	6	0		-0,0088	6	0	
-0,0099	8	0		-0,0133	8	0		-0,0099	8	0		-0,0132	8	0	
-0,0149	12	0		-0,0199	12	0		-0,0149	12	0		-0,0198	12	0	
-0,0223	19	0		-0,0298	19	0		-0,0223	19	0		-0,0296	19	0	
-0,0333	28	0		-0,0446	28	0		-0,0333	28	0		-0,0443	28	0	
-0,0498	42	0		-0,0665	42	0		-0,0498	42	0		-0,0660	42	0	
-0,0742	63	0		-0,0989	63	0		-0,0742	63	0		-0,0982	63	0	
-0,1102	95	0	E-ref	-0,1465	95	0	1/2 E-L	-0,1101	95	0	1/2 E-R	-0,1453	95	0	1/2 E-T
-0,1628	142	0		-0,2153	142	0		-0,1627	142	0		-0,2136	142	0	
-0,2387	213	0		-0,3135	213	0		-0,2387	213	0		-0,3111	213	0	
-0,3464	319	0		-0,4503	319	0		-0,3463	319	0		-0,4468	319	0	
-0,4950	479	0		-0,6341	479	0		-0,4949	479	0		-0,6293	479	0	
-0,6923	718	0		-0,8695	718	0		-0,6923	718	0		-0,8630	718	0	
-0,9406	1077	0		-1,1508	1077	0		-0,9405	1077	0		-1,1424	1077	0	
-1,2301	1616	0		-1,4566	1616	0		-1,2301	1616	0		-1,4463	1616	0	
-1,5350	2424	1		-1,7502	2424	1		-1,5350	2424	1		-1,7382	2424	1	
-1,8154	3636	1		-1,9902	3636	1		-1,8154	3636	1		-1,9768	3636	1	
-2,0326	5454	2		-2,1507	5454	2		-2,0327	5454	2		-2,1364	5454	2	
-2,1687	8181	2		-2,2351	8181	2		-2,1688	8181	2		-2,2204	8181	2	
-2,2350	12272	3		-2,2687	12272	3		-2,2351	12272	3		-2,2539	12272	3	
-2,2592	18408	5		-2,2785	18408	5		-2,2593	18408	5		-2,2637	18408	5	
-2,2657	27612	8		-2,2806	27612	8		-2,2658	27612	8		-2,2657	27612	8	
-2,2669	41418	12		-2,2809	41418	12		-2,2670	41418	12		-2,2660	41418	12	
-2,2670	62127	17		-2,2809	62127	17		-2,2671	62127	17		-2,2661	62127	17	
-2,2670	93191	26		-2,2809	93191	26		-2,2672	93191	26		-2,2661	93191	26	
-2,2670	139786	39		-2,2809	139786	39		-2,2672	139786	39		-2,2661	139786	39	
-2,2670	209680	58		-2,2809	209680	58		-2,2672	209680	58		-2,2661	209680	58	
-2,2670	314520	87		-2,2809	314520	87		-2,2672	314520	87		-2,2661	314520	87	
-2,2670	518400	144		-2,2809	518400	144		-2,2672	518400	144		-2,2661	518400	144	

Displ [mm]	time [sec.]	time (h)	Crook	Displ [mm]	time [sec.]	time (h)	Crook	Displ [mm]	time [sec.]	time (h)	Crook	Displ [mm]	time [sec.]	time (h)	Crook
-0,0001	0	0		-0,0001	0	0		-0,0001	0	0		-0,0001	0	0	
-0,0002	0	0		-0,0002	0	0		-0,0002	0	0		-0,0002	0	0	
-0,0004	0	0		-0,0004	0	0		-0,0004	0	0		-0,0004	0	0	
-0,0005	0	0		-0,0005	0	0		-0,0005	0	0		-0,0005	0	0	
-0,0008	1	0		-0,0008	1	0		-0,0008	1	0		-0,0008	1	0	
-0,0013	1	0		-0,0013	1	0		-0,0013	1	0		-0,0013	1	0	
-0,0019	2	0		-0,0019	2	0		-0,0019	2	0		-0,0019	2	0	
-0,0029	2	0		-0,0029	2	0		-0,0029	2	0		-0,0029	2	0	
-0,0044	4	0		-0,0044	4	0		-0,0044	4	0		-0,0044	4	0	
-0,0066	6	0		-0,0066	6	0		-0,0066	6	0		-0,0066	6	0	
-0,0099	8	0		-0,0099	8	0		-0,0099	8	0		-0,0099	8	0	
-0,0149	12	0		-0,0148	12	0		-0,0149	12	0		-0,0149	12	0	
-0,0223	19	0		-0,0222	19	0		-0,0223	19	0		-0,0223	19	0	
-0,0333	28	0		-0,0332	28	0		-0,0333	28	0		-0,0333	28	0	
-0,0498	42	0		-0,0496	42	0		-0,0498	42	0		-0,0498	42	0	
-0,0742	63	0		-0,0740	63	0		-0,0742	63	0		-0,0742	63	0	
-0,1102	95	0	G-ref	-0,1098	95	0	1/2 G-LT	-0,1102	95	0	1/2 G-LR	-0,1102	95	0	1/2 G-TR
-0,1628	142	0		-0,1623	142	0		-0,1628	142	0		-0,1628	142	0	
-0,2387	213	0		-0,2380	213	0		-0,2387	213	0		-0,2387	213	0	
-0,3464	319	0		-0,3453	319	0		-0,3464	319	0		-0,3464	319	0	
-0,4950	479	0		-0,4935	479	0		-0,4950	479	0		-0,4950	479	0	
-0,6923	718	0		-0,6903	718	0		-0,6923	718	0		-0,6923	718	0	
-0,9406	1077	0		-0,9380	1077	0		-0,9406	1077	0		-0,9406	1077	0	
-1,2301	1616	0		-1,2268	1616	0		-1,2301	1616	0		-1,2301	1616	0	
-1,5350	2424	1		-1,5310	2424	1		-1,5350	2424	1		-1,5350	2424	1	
-1,8154	3636	1		-1,8109	3636	1		-1,8154	3636	1		-1,8154	3636	1	
-2,0326	5454	2		-2,0277	5454	2		-2,0326	5454	2		-2,0326	5454	2	
-2,1687	8181	2		-2,1635	8181	2		-2,1687	8181	2		-2,1687	8181	2	
-2,2350	12272	3		-2,2297	12272	3		-2,2350	12272	3		-2,2350	12272	3	
-2,2592	18408	5		-2,2539	18408	5		-2,2592	18408	5		-2,2592	18408	5	
-2,2657	27612	8		-2,2603	27612	8		-2,2656	27612	8		-2,2656	27612	8	
-2,2669	41418	12		-2,2615	41418	12		-2,2669	41418	12		-2,2669	41418	12	
-2,2670	62127	17		-2,2617	62127	17		-2,2670	62127	17		-2,2670	62127	17	
-2,2670	93191	26		-2,2617	93191	26		-2,2670	93191	26		-2,2670	93191	26	
-2,2670	139786	39		-2,2617	139786	39		-2,2670	139786	39		-2,2670	139786	39	
-2,2670	209680	58		-2,2617	209680	58		-2,2670	209680	58		-2,2670	209680	58	
-2,2670	314520	87		-2,2617	314520	87		-2,2670	314520	87		-2,2670	314520	87	
-2,2670	518400	144		-2,2617	518400	144		-2,2670	518400	144		-2,2670	518400	144	

Displ [mm]	time [sec.]	time (h)	Crook	Displ [mm]	time [sec.]	time (h)	Crook	Displ [mm]	time [sec.]	time (h)	Crook	Displ [mm]	time [sec.]	time (h)	Crook
0,00	0	0		-0,0001	0	0		0,00	0	0		0,00	0	0	
0,00	0	0		-0,0002	0	0		0,00	0	0		0,00	0	0	
0,00	0	0		-0,0004	0	0		0,00	0	0		0,00	1	0	
0,00	0	0		-0,0005	0	0		0,00	0	0		0,00	1	0	
0,00	1	0		-0,0008	1	0		0,00	1	0		0,00	2	0	
0,00	1	0		-0,0013	1	0		0,00	1	0		0,00	3	0	
0,00	2	0		-0,0019	2	0		0,00	2	0		0,00	4	0	
0,00	2	0		-0,0029	2	0		0,00	2	0		0,00	6	0	
0,00	4	0		-0,0044	4	0		0,00	4	0		-0,01	10	0	
-0,01	6	0		-0,0066	6	0		-0,01	6	0		-0,01	15	0	
-0,01	8	0		-0,0099	8	0		-0,01	8	0		-0,01	22	0	
-0,01	12	0		-0,0149	12	0		-0,02	12	0		-0,02	33	0	
-0,02	19	0		-0,0223	19	0		-0,03	19	0		-0,03	50	0	
-0,03	28	0		-0,0333	28	0		-0,04	28	0		-0,04	75	0	
-0,05	42	0		-0,0498	42	0		-0,06	42	0		-0,06	112	0	
-0,07	63	0		-0,0742	63	0		-0,08	63	0		-0,09	168	0	
-0,11	95	0	α-ref	-0,1102	95	0	1/2 α-L	-0,12	95	0	1/2 α-T	-0,14	252	0	1/2 α-R
-0,16	142	0		-0,1628	142	0		-0,18	142	0		-0,20	378	0	
-0,24	213	0		-0,2387	213	0		-0,27	213	0		-0,28	567	0	
-0,35	319	0		-0,3464	319	0		-0,39	319	0		-0,39	851	0	
-0,49	479	0		-0,4950	479	0		-0,55	479	0		-0,52	1277	0	
-0,69	718	0		-0,6923	718	0		-0,76	718	0		-0,67	1915	1	
-0,94	1077	0		-0,9406	1077	0		-1,03	1077	0		-0,82	2873	1	
-1,23	1616	0		-1,2301	1616	0		-1,33	1616	0		-0,95	4309	1	
-1,53	2424	1		-1,5350	2424	1		-1,63	2424	1		-1,04	6464	2	
-1,82	3636	1		-1,8154	3636	1		-1,90	3636	1		-1,09	9696	3	
-2,03	5454	2		-2,0326	5454	2		-2,09	5454	2		-1,11	14545	4	
-2,17	8181	2		-2,1687	8181	2		-2,21	8181	2		-1,12	21817	6	
-2,24	12272	3		-2,2350	12272	3		-2,26	12272	3		-1,12	32725	9	
-2,26	18408	5		-2,2592	18408	5		-2,28	18408	5		-1,12	49088	14	
-2,27	27612	8		-2,2656	27612	8		-2,28	27612	8		-1,12	73632	20	
-2,27	41418	12		-2,2669	41418	12		-2,28	41418	12		-1,12	110448	31	
-2,27	62127	17		-2,2670	62127	17		-2,28	62127	17		-1,12	165673	46	
-2,27	93191	26		-2,2670	93191	26		-2,28	93191	26		-1,12	248509	69	
-2,27	139786	39		-2,2670	139786	39		-2,28	139786	39		-1,12	414182	115	
-2,27	209680	58		-2,2670	209680	58		-2,28	209680	58		-1,12	518400	144	
-2,27	314520	87		-2,2670	314520	87		-2,28	314520	87					
-2,27	518400	144		-2,2670	518400	144		-2,28	518400	144					

Appendix H: Data moisture distribution due to thickness Gesso layer

Temp.	Time [sec.]	Time [h]	
14,00	0	0	
14,00	0	0	
14,00	0	0	
14,00	0	0	
14,00	1	0	
14,00	1	0	
14,00	2	0	
14,00	3	0	
14,00	7	0	
14,00	13	0	
14,00	26	0	
14,00	45	0	
14,00	74	0	
14,00	117	0	
14,00	182	0	
14,00	279	0	
14,00	425	0	Reference
13,99	643	0	
13,99	971	0	
13,98	1464	0	
13,95	2202	1	
13,90	3309	1	
13,82	4970	1	
13,68	7461	2	
13,47	11197	3	
13,16	16802	5	
12,71	25210	7	
12,11	37821	11	
11,33	56738	16	
10,38	85114	24	
9,33	127677	35	
8,28	191522	53	
7,36	287289	80	
6,68	430941	120	
6,27	518400	144	

Temp	Time [sec.]	Time [h]	
14,00	0	0	
14,00	0	0	
14,00	0	0	
14,00	0	0	
14,00	1	0	
14,00	1	0	
14,00	2	0	
14,00	3	0	
14,00	7	0	
14,00	13	0	
14,00	26	0	
14,00	45	0	
14,00	74	0	
14,00	117	0	
14,00	182	0	
14,00	279	0	
14,00	425	0	2 mm Gesso
14,00	643	0	
13,99	971	0	
13,99	1464	0	
13,97	2202	1	
13,95	3309	1	
13,91	4970	1	
13,84	7461	2	
13,73	11197	3	
13,57	16802	5	
13,33	25210	7	
12,99	37821	11	
12,53	56738	16	
11,92	85114	24	
11,16	127677	35	
10,24	191522	53	
9,23	287289	80	
8,21	430941	120	
7,32	518400	144	

Temp	Time [sec.]	Time [h]	
14,00	0	0	
14,00	0	0	
14,00	0	0	
14,00	0	0	
14,00	1	0	
14,00	1	0	
14,00	2	0	
14,00	3	0	
14,00	7	0	
14,00	13	0	
14,00	26	0	
14,00	45	0	
14,00	74	0	
14,00	117	0	
14,00	182	0	
14,00	279	0	
14,00	425	0	0,2 mm Gesso
14,00	643	0	
13,99	971	0	
13,99	1464	0	
13,97	2202	1	
13,94	3309	1	
13,89	4970	1	
13,80	7461	2	
13,66	11197	3	
13,42	16802	5	
13,06	25210	7	
12,53	37821	11	
11,79	56738	16	
10,86	85114	24	
9,77	127677	35	
8,64	191522	53	
7,62	287289	80	
6,84	430941	120	
6,35	518400	144	

Temp	Time [sec.]	Time [h]	
14,00	0	0	
14,00	0	0	
14,00	0	0	
14,00	0	0	
14,00	1	0	
14,00	1	0	
14,00	2	0	
14,00	3	0	
14,00	7	0	
14,00	13	0	
14,00	26	0	
14,00	45	0	
14,00	74	0	
14,00	117	0	
14,00	182	0	
14,00	279	0	
14,00	425	0	0,6 mm Gesso
14,00	643	0	
13,99	971	0	
13,99	1464	0	
13,97	2202	1	
13,95	3309	1	
13,91	4970	1	
13,83	7461	2	
13,71	11197	3	
13,52	16802	5	
13,23	25210	7	
12,81	37821	11	
12,21	56738	16	
11,40	85114	24	
10,39	127677	35	
9,27	191522	53	
8,15	287289	80	
7,21	430941	120	
6,56	518400	144	

Temp	Time [sec.]	Time [h]	
14,00	0	0	
14,00	0	0	
14,00	0	0	
14,00	0	0	
14,00	1	0	
14,00	1	0	
14,00	2	0	
14,00	3	0	
14,00	7	0	
14,00	13	0	
14,00	26	0	
14,00	45	0	
14,00	74	0	
14,00	117	0	
14,00	182	0	
14,00	279	0	
14,00	425	0	1,0 mm Gesso
14,00	643	0	
13,99	971	0	
13,99	1464	0	
13,97	2202	1	
13,95	3309	1	
13,91	4970	1	
13,84	7461	2	
13,72	11197	3	
13,54	16802	5	
13,28	25210	7	
12,90	37821	11	
12,37	56738	16	
11,65	85114	24	
10,75	127677	35	
9,68	191522	53	
8,57	287289	80	
7,56	430941	120	
6,79	518400	144	

Appendix I: Data influence of pith orientation on bow

Displ [mm]	Time [sec]	Time [h]	e = 200 mm	Displ [mm]	Time [sec]	Time [h]	e = 107.5 mm	Displ [mm]	Time [sec]	Time [h]	e = 7,5 mm
0,0002	0	0		0,0006	0	0		0,0001	0	0	
0,0003	0	0		0,0010	0	0		0,0002	0	0	
0,0005	0	0		0,0015	0	0		0,0004	0	0	
0,0008	0	0		0,0024	0	0		0,0006	0	0	
0,0012	0	0		0,0036	1	0		0,0009	0	0	
0,0019	0	0		0,0054	1	0		0,0014	0	0	
0,0028	1	0		0,0082	1	0		0,0022	0	0	
0,0043	1	0		0,0123	2	0		0,0033	1	0	
0,0065	1	0		0,0185	3	0		0,0050	1	0	
0,0097	2	0		0,0278	4	0		0,0076	1	0	
0,0146	3	0		0,0417	6	0		0,0114	2	0	
0,0219	4	0		0,0624	9	0		0,0171	3	0	
0,0329	6	0		0,0932	14	0		0,0257	4	0	
0,0492	9	0		0,1390	21	0		0,0385	6	0	
0,0735	14	0		0,2066	32	0		0,0577	9	0	
0,1096	21	0		0,3057	47	0		0,0864	14	0	
0,1628	32	0		0,4493	71	0		0,1291	21	0	
0,2407	47	0		0,6539	106	0		0,1923	32	0	
0,3533	71	0		0,9384	160	0		0,2856	47	0	
0,5133	106	0		1,3210	239	0		0,4220	71	0	
0,7347	160	0		1,8109	359	0		0,6189	106	0	
1,0303	239	0		2,3991	539	0		0,8982	160	0	
1,4052	359	0		3,0479	808	0		1,2841	239	0	
1,8491	539	0		3,6922	1212	0		1,7974	359	0	
2,3297	808	0		4,2567	1818	1		2,4452	539	0	
2,7954	1212	0		4,6838	2727	1		3,2061	808	0	
3,1912	1818	1		4,9531	4091	1		4,0197	1212	0	
3,4776	2727	1		5,0822	6136	2		4,7951	1818	1	
3,6405	4091	1		5,1119	9204	3		5,4479	2727	1	
3,6882	6136,02	2		5,0840	13806	4		5,9497	4091	1	
3,6433	9204,04	3		5,0257	20709	6		6,3461	6136	2	
3,5313	13806,1	4		4,9505	31064	9		6,7244	9204	3	
3,3715	20709,1	6		4,8665	46596	13		7,1611	13806	4	
3,1777	31063,7	9		4,7830	69893	19		7,6938	20709	6	
2,9667	46595,5	13		4,7107	104840	29		8,3176	31064	9	
2,7614	69893,2	19		4,6582	157260	44		8,9887	46596	13	
2,5887	104840	29		4,6277	235890	66		9,6337	69893	19	
2,4674	157260	44		4,6141	353835	98		10,1688	104840	29	
2,3994	235890	66		4,6097	518400	144		10,5378	157260	44	
2,3702	353835	98						10,7407	235890	66	
2,3610	518400	144						10,8260	353835	98	
								10,8520	518400	144	

Appendix J: Data influence of elastic moduli Gesso on bow deformation

Displ [mm]	Time [sec.]	Time [h.]	E = 760 Mpa
0,0000	0	0	
0,0000	0	0	
0,0001	0	0	
0,0001	0	0	
0,0002	0	0	
0,0003	0	0	
0,0007	0	0	
0,0013	0	0	
0,0025	0	0	
0,0044	0	0	
0,0071	0	0	
0,0113	0	0	
0,0176	0	0	
0,0270	1	0	
0,0410	1	0	
0,0621	2	0	
0,0937	2	0	Bow
0,1411	4	0	
0,2120	6	0	
0,3179	8	0	
0,4762	12	0	
0,7118	19	0	
1,0615	28	0	
1,5778	42	0	
2,3341	63	0	
3,4291	95	0	
4,9879	142	0	
7,1524	213	0	
10,0526	319	0	
13,7462	479	0	
18,1304	718	0	
22,8590	1077	0	
27,3506	1616	0	
30,9697	2424	1	
33,3273	3636	1	
34,4659	5454	2	
34,7279	8181	2	
34,4402	12272	3	
33,7175	18408	5	
32,4762	27612	8	
30,5452	41418	12	
27,7914	62127	17	
24,9142	86400	24	

Displ [mm]	Time [sec.]	Time [h.]	E = 500 Mpa
0,0000	0	0	
0,0000	0	0	
0,0001	0	0	
0,0001	0	0	
0,0002	0	0	
0,0004	0	0	
0,0007	0	0	
0,0013	0	0	
0,0026	0	0	
0,0045	0	0	
0,0073	0	0	
0,0116	0	0	
0,0180	0	0	
0,0276	1	0	
0,0420	1	0	
0,0636	2	0	
0,0960	2	0	Bow
0,1444	4	0	
0,2170	6	0	
0,3255	8	0	
0,4875	12	0	
0,7287	19	0	
1,0867	28	0	
1,6152	42	0	
2,3893	63	0	
3,5101	95	0	
5,1055	142	0	
7,3205	213	0	
10,2878	319	0	
14,0659	479	0	
18,5483	718	0	
23,3795	1077	0	
27,9634	1616	0	
31,6492	2424	1	
34,0392	3636	1	
35,1772	5454	2	
35,4121	8181	2	
35,0745	12272	3	
34,2773	18408	5	
32,9300	27612	8	
30,8547	41418	12	
27,9150	62127	17	
24,8567	86400	24	

Displ [mm]	Time [sec.]	Time [h.]	E = 600 Mpa
0,0000	0	0	
0,0000	0	0	
0,0001	0	0	
0,0001	0	0	
0,0002	0	0	
0,0004	0	0	
0,0007	0	0	
0,0013	0	0	
0,0025	0	0	
0,0044	0	0	
0,0073	0	0	
0,0115	0	0	
0,0178	0	0	
0,0274	1	0	
0,0416	1	0	
0,0630	2	0	
0,0951	2	0	Bow
0,1431	4	0	
0,2150	6	0	
0,3225	8	0	
0,4830	12	0	
0,7220	19	0	
1,0767	28	0	
1,6004	42	0	
2,3675	63	0	
3,4781	95	0	
5,0591	142	0	
7,2542	213	0	
10,1950	319	0	
13,9398	479	0	
18,3834	718	0	
23,1741	1077	0	
27,7217	1616	0	
31,3812	2424	1	
33,7585	3636	1	
34,8968	5454	2	
35,1423	8181	2	
34,8243	12272	3	
34,0564	18408	5	
32,7506	27612	8	
30,7319	41418	12	
27,8651	62127	17	
24,8776	86400	24	

Displ [mm]	Time [sec.]	Time [h.]	E = 900 Mpa
0,0000	0	0	
0,0000	0	0	
0,0001	0	0	
0,0001	0	0	
0,0002	0	0	
0,0003	0	0	
0,0006	0	0	
0,0013	0	0	
0,0025	0	0	
0,0043	0	0	
0,0071	0	0	
0,0112	0	0	
0,0174	0	0	
0,0266	1	0	
0,0405	1	0	
0,0614	2	0	
0,0926	2	0	Bow
0,1394	4	0	
0,2094	6	0	
0,3141	8	0	
0,4705	12	0	
0,7033	19	0	
1,0488	28	0	
1,5589	42	0	
2,3062	63	0	
3,3882	95	0	
4,9285	142	0	
7,0675	213	0	
9,9338	319	0	
13,5848	479	0	
17,9193	718	0	
22,5959	1077	0	
27,0408	1616	0	
30,6260	2424	1	
32,9671	3636	1	
34,1060	5454	2	
34,3818	8181	2	
34,1195	12272	3	
33,4349	18408	5	
32,2478	27612	8	
30,3909	41418	12	
27,7326	62127	17	
24,9486	86400	24	

Displ [mm]	Time [sec.]	Time [h.]	E = 1000 Mpa
0,0000	0	0	
0,0000	0	0	
0,0001	0	0	
0,0001	0	0	
0,0002	0	0	
0,0003	0	0	
0,0006	0	0	
0,0012	0	0	
0,0025	0	0	
0,0043	0	0	
0,0070	0	0	
0,0111	0	0	
0,0172	0	0	
0,0264	1	0	
0,0402	1	0	
0,0609	2	0	
0,0918	2	0	Bow
0,1382	4	0	
0,2077	6	0	
0,3115	8	0	
0,4665	12	0	
0,6974	19	0	
1,0401	28	0	
1,5460	42	0	
2,2870	63	0	
3,3600	95	0	
4,8876	142	0	
7,0091	213	0	
9,8520	319	0	
13,4737	479	0	
17,7740	718	0	
22,4149	1077	0	
26,8275	1616	0	
30,3893	2424	1	
32,7190	3636	1	
33,8580	5454	2	
34,1434	8181	2	
33,8986	12272	3	
33,2405	18408	5	
32,0910	27612	8	
30,2855	41418	12	
27,6935	62127	17	
24,9743	86400	24	

Displ [mm]	Time [sec.]	Time [h.]	E = 1100 Mpa
0,0000	0	0	
0,0000	0	0	
0,0000	0	0	
0,0001	0	0	
0,0002	0	0	
0,0003	0	0	
0,0006	0	0	
0,0012	0	0	
0,0024	0	0	
0,0042	0	0	
0,0069	0	0	
0,0110	0	0	
0,0171	0	0	
0,0262	1	0	
0,0399	1	0	
0,0604	2	0	
0,0911	2	0	Bow
0,1371	4	0	
0,2060	6	0	
0,3090	8	0	
0,4627	12	0	
0,6917	19	0	
1,0316	28	0	
1,5334	42	0	
2,2684	63	0	
3,3327	95	0	
4,8480	142	0	
6,9525	213	0	
9,7727	319	0	
13,3659	479	0	
17,6331	718	0	
22,2392	1077	0	
26,6205	1616	0	
30,1596	2424	1	
32,4782	3636	1	
33,6174	5454	2	
33,9120	8181	2	
33,6844	12272	3	
33,0520	18408	5	
31,9392	27612	8	
30,1838	41418	12	
27,6565	62127	17	
25,0006	86400	24	

Appendix K: Data influence of elastic moduli Gesso on cup deformation

Displ [mm]	Time [sec.]	Time [h.]	E = 760 Mpa
0,0000	0	0	
0,0000	0	0	
0,0000	0	0	
0,0000	0	0	
0,0000	0	0	
0,0000	0	0	
0,0001	0	0	
0,0001	0	0	
0,0003	0	0	
0,0004	0	0	
0,0007	0	0	
0,0011	0	0	
0,0018	0	0	
0,0027	1	0	
0,0042	1	0	
0,0063	2	0	
0,0095	2	0	Cup
0,0143	4	0	
0,0215	6	0	
0,0322	8	0	
0,0483	12	0	
0,0722	19	0	
0,1076	28	0	
0,1599	42	0	
0,2365	63	0	
0,3472	95	0	
0,5047	142	0	
0,7230	213	0	
1,0147	319	0	
1,3848	479	0	
1,8218	718	0	
2,2901	1077	0	
2,7315	1616	0	
3,0843	2424	1	
3,3140	3636	1	
3,4296	5454	2	
3,4684	8181	2	
3,4648	12272	3	
3,4325	18408	5	
3,3681	27612	8	
3,2624	41418	12	
3,1109	62127	17	
2,9569	86400	24	

Displ [mm]	Time [sec.]	Time [h.]	E = 500 Mpa
0,0000	0	0	
0,0000	0	0	
0,0000	0	0	
0,0000	0	0	
0,0000	0	0	
0,0000	0	0	
0,0001	0	0	
0,0001	0	0	
0,0003	0	0	
0,0004	0	0	
0,0007	0	0	
0,0011	0	0	
0,0018	0	0	
0,0027	1	0	
0,0041	1	0	
0,0062	2	0	
0,0094	2	0	Cup
0,0141	4	0	
0,0212	6	0	
0,0318	8	0	
0,0476	12	0	
0,0712	19	0	
0,1061	28	0	
0,1577	42	0	
0,2332	63	0	
0,3423	95	0	
0,4975	142	0	
0,7124	213	0	
0,9993	319	0	
1,3629	479	0	
1,7914	718	0	
2,2490	1077	0	
2,6777	1616	0	
3,0168	2424	1	
3,2317	3636	1	
3,3310	5454	2	
3,3505	8181	2	
3,3227	12272	3	
3,2598	18408	5	
3,1576	27612	8	
3,0070	41418	12	
2,8054	62127	17	
2,6078	86400	24	

Displ [mm]	Time [sec.]	Time [h.]	E = 600 Mpa
0,0000	0	0	
0,0000	0	0	
0,0000	0	0	
0,0000	0	0	
0,0000	0	0	
0,0000	0	0	
0,0001	0	0	
0,0001	0	0	
0,0003	0	0	
0,0004	0	0	
0,0007	0	0	
0,0011	0	0	
0,0018	0	0	
0,0027	1	0	
0,0041	1	0	
0,0062	2	0	
0,0094	2	0	Cup
0,0142	4	0	
0,0213	6	0	
0,0320	8	0	
0,0479	12	0	
0,0716	19	0	
0,1067	28	0	
0,1586	42	0	
0,2345	63	0	
0,3443	95	0	
0,5004	142	0	
0,7167	213	0	
1,0055	319	0	
1,3717	479	0	
1,8037	718	0	
2,2656	1077	0	
2,6994	1616	0	
3,0440	2424	1	
3,2649	3636	1	
3,3708	5454	2	
3,3981	8181	2	
3,3800	12272	3	
3,3293	18408	5	
3,2423	27612	8	
3,1097	41418	12	
2,9281	62127	17	
2,7479	86400	24	

Displ [mm]	Time [sec.]	Time [h.]	E = 900 Mpa
0,0000	0	0	
0,0000	0	0	
0,0000	0	0	
0,0000	0	0	
0,0000	0	0	
0,0000	0	0	
0,0001	0	0	
0,0001	0	0	
0,0003	0	0	
0,0004	0	0	
0,0007	0	0	
0,0012	0	0	
0,0018	0	0	
0,0028	1	0	
0,0042	1	0	
0,0063	2	0	
0,0096	2	0	Cup
0,0144	4	0	
0,0216	6	0	
0,0324	8	0	
0,0486	12	0	
0,0726	19	0	
0,1083	28	0	
0,1609	42	0	
0,2380	63	0	
0,3496	95	0	
0,5081	142	0	
0,7280	213	0	
1,0220	319	0	
1,3952	479	0	
1,8364	718	0	
2,3098	1077	0	
2,7571	1616	0	
3,1166	2424	1	
3,3534	3636	1	
3,4768	5454	2	
3,5249	8181	2	
3,5330	12272	3	
3,5156	18408	5	
3,4696	27612	8	
3,3858	41418	12	
3,2588	62127	17	
3,1262	86400	24	

Displ [mm]	Time [sec.]	Time [h.]	E = 1000 Mpa
0,0000	0	0	
0,0000	0	0	
0,0000	0	0	
0,0000	0	0	
0,0000	0	0	
0,0000	0	0	
0,0001	0	0	
0,0001	0	0	
0,0003	0	0	
0,0004	0	0	
0,0007	0	0	
0,0012	0	0	
0,0018	0	0	
0,0028	1	0	
0,0042	1	0	
0,0064	2	0	
0,0096	2	0	Cup
0,0145	4	0	
0,0217	6	0	
0,0326	8	0	
0,0488	12	0	
0,0729	19	0	
0,1088	28	0	
0,1617	42	0	
0,2391	63	0	
0,3511	95	0	
0,5104	142	0	
0,7314	213	0	
1,0269	319	0	
1,4022	479	0	
1,8461	718	0	
2,3230	1077	0	
2,7743	1616	0	
3,1381	2424	1	
3,3797	3636	1	
3,5084	5454	2	
3,5627	8181	2	
3,5787	12272	3	
3,5712	18408	5	
3,5376	27612	8	
3,4686	41418	12	
3,3583	62127	17	
3,2402	86400	24	

Displ [mm]	Time [sec.]	Time [h.]	E = 1100 Mpa
0,0000	0	0	
0,0000	0	0	
0,0000	0	0	
0,0000	0	0	
0,0000	0	0	
0,0000	0	0	
0,0001	0	0	
0,0001	0	0	
0,0003	0	0	
0,0004	0	0	
0,0007	0	0	
0,0012	0	0	
0,0018	0	0	
0,0028	1	0	
0,0042	1	0	
0,0064	2	0	
0,0096	2	0	Cup
0,0145	4	0	
0,0218	6	0	
0,0327	8	0	
0,0490	12	0	
0,0732	19	0	
0,1092	28	0	
0,1623	42	0	
0,2401	63	0	
0,3526	95	0	
0,5126	142	0	
0,7346	213	0	
1,0315	319	0	
1,4088	479	0	
1,8554	718	0	
2,3354	1077	0	
2,7905	1616	0	
3,1586	2424	1	
3,4046	3636	1	
3,5383	5454	2	
3,5986	8181	2	
3,6220	12272	3	
3,6241	18408	5	
3,6023	27612	8	
3,5474	41418	12	
3,4530	62127	17	
3,3488	86400	24	

Appendix L: Data influence of diffusivity Gesso on bow deformation

Displ [mm]	Time [sec.]	Time [h.]	D = 0,0
0,0001	0	0	
0,0002	0	0	
0,0003	0	0	
0,0007	0	0	
0,0013	0	0	
0,0025	0	0	
0,0044	0	0	
0,0071	0	0	
0,0113	0	0	
0,0176	0	0	
0,0270	1	0	
0,0410	1	0	
0,0621	2	0	
0,0937	2	0	
0,1411	4	0	
0,2120	6	0	
0,3180	8	0	Bow
0,4762	12	0	
0,7118	19	0	
1,0616	28	0	
1,5780	42	0	
2,3346	63	0	
3,4302	95	0	
4,9902	142	0	
7,1572	213	0	
10,0620	319	0	
13,7643	479	0	
18,1633	718	0	
22,9159	1077	0	
27,4447	1616	0	
31,1194	2424	1	
33,5581	3636	1	
34,8129	5454	2	
35,2376	8181	2	
35,1706	12272	3	
34,7345	18408	5	
33,8430	27612	8	
32,3026	41418	12	
29,9303	62127	17	
27,3152	86400	24	

Displ [mm]	Time [sec.]	Time [h.]	D = 0,1
0,0003	0	0	
0,0006	0	0	
0,0009	0	0	
0,0014	0	0	
0,0022	0	0	
0,0034	0	0	
0,0051	0	0	
0,0078	0	0	
0,0116	0	0	
0,0174	0	0	
0,0260	1	0	
0,0386	1	0	
0,0569	2	0	
0,0834	2	0	
0,1210	4	0	
0,1736	5	0	
0,2458	8	0	Bow
0,3444	12	0	
0,4792	18	0	
0,6664	27	0	
0,9314	40	0	
1,3106	60	0	
1,8504	90	0	
2,6042	135	0	
3,6218	202	0	
4,9265	303	0	
6,4732	455	0	
8,0988	682	0	
9,4996	1023	0	
10,3039	1534	0	
10,2767	2301	1	
9,5391	3452	1	
8,5534	5177	1	
7,7951	7766	2	
7,4382	11649	3	
7,3788	17473	5	
7,4554	26210	7	
7,5710	39315	11	
7,6845	58972	16	
7,7729	86400	24	

Displ [mm]	Time [sec.]	Time [h.]	D = 0,01
0,0002	0	0	
0,0003	0	0	
0,0007	0	0	
0,0013	0	0	
0,0022	0	0	
0,0036	0	0	
0,0057	0	0	
0,0088	0	0	
0,0135	0	0	
0,0205	0	0	
0,0310	1	0	
0,0467	1	0	
0,0702	2	0	
0,1052	2	0	
0,1571	4	0	
0,2340	5	0	
0,3469	8	0	Bow
0,5112	12	0	
0,7474	18	0	
1,0812	27	0	
1,5433	40	0	
2,1684	60	0	
2,9943	90	0	
4,0618	135	0	
5,4073	202	0	
7,0353	303	0	
8,8612	455	0	
10,6455	682	0	
11,9876	1023	0	
12,4600	1534	0	
11,8865	2301	1	
10,5632	3452	1	
9,1307	5177	1	
8,1248	7766	2	
7,6634	11649	3	
7,5612	17473	5	
7,6086	26210	7	
7,6931	39315	11	
7,7728	58972	16	
7,8110	86400	24	

Displ [mm]	Time [sec.]	Time [h.]	D = 0,001
0,0001	0	0	
0,0002	0	0	
0,0003	0	0	
0,0007	0	0	
0,0013	0	0	
0,0025	0	0	
0,0044	0	0	
0,0071	0	0	
0,0113	0	0	
0,0176	0	0	
0,0270	1	0	
0,0410	1	0	
0,0621	2	0	
0,0937	2	0	
0,1409	4	0	
0,2116	5	0	
0,3170	8	0	Bow
0,4741	12	0	
0,7072	18	0	
1,0513	27	0	
1,5555	40	0	
2,2858	60	0	
3,3268	90	0	
4,7764	135	0	
6,7299	202	0	
9,2441	303	0	
12,2766	455	0	
15,6072	682	0	
18,7741	1023	0	
21,1064	1534	0	
21,9385	2301	1	
20,9688	3452	1	
18,5151	5177	1	
15,4047	7766	2	
12,5436	11649	3	
10,4865	17473	5	
9,2888	26210	7	
8,6791	39315	11	
8,3587	58972	16	
8,1856	86400	24	

Displ [mm]	Time [sec.]	Time [h.]	D = 0,0001
0,0001	0	0	
0,0002	0	0	
0,0003	0	0	
0,0007	0	0	
0,0013	0	0	
0,0025	0	0	
0,0044	0	0	
0,0071	0	0	
0,0113	0	0	
0,0176	0	0	
0,0270	1	0	
0,0410	1	0	
0,0621	2	0	
0,0937	2	0	
0,1411	4	0	
0,2119	6	0	
0,3179	8	0	Bow
0,4760	12	0	
0,7114	19	0	
1,0606	28	0	
1,5757	42	0	
2,3295	63	0	
3,4193	95	0	
4,9673	142	0	
7,1102	213	0	
9,9689	319	0	
13,5874	479	0	
17,8431	718	0	
22,3653	1077	0	
26,5422	1616	0	
29,7005	2424	1	
31,4047	3636	1	
31,6454	5454	2	
30,7230	8181	2	
28,9619	12272	3	
26,5561	18408	5	
23,6236	27612	8	
20,3243	41418	12	
16,9243	62127	17	
14,2513	86400	24	

Displ [mm]	Time [sec.]	Time [h.]	D = 0,00001
0,0001	0	0	
0,0002	0	0	
0,0003	0	0	
0,0007	0	0	
0,0013	0	0	
0,0025	0	0	
0,0044	0	0	
0,0071	0	0	
0,0113	0	0	
0,0176	0	0	
0,0270	1	0	
0,0410	1	0	
0,0621	2	0	
0,0937	2	0	
0,1411	4	0	
0,2120	6	0	
0,3179	8	0	Bow
0,4762	12	0	
0,7118	19	0	
1,0615	28	0	
1,5778	42	0	
2,3341	63	0	
3,4291	95	0	
4,9879	142	0	
7,1524	213	0	
10,0526	319	0	
13,7462	479	0	
18,1304	718	0	
22,8590	1077	0	
27,3506	1616	0	
30,9697	2424	1	
33,3273	3636	1	
34,4659	5454	2	
34,7279	8181	2	
34,4402	12272	3	
33,7175	18408	5	
32,4762	27612	8	
30,5452	41418	12	
27,7914	62127	17	
24,9142	86400	24	

Appendix M: Data influence of diffusivity Gesso on cup deformation

Displ [mm]	Time [sec.]	Time [h.]	D = 0,0
0,0001	0	0	
0,0003	0	0	
0,0004	0	0	
0,0007	0	0	
0,0011	0	0	
0,0018	0	0	
0,0027	1	0	
0,0042	1	0	
0,0063	2	0	
0,0095	2	0	
0,0143	4	0	
0,0215	6	0	
0,0322	8	0	
0,0483	12	0	
0,0722	19	0	
0,1076	28	0	
0,1599	42	0	Cup
0,2365	63	0	
0,3473	95	0	
0,5049	142	0	
0,7234	213	0	
1,0154	319	0	
1,3862	479	0	
1,8245	718	0	
2,2946	1077	0	
2,7388	1616	0	
3,0957	2424	1	
3,3314	3636	1	
3,4552	5454	2	
3,5051	8181	2	
3,5158	12272	3	
3,5008	18408	5	
3,4556	27612	8	
3,3683	41418	12	
3,2305	62127	17	
3,0821	86400	24	

Displ [mm]	Time [sec.]	Time [h.]	D = 0,1
0,0001	0	0	
0,0002	0	0	
0,0003	0	0	
0,0005	0	0	
0,0008	0	0	
0,0012	0	0	
0,0018	0	0	
0,0026	1	0	
0,0039	1	0	
0,0058	2	0	
0,0086	2	0	
0,0125	4	0	
0,0181	5	0	
0,0260	8	0	
0,0370	12	0	
0,0523	18	0	
0,0740	27	0	Cup
0,1052	40	0	
0,1501	60	0	
0,2144	90	0	
0,3049	135	0	
0,4286	202	0	
0,5901	303	0	
0,7877	455	0	
1,0075	682	0	
1,2202	1023	0	
1,3872	1534	0	
1,4799	2301	1	
1,5032	3452	1	
1,4976	5177	1	
1,5103	7766	2	
1,5645	11649	3	
1,6561	17473	5	
1,7702	26210	7	
1,8908	39315	11	
2,0032	58972	16	
2,0907	86400	24	

Displ [mm]	Time [sec.]	Time [h.]	D = 0,01
0,0001	0	0	
0,0002	0	0	
0,0004	0	0	
0,0006	0	0	
0,0009	0	0	
0,0014	0	0	
0,0021	1	0	
0,0031	1	0	
0,0047	1	0	
0,0071	2	0	
0,0107	3	0	
0,0160	4	0	
0,0238	6	0	
0,0354	9	0	
0,0523	14	0	
0,0768	21	0	
0,1117	32	0	Cup
0,1607	47	0	
0,2281	71	0	
0,3190	106	0	
0,4395	160	0	
0,5951	239	0	
0,7889	359	0	
1,0148	539	0	
1,2515	808	0	
1,4601	1212	0	
1,5970	1818	1	
1,6401	2727	1	
1,6115	4091	1	
1,5688	6136	2	
1,5647	9204	3	
1,6163	13806	4	
1,7104	20709	6	
1,8256	31064	9	
1,9426	46596	13	
2,0462	69893	19	
2,0962	86400	24	

Displ [mm]	Time [sec.]	Time [h.]	D = 0,001
0,0001	0	0	
0,0001	0	0	
0,0003	0	0	
0,0004	0	0	
0,0007	0	0	
0,0011	0	0	
0,0018	1	0	
0,0027	1	0	
0,0042	1	0	
0,0063	2	0	
0,0095	3	0	
0,0143	4	0	
0,0215	6	0	
0,0322	9	0	
0,0481	14	0	
0,0718	21	0	
0,1068	32	0	Cup
0,1581	47	0	
0,2325	71	0	
0,3388	106	0	
0,4873	160	0	
0,6884	239	0	
0,9489	359	0	
1,2661	539	0	
1,6200	808	0	
1,9672	1212	0	
2,2447	1818	1	
2,3913	2727	1	
2,3819	4091	1	
2,2495	6136	2	
2,0714	9204	3	
1,9285	13806	4	
1,8672	20709	6	
1,8876	31064	9	
1,9583	46596	13	
2,0433	69893	19	
2,1071	86400	24	

Displ [mm]	Time [sec.]	Time [h.]	D = 0,0001
0,0001	0	0	
0,0001	0	0	
0,0003	0	0	
0,0004	0	0	
0,0007	0	0	
0,0011	0	0	
0,0018	0	0	
0,0027	1	0	
0,0042	1	0	
0,0063	2	0	
0,0095	2	0	
0,0143	4	0	
0,0215	6	0	
0,0322	8	0	
0,0483	12	0	
0,0721	19	0	
0,1075	28	0	Cup
0,1597	42	0	
0,2361	63	0	
0,3464	95	0	
0,5030	142	0	
0,7195	213	0	
1,0079	319	0	
1,3719	479	0	
1,7989	718	0	
2,2511	1077	0	
2,6685	1616	0	
2,9871	2424	1	
3,1694	3636	1	
3,2217	5454	2	
3,1801	8181	2	
3,0819	12272	3	
2,9505	18408	5	
2,8006	27612	8	
2,6466	41418	12	
2,5038	62127	17	
2,4029	86400	24	

Displ [mm]	Time [sec.]	Time [h.]	D = 0,00001
0,0001	0	0	
0,0001	0	0	
0,0003	0	0	
0,0004	0	0	
0,0007	0	0	
0,0011	0	0	
0,0018	0	0	
0,0027	1	0	
0,0042	1	0	
0,0063	2	0	
0,0095	2	0	
0,0143	4	0	
0,0215	6	0	
0,0322	8	0	
0,0483	12	0	
0,0722	19	0	
0,1076	28	0	Cup
0,1599	42	0	
0,2365	63	0	
0,3472	95	0	
0,5047	142	0	
0,7230	213	0	
1,0147	319	0	
1,3848	479	0	
1,8218	718	0	
2,2901	1077	0	
2,7315	1616	0	
3,0843	2424	1	
3,3140	3636	1	
3,4296	5454	2	
3,4684	8181	2	
3,4648	12272	3	
3,4325	18408	5	
3,3681	27612	8	
3,2624	41418	12	
3,1109	62127	17	
2,9569	86400	24	

Appendix N: Data Influence of elastic moduli Gesso on twist deformation

Displ [mm]	1/2 Width	Twist [degrees]	time [sec.]	time (h)	E = 760 MPa
-0,0001	100	-7,17504E-05	0	0	
-0,0002	100	-0,000139277	0	0	
-0,0005	100	-0,000274324	0	0	
-0,0008	100	-0,000476876	0	0	
-0,0014	100	-0,000780666	0	0	
-0,0022	100	-0,00123626	0	0	
-0,0034	100	-0,001919454	0	0	
-0,0051	100	-0,002943806	1	0	
-0,0078	100	-0,004479315	1	0	
-0,0118	100	-0,006780325	2	0	
-0,0178	100	-0,010226781	2	0	
-0,0269	100	-0,01538512	4	0	
-0,0403	100	-0,023097131	6	0	
-0,0604	100	-0,034608194	8	0	
-0,0903	100	-0,051747872	12	0	
-0,1347	100	-0,077175649	19	0	
-0,2002	100	-0,114695684	28	0	Twist
-0,2960	100	-0,169619076	42	0	
-0,4347	100	-0,249083811	63	0	
-0,6320	100	-0,362115391	95	0	
-0,9059	100	-0,519001342	142	0	
-1,2729	100	-0,72928432	213	0	
-1,7411	100	-0,997476033	319	0	
-2,2972	100	-1,315984375	479	0	
-2,8908	100	-1,655850974	718	0	
-3,4213	100	-1,959490471	1077	0	
-3,7437	100	-2,143980855	1616	0	
-3,7112	100	-2,125391284	2424	1	
-3,2478	100	-1,860204176	3636	1	
-2,4033	100	-1,376718725	5454	2	
-1,3403	100	-0,767889354	8181	2	
-0,2627	100	-0,150522542	12272	3	
0,6686	100	0,38305955	18408	5	
1,3882	100	0,795328925	27612	8	
1,9210	100	1,100516565	41418	12	
2,3226	100	1,330506836	62127	17	
2,5843	100	1,480371055	86400	24	

Displ [mm]	1/2 Width	Twist [degrees]	time [sec.]	time (h)	E = 500 MPa
-0,0001	100	-7,2403E-05	0	0	
-0,0002	100	-0,000140544	0	0	
-0,0005	100	-0,000276819	0	0	
-0,0008	100	-0,000481213	0	0	
-0,0014	100	-0,000787765	0	0	
-0,0022	100	-0,001247501	0	0	
-0,0034	100	-0,001936907	0	0	
-0,0052	100	-0,002970563	1	0	
-0,0079	100	-0,004520024	1	0	
-0,0119	100	-0,006841918	2	0	
-0,0180	100	-0,010319657	2	0	
-0,0271	100	-0,015524635	4	0	
-0,0407	100	-0,023306318	6	0	
-0,0609	100	-0,034921028	8	0	
-0,0911	100	-0,052214202	12	0	
-0,1359	100	-0,077867781	19	0	
-0,2020	100	-0,115717837	28	0	Twist
-0,2987	100	-0,171115629	42	0	
-0,4385	100	-0,251247831	63	0	
-0,6374	100	-0,365191478	95	0	
-0,9133	100	-0,523268379	142	0	
-1,2829	100	-0,734995777	213	0	
-1,7538	100	-1,004761831	319	0	
-2,3123	100	-1,324625718	479	0	
-2,9069	100	-1,665056399	718	0	
-3,4354	100	-1,967565414	1077	0	
-3,7510	100	-2,148163303	1616	0	
-3,7051	100	-2,121901041	2424	1	
-3,2208	100	-1,844756205	3636	1	
-2,3486	100	-1,345418522	5454	2	
-1,2534	100	-0,718101968	8181	2	
-0,1421	100	-0,08142355	12272	3	
0,8215	100	0,470650751	18408	5	
1,5704	100	0,899710423	27612	8	
2,1293	100	1,219808977	41418	12	
2,5536	100	1,462764223	62127	17	
2,8311	100	1,621690544	86400	24	

Displ [mm]	1/2 Width	Twist [degrees]	time [sec.]	time (h)	E = 600 MPa
-0,0001	100	-7,21423E-05	0	0	
-0,0002	100	-0,000140038	0	0	
-0,0005	100	-0,000275822	0	0	
-0,0008	100	-0,00047948	0	0	
-0,0014	100	-0,000784929	0	0	
-0,0022	100	-0,001243009	0	0	
-0,0034	100	-0,001929934	0	0	
-0,0052	100	-0,002959871	1	0	
-0,0079	100	-0,004503758	1	0	
-0,0119	100	-0,006817338	2	0	
-0,0179	100	-0,01028253	2	0	
-0,0270	100	-0,015468886	4	0	
-0,0405	100	-0,02322278	6	0	
-0,0607	100	-0,034796009	8	0	
-0,0908	100	-0,052027877	12	0	
-0,1354	100	-0,077591043	19	0	
-0,2013	100	-0,115309319	28	0	Twist
-0,2976	100	-0,170517466	42	0	
-0,4370	100	-0,250382681	63	0	
-0,6352	100	-0,363960814	95	0	
-0,9103	100	-0,521560533	142	0	
-1,2789	100	-0,73271005	213	0	
-1,7487	100	-1,001840642	319	0	
-2,3063	100	-1,321149718	479	0	
-2,9004	100	-1,661341036	718	0	
-3,4297	100	-1,964274784	1077	0	
-3,7479	100	-2,146389627	1616	0	
-3,7073	100	-2,123142654	2424	1	
-3,2312	100	-1,850708771	3636	1	
-2,3700	100	-1,357627187	5454	2	
-1,2874	100	-0,737602304	8181	2	
-0,1894	100	-0,108540995	12272	3	
0,7614	100	0,436240489	18408	5	
1,4988	100	0,858684849	27612	8	
2,0474	100	1,172909919	41418	12	
2,4627	100	1,410760914	62127	17	
2,7341	100	1,566116565	86400	24	

Displ [mm]	1/2 Width	Twist [degrees]	time [sec.]	time (h)	E = 900 MPa
-0,0001	100	-7,14306E-05	0	0	
-0,0002	100	-0,000138656	0	0	
-0,0005	100	-0,000273101	0	0	
-0,0008	100	-0,000474751	0	0	
-0,0014	100	-0,000777183	0	0	
-0,0021	100	-0,001230753	0	0	
-0,0033	100	-0,0019109	0	0	
-0,0051	100	-0,002930685	1	0	
-0,0078	100	-0,004459365	1	0	
-0,0118	100	-0,00675013	2	0	
-0,0178	100	-0,010181288	2	0	
-0,0267	100	-0,015316708	4	0	
-0,0401	100	-0,022994571	6	0	
-0,0601	100	-0,034454927	8	0	
-0,0899	100	-0,051519377	12	0	
-0,1341	100	-0,076836459	19	0	
-0,1993	100	-0,114195494	28	0	Twist
-0,2948	100	-0,168887415	42	0	
-0,4329	100	-0,248025578	63	0	
-0,6294	100	-0,360611437	95	0	
-0,9022	100	-0,516918811	142	0	
-1,2681	100	-0,726500195	213	0	
-1,7349	100	-0,993947678	319	0	
-2,2900	100	-1,311815435	479	0	
-2,8831	100	-1,651460047	718	0	
-3,4147	100	-1,955730531	1077	0	
-3,7407	100	-2,14224722	1616	0	
-3,7151	100	-2,127588413	2424	1	
-3,2623	100	-1,86846893	3636	1	
-2,4318	100	-1,393015579	5454	2	
-1,3851	100	-0,793535911	8181	2	
-0,3245	100	-0,185939049	12272	3	
0,5904	100	0,338274935	18408	5	
1,2952	100	0,742030529	27612	8	
1,8147	100	1,039638127	41418	12	
2,2048	100	1,263041257	62127	17	
2,4585	100	1,408304412	86400	24	

Displ [mm]	1/2 Width	Twist [degrees]	time [sec.]	time (h)	E = 1000 MPa
-0,0001	100	-7,12141E-05	0	0	
-0,0002	100	-0,000138236	0	0	
-0,0005	100	-0,000272273	0	0	
-0,0008	100	-0,000473311	0	0	
-0,0014	100	-0,000774828	0	0	
-0,0021	100	-0,001227018	0	0	
-0,0033	100	-0,001905108	0	0	
-0,0051	100	-0,002921804	1	0	
-0,0078	100	-0,004445849	1	0	
-0,0117	100	-0,006729676	2	0	
-0,0177	100	-0,010150463	2	0	
-0,0267	100	-0,015270413	4	0	
-0,0400	100	-0,022925186	6	0	
-0,0600	100	-0,034351108	8	0	
-0,0896	100	-0,051364679	12	0	
-0,1337	100	-0,076606703	19	0	
-0,1987	100	-0,113856304	28	0	Twist
-0,2939	100	-0,168391811	42	0	
-0,4316	100	-0,247309394	63	0	
-0,6276	100	-0,35959505	95	0	
-0,8998	100	-0,515512313	142	0	
-1,2648	100	-0,724621194	213	0	
-1,7308	100	-0,99156489	319	0	
-2,2851	100	-1,309020864	479	0	
-2,8780	100	-1,64853466	718	0	
-3,4104	100	-1,953263955	1077	0	
-3,7389	100	-2,141205893	1616	0	
-3,7180	100	-2,129264864	2424	1	
-3,2725	100	-1,874341208	3636	1	
-2,4517	100	-1,404422098	5454	2	
-1,4162	100	-0,811391503	8181	2	
-0,3675	100	-0,210536978	12272	3	
0,5362	100	0,307214734	18408	5	
1,2307	100	0,705092104	27612	8	
1,7411	100	0,997464577	41418	12	
2,1232	100	1,216309787	62127	17	
2,3713	100	1,358388793	86400	24	

Displ [mm]	1/2 Width	Twist [degrees]	time [sec.]	time (h)	E = 1100 MPa
-0,0001	100	-7,10061E-05	0	0	
-0,0002	100	-0,000137833	0	0	
-0,0005	100	-0,000271479	0	0	
-0,0008	100	-0,000471932	0	0	
-0,0013	100	-0,000772571	0	0	
-0,0021	100	-0,001223443	0	0	
-0,0033	100	-0,001899561	0	0	
-0,0051	100	-0,002913296	1	0	
-0,0077	100	-0,004432906	1	0	
-0,0117	100	-0,006710138	2	0	
-0,0177	100	-0,010120956	2	0	
-0,0266	100	-0,015226067	4	0	
-0,0399	100	-0,022858666	6	0	
-0,0598	100	-0,034251699	8	0	
-0,0894	100	-0,051216512	12	0	
-0,1333	100	-0,076386688	19	0	
-0,1982	100	-0,113532011	28	0	Twist
-0,2931	100	-0,167917406	42	0	
-0,4304	100	-0,246624149	63	0	
-0,6259	100	-0,358622779	95	0	
-0,8974	100	-0,514168263	142	0	
-1,2616	100	-0,722828123	213	0	
-1,7268	100	-0,989302382	319	0	
-2,2804	100	-1,306363724	479	0	
-2,8732	100	-1,64576956	718	0	
-3,4064	100	-1,950963337	1077	0	
-3,7373	100	-2,140301883	1616	0	
-3,7211	100	-2,131021414	2424	1	
-3,2827	100	-1,880179106	3636	1	
-2,4713	100	-1,415650997	5454	2	
-1,4468	100	-0,828891777	8181	2	
-0,4094	100	-0,234586518	12272	3	
0,4832	100	0,276877407	18408	5	
1,1677	100	0,669029598	27612	8	
1,6692	100	0,956303799	41418	12	
2,0436	100	1,170710682	62127	17	
2,2862	100	1,309690874	86400	24	

Appendix O: Data influence of elastic moduli Gesso on bow deformation

Displ [mm]	Time [sec.]	Time [h.]	E = 760 Mpa
0,0000	0	0	
0,0000	0	0	
-0,0001	0	0	
-0,0002	0	0	
-0,0003	0	0	
-0,0005	0	0	
-0,0010	0	0	
-0,0019	0	0	
-0,0038	0	0	
-0,0067	0	0	
-0,0109	0	0	
-0,0173	0	0	
-0,0268	0	0	
-0,0411	1	0	
-0,0625	1	0	
-0,0946	2	0	
-0,1427	2	0	Bow
-0,2148	4	0	
-0,3225	6	0	
-0,4834	8	0	
-0,7232	12	0	
-1,0795	19	0	
-1,6062	28	0	
-2,3794	42	0	
-3,5030	63	0	
-5,1112	95	0	
-7,3637	142	0	
-10,4226	213	0	
-14,3982	319	0	
-19,2527	479	0	
-24,6689	718	0	
-29,9368	1077	0	
-33,9875	1616	0	
-35,7189	2424	1	
-34,5564	3636	1	
-30,8614	5454	2	
-25,8006	8181	2	
-20,7858	12272	3	
-16,8945	18408	5	
-14,5392	27612	8	
-13,4876	41418	12	
-13,2100	62127	17	
-13,2314	86400	24	

Displ [mm]	Time [sec.]	Time [h.]	E = 500 Mpa
0,0000	0	0	
-0,0001	0	0	
-0,0001	0	0	
-0,0002	0	0	
-0,0003	0	0	
-0,0006	0	0	
-0,0011	0	0	
-0,0020	0	0	
-0,0040	0	0	
-0,0070	0	0	
-0,0114	0	0	
-0,0181	0	0	
-0,0281	0	0	
-0,0431	1	0	
-0,0656	1	0	
-0,0993	2	0	
-0,1497	2	0	Bow
-0,2253	4	0	
-0,3383	6	0	
-0,5071	8	0	
-0,7585	12	0	
-1,1321	19	0	
-1,6842	28	0	
-2,4945	42	0	
-3,6715	63	0	
-5,3550	95	0	
-7,7108	142	0	
-10,9055	213	0	
-15,0497	319	0	
-20,0960	479	0	
-25,7016	718	0	
-31,1106	1077	0	
-35,1910	1616	0	
-36,7776	2424	1	
-35,2627	3636	1	
-31,0279	5454	2	
-25,3095	8181	2	
-19,6106	12272	3	
-15,0852	18408	5	
-12,1819	27612	8	
-10,6557	41418	12	
-9,9951	62127	17	
-9,7434	86400	24	

Displ [mm]	Time [sec.]	Time [h.]	E = 600 Mpa
0,0000	0	0	
-0,0001	0	0	
-0,0001	0	0	
-0,0002	0	0	
-0,0003	0	0	
-0,0005	0	0	
-0,0010	0	0	
-0,0020	0	0	
-0,0039	0	0	
-0,0069	0	0	
-0,0112	0	0	
-0,0178	0	0	
-0,0276	0	0	
-0,0423	1	0	
-0,0644	1	0	
-0,0974	2	0	
-0,1469	2	0	Bow
-0,2211	4	0	
-0,3320	6	0	
-0,4976	8	0	
-0,7445	12	0	
-1,1111	19	0	
-1,6531	28	0	
-2,4486	42	0	
-3,6043	63	0	
-5,2578	95	0	
-7,5724	142	0	
-10,7130	213	0	
-14,7900	319	0	
-19,7599	479	0	
-25,2900	718	0	
-30,6429	1077	0	
-34,7117	1616	0	
-36,3563	2424	1	
-34,9822	3636	1	
-30,9630	5454	2	
-25,5072	8181	2	
-20,0815	12272	3	
-15,8094	18408	5	
-13,1250	27612	8	
-11,7945	41418	12	
-11,2810	62127	17	
-11,1384	86400	24	

Displ [mm]	Time [sec.]	Time [h.]	E = 900 Mpa
0,0000	0	0	
-0,0001	0	0	
-0,0001	0	0	
-0,0002	0	0	
-0,0003	0	0	
-0,0005	0	0	
-0,0010	0	0	
-0,0019	0	0	
-0,0037	0	0	
-0,0065	0	0	
-0,0106	0	0	
-0,0168	0	0	
-0,0261	0	0	
-0,0401	1	0	
-0,0610	1	0	
-0,0924	2	0	
-0,1393	2	0	Bow
-0,2096	4	0	
-0,3148	6	0	
-0,4718	8	0	
-0,7059	12	0	
-1,0536	19	0	
-1,5678	28	0	
-2,3227	42	0	
-3,4200	63	0	
-4,9912	95	0	
-7,1929	142	0	
-10,1848	213	0	
-14,0772	319	0	
-18,8372	479	0	
-24,1598	718	0	
-29,3578	1077	0	
-33,3933	1616	0	
-35,1953	2424	1	
-34,2052	3636	1	
-30,7747	5454	2	
-26,0362	8181	2	
-21,3567	12272	3	
-17,7761	18408	5	
-15,6891	27612	8	
-14,8649	41418	12	
-14,7795	62127	17	
-14,9346	86400	24	

Displ [mm]	Time [sec.]	Time [h.]	E = 1000 Mpa
0,0000	0	0	
-0,0001	0	0	
-0,0001	0	0	
-0,0002	0	0	
-0,0003	0	0	
-0,0005	0	0	
-0,0010	0	0	
-0,0019	0	0	
-0,0037	0	0	
-0,0064	0	0	
-0,0105	0	0	
-0,0166	0	0	
-0,0257	0	0	
-0,0394	1	0	
-0,0600	1	0	
-0,0908	2	0	
-0,1370	2	0	Bow
-0,2061	4	0	
-0,3095	6	0	
-0,4639	8	0	
-0,6941	12	0	
-1,0360	19	0	
-1,5417	28	0	
-2,2843	42	0	
-3,3637	63	0	
-4,9097	95	0	
-7,0769	142	0	
-10,0235	213	0	
-13,8595	319	0	
-18,5553	479	0	
-23,8143	718	0	
-28,9647	1077	0	
-32,9897	1616	0	
-34,8391	2424	1	
-33,9655	3636	1	
-30,7140	5454	2	
-26,1934	8181	2	
-21,7407	12272	3	
-18,3702	18408	5	
-16,4646	27612	8	
-15,7941	41418	12	
-15,8386	62127	17	
-16,0839	86400	24	

Displ [mm]	Time [sec.]	Time [h.]	E = 1100 Mpa
0,0000	0	0	
-0,0001	0	0	
-0,0001	0	0	
-0,0002	0	0	
-0,0003	0	0	
-0,0005	0	0	
-0,0009	0	0	
-0,0018	0	0	
-0,0036	0	0	
-0,0063	0	0	
-0,0103	0	0	
-0,0163	0	0	
-0,0253	0	0	
-0,0388	1	0	
-0,0590	1	0	
-0,0893	2	0	
-0,1347	2	0	Bow
-0,2027	4	0	
-0,3045	6	0	
-0,4564	8	0	
-0,6828	12	0	
-1,0192	19	0	
-1,5167	28	0	
-2,2474	42	0	
-3,3098	63	0	
-4,8317	95	0	
-6,9658	142	0	
-9,8688	213	0	
-13,6507	319	0	
-18,2848	479	0	
-23,4829	718	0	
-28,5875	1077	0	
-32,6021	1616	0	
-34,4968	2424	1	
-33,7346	3636	1	
-30,6541	5454	2	
-26,3422	8181	2	
-22,1064	12272	3	
-18,9368	18408	5	
-17,2047	27612	8	
-16,6810	41418	12	
-16,8497	62127	17	
-17,1812	86400	24	

Appendix P: Data influence of diffusivity Gesso on twist deformation

Displ [mm]	1/2 Width	Twist [degrees]	Time [sec.]	Time [h.]	D = 0,0
-0,0001	100	-7,17509E-05	0	0	
-0,0002	100	-0,000139279	0	0	
-0,0005	100	-0,000274332	0	0	
-0,0008	100	-0,000476899	0	0	
-0,0014	100	-0,000780724	0	0	
-0,0022	100	-0,001236409	0	0	
-0,0034	100	-0,00191981	0	0	
-0,0051	100	-0,002944625	1	0	
-0,0078	100	-0,004481212	1	0	
-0,0118	100	-0,00678468	2	0	
-0,0179	100	-0,010236636	2	0	
-0,0269	100	-0,015407293	4	0	
-0,0404	100	-0,02314715	6	0	
-0,0606	100	-0,034720436	8	0	
-0,0908	100	-0,051998885	12	0	
-0,1357	100	-0,077734282	19	0	
-0,2023	100	-0,115932695	28	0	Cup
-0,3008	100	-0,172333153	42	0	
-0,4450	100	-0,254963963	63	0	
-0,6539	100	-0,374637439	95	0	
-0,9513	100	-0,545035445	142	0	
-1,3644	100	-0,781689383	213	0	
-1,9179	100	-1,09871814	319	0	
-2,6222	100	-1,502065723	479	0	
-3,4559	100	-1,979308566	718	0	
-4,3489	100	-2,490149911	1077	0	
-5,1835	100	-2,967248221	1616	0	
-5,8316	100	-3,337486494	2424	1	
-6,2161	100	-3,556991983	3636	1	
-6,3459	100	-3,631041117	5454	2	
-6,2842	100	-3,595875698	8181	2	
-6,0837	100	-3,481418212	12272	3	
-5,7500	100	-3,290900818	18408	5	
-5,2508	100	-3,005720752	27612	8	
-4,5414	100	-2,600226751	41418	12	
-3,5953	100	-2,059045381	62127	17	
-2,4261	100	-1,389797455	86400	24	

Displ [mm]	1/2 Width	wist [degrees	Time [sec.]	Time [h.]	D = 0,1
-0,0001	100	-6,3253E-05	0	0	
-0,0002	100	-0,00010115	0	0	
-0,0003	100	-0,00015793	0	0	
-0,0004	100	-0,00024293	0	0	
-0,0006	100	-0,00037007	0	0	
-0,0010	100	-0,00055996	0	0	
-0,0015	100	-0,00084296	0	0	
-0,0022	100	-0,00126342	0	0	
-0,0033	100	-0,00188517	0	0	
-0,0049	100	-0,00279827	1	0	
-0,0072	100	-0,00412586	1	0	
-0,0105	100	-0,00602855	2	0	
-0,0152	100	-0,00870134	2	0	
-0,0216	100	-0,01235589	4	0	
-0,0300	100	-0,0171869	5	0	
-0,0407	100	-0,02333777	8	0	
-0,0540	100	-0,03092156	12	0	Cup
-0,0701	100	-0,04017018	18	0	
-0,0903	100	-0,05171407	27	0	
-0,1166	100	-0,06682862	40	0	
-0,1526	100	-0,0874161	60	0	
-0,2019	100	-0,11566341	90	0	
-0,2677	100	-0,15337757	135	0	
-0,3504	100	-0,20075671	202	0	
-0,4434	100	-0,25404266	303	0	
-0,5268	100	-0,30182966	455	0	
-0,5608	100	-0,32129704	682	0	
-0,4865	100	-0,27871484	1023	0	
-0,2464	100	-0,14117136	1534	0	
0,1716	100	0,09829196	2301	1	
0,6970	100	0,39935887	3452	1	
1,2009	100	0,68800903	5177	1	
1,5840	100	0,90746061	7766	2	
1,8421	100	1,05530329	11649	3	
2,0361	100	1,16642101	17473	5	
2,2217	100	1,27274814	26210	7	
2,4174	100	1,38478701	39315	11	
2,6119	100	1,49617402	58972	16	
2,7744	100	1,58920071	86400	24	

Displ [mm]	1/2 Width	wist [degrees	Time [sec.]	Time [h.]	D = 0,01
-0,0001	100	-7,1743E-05	0	0	
-0,0002	100	-0,00013925	0	0	
-0,0004	100	-0,00024049	0	0	
-0,0007	100	-0,00039228	0	0	
-0,0011	100	-0,00061985	0	0	
-0,0017	100	-0,00096091	0	0	
-0,0026	100	-0,00147184	0	0	
-0,0039	100	-0,00223678	1	0	
-0,0059	100	-0,0033809	1	0	
-0,0089	100	-0,00508974	1	0	
-0,0133	100	-0,00763667	2	0	
-0,0199	100	-0,01142065	3	0	
-0,0297	100	-0,01701644	4	0	
-0,0440	100	-0,02523489	6	0	
-0,0649	100	-0,0371849	9	0	
-0,0948	100	-0,05431323	14	0	
-0,1368	100	-0,0783737	21	0	Cup
-0,1942	100	-0,11126082	32	0	
-0,2699	100	-0,15465812	47	0	
-0,3658	100	-0,20957156	71	0	
-0,4817	100	-0,2760071	106	0	
-0,6161	100	-0,35298624	160	0	
-0,7649	100	-0,4382652	239	0	
-0,9180	100	-0,52593355	359	0	
-1,0485	100	-0,60072424	539	0	
-1,1031	100	-0,6320213	808	0	
-1,0049	100	-0,57573445	1212	0	
-0,6862	100	-0,39316033	1818	1	
-0,1477	100	-0,08463669	2727	1	
0,5048	100	0,28924096	4091	1	
1,1077	100	0,63462221	6136	2	
1,5520	100	0,88918202	9204	3	
1,8461	100	1,0576287	13806	4	
2,0653	100	1,18313289	20709	6	
2,2704	100	1,30063138	31067	9	
2,4779	100	1,41946456	46596	13	
2,6731	100	1,53122602	69893	19	
2,7718	100	1,58771217	86400	24	

Displ [mm]	1/2 Width	wist [degrees	Time [sec.]	Time [h.]	D = 0,001
-0,0001	100	-7,17498E-05	0	0	
-0,0002	100	-0,000139276	0	0	
-0,0005	100	-0,000274321	0	0	
-0,0008	100	-0,000476866	0	0	
-0,0014	100	-0,000780638	0	0	
-0,0022	100	-0,001236197	0	0	
-0,0033	100	-0,001919305	0	0	
-0,0051	100	-0,00294345	1	0	
-0,0078	100	-0,004478507	1	0	
-0,0118	100	-0,006778492	2	0	
-0,0178	100	-0,010222598	2	0	
-0,0268	100	-0,015375609	4	0	
-0,0403	100	-0,023075817	6	0	
-0,0603	100	-0,034560352	8	0	
-0,0901	100	-0,051641073	12	0	
-0,1343	100	-0,076938445	19	0	
-0,1993	100	-0,114174295	28	0	Cup
-0,2941	100	-0,16848463	42	0	
-0,4305	100	-0,246652796	63	0	
-0,6231	100	-0,357020851	95	0	
-0,8878	100	-0,508650546	142	0	
-1,2376	100	-0,709079283	213	0	
-1,6757	100	-0,959998344	319	0	
-2,1828	100	-1,25047661	479	0	
-2,7035	100	-1,548637085	718	0	
-3,1347	100	-1,795485756	1077	0	
-3,3341	100	-1,909574043	1616	0	
-3,1657	100	-1,813229838	2424	1	
-2,5774	100	-1,476391649	3636	1	
-1,6551	100	-0,948210142	5454	2	
-0,5985	100	-0,342927188	8181	2	
0,3778	100	0,216481905	12272	3	
1,1462	100	0,656706925	18408	5	
1,7009	100	0,974432766	27612	8	
2,1090	100	1,20821179	41418	12	
2,4310	100	1,392591841	62127	17	
2,6496	100	1,517748141	86400	24	

Displ [mm]	1/2 Width	wist [degrees	Time [sec.]	Time [h.]	D = 0,0001
-0,0001	100	-7,1751E-05	0	0	
-0,0002	100	-0,00013928	0	0	
-0,0005	100	-0,00027433	0	0	
-0,0008	100	-0,0004769	0	0	
-0,0014	100	-0,00078072	0	0	
-0,0022	100	-0,00123639	0	0	
-0,0034	100	-0,00191976	0	0	
-0,0051	100	-0,0029445	1	0	
-0,0078	100	-0,00448094	1	0	
-0,0118	100	-0,00678405	2	0	
-0,0179	100	-0,0102352	2	0	
-0,0269	100	-0,01540414	4	0	
-0,0404	100	-0,02313999	6	0	
-0,0606	100	-0,03470434	8	0	
-0,0907	100	-0,05196285	12	0	
-0,1355	100	-0,07765407	19	0	
-0,2020	100	-0,11575451	28	0	Cup
-0,3001	100	-0,17193953	42	0	
-0,4435	100	-0,25410569	63	0	
-0,6507	100	-0,37279202	95	0	
-0,9445	100	-0,54114484	142	0	
-1,3505	100	-0,77370955	213	0	
-1,8903	100	-1,08292742	319	0	
-2,5699	100	-1,47214312	479	0	
-3,3617	100	-1,9253757	718	0	
-4,1875	100	-2,39783126	1077	0	
-4,9201	100	-2,81674397	1616	0	
-5,4197	100	-3,10219577	2424	1	
-5,5939	100	-3,20174323	3636	1	
-5,4349	100	-3,11089058	5454	2	
-4,9918	100	-2,85769009	8181	2	
-4,3150	100	-2,47075158	12272	3	
-3,4335	100	-1,96644946	18408	5	
-2,3758	100	-1,3609542	27612	8	
-1,2002	100	-0,68760801	41418	12	
-0,0047	100	-0,00269492	62127	17	
0,9232	100	0,528941901	86400	24	

Displ [mm]	1/2 Width	wist [degree	Time [sec.]	Time [h.]	D = 0,00001
-0,0001	100	-7,1751E-05	0	0	
-0,0002	100	-0,00013928	0	0	
-0,0005	100	-0,00027433	0	0	
-0,0008	100	-0,0004769	0	0	
-0,0014	100	-0,00078072	0	0	
-0,0022	100	-0,00123641	0	0	
-0,0034	100	-0,0019198	0	0	
-0,0051	100	-0,00294461	1	0	
-0,0078	100	-0,00448118	1	0	
-0,0118	100	-0,00678457	2	0	
-0,0179	100	-0,01023646	2	0	
-0,0269	100	-0,01540701	4	0	
-0,0404	100	-0,02314641	6	0	
-0,0606	100	-0,03471883	8	0	
-0,0907	100	-0,05199528	12	0	
-0,1357	100	-0,07772626	19	0	
-0,2023	100	-0,11591493	28	0	Cup
-0,3007	100	-0,17229362	42	0	
-0,4448	100	-0,25487802	63	0	
-0,6536	100	-0,37445238	95	0	
-0,9506	100	-0,54464358	142	0	
-1,3630	100	-0,78088739	213	0	
-1,9151	100	-1,09712018	319	0	
-2,6169	100	-1,49901395	479	0	
-3,4463	100	-1,97378038	718	0	
-4,3322	100	-2,48061095	1077	0	
-5,1560	100	-2,95155674	1616	0	
-5,7881	100	-3,31266381	2424	1	
-6,1494	100	-3,51892123	3636	1	
-6,2461	100	-3,57407999	5454	2	
-6,1383	100	-3,51259673	8181	2	
-5,8756	100	-3,36262768	12272	3	
-5,4620	100	-3,12639463	18408	5	
-4,8664	100	-2,78605534	27612	8	
-4,0515	100	-2,32004674	41418	12	
-3,0060	100	-1,7217812	62127	17	
-1,9937	100	-1,14217755	86400	24	